

**Regulation of the carbon/nitrogen storage polymer
cyanophycin by the signal transduction protein P_{II} in
Synechocystis sp. PCC 6803**

Dissertation

der Mathematisch-Naturwissenschaftlichen Fakultät
der Eberhard Karls Universität Tübingen
zur Erlangung des Grades eines
Doktors der Naturwissenschaften
(Dr. rer. nat.)

vorgelegt von
Björn Watzer
aus Heidelberg

Tübingen
2018

Gedruckt mit Genehmigung der Mathematisch-Naturwissenschaftlichen Fakultät der
Eberhard Karls Universität Tübingen.

Tag der mündlichen Qualifikation:	09.04.2019
Dekan:	Prof. Dr. Wolfgang Rosenstiel
1. Berichterstatter:	Prof. Dr. Karl Forchhammer
2. Berichterstatter:	Prof. Dr. Heike Brötz-Oesterhelt

Erklärung

Ich erkläre hiermit, dass ich die zur Promotion eingereichte Arbeit selbständig verfasst, nur die angegebenen Quellen und Hilfsmittel benutzt und Stellen, die wörtlich oder inhaltlich nach den Werken anderer Autoren entnommen sind, als solche gekennzeichnet habe. Eine detaillierte Abgrenzung meiner eigenen Leistungen von den Beiträgen meiner Kooperationspartner habe ich in „Declaration of author contribution“ vorgenommen.

Tübingen, den 12.12.2018

Björn Watser

Table of contents

I.	ABBREVIATIONS.....	1
II.	SUMMARY	2
III.	ZUSAMMENFASSUNG	3
IV.	PUBLICATIONS.....	5
1.	Accepted Papers	5
1.	Publication.....	5
2.	Publication.....	5
3.	Publication.....	5
4.	Publication.....	5
5.	Publication.....	6
6.	Publication.....	6
2.	Manuscripts in preparation.....	6
7.	Publication.....	6
3.	Declaration of personal contribution to the publications.....	7
3.1	1. Publication	7
3.2	2. Publication	7
3.3	3. Publication	7
3.4	4. Publication	8
3.5	5. Publication	8
3.6	6. Publication	8
3.7	7. Publication	8
V.	INTRODUCTION	9
1.	Cyanobacteria.....	9
2.	Carbon metabolism	9
2.1	Carbon fixation.....	9
2.2	The cyanobacterial TCA cycle	10
2.3	Carbon storage polymers.....	11
2.3.1	Glycogen in cyanobacteria	11
2.3.2	Polyhydroxybutyrate in cyanobacteria	11
3.	Nitrogen metabolism	12
3.1	2-oxoglutarate as regulatory metabolite	12
3.2	Nitrogen starvation response	15
3.3	Resuscitation from nitrogen starvation.....	15
3.4	P _{II} signal transduction protein ¹	16
3.4.1	NtcA coactivator PipX	17
3.4.2	N-acetylglutamate kinase ¹	18
3.4.3	Ammonium Channel AmtB.....	20

4.	Cyanophycin a carbon/nitrogen storage polymer ¹	20
4.1	Natural occurrence of cyanophycin ¹	21
4.2	Biochemical characteristics of Cyanophycin ¹	22
4.3	Cyanophycin metabolism ¹	23
4.3.1	Cyanophycin Synthetase	23
4.3.2	Cyanophycinase ¹	25
4.3.3	Aspartyl-arginine dipeptidase ¹	26
4.4	Regulation of cyanophycin metabolism ¹	28
4.4.1	Genetic organization of CphA and CphB	28
4.4.2	Influence of arginine to the cyanophycin metabolism ¹	29
4.5	Industrial applications ¹	30
4.6	Biotechnological production of cyanophycin ¹	31
5.	Research objective.....	34
VI.	RESULTS	35
1.	The P _{II} (I86N) regulatory network.....	36
1.1	P _{II} (I86N) variant, a super activator of NAGK	36
1.1.1	Strain BW86 process optimization	38
1.2	P _{II} (I86N) and Amt1 ammonium permease	40
1.3	P _{II} localization changes under different nitrogen supplementations.....	41
1.4	P _{II} (I86N) and the NrtABCD nitrate/nitrite transporter	42
1.5	P _{II} I86N and the UrtABCDE urea transporter	43
1.6	Additional research	43
1.6.1	P _{II} (I86N) and PipX.....	43
1.6.2	P _{II} I86N and nitrogen starvation response	46
1.6.3	P _{II} (I86N) causes decreased PHB accumulation	48
2.	Cell biology of the nitrogen storage polymer cyanophycin.....	49
2.1	CphA localization changes during cyanophycin accumulation and degradation.....	49
2.2	Physiological function of cyanophycin in non-diazotrophic cyanobacteria.....	50
2.2.1	Cyanophycin-deficient mutant has a growth advantage under standard laboratory conditions	50
2.2.2	Cyanophycin accumulation is beneficial under natural conditions.....	51
2.3	Additional research	52
2.3.1	Extraction of an unidentified polymer from a cyanophycin-deficient mutant.....	52
VII.	DISCUSSION	55
1.	Metabolic engineering using custom- tailored P _{II} signaling proteins.....	55
1.1	Is the <i>Synechocystis</i> sp. BW86 an economical alternative to heterotrophic cyanophycin production?	56
1.2	Further physiological impact by the P _{II} (I86N)	56
1.2.1	P _{II} (I86N) and the NtcA co-activator PipX	56
1.2.2	P _{II} (I86N) influences PHB accumulation.....	57
2.	The signal transduction protein P _{II} controls nitrogen uptake.....	58
2.1	P _{II} regulate ammonium uptake	58
2.2	P _{II} regulates nitrate uptake	58
2.3	P _{II} regulate urea uptake.....	60

3.	Cell biology of the nitrogen storage polymer cyanophycin.....	62
3.1	CphA localization change indicates active and inactive forms	62
3.2	CphA biochemical properties.....	62
3.3	Physiological role of cyanophycin in cyanobacteria	65
3.3.1	Growth advantage of cyanophycin-deficient mutant under standard laboratory conditions	65
3.3.2	Cyanophycin accumulation provides fitness advantage under natural conditions	66
4.	Final conclusions.....	68
VIII.	REFERENCES	69
IX.	APPENDIX.....	84
1.	Accepted publication	
2.	Accepted publication	
3.	Accepted publication	
4.	Accepted publication	
5.	Accepted publication	
6.	Accepted publication	
7.	Manuscript in preparation	
X.	ACKNOWLEDGEMENTS	

I. Abbreviations

2-OG	2-oxoglutarate	LED	Light-emitting diode
3-PGA	3-phosphoglycerate	MS	Mass spectrometry
Å	Ångström	MSX	L-methionine-d,l-sulfoximine
AC	Adenylate cyclase	NADPH	Nicotinamide adenine dinucleotide phosphate
ACC	Acetyl-CoA carboxylase	NAGK	N-acetylglutamate kinase
Ac-Glu	N-acetylglutamate	NTA	Nitrilotriacetic acid
Ac-Glu-P	N-acetylglutamyl-phosphate	OD ₇₅₀	Optical density at 750nm
ADP	Adenosine diphosphate	OGDC	2-oxoglutarate decarboxylase
AMP	Adenosine monophosphate	OGDH	2-oxoglutarate dehydrogenase
ATP	Adenosine triphosphate	OPLS	Orthogonal projections to latent structures
BCCP	Biotin carboxyl carrier protein	ORF	Open reading frame
BSA	Bovine serum albumin	PAA	Poly(α -L-aspartic acid)
CA	Carbonic anhydrase	PAGE	Polyacrylamide gel electrophoresis
cAMP	Cyclic AMP	PCA	Principal component analysis
CCM	CO ₂ -concentrating-mechanism	PCC	Pasteur culture collection
CCR	Carbon catabolite repression	PCE	Photo conversion efficiency
CD	Circular dichroism	PHA	Polyhydroxyalkanoates
CDM	Cell dry matter	PHB	Poly- β -hydroxybutyrate
CoA	Coenzyme-A	PTS	Phosphotransferase system
CRP	cAMP receptor protein	RubisCO	Ribulose-1,5-bisphosphate carboxylase/oxygenase
Crp	cAMP receptor protein	RUs	Response units
DTT	Dithiothreitol	SDS	Natriumdodecylsulfat
EI	Enzyme I	SPR	Surface plasmon resonance
GDH	Glutamate dehydrogenase	SSADH	Succinic semialdehyde dehydrogenase
GOGAT	Glutamine 2-oxoglutarate aminotransferase	TCA	Tricarboxylic acid
GS	Glutamine synthetase	V_{max}	Maximum reaction rate
kDa	Kilo dalton	w/v	Weight per volume
K_m	Michaelis constant	w/w	Weight per weight

II. Summary

Cyanobacteria are one of the deepest branching bacterial phyla on earth. Today, cyanobacteria occupy almost all illuminated habitats, where they utilize various nitrogen sources. Nitrogen assimilation strictly depends on carbon and nitrogen availability and requires a fine-tuned regulatory network involving the P_{II} signal transduction protein. In the present study I focused on the regulation of the carbon/nitrogen storage polymer cyanophycin by the P_{II} signaling protein. Cyanophycin is a non-ribosomal synthesized polyamide consisting of arginine and aspartate. Cyanophycin accumulation depends on the arginine availability. P_{II} controls the rate limiting step of arginine biosynthesis by regulating the key enzyme N-acetylglutamate kinase (NAGK). A P_{II} variant with a single point mutation (I86N) was previously identified as a NAGK super activator *in vitro*. By introducing P_{II}(I86N) in *Synechocystis* sp. PCC 6803, we created a strain which strongly overproduces cyanophycin up to 57 % of the cell dry mass. Since cyanophycin is a bio-polymer with high industrial interest, we performed several process optimization studies. During these studies, we observed that *Synechocystis* sp. PCC 6803 harboring the P_{II} (I86N) variant showed impaired ammonium utilization. By analyzing this behavior, we could clarify that P_{II} regulates ammonium uptake by interacting with Amt1 ammonium permease. We could further demonstrate that P_{II} mediates the light and ammonium dependent inhibition of nitrate uptake by interacting with the NrtC and NrtD subunits of the nitrate/nitrite transporter NrtABCD. During this study, we could also identify the UrtE subunit of the ABC-type urea transporter UrtABCDE as novel P_{II} target. The interaction of P_{II} with the UrtE subunit regulates the urea uptake in cyanobacteria.

The occurrence of cyanophycin in cyanobacteria was known for more than 100 years; however, the biological function remained largely uninvestigated. During localization studies in *Synechocystis* sp. PCC 6803, we could show that the cyanophycin synthesizing enzyme CphA resides in an active and inactive state. When CphA was inactive, it localized diffusely in the cytoplasm. When cyanophycin synthesis was triggered, CphA first aggregated into foci and was later localized on the surface of the cyanophycin granules. During degradation, CphA dissociates from the granule surface. Under standard laboratory conditions, the ability to synthesize cyanophycin did not confer a fitness advantage, however with a fluctuating and limiting nitrogen supplementation in combination with day/night cycles, the accumulation of the polymer provides a clear fitness advantage. Furthermore cyanophycin acts as a temporary nitrogen storage which allows nitrogen assimilation during the night. The accumulated cyanophycin can be subsequently used as an internal nitrogen source during the day.

III. Zusammenfassung

In der Domäne der Bakterien bilden die Cyanobakterien eine der ältesten Abteilungen und sind heute in nahezu allen lichtzugänglichen Habitaten angesiedelt. Cyanobakterien können eine Vielzahl organischer und anorganischer Stickstoffquellen verstoffwechseln, wobei die Stickstoffassimilation über die intrazelluläre Kohlenstoff- und Stickstoffbalance reguliert wird. Das P_{II} Signaltransduktions-Proteins erfüllt hierbei eine zentrale Rolle. Die vorliegende Arbeit befasst sich mit der Regulation des Kohlenstoff-/Stickstoff- Speicherpolymers Cyanophycin durch das P_{II} Protein. Cyanophycin ist ein nicht-ribosomal synthetisiertes Polyamid bestehend aus Arginin und Asparaginsäure. Die Akkumulation von Cyanophycin ist von der Argininverfügbarkeit abhängig. Das P_{II} Protein reguliert die Argininbiosynthese durch die Interaktion mit der N-Acetylglutamat Kinase (NAGK), dem Schlüssel-Enzym der Argininbiosynthese. Vorangegangene Studien zeigten, dass eine Punktmutation (I86N) in P_{II} die aktivierende Wirkung auf NAGK *in vitro* deutlich verstärkt. Folglich konnten wir durch das Einbringen dieser P_{II} (I86N) Variante in *Synechocystis* sp. PCC 6803 einen Stamm kreieren, der eine erhebliche Überproduktion von Arginin und ein Cyanophycinanteil von bis zu 57 % zur Zelltrockenmaße aufwies. Da Cyanophycin von industriellem Interesse ist, wurden verschiedene Prozessoptimierungsstudien angefertigt. Im Zuge dieser Studien stellte sich heraus, dass die P_{II} (I86N) Variante die Ammoniumverwertung von *Synechocystis* sp. PCC 6803 negativ beeinflusst. Bei näheren Untersuchungen zeigte sich, dass P_{II} die Ammoniumaufnahme durch die Interaktion mit der Amt1 Ammoniumpermease reguliert. Wir konnten ebenfalls demonstrieren, dass P_{II} die licht- und ammoniumabhängige Nitrataufnahme-Inhibition durch die Interaktion mit der NrtC und NrtD Untereinheit des Nitrit/Nitrat Transporter NrtABCD vermittelt. Darüber hinaus konnte nachgewiesen werden, dass P_{II} mit der UrtE Untereinheit des ABC-Typ Urea Transporter UrtABCDE interagiert und hierdurch die Ureaaufnahme reguliert.

Das Auftreten von Cyanophycin in Cyanobakterien wurde bereits vor mehr als 100 Jahren beschrieben, jedoch blieb bis heute dessen biologische Funktion ungeklärt. Lokalisationsstudien in *Synechocystis* sp. PCC 6803, bei denen das Cyanophycin synthetisierende Enzym CphA mit eGFP fusioniert wurde, ergaben, dass CphA eine aktive und inaktive Form aufweist. In seiner inaktiven Form ist CphA diffus im Zytoplasma verteilt. Wird die Cyanophycinakkumulation induziert, aggregiert CphA zunächst in Focis und ist später an der Oberfläche der Cyanophycingranula lokalisiert. Während dem Abbau dissoziiert CphA von der Granulaoberfläche und geht wieder in die inaktive Form über. Überraschenderweise hatten Cyanophycin freien Zellen unter Standard-Laborbedingungen einen Wachstumsvorteil gegenüber dem Wild-Typ. Um die Situation eines natürlichen

Habitats zu imitieren, kultivierten wir beide Stämme bei schwankender Stickstoffversorgung zusammen mit Tag/Nacht-Zyklen. Unter diesen Bedingungen hatten die Cyanophycin akkumulierenden Zellen einen klaren Vorteil. Darüber hinaus konnten wir vorweisen, dass Cyanophycin als temporärer Stickstoffspeicher dient, der die Stickstoffassimilation in der Nacht ermöglicht. In der Nacht akkumuliertes Cyanophycin kann während des Tages als Stickstoffquelle genutzt werden.

IV. Publications

1. Accepted Papers

1. Publication

Research Article

Watzer, B., Engelbrecht, A., Hauf, W., Stahl, M., Maldener, I. & Forchhammer, K. (2015).

Metabolic pathway engineering using the central signal processor P_{II}.

Microbial cell factories, 14(1), 192.

2. Publication

Commentary

Forchhammer, K. & **Watzer, B.** (2016).

Closing a gap in cyanophycin metabolism (Microbiology Comment).

Microbiology, 162(5), 727-729.

3. Publication

Research Article

Trautmann, A., **Watzer, B.**, Wilde, A., Forchhammer, K. & Posten, C. (2016).

Effect of phosphate availability on cyanophycin accumulation in *Synechocystis* sp. PCC 6803 and the production strain BW86.

Algal research, 20, 189-196.

4. Publication

Research Article

Lüddecke, J., Francois, L., Spät, P., **Watzer, B.**, Chilczuk, T., Poschet, G., Hell, R., Radlwimmer, B. & Forchhammer, K. (2017).

P_{II} protein-derived FRET sensors for quantification and live-cell imaging of 2-oxoglutarate.

Scientific reports, 7(1), 1437

5. Publication

Book Chapter

Watzer, B. & Forchhammer, K. (2018).

Cyanophycin, a nitrogen-rich reserve polymer.

Cyanobacteria, ISBN: 978-953-51-6243-8

6. Publication

Research Article

Watzer, B. & Forchhammer, K. (2018).

Cyanophycin synthesis optimizes nitrogen utilization in the unicellular cyanobacterium *Synechocystis* sp. PCC 6803.

Applied and environmental microbiology, 84: e01298-18

2. Manuscripts in preparation

7. Publication

Research Article (Preliminary manuscript from 07.12.2018)

Watzer, B., Spät, P., Neumann, N., Koch, M., Hennrich, O. & Forchhammer, K.

The signal transduction protein P_{II} controls ammonium, nitrate and urea uptake in cyanobacteria

Final version of the manuscript was submitted to *Frontiers in Microbiology* (ISSN 1664302x) on 09.04.2019

3. Declaration of personal contribution to the publications

3.1 1. Publication

Metabolic pathway engineering using the central signal processor P_{II}.

I performed, evaluated and interpreted the *In vivo* NAGK activity assays, the determination of P_{II} phosphorylation via western blot, cyanophycin extraction and quantification under several conditions, cyanophycin isolation and determination of molecular mass, light microscopic studies and all cyanobacterial cultivation methods.

Sample collection and preparation for metabolome analysis was performed by me; Dr. Mark Stahl performed the quantitative measurement of metabolites via UPLC/ MS and evaluated the data.

Sample collection for transmission electron microscopy was done by me; Dr. Iris Maldener and Claudia Menzel performed sample preparation and transmission electron microscopy.

The manuscript was prepared by me and Prof. Karl Forchhammer with input from all co-authors. I took part in the revision process. During the whole study I was under the supervision of Prof. Karl Forchhammer.

3.2 2. Publication

Closing a gap in cyanophycin metabolism (Microbiology Comment).

I created the figure of cyanophycin metabolism shown in this publication and proof read the manuscript.

3.3 3. Publication

*Effect of phosphate availability on cyanophycin accumulation in *Synechocystis* sp. PCC 6803 and the production strain BW86.*

I provided and established methods of cyanobacterial cultivation, cyanophycin extraction and quantification in the group of Prof. Clemens Posten (Karlsruher Institut für Technologie). Strains used in this study were provided by me. I gave input and proof read the manuscript.

3.4 4. Publication

P_{II} protein-derived FRET sensors for quantification and live-cell imaging of 2-oxoglutarate.

Dr. Jan Lüddecke and I established the *In situ* fdGOGAT -assay described in this publication. Furthermore, physiological characterization using the novel *In situ* fdGOGAT -assay in the unicellular cyanobacterium *Synechococcus elongates*, was performed by me. I gave input to the manuscript.

3.5 5. Publication

Cyanophycin, a nitrogen-rich reserve polymer.

The manuscript and figures of this publication were prepared by me and proof read by Prof. Karl Forchhammer.

3.6 6. Publication

*Cyanophycin synthesis optimizes nitrogen utilization in the unicellular cyanobacterium *Synechocystis* sp. PCC 6803.*

All experiments shown in this publication were planned, performed and evaluated by me under the supervision of Prof. Karl Forchhammer. The manuscript was written by me and Prof. Karl Forchhammer. I took part in the revision process.

3.7 7. Publication (preliminary manuscript from 07.12.2018)

The signal transduction protein P_{II} controls ammonium, nitrate and urea uptake in cyanobacteria

I performed all nitrogen utilization experiments, the determination of P_{II} localization in dependence of nitrogen availability and cyanobacterial cultivation methods (drop plate methods). I evaluated and interpreted the collected data.

Dr. Philipp Spät performed and evaluated the protein pull down assays. Niels Neumann and Mortiz Koch performed the bacterial two-hybrid assays. The manuscript was prepared by me with input from all co-authors. During the whole study I was under the supervision of Prof. Karl Forchhammer.

V. Introduction

1. Cyanobacteria

The biologically induced enrichment of oxygen in the atmosphere marks one of the most important steps in earth history. This change in the redox-state of the atmosphere, called "great oxidation event" was triggered by the emergence of oxygenic photosynthesis by ancestors of present cyanobacteria, at least 2.3 billion years ago [1].

Cyanobacteria are photoautotrophic prokaryotes, classified in the phylum *Cyanophyta* in the kingdom of *Bacteria* [2]. In six known phyla of photosynthetic bacteria, only cyanobacteria are able to perform oxygenic photosynthesis [3]. Cyanobacteria occupy almost all illuminated habitats, together they represent one of the quantitatively most abundant organisms on earth [2]. As primary producers, cyanobacteria play a key role in the global carbon cycle. Furthermore, diazotrophic cyanobacteria are the dominant N₂ fixers in the ocean, introducing combined nitrogen into the global nitrogen cycle [4].

Cyanobacteria can be classified in five sections, each distinguished by particular patterns of structure and development [5]. Section I contain unicellular cyanobacteria, which divide by binary fission or budding. Cyanobacteria of section II are also unicellular; however, they divide by multiple fissions of the mother cell to smaller daughter cells, named baeocytes. Section III contains multicellular filament forming cyanobacteria without specialized cells. Section IV includes filamentous cyanobacteria, which are able to differentiate specialized cells, including heterocysts (specialized cells for N₂ fixation), akinetes (resting spore-like cells) and hormogonia (short and motile filaments). Branched filamentous cyanobacteria of section V are multicellular and divide in more than one plane and differentiate specialized cells [5].

2. Carbon metabolism

2.1 Carbon fixation

Cyanobacteria play a key role in the global carbon cycle, mainly through their autotrophic carbon dioxide (CO₂) fixation coupled to oxygenic photosynthesis. Cyanobacteria use the energy and reducing equivalents (NADPH) obtained from photosynthesis to fix CO₂ through the Calvin-Benson-Bassham cycle [6]. Key enzyme of the Calvin-Benson-Bassham cycle is the Ribulose-1,5-bisphosphate carboxylase/oxygenase (RubisCO), which is responsible for CO₂ fixation. RubisCO fixes CO₂ by carboxylation of Ribulose-1,5-bisphosphate to yield two molecules 3-phosphoglycerate (3-PGA) [6].

However, the affinity of RubisCO to CO₂ is low compared to molecular oxygen (O₂). When RubisCO react with O₂, this leads to the formation of phosphoglycolate, a toxic component which has to be recycled in a process called photorespiration [7]. The photorespiratory metabolism allows cyanobacteria and plants to tolerate high concentrations of O₂. To avoid photorespiration, cyanobacteria have evolved a CO₂-concentrating-mechanism (CCM) that improves photosynthetic activity and survival under CO₂ limiting conditions [8]. In CCM, both, CO₂ and hydrogencarbonate (HCO₃⁻), are taken up; however HCO₃⁻ represents the predominant species of inorganic carbon in the cytoplasm [8]. Cytoplasmic HCO₃⁻ diffuses through the proteinaceous shell of micro-compartments called carboxysomes. The latter are polyhedral bodies featuring high amounts of RubisCO molecules covered by a protein shell [9]. Inside the carboxysome, HCO₃⁻ is converted into CO₂ by the carbonic anhydrase (CA). The protein shell of the carboxysome represents a gas diffusion barrier, which enables a high local concentration of CO₂ around tightly packed RubisCO molecules, leading to an efficient carboxylation reaction. Molecules like Ribulose-1,5-bisphosphate, 3-PGA and HCO₃⁻ are able to pass the protein shell. 5/6 of 3-PGA is converted in the Calvin-Benson-Bassham cycle to regenerate Ribulose-1,5-bisphosphate and 1/6 is used in the central metabolism [9].

2.2 The cyanobacterial TCA cycle

The tricarboxylic acid (TCA) cycle is a fundamental metabolic pathway among all aerobic organisms. Generally, the TCA cycle has two functions: First, it oxidizes two-carbon units derived from acetyl coenzyme-A (CoA), producing CO₂ and reduced NADH to provide electrons for the oxidative phosphorylation. Second, the TCA cycle provides precursor metabolites that are required for other anabolic pathways, like non-essential amino acid synthesis or fatty acid synthesis [10].

In 1967, Smith *et al.* and Pearce *et al.* reported the absence of the 2-oxoglutarate dehydrogenase (OGDH), an enzyme that converts 2-oxoglutarate (2-OG) to succinyl-CoA in several cyanobacteria [11, 12]. Due to these observations it became common knowledge that cyanobacteria possess an incomplete TCA cycle. The glyoxylate shunt and aspartate transaminase reactions are believed to permit the recycling of TCA cycle metabolites and thereby complete the cycle (for review see [13]). In 2011, Zhang *et al.* reported the presence of two other enzymes, which functionally substitute the OGDH and succinyl-CoA ligase to generate succinate from 2-OG and closing the TCA cycle. Here, 2-OG is converted to succinic semialdehyde by the 2-OG decarboxylase and is subsequently oxidized to succinate by the succinic semialdehyde dehydrogenase (figure 1). This alternative TCA cycle is highly conserved in the majority of cyanobacteria, with the exception of *Prochlorococcus* and marine *Synechococcus* species [10].

2.3 Carbon storage polymers

The most common carbon storage polymers, which are widely distributed among microorganisms, are glycogen and poly- β -hydroxybutyrate (PHB). The unicellular and non-diazotrophic cyanobacterium *Synechocystis* sp. PCC 6803 is able to synthesize both, glycogen and PHB, in contrast to most other microorganisms, which mostly produce only one of these carbon storage compounds [14].

2.3.1 Glycogen in cyanobacteria

Glycogen is a highly branched homopolymer of glucose which serves as energy and carbon storage in most organisms. Glycogen is composed of α -D-glycosyl units connected by α -1,4-glycosidic linkages and branched by α -1,6 glycosidic linkages [15]. The accumulation of glycogen occurs in form of cytoplasmic granules, with a homogeneous size of less than 50 nm [16, 17]. In the first step of the biosynthesis in bacteria, the ADP-Glucose pyrophosphorylase (GlgC) catalyses the syntheses of ADP-Glucose by using ATP and glucose 1-phosphate [15]. Afterwards, the glycogen synthetase (GlgA) catalyses the successive addition of α -1,4-linked glucose to the non-reduced end of glycogen by using ADP-Glucose [18]. The glycogen branching enzyme (GlgB) introduces α -1,6 glucosidic branches into the growing polymer [19]. During glycogen degradation, the glycogen phosphorylase (GlgP) transfers an orthophosphate to the non-reduced end and thereby releases glucose 1-phosphate. This process continues until the glycogen phosphorylase reaches the last four glucose moieties left on each branch [20]. The glycogen debranching enzyme (GlgX) catalyses the hydrolysis of the α -1,6 glucosidic linkage [20, 21].

Accumulation of glycogen occurs under adverse growth conditions, which provide carbon in sufficient amounts. Here the exact physiological role of glycogen differs from strain to strain. Depending on the microorganism, glycogen accumulation can be beneficial in survival of macronutrient starvation, symbiotic performance, colonization or virulence [22, 23]. In cyanobacteria, the ability for glycogen synthesis is highly conserved [24]. It was shown that a glycogen-deficient mutant of *Synechocystis* sp. PCC 6803 shows a reduced viability during light-dark transitions. Furthermore, glycogen accumulation seems to be crucial for survival of nitrogen starvation [22]. Recently, glycogen was also identified to play a fundamental role during resuscitation from nitrogen starvation in *Synechocystis* sp. PCC 6803, by providing energy and carbon for anabolic reactions [25, 26].

2.3.2 Polyhydroxybutyrate in cyanobacteria

Polyhydroxybutyrate (PHB) is a carbon and redox storage compound, widely distributed in *Eubacteria* and *Archaea*. PHB is a bio-polymer with high industrial interest, due to its

potential use as biodegradable plastic substituent [27, 28]. Therefore, several PHB-accumulating cyanobacteria, like *Synechocystis* sp. PCC 6803, come into focus of PHB research [29].

PHB accumulation is triggered by several adverse growth conditions, which lower the growth rate. For *Synechocystis* sp. PCC 6803, nitrogen and phosphate starvation have been described as reliable and strong trigger for PHB accumulation [30, 31]. In the first step of PHB synthesis, two molecules of acetyl coenzyme-A (CoA) condensate to acetoacetyl-CoA, catalyzed by the enzyme PhaA. Subsequently, PhaB reduces acetoacetyl-CoA to 3-hydroxybutyryl-CoA by utilizing NADPH [32]. Finally, 3-hydroxybutyryl-CoA is polymerized to PHB by the PHB-synthase. The latter can be divided into four subclasses [33]. *Synechocystis* sp. PCC 6803 possesses a type III PHB synthase, containing two subunits, both with a size of around 40 kDa, called PhaC and PhaE [34]. The PhaEC heterodimer is attached to the PHB granule surface. PHB granules, also named carbonosomes, contain a PHB polymer core and a surface layer of structural and functional proteins [35]. Based on *in vitro* analysis of isolated PHB granules, it was suggested that the surface of these granules contain a phospholipid membrane. However, a recent study refuted this suggestion and concluded that the PHB granule surface is exclusively composed of proteins [36]. Next to PHB-synthase and PHB-depolymerase, a third class of PHB associated proteins is known, called phasins. The functions of phasins are manifold, ranging from activation of the PHB-synthase, over equally distribution of the PHB granules during cell division, to the regulation of the PHB granule surface to volume ratio [37-39].

3. Nitrogen metabolism

3.1 2-oxoglutarate as regulatory metabolite

Cyanobacteria can assimilate several different nitrogen sources. Nitrogen assimilation is tightly regulated by the carbon and nitrogen availability. The interconnection of the carbon and nitrogen metabolism relies primarily on the glutamine synthetase / glutamine-2-oxoglutarate-aminotransferase (GS/GOGAT) reaction. 2-OG, an intermediate of the TCA-cycle, provides the carbon skeleton for inorganic nitrogen incorporation by the GS/GOGAT cycle. The GOGAT converts one molecule of each, 2-OG and glutamine, in two molecules of glutamate, by using reduction equivalents. Subsequently, the GS catalyzes the assimilation of ammonium through amidation of one glutamate yielding glutamine. The net balance of the GS/GOGAT cycle includes one ammonium per TCA cycle derived 2-OG for the synthesis of two molecules of glutamate, whereas one glutamate stays in the cycle to regenerate glutamine (figure 1) [4, 40]. Due to this mechanism, 2-OG is not only the link between carbon and nitrogen metabolism, but also an indicator for the intracellular carbon/nitrogen balance

[41-43]. In case of nitrogen limitation or carbon excess, the GS/GOGAT cycle runs out of ammonium, leading to an elevated 2-OG level. In contrast, under nitrogen excess or carbon limitation, the 2-OG level declines to a minimum [40-43]. The transient 2-OG level fluctuation in dependence of nitrogen and carbon supply occurs within a short time and has been reported in various microorganisms [42, 44-48].

Due to its role as indicator for intracellular carbon/nitrogen ratio, several 2-OG sensing proteins have evolved. The regulation of nitrogen metabolism mainly depends on the global transcription factor NtcA, which regulates the expression of genes involved in nitrogen metabolism, and the signal transduction protein P_{II}, which controls a high variety cellular processes by direct protein-protein interaction. Both, NtcA and P_{II}, can bind 2-OG and thereby modulate their regulatory functions [49-51], as further described in chapter 3.4 and 3.4.2, respectively.

Another example of a 2-OG dependent regulation is the carbohydrate phosphotransferase system (PTS) in *E.coli*. The PTS is responsible for phosphorylation and subsequent uptake of several sugars [52]. The first protein of the phosphorylation cascade, called enzyme I (EI), is regulated by the 2-OG / phosphoenolpyruvate ratio [53]. Furthermore, the PTS has regulatory influence to the activity of the adenylate cyclase (AC) [54]. The AC is responsible for cyclic AMP (cAMP) formation, which acts as coactivator of the important global transcription factor CRP (cAMP receptor protein). Together, cAMP and CRP regulate the expression of many catabolic enzymes, as part of a process called carbon catabolite repression (CCR) [55, 56]. Due to its involvement in PTS regulation, 2-OG is also indirectly involved in CCR regulation. Overall, 2-OG is involved in manifold cellular regulatory circuits and has been proposed to be a "master regulatory metabolite" in many organisms (for further review see [57]).

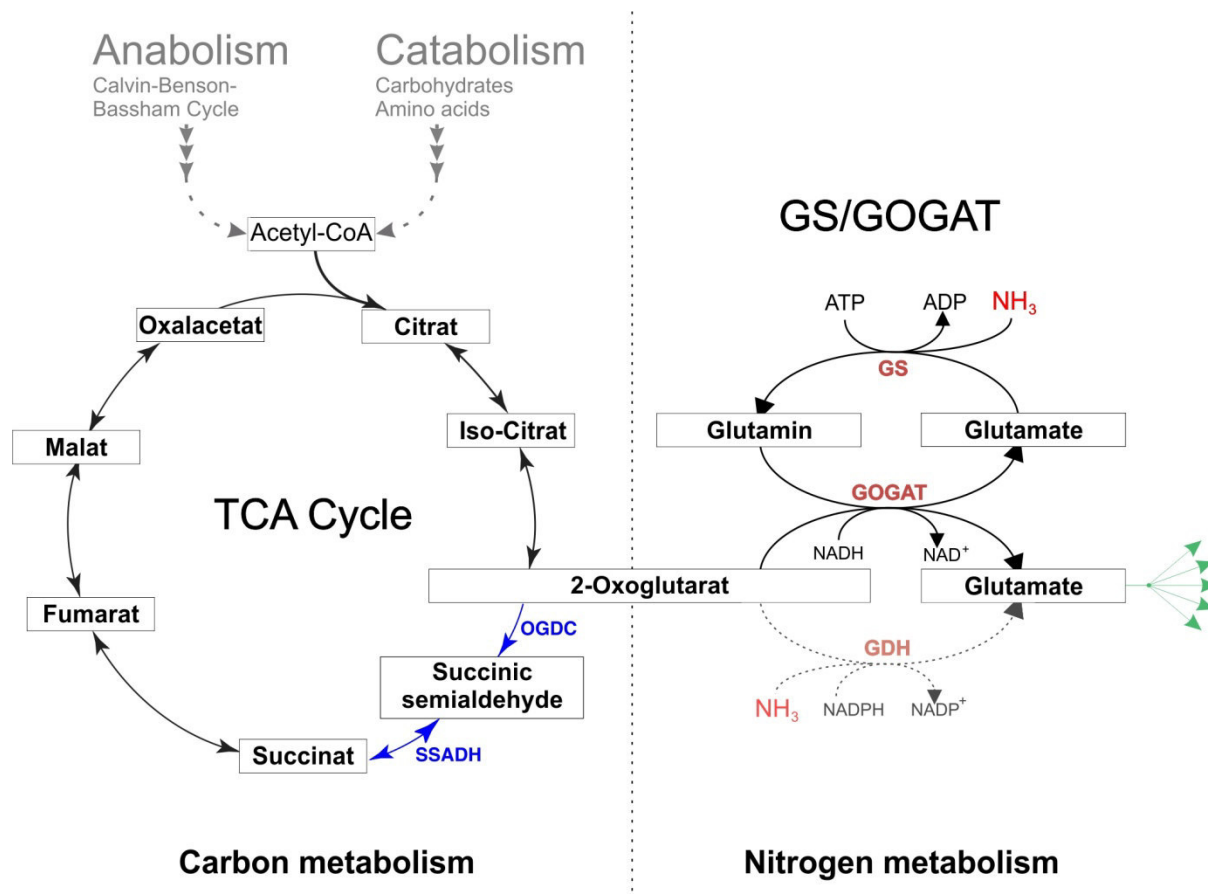


Figure 1 Connection of the carbon and nitrogen metabolism by 2-OG in cyanobacteria. Carbon derived from catabolic reactions like degradation of proteins, fats or polysaccharides and fixed carbon from the Calvin-Benson-Bassham cycle flow into the TCA cycle (left). Cyanobacteria possess an alternative TCA cycles (shown in blue) characterized by the presence of two other enzymes. Here, 2-OG is converted to succinic semialdehyde by the 2-OG decarboxylase (OGDC) and is subsequently oxidized to succinate by the succinic semialdehyde dehydrogenase (SSADH). The 2-OG acts a carbon skeleton for nitrogen assimilation by the GS/GOGAT cycle (right) and thereby connects both pathways. The GOGAT converts one molecule of each, 2-OG and glutamine, into two molecules of glutamate. The GS catalyzes the ATP-dependent amidation of glutamate to glutamine and thereby assimilates ammonium. The green arrows indicate the release of glutamate into the metabolism as precursor of various biosynthetic processes. Abbreviations: OGDC: 2-OG decarboxylase; SSADH: succinic semialdehyde dehydrogenase; GS: glutamine synthetase; GOGAT: glutamine 2-oxoglutarate aminotransferase; GDH: glutamate dehydrogenase.

3.2 Nitrogen starvation response

Nitrogen is an essential macronutrient for all living organisms and therefore constitutes an important growth limiting factor in many natural habitats [58]. Cyanobacteria can utilize several organic and inorganic nitrogen sources, including ammonium, nitrate, nitrite, dinitrogen, urea and several amino acids. These nitrogen sources are utilized in a hierarchical order, in which ammonia represents the preferred nitrogen sources [2, 59, 60]. In absence of a suitable nitrogen source these cyanobacteria face nitrogen starvation; a situation which results in the repression of anabolic metabolism and finally leads to dormancy [61]. This process of nitrogen starvation is called chlorosis, which describes the color change from a typical blue-green to yellow; comparable to the color change of trees in autumn.

During the process of nitrogen starvation, genes involved in transcription, translation and biosynthetic processes are down-regulated [62]. Due to an elevated intracellular 2-OG concentration, the NtcA regulon is activated, which influences a large number of nitrogen starvation associated genes, including nitrogen uptake and assimilation involved genes [63]. The phycobilisomes are proteinaceous light harvesting complexes, which can constitute up to 50 % of the total soluble protein mass of a vegetative cell [64]. The degradation of phycobilisomes leads to the noticeable color change from blue-green to yellow and frees a large pool of nitrogen to maintain essential cellular functions. The Clp protease-associated adaptor polypeptide NblA plays an essential role in phycobilisome degradation [65]. The expression of *nblA* triggers the phycobilisome degradation and is therefore tightly regulated by NtcA and the Nbl-System, involving the two-component system NblS/ RpaB and the one-component system NblR [66-70]. While the phycobilisomes are degraded, the cells commit a last division and start to accumulate carbon storage biopolymers, like glycogen or PHB [25, 71]. When the nitrogen starvation is prolonged, the cells start the degradation of photosystem I and the associated chlorophyll *a* [72]. As shown for *Synechococcus elongatus*, the cells degrade the majority of their cellular proteins as well as their thylakoid membranes until they reach the final chlorotic stage, with a residual photosynthetic activity of ~0.1 % of the initial capacity [73, 74]. These non-pigmented and dormant cells are able to survive long periods of starvation and they are still able to return to their vegetative cell cycle after the addition of a suitable nitrogen source [25, 74].

3.3 Resuscitation from nitrogen starvation

Recently, the process of resuscitation from nitrogen starvation was comprehensively investigated in the unicellular cyanobacterium *Synechocystis* sp. PCC 6803 [25]. The addition of a suitable nitrogen source to nitrogen-starved chlorotic cyanobacteria initiates a genetically determined program, in which the cells resuscitate their pigmentation and return

to vegetative growth. The re-greening of fully chlorotic cells, with a complete restoring of the vegetative cell cycle, takes 48 h and can be divided into two phases. In the first phase the cells respire to gain energy. The carbon storage polymer glycogen has been identified as main source of energy and carbon during this process, while PHB plays a minor role [25, 26]. According to a transcriptome study in this early stage of resuscitation, the cells re-install their translational machinery to enable *de novo* protein synthesis [25]. In the second phase of resuscitation, around 12-16 h after the addition of nitrogen, the cells start to reassemble their photosynthetic apparatus and re-green. In this phase the cells switch from oxygen consumption to oxygen production. After 48 h, the cells regain full photosynthetic capacity and enter the vegetative cell cycle [25].

3.4 P_{II} signal transduction protein¹

P_{II} signal transduction proteins are widely spread in all domains of life, where they represent one of the largest and most ancient family of signaling proteins. P_{II} proteins are involved in the regulation of various carbon and nitrogen metabolism related processes [43, 49, 75].

P_{II} proteins can be classified in three groups based in their sequence and phylogeny: GlnB, GlnK and NifI [76]. GlnB can be predominantly found in proteobacteria, cyanobacteria and plants. Homologues of *glnB* are often genetically organized in an operon together with *glnA* (glutamine synthetase I) or *nadE* (a gene encoding ammonia-dependent NAD synthetase). GlnK homologues are more widely distributed and often genetically associated with the ammonium channel AmtB. NifI proteins are associated with the nitrogen fixing genes (*nif*-cluster) and can be found in nitrogen fixing archaea and anaerobic bacteria [76].

P_{II} proteins are highly conserved homo-trimeric proteins with three characteristic loop regions. These loop regions, called B-, C- and T-loops are located near the inter-subunit clefts and play a major role in ligand binding and protein-protein interactions [49, 50, 75, 77-81]. Canonical P_{II} proteins sense the energy status of the cell by binding ATP or ADP in a competitive way [77]. Binding of ATP and synergistic binding of 2-OG allows P_{II} to sense the current carbon/nitrogen status of the cell [50]. Besides metabolite binding, post translational modifications represent a second level of regulation. Depending on the nitrogen supply, the cyanobacterial P_{II} can be phosphorylated at the apex of the T-loop at position Ser49 [82, 83]. In other prokaryotes, like *E.coli*, P_{II} is uridylylated, instead of phosphorylated, at Tyr51 in dependence of nitrogen availability [84]. Furthermore, in *Actinobacteria* adenylation of Tyr51 has been reported [85].

¹ Paragraph adapted from Watzer, B. & Forchhammer, K. (2018) Cyanophycin, a nitrogen-rich reserve polymer. *Cyanobacteria*, ISBN: 978-953-51-6243-8

P_{II} acts as a central information processing unit: binding of metabolites as well as post translational modifications enable P_{II} to integrate different signals. Based on these inputs, P_{II} triggers a specific output signal by interacting with other proteins. Binding of the effector molecules ATP, ADP and 2-OG as well as post translational modifications lead to a conformational rearrangement of the large surface-exposed T-loop, P_{II} 's major protein-interaction structure [86]. These conformational states direct the interaction of P_{II} with its various interaction partners and thereby regulate the cellular carbon/nitrogen balance [75].

In cyanobacteria, P_{II} regulates the global nitrogen control transcription factor NtcA, through binding to the NtcA co-activator PipX [87]. In common with other bacteria, the cyanobacterial P_{II} protein can interact with the biotin carboxyl carrier protein (BCCP) of acetyl-CoA carboxylase (ACC) and thereby control the acetyl-CoA levels [88]. Plant and cyanobacterial P_{II} proteins control arginine biosynthesis by regulating NAGK [89-91]. Furthermore, P_{II} is involved in nitrate assimilation, since a P_{II} deficient mutant shows ammonium-insensitive nitrate utilization [92]. The following sections provide a selection of some well-studied P_{II} interactions.

3.4.1 NtcA coactivator PipX

NtcA is a homodimeric DNA-binding protein that belongs to the CRP family (cAMP receptor protein) of bacterial transcription factors [63]. NtcA is responsible for activation or repression of several genes involved in nitrogen metabolism, in dependence of nitrogen availability (for review [93]). PipX, a protein uniquely found in cyanobacteria, can interact with both, P_{II} and NtcA, acting as a co-activator of the latter [87].

In case of nitrogen excess conditions, indicated by a low 2-OG level, the sequestration of PipX by P_{II} leads to a decreased NtcA-PipX complex formation [94, 95]. Crystal structures of the P_{II} -PipX complex show that one P_{II} trimer binds three PipX monomers at the base of the T-loop [81]. The interaction of P_{II} and PipX is highly sensitive to the ATP/ADP ratio. Complex formation with PipX increases the affinity of P_{II} for ADP [77]. ADP stabilizes the P_{II} -PipX complex, while the addition of ATP and 2-OG leads to its dissociation [95, 96]. P_{II} -PipX complex formation is impaired under low nitrogen availability, due to the elevated presence of ATP and 2-OG [95]. In consequence, free PipX can bind and activate NtcA, which leads to an activation of the NtcA regulon [95] (Figure 2)

The 2-OG mediated partner switch of PipX provides the link between P_{II} signaling and the NtcA dependent gene expression [94]. *In vivo*, PipX interaction with NtcA is required for NtcA mediated gene expression under nitrogen limiting conditions [87, 94, 97].

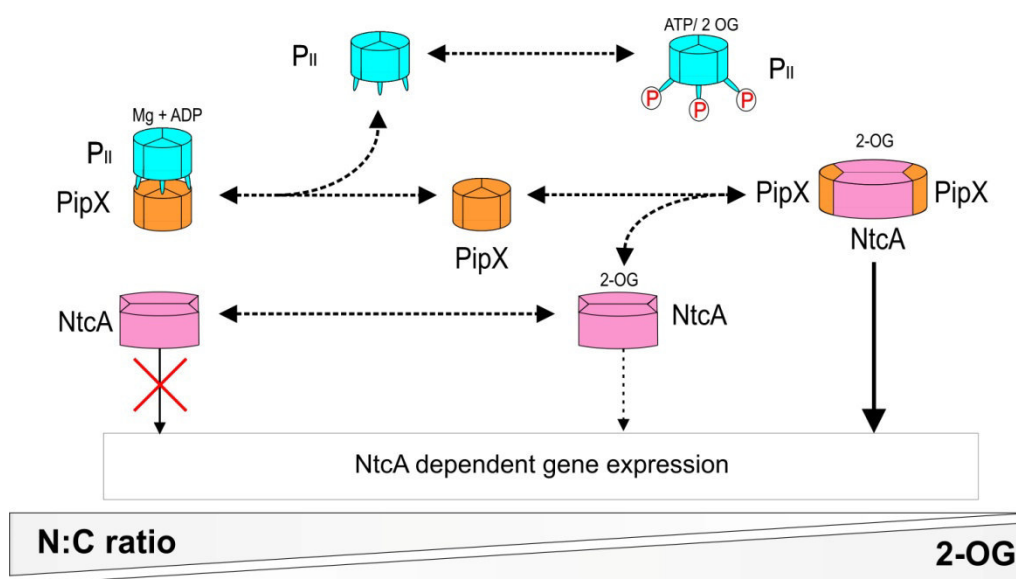


Figure 2 Nitrogen depending regulatory network of P_{II}, PipX and NtcA. Under nitrogen excess conditions, indicated by a low 2-OG level, no NtcA mediated gene expression occurs due to the strong sequestration of PipX by P_{II}. Rising 2-OG concentrations trigger the dissociation of the P_{II}-PipX complex. In consequence free PipX can bind and activate NtcA, which leads to an activation of the NtcA regulon under nitrogen depletion. Simultaneously, P_{II} becomes phosphorylated due to the low nitrogen availability.

3.4.2 N-acetylglutamate kinase¹

Bacteria produce arginine from glutamate in eight steps. The first five steps involving N-acetylated intermediates lead to ornithine. The conversion of ornithine to arginine requires three additional steps [98]. The second enzyme of ornithine biosynthesis is the N-acetylglutamate kinase (NAGK), which catalyses the phosphorylation of N-acetyl glutamate to N-acetylglutamyl-phosphate. This is the controlling step in arginine biosynthesis [99], since NAGK activity is subjected to allosteric feedback-inhibition by arginine and is, moreover, positively controlled by the P_{II} signal transduction protein [91, 99].

If sufficient energy and nitrogen is available, indicated by a high ATP and low 2-OG level, non-phosphorylated P_{II} forms an activating complex with NAGK. The P_{II}-NAGK complex consists of two P_{II} trimers and one NAGK homohexamer (trimer of dimers) [80]. Each P_{II} subunit contacts one NAGK subunit [80]. Two parts of P_{II} are involved in the interaction with NAGK. The first structure, called B-loop, is located on the P_{II} body and interacts with the C-domain of a NAGK subunit, involving residue Glu85. The interaction of the B-loop is the

¹ Paragraph adapted from Watzler, B. & Forchhammer, K. (2018) Cyanophycin, a nitrogen-rich reserve polymer. *Cyanobacteria*, ISBN: 978-953-51-6243-8

first step in complex formation. Second, the T-loop must adopt a bent conformation and insert into the interdomain cleft of NAGK [100]. This enhances the catalytic efficiency of NAGK, with the V_{max} increasing 4-fold and the K_m for N-acetylglutamate decreasing by a factor of 10 [89]. Furthermore, feedback inhibition of NAGK by arginine is strongly decreased in presence of P_{II} [89]. During mutational analysis of the P_{II} protein, a variant was identified that binds constitutively NAGK *in vitro*. This P_{II} variant exhibits a single amino acid replacement, Ile86 to Asn86, hereafter referred as $P_{II}(I86N)$ [100]. The crystal structure of $P_{II}(I86N)$ has been solved, showing an almost identical backbone than wild-type P_{II} . However, the T-loop adopts a compact conformation, which is a structural mimic of P_{II} in the NAGK complex [100, 101]. Addition of 2-OG in presence of ATP normally leads to a dissociation of the P_{II} -NAGK complex, however $P_{II}(I86N)$ no longer responds to 2-OG [101].

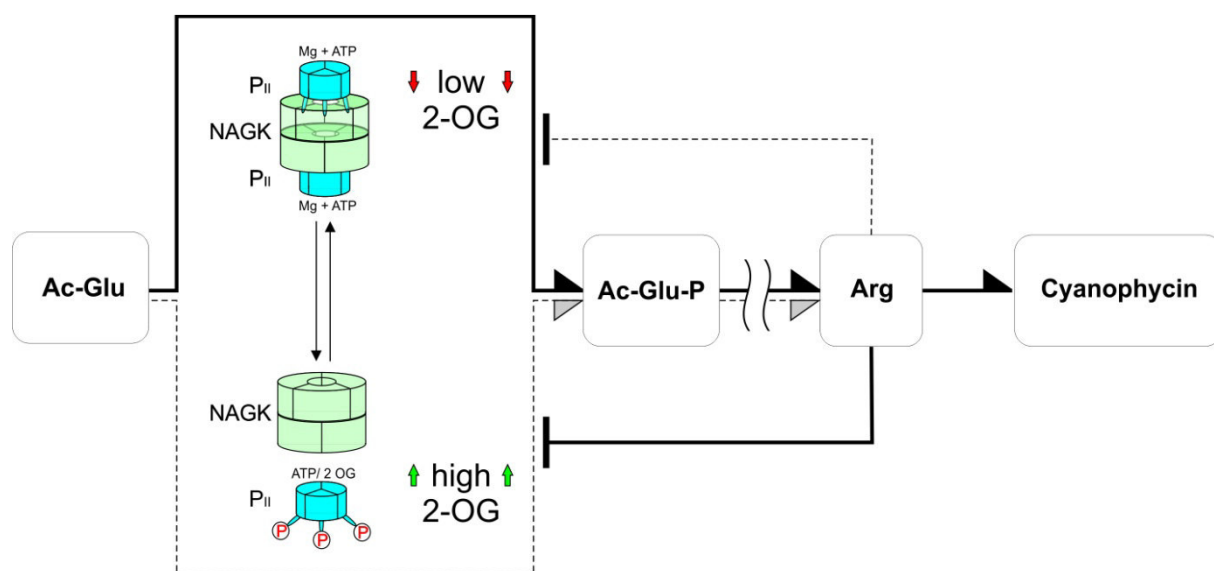


Figure 3 Regulation of the arginine and cyanophycin biosynthesis by P_{II} . The conversion of N-acetylglutamate (Ac-Glu) to N-acetylglutamyl-phosphate (Ac-Glu-P) is the rate-limiting step in the arginine (Arg) synthesis catalyzed by NAGK. NAGK activity is controlled by complex formation with P_{II} . If sufficient energy and nitrogen is available, indicated by a high ATP and low 2-OG level, non-phosphorylated P_{II} forms an activating complex with NAGK. Increasing 2-OG levels in presence of ATP lead to a dissociation of the complex. Unbound NAGK has low activity (dashed line) and is highly susceptible to arginine feedback inhibition, whereas NAGK bound to P_{II} has high activity (solid black line) and is much less sensitive towards arginine feedback inhibition. When excess arginine (Arg) is produced cyanophycin is synthesized. Abbreviations: Ac-Glu: N-acetylglutamate; Ac-Glu-P: N-acetylglutamyl-phosphate; Arg: arginine.

3.4.3 Ammonium Channel AmtB

The ammonium transporter family (Amt) is ubiquitous among all domains of life [102]. The AmtB protein from *E.coli* has become the paradigm for studies on the biology of Amt-proteins [103]. AmtB forms a homotrimer located in the cytoplasmic membrane. Each monomer of the trimeric AmtB forms a mainly hydrophobic and ~ 20 Å long pore, which enables bidirectional flux of ammonia [104-106]. The *E.coli* P_{II} homolog GlnK regulates AmtB by direct protein-protein interaction to prevent uncontrolled influx of ammonia. When the cells experience an ammonia excess, the intracellular 2-OG level decreases rapidly and GlnK become deuridylyated. In its ADP bound and deuridylyated state GlnK can block the ammonia influx by inserting the tip of its large surface exposed T-loops into the cytoplasmic exits of the pores [103]. AmtB-GlnK complex responds to the ATP/ADP ratio. While ADP stabilizes the complex, ATP and synergistically bound 2-OG promote its dissociation in response to nitrogen limitation [107-109]. The subsequent complete uridylylation of GlnK under nitrogen depletion prevents the re-association with AmtB [109]. Also, partially uridylylated P_{II} trimers can interact with AmtB in the presence of ADP. It was suggested that fluctuating environmental ammonia concentrations lead to partially uridylylated P_{II} trimers. Such forms of P_{II} can bind to AmtB and can probably allow partial AmtB activity, while fully uridylylated P_{II} is unable to bind AmtB. The physiological significance of this behavior is fine tuning of AmtB activity under fluctuating environmental ammonia availability [109].

4. Cyanophycin a carbon/nitrogen storage polymer¹

Cyanophycin, is in addition to poly- γ -glutamic acid and poly- ϵ -lysine the third polyamino acid known to occur in nature [110]. It serves as a nitrogen/carbon reserve polymer in many cyanobacterial strains as well as in a few heterotrophic bacteria. Cyanophycin consists of the two amino acids aspartate and arginine, forming a poly-L-aspartic acid backbone with arginine side chains. The arginine residues are linked to the β -carboxyl group of every aspartyl moiety via isopeptide bond [111].

Cyanophycin was discovered in 1887 by the botanist Antonio Borzi during microscopic studies of filamentous cyanobacteria [112]. He observed opaque and light scattering inclusions by using light microscopy and created the name *cianoficina*. Early electron microscopic studies showed a strong structure variation of the cyanophycin granules, depending on the fixatives and poststains used during electron microscopic examinations [113, 114]. This led to a controversy about the ultra structure of these inclusions until the

¹ Paragraph adapted from Watzler, B. & Forchhammer, K. (2018) Cyanophycin, a nitrogen-rich reserve polymer. *Cyanobacteria*, ISBN: 978-953-51-6243-8

70ies. Later electron microscopic studies described cyanophycin granules as membrane less, electron dense and highly structured cytoplasmic inclusions [115, 116].

With a carbon/nitrogen ratio of 2:1, cyanophycin is extremely rich in nitrogen and consequently an excellent nitrogen storage compound. During the degradation of cyanophycin and subsequent degradation of arginine, a function as energy source was also proposed [117].

4.1 Natural occurrence of cyanophycin¹

Most cyanobacteria, including unicellular and filamentous, as well as diazotrophic and non-diazotrophic groups are able to accumulate cyanophycin. In non-diazotrophic cyanobacteria, the amount of cyanophycin is usually less than 1 % of the cell dry mass during exponential growth. Cyanophycin accumulates conspicuously under unbalanced growth conditions including stationary phase, light stress or nutrient limitation (sulfate, phosphate or potassium starvation) that do not involve nitrogen starvation [118, 119]. Under such unbalanced conditions the amount of cyanophycin may increase up to 18 % of the cell dry mass [119]. During the recovery from nitrogen starvation by the addition of a usable nitrogen source, cyanophycin is transiently accumulated [25, 120].

In the unicellular diazotrophic cyanobacterium *Cyanothece* sp. ATCC 51142 nitrogen fixation and photosynthesis can coexist in the same cell, but are temporarily separated. The nitrogen-fixing enzyme, nitrogenase, is highly sensitive to oxygen. Nitrogen fixation occurs in dark periods and the fixed nitrogen is stored in cyanophycin. In the light period, when photosynthesis is performed, the cyanophycin is degraded to mobilize the fixed nitrogen [121]. Transient cyanophycin accumulation during dark periods was also reported in the filamentous cyanobacterium *Trichodesmium* sp., which has a high abundance in tropical and subtropical seas and is an important contributor to global N and C cycling [122].

Furthermore, in heterocysts of diazotrophic cyanobacteria of the order *Nostocales*, polar nodules consisting of cyanophycin are deposited at the contact site to adjacent vegetative cells [123]. The heterocystous cyanophycin seems to be involved in transport of fixed nitrogen to the adjacent photosynthetically active vegetative cell. Cyanophycin catabolic enzymes are present at significantly higher levels in vegetative cells than in heterocysts. Moreover, cyanophycin could serve as a sink for fixed nitrogen in the heterocyst to avoid feedback inhibition from soluble products of nitrogen fixation [124, 125]. In *Anabaena* sp. PCC 7120 and *Anabaena variabilis*, mutational studies have shown that strains lacking

¹ Paragraph adapted from Watzler, B. & Forchhammer, K. (2018) Cyanophycin, a nitrogen-rich reserve polymer. *Cyanobacteria*, ISBN: 978-953-51-6243-8

cyanophycin synthetic genes are little affected in diazotrophic growth under standard laboratory conditions [123, 126]. However, a growth defect was observed under high light conditions [123]. Moreover, diazotrophic growth is significantly decreased in strains which are unable to degrade cyanophycin [124, 126].

Akinetes are resting spore-like cells of a subgroup of heterocyst-forming cyanobacteria for surviving long periods of unfavorable conditions. During akinete development, the cells transiently accumulate storage compounds, namely glycogen, lipid droplets and cyanophycin [127, 128]. Cyanophycin granules also appear during germination of dormant akinetes [129]. *Anabaena variabilis* akinetes lacking cyanophycin granules were also able to germinate. This behavior agrees with early observations that cyanophycin is not the direct nitrogen source for protein biosynthesis and therefore not essential for akinete germination [129, 130].

Cyanophycin was previously thought to be unique in cyanobacteria. In 2002 Krehenbrink *et al.* and Ziegler *et al.* discovered through evaluation of obligate heterotrophic bacteria genomes, that many heterotrophic bacteria possess cyanophycin synthetase genes [131, 132]. Genes of cyanophycin metabolism occur in a wide range of different phylogenetic taxa, and not closely related to cyanobacteria [133].

4.2 Biochemical characteristics of Cyanophycin¹

In 1971, Robert Simon isolated cyanophycin granules for the first time, by using differential centrifugation. Along with this study, cyanophycin has shown its special and unique solubility behavior [134]. Cyanophycin is insoluble at physiological ionic strength and at neutral pH, but soluble in solutions which are acidic, basic or highly ionic. In non-ionic detergent such as Triton X-100, cyanophycin is insoluble, however in ionic detergents like SDS it is soluble [115]. Present-day cyanophycin extraction methods are based on its solubility at low pH and insolubility at neutral pH [135]. The chemical structure of cyanophycin was proposed in 1976 by Simon and Weathers [111]. According to this model, cyanophycin has a polymer backbone consisting of α -linked aspartic acid residues. The α -amino group of arginine is linked via isopeptide-bonds to the β -carboxylic group of every aspartyl moiety. Because every aspartate residue is linked to an arginine residue, cyanophycin contains equimolar amounts of aspartate and arginine [111]. This structure has been confirmed via enzymatic degradation studies. Cyanophycin degrading enzymes (see below) release β -Asp-Arg dipeptides [136]. CD spectroscopy data suggest that the acid-

¹ Paragraph adapted from Watzer, B. & Forchhammer, K. (2018) Cyanophycin, a nitrogen-rich reserve polymer. *Cyanobacteria*, ISBN: 978-953-51-6243-8

soluble and neutral insoluble form of cyanophycin have similar conformations. Both forms contain substantial fractions of β -pleated sheet structure [137].

Cyanobacterial cyanophycin has a molecular weight and polydispersity ranging from 25 to 100 kDa [134]. In contrast, the native cyanophycin producer *Acinetobacter* sp. ADP1 synthesizes cyanophycin with a lower molecular weight ranging from 21 to 28 kDa [138]. Recombinant bacteria or genetically engineered yeast harboring heterologous expression of cyanobacterial cyanophycin synthesis genes, also show a lower molecular weight of 25–45 kDa [135, 139]. From transgenic plant-produced cyanophycin also shows a reduced polydispersity between 20 and 35 kDa [140]. A possible explanation would be that cyanophycin synthesis in the native cyanobacterial background involves additional factors contributing the polymer length. These additional factors should be also absent in *Acinetobacter* sp. ADP1.

Native cyanophycin is exclusively composed of aspartate and arginine. By contrast, in cyanophycin isolated from recombinant *E. coli* expressing cyanophycin synthetase (see below) from *Synechocystis* sp. PCC 6803, besides aspartate and arginine, lysine has been found [141]. The amount of incorporated lysine in cyanophycin influences its solubility behavior. Recombinant cyanophycin with a high lysine amount (higher than 31 mol%) is soluble at neutral pH [142].

4.3 Cyanophycin metabolism¹

4.3.1 Cyanophycin Synthetase¹

Cyanophycin is nonribosomally synthesized from aspartate and arginine by cyanophycin synthetase (CphA1) (Figure 4). In 1976, CphA1 was enriched and characterized for the first time by Simion [143]. The enzyme incorporates aspartate and arginine in an elongation reaction, which requires ATP, KCl, MgCl₂ and a sulfdryl reagent (β -mercaptoethanol or DTT). For its activity, CphA1 needs a so far unknown cyanophycin primer, as a starting point of the elongation reaction [143]. By using synthetic primers, Berg *et al.* could show that a single building block of cyanophycin (β -Asp-Arg) does not serve as an efficient primer for CphA1 elongation reaction *in vitro*. The primers need to consist of at least three Asp-Arg building blocks (β -Asp-Arg)₃ to detect CphA1 activity [144]. Other peptides, like cell wall peptides, have been suggested to serve as an alternative priming substance for the CphA1 reaction [145]. This could be an explanation for the functionality of cyanophycin synthesis in recombinant bacteria, without the ability to produce native cyanophycin primers [146].

¹ Paragraph adapted from Watzer, B. & Forchhammer, K. (2018) Cyanophycin, a nitrogen-rich reserve polymer. *Cyanobacteria*, ISBN: 978-953-51-6243-8

Interestingly, the CphA1 of *Thermosynechococcus elongates* strain BP-1 shows primer-independent cyanophycin synthesis [147].

Today, CphA1 enzymes from several bacteria including cyanobacteria and heterotrophic bacteria have been purified and characterized [141, 147-150]. The molecular mass of the characterized CphA1 enzymes ranges from 90 to 130 kDa. The active form of CphA1s from *Synechocystis* sp. PCC6308 and *Anabaena variabilis* PCC7937 is most likely homodimeric [141, 149], while the primer-independent CphA1 from *Thermosynechococcus elongates* strain BP-1 forms a homotetramer [147]. The primary structure of cyanobacterial CphA1 can be divided into two regions [141]. The C-terminal region shows sequence similarities to peptide ligases that include murein ligases and folyl poly- γ -glutamate ligase. The N-terminal part of CphA1 shows sequence similarities with another superfamily of ATP-dependent ligases that includes carboxylate-thiol and carboxylate-amine ligase. Since the C- and N-terminal part show similarity to different superfamilies of ATP-dependent ligases, two ATP-binding sites and two different active sites have been predicted [144]. *In vitro* experiments revealed that arginine is probably bound in the C-terminal and aspartate in the N-terminal active site [151].

The mechanism of cyanophycin synthesis by CphA1 has been suggested by Berg *et al.* in 2000, by measuring the step-wise incorporation of amino acids to the C-terminus of the CGP primer. The putative cyanophycin elongation cycle starts at the C-terminal end of the poly-aspartate backbone. First, the carboxylic acid group of the poly-aspartate backbone is activated by transfer of the γ -phosphoryl group of ATP. In the second step, one aspartate is bound at the C-terminus of the growing polymer by its amino group, forming a peptide bound. Subsequently, the intermediate (β -Asp-Arg)_n-Asp is transferred to the second active site of CphA1 and phosphorylated at the β -carboxyl group of the aspartate. Finally, the α -group of arginine is linked to the β -carboxyl group of aspartate, forming an isopeptide bound [144].

Various CphA1 enzymes have been characterized with respect to their substrate affinity and specificity. For CphA1 of *Synechocystis* sp. PCC 6308, apparent K_m values were determined to be 450 μ M for aspartate, 49 μ M for arginine, 200 μ M for ATP and 35 μ g/ml for cyanophycin as priming substance. The lower K_m of arginine compared to aspartate indicates a higher affinity of CphA1 towards arginine. During the *in vitro* reaction, CphA1 converts per mol incorporated amino acid 1.3 \pm 0.1 mol ATP to ADP. The optimal reaction conditions of this enzyme were at pH 8.2 and 50°C [149, 152].

CphA homologues are widely distributed in eubacteria. *In silico* analysis proposes ten different groups of cyanophycin synthetases [133]. In cyanobacteria cyanophycin synthetases of group I - III (CphA, CphA2 and CphA2') can be found.

Recently, the function of a cyanophycin synthetase of group II (CphA2) has been characterized. Most non-diazotrophic cyanobacteria use a single type of cyanophycin synthetase (CphA1). However, in many nitrogen-fixing cyanobacteria, an additional version of CphA1 is present, termed CphA2. In 2016, Klemke *et al.* resolved the function of CphA2 [153]. Compared to CphA1, CphA2 has a reduced size and just one ATP-binding site. CphA2 uses the product of cyanophycin hydrolysis, β -aspartyl-arginine dipeptide as substrate to re-synthesize cyanophycin, consuming one molecule of ATP per elongation reaction. A mutant lacking CphA2 shows only a minor decrease in the overall cyanophycin content. However, a CphA2-deficient mutant displays similar defects under diazotrophic and high light conditions than a CphA1 mutant [123, 153]. This observation suggests that the apparent "futile cycle" of cyanophycin hydrolysis and immediate re-polymerization is probably of physiological significance in the context of nitrogen-fixation [125].

4.3.2 Cyanophycinase¹

Since 1976 it is known that cyanophycin is resistant against hydrolytic cleavage by several proteases or arginase [111, 154]. This resistance is probably due to the branched structure of cyanophycin [146]. Therefore, the presence of a highly specified peptidase for cyanophycin hydrolysis was suggested.

In 1999, Richter *et al.* reported a cyanophycin hydrolyzing enzyme from the unicellular cyanobacterium *Synechocystis* sp. PCC 6803, called CphB [136] (Figure 4). During this study, CphB was purified and studied in detail. CphB is a 29.4 kDa C-terminal exopeptidase, catalyzing the hydrolysis of cyanophycin to β -Asp-Arg dipeptides [136]. Based on sequence analysis and inhibitor sensitivity to serine protease inhibitors, CphB appears to be a serine-type exopeptidase related to dipeptidase E (PepE) [136]. According to its sequence, CphB contains a serine residue within a lipase box motive (Gly-Xaa-Ser-Xaa-Gly). The serine residue together with a glutamic acid residue and a histidine residue forms the catalytic triad, which is typical for serine-type peptidases [136]. In 2009, the crystal structure has been solved at a resolution of 1.5 Å, showing that CphB forms a dimer. Site-directed mutagenesis confirms that CphB is a serine-type peptidase, consisting of a conserved pocket with the catalytic Ser at position 132 [155]. Structure modeling indicates that the cleavage specificity occurs due to an extended conformation in the active site pocket. The unique conformation

¹ Paragraph adapted from Watzer, B. & Forchhammer, K. (2018) Cyanophycin, a nitrogen-rich reserve polymer. *Cyanobacteria*, ISBN: 978-953-51-6243-8

of the active site pocket requires β -linked aspartyl peptides for binding and catalysis, preventing CphB from non-specific cleavage of other polypeptides next to cyanophycin [155].

Next to CphB, which catalyzes the intracellular cleavage of cyanophycin, other versions of cyanophycinases exist, catalyzing the extracellular hydrolysis of cyanophycin. In 2002, Obst *et al.* isolated several Gram-negative bacteria from different habitats, which were able to utilize cyanophycin as a source of carbon and energy [156, 157]. One isolate was affiliated as *Pseudomonas anguilliseptica* strain BI. In the supernatant of a *Pseudomonas anguilliseptica* culture, a cyanophycinase was found and purified, called CphE [156]. CphE exhibits a high specificity for cyanophycin; however proteins were not or only marginally hydrolyzed. Degradation products of CphE are β -Asp-Arg dipeptides. Inhibitor sensitivity studies indicated that the catalytic mechanism of CphE is related to serine-type proteases. CphE from *Pseudomonas anguilliseptica* strain BI exhibits an amino acid sequence identity 27-28% to intracellular CphB enzymes of cyanobacteria [156]. Today, extracellular cyanophycinases has been found in a high variety of bacteria including Gram-positive, Gram-negative, aerobic and anaerobic strains. This indicates that the extracellular cleavage and utilization of cyanophycin as carbon, nitrogen and energy source is a common principle in nature [156-162].

In 2007, *in silico* analysis have shown that CphB homologes are widely distributed in eubacteria, proposing eight different groups including intracellular and extracellular cyanophycinases. Cyanophycinases from cyanobacteria belong to group I, II and partially group III (CphB₁₋₃). Group IV - VIII, including CphE, are present in a large variety of non-photosynthetic bacteria [133].

4.3.3 Aspartyl-arginine dipeptidase¹

The last step in catabolism of cyanophycin is the cleavage of β -Asp-Arg dipeptides to monomeric amino acids arginine and aspartate (Figure 4). In 1999, Richter *et al.* found β -Asp-Arg dipeptides hydrolysing activity in extracts of *Synechocystis* sp. PCC 6803 [136]. In *Synechocystis* sp. PCC 6803, the ORF *sll0422* as well as ORF *all3922* from *Anabaena* sp. PCC 7120 are annotated as "plant-type asparaginase", because of sequence similarities to the first cloned asparaginase from plants [163]. During characterization of plant-type asparaginase in general, including *Sll0422* and *All3922*, Hejazi *et al.* were able to show that these enzymes are able to hydrolyse a wide range of isoaspartyl dipeptides [164]. Isoaspartyl peptides arise from two biological pathways: First, proteolytic degradation of modified proteins containing

¹ Paragraph adapted from Watzer, B. & Forchhammer, K. (2018) Cyanophycin, a nitrogen-rich reserve polymer. *Cyanobacteria*, ISBN: 978-953-51-6243-8

isoaspartyl residues and second, as primary degradation product of cyanophycin cleavage from cyanophycinases. Thus, the plant-type asparaginases Sll0422 and All3922 have not only a function in asparagine catabolism but also in the final step of cyanophycin and protein degradation [164].

The mature isoaspartyl dipeptidases of *Synechocystis* sp. PCC 6803 and *Anabaena* sp. PCC 7120 consist of two protein subunits that are generated by auto-cleavage of the primary translation product between Gly172 and Thr173 (numbering according to *Synechocystis* sp. PCC 6803) within the conserved consensus sequence GT(I/V)G [164]. The native molecular weight of approximately 70kD of this enzyme suggests that it has a subunit structure of $\alpha_2\beta_2$ (α derived from the N-terminal part and β form the C-terminal part of the precursor) [164].

In *Anabaena* sp. PCC 7120, all genes involved in cyanophycin metabolism as well as the isoaspartyl dipeptidases All3922 are expressed in vegetative cells and heterocysts but in different expression levels. Both, cyanophycin synthetases and cyanophycinases are much higher expressed in heterocysts than in vegetative cells [165]. However, asparaginase All3922 is present in significantly lower levels in heterocysts than in vegetative cells [124]. A deletion of All3922 in *Anabaena* sp. PCC 7120 causes an increased accumulation of cyanophycin and β -Asp-Arg dipeptides. Furthermore, a deletion mutant shows an impaired diazotrophic growth similar to the phenotype known from CphB deletion mutants in *Anabaena* sp. PCC 7120 [124, 126]. This observation implies that the first step of cyanophycin catabolism, the cleavage catalyzed by CphB, takes place in the heterocyst. The released β -Asp-Arg dipeptides are transported to the adjacent vegetative cells. Isoaspartyl dipeptidase All3922, present in the vegetative cells, cleaves the β -Asp-Arg dipeptides and release monomeric aspartate and arginine [124]. When cyanophycin synthesis is not possible, due to a deletion of CphA, arginine and aspartate might be transferred directly from heterocysts. This explains the minor effects on diazotrophic growth in a CphA deletion mutant [123]. These results identified β -Asp-Arg dipeptides as nitrogen vehicle in diazotrophic heterocyst forming cyanobacteria, next to glutamine and arginine alone or with aspartate [124, 166, 167]. A benefit of β -Asp-Arg dipeptides as nitrogen transport substance is avoiding the release of amino acids back in the heterocyst. This suggests that cyanophycin metabolism may have evolved in multicellular heterocyst-forming cyanobacteria to increase the efficiency of nitrogen fixation [124].

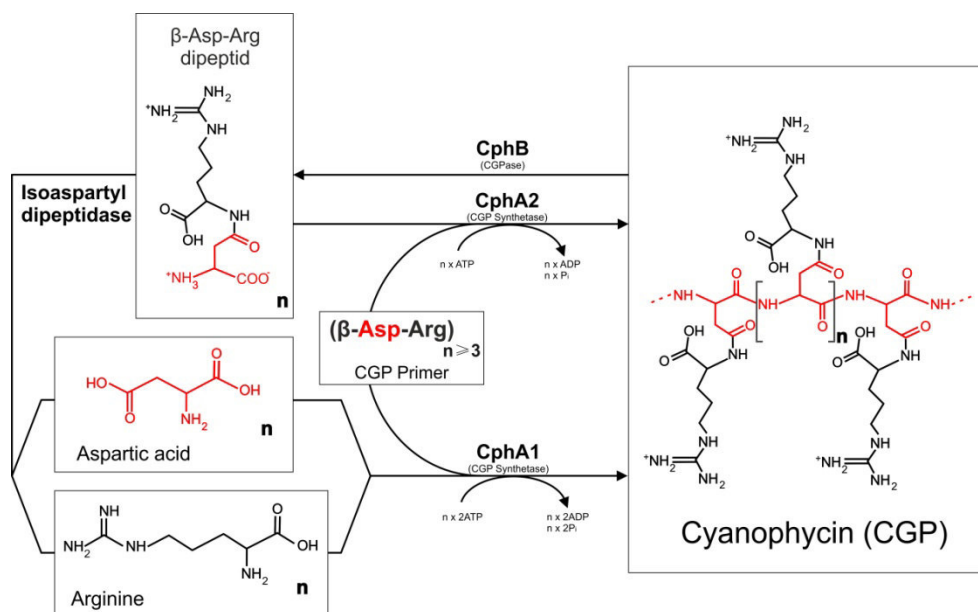


Figure 4 Schematic illustration of cyanophycin metabolism in cyanobacteria. Cyanophycin is synthesized from aspartate and arginine by cyanophycin synthetase (CphA1) in an ATP-dependent elongation reaction using cyanophycin primers, containing of at least three Asp-Arg building blocks. Intracellular cyanophycin degradation is catalyzed by the cyanophycinase (CphB). The β -Asp-Arg dipeptides resulting from cleavage of cyanophycin are further hydrolysed by isoaspartyl dipeptidase, releasing aspartate and arginine. In many nitrogen-fixing cyanobacteria, an additional cyanophycin synthetase is present, termed CphA2. CphA2 can use β -aspartyl-arginine dipeptides to re-synthesize cyanophycin. Figure adapted from publication 5 Watzer, B. & Forchhammer, K. (2018). Cyanophycin, a nitrogen-rich reserve polymer. *Cyanobacteria*, ISBN: 978-953-51-6243-8

4.4 Regulation of cyanophycin metabolism¹

4.4.1 Genetic organization of CphA and CphB¹

Usually, genes involved in cyanophycin metabolism are clustered. The organization of these clusters can be different, depending on the respective organism [133]. In *Synechocystis* sp. PCC 6803, *cphA* and *cphB* are adjacent, however there are expressed independently [168]. A hypothetical protein named *slr2003* is located downstream of *cphA* and is transcribed in a polycistronic unit with *cphA* [168]. However, the function of Slr2003 is unknown. In the gene of CphB (*slr2001*) a small antisense RNA was detected (transcriptional unit 1486) [168].

¹ Paragraph adapted from Watzer, B. & Forchhammer, K. (2018) Cyanophycin, a nitrogen-rich reserve polymer. *Cyanobacteria*, ISBN: 978-953-51-6243-8

In *Anabaena* sp. PCC 7120, two clusters containing CphA and CphB were identified [126]. In Cluster *cph1*, *cphB1* and *cphA1* were expressed under ammonia and nitrate supplemented growth, but the expression of both genes was higher in the absence of combined nitrogen in heterocysts and vegetative cells. In the *cph1* operon, *cphB1* and *cphA1* were co-transcribed. In addition, *cphA1* can be expressed from independent promoters, of which one is constitutive and the other regulated by the global nitrogen control transcriptional factor NtcA [126].

In cluster *cph2*, the *cphB2* and *cphA2* genes were found in opposite orientation and both genes were expressed monocistronically. The genes were expressed under conditions of ammonia, nitrate or N₂ supplementation, but the expression was higher in absence of ammonia. Generally the expression of the *cph2* is lower compared to *cph1* [126]. In addition to these two gene clusters, a third set of ORFs containing putative *cphA* and *cphB* genes were found in *Nostoc punctiforme* PCC 73102 and *Anabaena variabilis* ATCC 29413 [133].

4.4.2 Influence of arginine to the cyanophycin metabolism¹

Generally, cyanophycin accumulation is triggered by cell-growth arresting stress-conditions, such as entry into stationary phase, light or temperature stress, limitation of macronutrients (with the exception of nitrogen starvation) or inhibition of translation by adding antibiotics like chloramphenicol [118, 119, 169]. All of these cyanophycin triggering conditions result in a reduced or arrested growth. In exponential growth phase, the amino acids arginine and aspartate are mostly used for protein biosynthesis with the consequence of a low intracellular level of free amino acids. Under growth-limiting conditions, protein biosynthesis is slowed down, which yields an excess of monomeric amino acids in the cytoplasm, triggering the cyanophycin biosynthesis [119]. Cyanophycin accumulation also requires an excess of nitrogen. For the filamentous cyanobacterium *Calothrix* sp. strain PCC 7601, it was shown that cyanophycin accumulation occurs preferably in presence of ammonia [170]. The addition of amino acids to the media further increased cyanophycin formation [171]. During process optimization studies for heterotrophic cyanophycin production in the strain *Acinetobacter calcoaceticus* ADP1, it was shown that addition of arginine to the medium as sole carbon source increased cyanophycin accumulation drastically. When in *A. calcoaceticus* strain ADP1, cyanophycin synthesis is induced by phosphate starvation, it accounts to 3.5% (w/w) of the cell dry matter (CDM) with ammonia as nitrogen source. Additional supply of the medium with arginine increases the cyanophycin amount to 41.4% (w/w) (CDM). Notably, a combined supply of arginine and aspartate has a much lower stimulating effect to cyanophycin accumulation than arginine alone [138].

¹ Paragraph adapted from Watzer, B. & Forchhammer, K. (2018) Cyanophycin, a nitrogen-rich reserve polymer. *Cyanobacteria*, ISBN: 978-953-51-6243-8

A potential link between regulation of arginine biosynthesis and cyanophycin metabolism was suggested in many previous studies. In a transposon mutagenesis study in the filamentous cyanobacterium *Nostoc ellipsosporum*, an arginine biosynthesis gene, *argL*, was interrupted by a transposon. This mutation partially impairs arginine biosynthesis, but does not strictly result in L-arginine auxotrophy. Without arginine supplementation, heterocysts failed to fix nitrogen, akinetes were unable to germinate and cyanophycin granules did not appear. However, when both nitrate and arginine are present in the media, the impaired arginine biosynthesis is bypassed. Under this condition the mutant could form cyanophycin and was able to differentiate functional akinetes, which contained cyanophycin granules [172].

In metabolic engineering studies of the cyanophycin production strain *Acinetobacter calcoaceticus* ADP1, several genes related to the arginine biosyntheses or its regulation were modified to yield higher amounts of arginine. As a consequence, significant higher cyanophycin production was observed [173].

The nitrogen-regulated response regulator NrrA has also influence on arginine and cyanophycin biosynthesis. An NrrA-deficient mutant in *Synechocystis* sp. PCC 6803 shows reduced intracellular arginine levels and consequently, reduced cyanophycin amount [174].

Maheswaran *et al.* showed that arginine production and the following cyanophycin accumulation depend on the catalytic activation of NAGK by the signal transduction protein P_{II} [90]. In a P_{II}-deficient mutant of *Synechocystis* sp. PCC 6803, NAGK remained in a low activity state, which caused impaired cyanophycin accumulation [90].

All these results and observations point towards arginine as main bottleneck of cyanophycin biosynthesis, while aspartate plays a minor role. Cyanophycin accumulation occurs as a result of arginine enrichment in the cytoplasm. Reasons for increased arginine content in the cell are lowered protein biosynthesis as a result of various growth limiting conditions. Furthermore, an excess of nitrogen and energy, sensed by P_{II} leads to NAGK activation and thereby, increased arginine biosynthesis.

4.5 Industrial applications¹

Industrial applications for cyanophycin have previously mainly focused on chemical derivatives. Cyanophycin can be converted via hydrolytic β -cleavage to poly(α -L-aspartic acid) (PAA) and free arginine. PAA is biodegradable and has a high number of negatively charged carboxylic groups, making PAA to a possible substituent for polyacrylates [157, 159,

¹ Paragraph adapted from Watzer, B. & Forchhammer, K. (2018) Cyanophycin, a nitrogen-rich reserve polymer. *Cyanobacteria*, ISBN: 978-953-51-6243-8

175]. PAA can be employed as anti-scalant or dispersing ingredient in many fields of applications, including washing detergents or suntan lotions. Furthermore, PAA has potential application areas as an additive in paper, paint, building or oil industry [157, 159].

Cyanophycin can also serve as a source for dipeptides and amino acids in food, feed and pharmaceutical industry. The amino acids arginine (semi-essential), aspartate (non-essential) and lysine (essential) derived from cyanophycin have a broad spectrum of nutritional or therapeutic applications. Large scale production of these amino acids, as mixtures or dipeptides, is established in industry, with various commercial products already available on the market (reviewed by Sallam *et al.* 2010) [176].

Potential applications of non-modified cyanophycin have been discussed, but remain so-far largely unexplored. This can partially be explained by the lack of research being conducted on the material properties of cyanophycin. Recently in 2017, the first study regarding cyanophycin material properties has been published. In this study, Khlystov *et al.* focused on the structural, thermal, mechanical and solution properties of cyanophycin produced by recombinant *E. coli*, giving new insights in the nature of this polymer as bulk chemical [175]. They describe cyanophycin as an amorphous, glassy polyzwitterion with high thermo stability. The dry material is stiff and brittle. According to these properties cyanophycin could be used to synthesize zwitterionomeric copolymers or as reinforcing fillers [175].

4.6 Biotechnological production of cyanophycin¹

Previous ventures to produce cyanophycin in high amounts were mainly focused on heterotrophic bacteria, yeasts and plants as production host. These recombinant production hosts heterologously express cyanophycin synthetase genes, mostly from cyanobacteria. In this way, heterotrophic bacteria, which are established in biotechnological industry including *E. coli*, *Corynebacterium glutamicum*, *Cupriavidus necator* (previously known as *Ralstonia eutropha*) and *Pseudomonas putida*, were used for heterologous production of cyanophycin [177].

Strain *E. coli* DH1, containing *cphA* from *Synechocystis* sp. PCC6803, was used for large-scale production of cyanophycin in a culture volume of up to 500 liter, allowing the isolation of cyanophycin in a kilogram scale. During process optimization, the highest observed cyanophycin content was 24 % (w/w) per CDM. However, the synthesis of cyanophycin strongly depends on the presence of complex components in the medium (terrific broth complex medium). In mineral salt medium, cyanophycin accumulation only occurs in

¹ Paragraph adapted from Watzer, B. & Forchhammer, K. (2018) Cyanophycin, a nitrogen-rich reserve polymer. *Cyanobacteria*, ISBN: 978-953-51-6243-8

presence of casamino acids [135]. An engineered version of CphA from *Nostoc ellipsosporum*, transformed in *E.coli*, shows a further increase in cyanophycin production, up to 34.5 % (w/w) of CDM. However, this production strain also requires expensive complex growth media to yield such a high amount of cyanophycin [178].

Cupriavidus necator and *Pseudomonas putida* are known as model organisms for the industrial scale production of polyhydroxyalkanoates (PHA). Therefore, they have been considered as candidates for large scale cyanophycin production [177, 179]. Metabolic engineering and process optimization studies of *Cupriavidus necator* and *Pseudomonas putida* harboring *cphA* from *Synechocystis* sp. PCC 6803 or *Anabaena* sp. PCC 7120 were performed. Accumulation of cyanophycin depended on the source of the *cphA* gene, on the accumulation of other storage compounds like PHA as well as the addition of precursor components like arginine to the medium [180]. PHA-deficient mutants of *Cupriavidus necator* and *Pseudomonas putida* accumulate in general more cyanophycin compared to the PHA containing strains [180]. During genetic modification of *cphA* expression in *Cupriavidus necator*, cyanophycin accumulation turned out to be strongly affected by the expression system. A stabilized multi-copy *cphA* expression system, using the KDPG-aldolase gene (*eda*)-dependent addition system, allows cultivation without antibiotic selection. The multi-copy *cphA* expression results in a cyanophycin yield between 26.9 % and 40.0 % (w/w) of CDM. The maximum amount of 40.0% (w/w) of CDM was observed in a 30 and 500 liter pilot-plant. In the absence of the amino acids arginine and aspartic acid in the medium, the cyanophycin amount was still between 26.9% or 27.7% (w/w) of CDM [181].

The industrial established host *Saccharomyces cerevisiae* has also been used for cyanophycin production, by expression of *cphA* from *Synechocystis* sp. PCC 6803. *S. cerevisiae* harboring *cphA* accumulated up to 6.9% (w/w) of CDM. Two cyanophycin species were observed in this strain: water-soluble and the typical water-insoluble cyanophycin. Furthermore, the isolated polymer from this transgenic yeast contained 2 mol % lysine, which can be increased up to 10 mol % when the cultivation occurs with lysine in the medium [139]. During metabolic engineering studies, several arginine biosynthesis mutants have been analyzed concerning their cyanophycin accumulation abilities. Surprisingly, strains with defects in arginine degradation accumulated only 4 % cyanophycin (w/w) of CDM; however, arginine auxotrophic strains were able to accumulate up to 15.3 %. Depending on the cultivation conditions, between 30 and 90 % of the extracted cyanophycin was soluble at neutral pH. In addition to arginine, aspartate and lysine, further amino acids, like citrullin and ornithine have been detected in isolated cyanophycin from different arginine biosynthesis mutants

¹ Paragraph adapted from Watzer, B. & Forchhammer, K. (2018) Cyanophycin, a nitrogen-rich reserve polymer. *Cyanobacteria*, ISBN: 978-953-51-6243-8

[182]. Furthermore, it was also possible to produce cyanophycin and cyanophycin-derivates in *Pseudomonas putida* and the yeast *Pichia pastoris* [183, 184].

Cyanophycin and cyanophycin-derivates are important sources for β -dipeptides for several applications. A large-scale method was developed to convert cyanophycin into its constituting β -dipeptides by using CphE from *Pseudomonas alcaligenes*. This allows the large-scale production of customized β -dipeptides, depending on the composition of the cyanophycin-derivates [176, 185].

Production of cyanophycin has also been attempted in several transgenic plants. Here, ectopic expression of the primer-independent CphA from *Thermosynechococcus elongates* BP-1 leads to an accumulation of cyanophycin up to 6.8% (w/w) in tobacco leaves and to 7.5 % (w/w) of CDM in potato tubers [186, 187]. Cyanophycin production and extraction in plants can be coupled with the production of other plant products like starch [187]. The peculiarities and challenges of plant-produced cyanophycin have been reviewed by Nausch *et al.* [140].

5. Research objective

Previous research on cyanophycin mainly focused on its production by using heterologous expression systems with heterotrophic bacteria, genetically engineered yeast or plants harboring a cyanobacterial CphA gene [135, 139, 140, 179, 182]. However, future industry has to cope with manifold challenges to counteract environmental pollution and climate change. The use of cyanobacteria in biotechnological industry provides an environmentally friendly alternative to conventional approaches.

The present study aimed to explore the possibilities of a cyanobacterial cyanophycin producer strain. To realize this producer strain we used a novel metabolic engineering strategy by manipulating the P_{II} signaling protein. A P_{II} variant carrying a single point mutation (I86N) was previously shown to be a NAGK super activator *in vitro*. Since NAGK catalyzes the rate limiting step in the arginine biosynthesis, an over-activation leads to an increased production of arginine. Cyanophycin accumulation depends on the arginine availability. Therefore, a replacement of the native *glnB* gene by a modified *glnB* gene carrying the I86N mutation in the unicellular cyanobacterium *Synechocystis* sp. PCC 6803 leads to a strong cyanophycin production. To further increase the cyanophycin yield of the engineered producer strain, several process optimization studies have been performed. In order to gain new insights about the physiological impact of the P_{II}(I86N) variant, we investigated if the P_{II}(I86N) variant maintains the ability to interact with outer P_{II} interaction partners, namely PipX, Amt1, NrtABCD or UrtABCDE.

The presence of cyanophycin in cyanobacteria is known for more than 100 year. Previous research mainly focused on biotechnological purposes. However, the cell biology of cyanophycin remained largely uninvestigated. In order to gain new insights in the physiological role of cyanophycin we compared wild-type cells with cyanophycin deficient cells of *Synechocystis* sp. PCC 6803 under different conditions. To study the cellular localization of the cyanophycin-synthesizing enzyme CphA during cyanophycin synthesis and degradation, we fused it to green fluorescent protein and performed localization studies.

VI. Results

The main results of the following publications are summarized in section VI "Results". Section VI also provides non-published, additional results related to the publications.

- **Watzer, B.**, Engelbrecht, A., Hauf, W., Stahl, M., Maldener, I. & Forchhammer, K. (2015).
Metabolic pathway engineering using the central signal processor P_{II}.
Microbial cell factories, 14(1), 192.
- Trautmann, A., **Watzer, B.**, Wilde, A., Forchhammer, K. & Posten, C. (2016).
Effect of phosphate availability on cyanophycin accumulation in *Synechocystis* sp. PCC 6803 and the production strain BW86.
Algal research, 20, 189-196.
- **Watzer, B.** & Forchhammer, K. (2018).
Cyanophycin synthesis optimizes nitrogen utilization in the unicellular cyanobacterium *Synechocystis* sp. PCC 6803.
Applied and environmental microbiology, 84: e01298-18
- **Watzer, B.**, Spät, P., Neumann, N., Koch, M., Hennrich, O. & Forchhammer, K. (Preliminary manuscript from 07.12.2018).
The signal transduction protein P_{II} controls ammonium, nitrate and urea uptake in cyanobacteria
Final version of the manuscript was submitted to *Frontiers in Microbiology* (ISSN 1664302x) on 09.04.2019

1. The P_{II}(I86N) regulatory network

1.1 P_{II}(I86N) variant, a super activator of NAGK

The P_{II} signal transduction protein regulates the arginine biosynthesis by its interaction with the arginine controlling enzyme N-acetylglutamate kinase (NAGK). The NAGK (R233A) variant was previously shown to be unable to bind wild-type P_{II} *in vitro* [80]. To gain further insights in the nature of NAGK - P_{II} interaction, a screening for P_{II} variants with altered NAGK binding characteristics was performed. During this study two P_{II} variants were identified, both containing substitutions at position 86 (I86N and I86T). These two P_{II} variants are still able to interact with NAGK (R233A). Biochemical studies suggested that P_{II}(I86N) represents a super active NAGK binder. Dissociation of the P_{II}-NAGK complex is normally triggered by the addition of 2-OG in presence of ATP; however, P_{II}(I86N) no longer responds to 2-OG [100]. Determination of the three-dimensional structure of P_{II}(I86N) shows an almost identical backbone compared to the wild-type P_{II}. However, the T-loop adopts a compact bended conformation similar to that of wild-type P_{II} in NAGK complex [100].

The accumulation of the carbon/nitrogen storage polymer cyanophycin mainly depends on the availability of arginine. A P_{II}-deletion in *Synechocystis* sp. PCC 6803 leads to a low active NAGK, which caused impaired cyanophycin accumulation [90]. We expected the opposite phenotype if we replace the wild-type P_{II} with the NAGK super activator P_{II}(I86N). Strain BW86, containing the P_{II}(I86N) variant, showed an increased *in vivo* NAGK activity under different nitrogen supplementations (nitrate, ammonia and without nitrogen source) (figure 2 Publication 1). To determine the metabolic changes, which are caused by the elevated NAGK activity, a metabolom study with focus on primary metabolism was performed. According to PCA and OPLS-DA analysis, the only changing metabolites were arginine, citrate/isocitrate, succinate and glycerate-3-P. Remarkably, the arginine content in strain BW86 was more than tenfold higher compared to the wild-type. On the other hand, the pools of citrate/isocitrate, succinate and glycerate-3-P were decreased (figure 4 Publication 1). A possible explanation for this could be the accelerated metabolite flow into arginine, which drains the pools of metabolites from TCA cycle and carbon fixation.

Due to the high intracellular arginine concentration, the cyanophycin accumulation was highly increased. Under balanced growth conditions with nitrate as nitrogen source, strain BW86 accumulated up to 15.6 ± 5.4 % cyanophycin relative to the CDM, i.e. on average almost six times more than the wild-type cultivated under the same condition (figure 5 Publication 1). Surprisingly, strain BW86 showed impaired growth and cyanophycin production when cultivated with ammonia as only nitrogen source. This phenomenon is due to ammonia toxicity and will be discussed later in the paragraph "1.2 P_{II}(I86N) and Amt1

ammonium permease". Appropriate starvation conditions further increased the cyanophycin content of strain BW86 up to 47.4 ± 2.3 % of the CDM under phosphate starvation and 57.3 ± 11.1 % per CDM under potassium starvation (figure 5 Publication 1).

Furthermore, the cyanophycin produced by strain BW86 showed a high polydispersity ranging from 25 to 100 kDa, similar to the polydispersity of cyanobacterial wild-type cyanophycin (figure 6 Publication 2). Recombinant strains using heterologous expression systems with heterotrophic bacteria, yeasts or plants, produce cyanophycin with a size ranging of 25 - 45 kDa [135, 139, 140]. The higher polydispersity of cyanophycin produced by strain BW86 represents the most significant differences to other published cyanophycin producer strains.

Compared to bacteria which are used in biotechnological industry, cyanobacteria are unique as they use sunlight and CO₂ as energy and carbon source. Obviously, the importance of environmentally-friendly production processes increases. Hence, cyanobacteria are expected to play a major role in future industry. *Synechocystis* sp. PCC 6803 strain BW86 is the first reported bulk chemical producing cyanobacterial strain in the literature. Cyanophycin production in *Synechocystis* BW86 does not require organic carbon or cyanophycin-precursor substances, which enable low cost production of cyanophycin. With an amount of 57.3 ± 11.1 % cyanophycin per CDM, strain BW86 represents the cyanophycin producer strain with the highest observed cyanophycin content reported in literature so far.

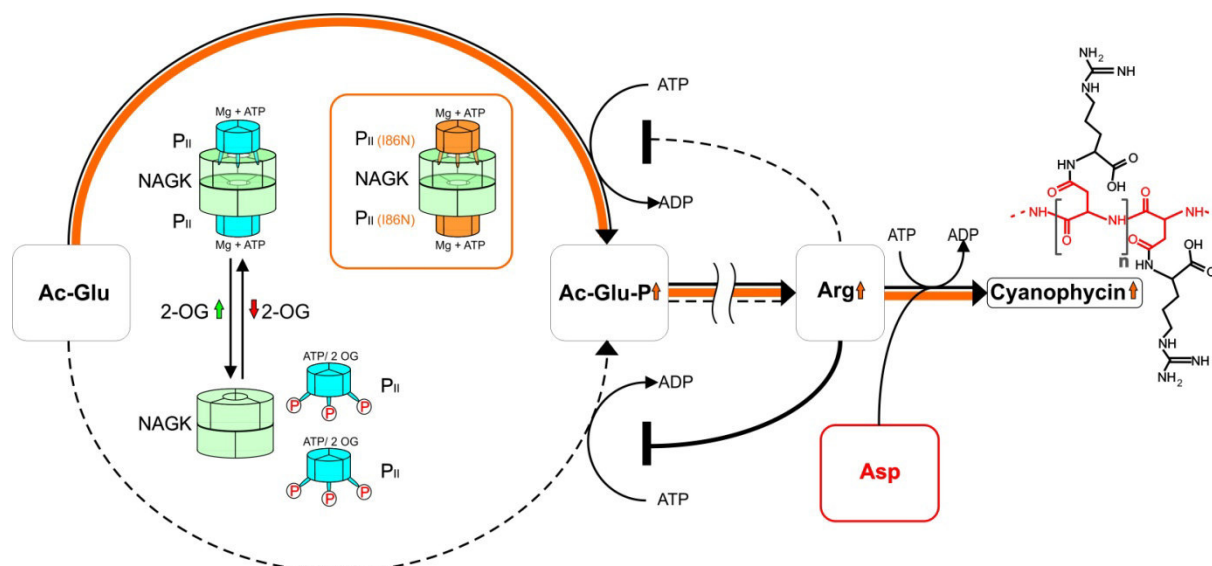


Figure 5 The strategy of metabolic engineering of the P_{II}(I86N) protein in *Synechocystis* sp. PCC 6803 for arginine/ cyanophycin overproduction. The conversion of *N*-acetylglutamate (Ac-Glu) to *N*-acetylglutamate-phosphate (Ac-Glu-P) is the rate-limiting step in the cyclic arginine synthesis pathway and is catalyzed by NAGK. NAGK activity is controlled by complex formation with the P_{II} protein, which senses the nitrogen status by 2-oxoglutarate (2-OG) binding. In the wild-type, unbound NAGK has low activity (*dashed line*) and is highly susceptible to arginine feedback inhibition, whereas NAGK bound to the P_{II} protein has high activity (*solid black line*) and much less sensitive towards arginine. The P_{II}(I86N) variant of strain BW86 (in *orange box*) permanently binds to NAGK, whereby its activity strongly increases (*solid orange line*) and the arginine feedback inhibition relieves. When excess arginine (Arg) is produced, cyanophycin is synthesized from arginine and aspartate (Asp in *red*). (Figure taken from Watzler *et al.* 2015 (Publication 1))

1.1.1 Strain BW86 process optimization

Strain BW86 demonstrated the potential of metabolic pathway engineering by using a variant of the central regulatory P_{II} signal transduction protein. However, to verify the industrial applicability of strain BW86, several process optimization studies have to be done. Previous characterization studies were performed under standard laboratory conditions using Erlenmeyer flasks with a maximal volume below one liter. In a first up-scale approach, it was possible to cultivate strain BW86 in flat plate photobioreactors (Midi-plate reactor system [188] and the similar Mini-plate reactor system). Both homologue reactor systems are smaller pilot constructions of industrial used flat plate photobioreactors. The cultivation compartment of the midi-plate reactor allowed a maximum volume of 1.2 liter, while the mini-plate reactor allowed a volume of 0.2 liter (setup shown in Figure 6).

In order to determine the optimal growth conditions of *Synechocystis* sp. PCC 6803 in flat plate photobioreactors, light kinetics were measured using warm-white LED illumination [189]. The maximum growth rate of 1.32 d^{-1} was observed at photon flux densities of $150 \mu\text{mol photons m}^{-2} \text{ s}^{-1}$. However, transition from photo-limitation to photo-saturation already occurred at $46 \mu\text{mol photons m}^{-2} \text{ s}^{-1}$. The growth rate was directly proportional to the irradiance under light limited conditions (below $46 \mu\text{mol photons m}^{-2} \text{ s}^{-1}$). Light intensities above $46 \mu\text{mol photons m}^{-2} \text{ s}^{-1}$ increased the growth rate slower and reached the maximum at $150 \mu\text{mol photons m}^{-2} \text{ s}^{-1}$ (figure 1 publication 3).

Strain BW86 produces $15.6 \pm 5.4 \%$ cyanophycin relative to the CDM under balanced growth conditions with nitrate as nitrogen source. Several growth limiting conditions, like phosphate or potassium starvation, increased the cyanophycin accumulation. However, growth limiting conditions also lower the overall biomass production. Therefore, it is necessary to find an optimal balance between enhanced cyanophycin production by stress factors and biomass production. According to our previous results (figure 5 Publication 1), we suggested phosphate limitation as best compromise between biomass and cyanophycin production. For this purpose, different initial phosphate concentrations were tested in batch cultivation approaches. Progressive phosphate limitation resulted in an increased cyanophycin accumulation. Phosphate quotas ranging from 1 to 4 mg phosphate per g CDM increased the cyanophycin production (figure 5 Publication 3). According to calculations of the photo conversion efficiency (PCE), *Synechocystis* sp. PCC6803 wild-type was more efficient in generating biomass from received light-energy than strain BW86. This behavior can be explained by the increased, high energy consuming cyanophycin production in strain BW86 (table 1 publication 3). Initial phosphate concentrations below 1 mg per g CDM led to a breakdown of the PCE. During these studies, BG-11 medium according to Rippka *et al.* [5] was used. Quantification of nitrate and sulfate consumption of strain BW86 in batch cultivation showed that both macronutrients are available in sufficient amounts over the whole cultivation procedure (figure 3 publication 3). In summary, to enable an increased cyanophycin production with a minimum impairment of the cell growth in flat plate photobioreactors, initial phosphate amounts of 1 to 4 mg per g CDM is required. Under these optimal conditions, the highest amount of cyanophycin was around 40% of CDM with a total yield of 340 mg cyanophycin per liter culture in 9 days.

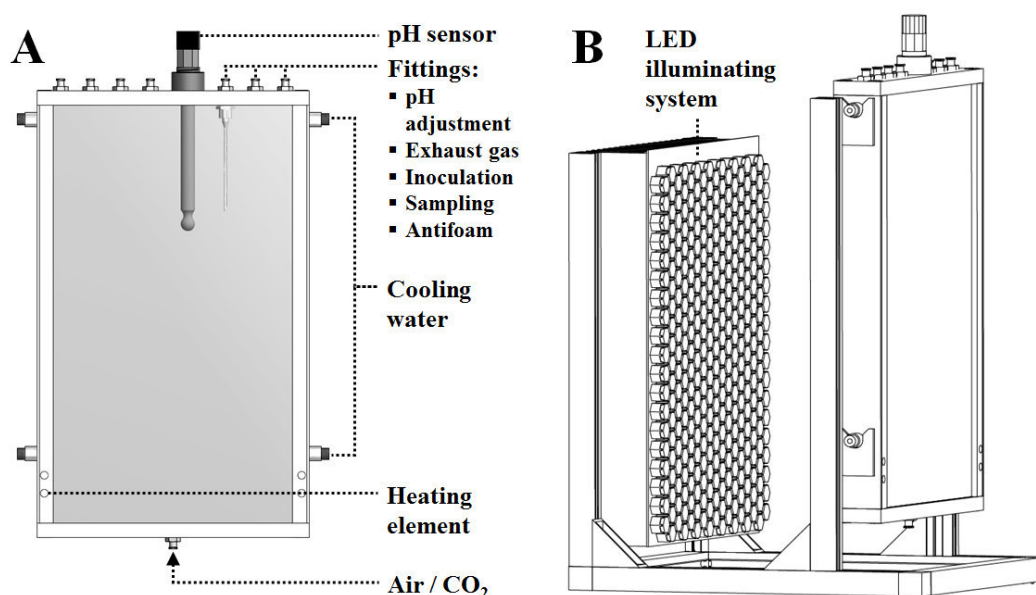


Figure 6 (A) Front and (B) side view of the Midi- and miniplate photobioreactor system. The Midiplate reactor (height, width and depth: 350 x 200 x 20 mm) allowing 1.2 liter volume, while the Miniplate reactor (height, width, depth of 140, 100, 20 mm) allowing 0.2 liter culture. (Figure taken from Trautmann *et al.* 2016 (Publication 3))

1.2 $P_{II}(I86N)$ and Amt1 ammonium permease

In order to find the best nitrogen source to maximize the cyanophycin yield of strain BW86 several nitrogen sources have been tested. It surprisingly turned out that strain BW86 is impaired in ammonium utilization (figure 5 and supplementary figure 2, Publication 1). In *E.coli* it is known that the P_{II} homolog GlnK regulates the ammonium influx by direct protein-protein interaction with the ammonium permease AmtB [103]. The observation regarding the impaired ammonium utilization of *Synechocystis* sp. harboring the $P_{II}(I86N)$ mutation implied a similar regulation in cyanobacteria. The $P_{II}(I86N)$ variant exhibits a modified T-loop structure while the P_{II} backbone appear almost identical with the P_{II} wild-type structure [100]. Therefore, the impaired ammonium utilization of strain BW86 could be caused by the altered T-loop structure.

To verify this suggestion, we tested the ammonium utilization of different P_{II} mutant strains, including a P_{II} deletion mutant (ΔP_{II}) [190]. To complement the P_{II} deletion, a *Synechocystis* sp. shuttle vector containing a P_{II} -Venus fusion was transformed in the P_{II} deletion mutant. To avoid steric hindrance of the T-loop we fused the Venus protein to the C-terminus of P_{II} . However, fusion to the C-terminus could instead lead to a steric hindrance of the B- and C-loop.

Growth experiments of *Synechocystis* sp. wild-type, ΔP_{II} , strain BW86 and a $\Delta P_{II} + P_{II}$ -Venus complementation strain have been performed to investigate the relation between P_{II} signaling and ammonium utilization (figure 1 and 2, publication 7). Both, the *Synechocystis* sp. ΔP_{II} mutant and strain BW86 showed impaired growth in presence of high ambient ammonium concentrations (≥ 10 mM ammonium) (figure 1, publication 7; supplementary figure 2, Publication 1). Quantification of ammonium utilization confirmed an uncontrolled influx of ammonium in the ΔP_{II} mutant and strain BW86, which led to intoxication in presence of high ambient ammonium concentrations. In contrast, *Synechocystis* sp. wild-type and the $\Delta P_{II} + P_{II}$ -Venus complementation strain maintained normal growth and ammonium tolerance (figure 1 and 2, publication 7).

Ammonium uptake in *Synechocystis* sp. mainly depends on the Amt1 permease [191]. In order to verify a possible interaction between P_{II} and Amt1 we performed pull down assays, using a C-terminal 3xflag-tagged P_{II} as bait. The fusion protein and its interacting proteins were purified by immunoprecipitation and subsequently identified by mass spectroscopy (MS). Since protein identification by MS is extremely sensitive, we performed a negative control using *Synechocystis* sp. wild-type, processed in the same way as the *Synechocystis* sp. P_{II} 3xFlag strain, to identify unspecific purified proteins. With this approach, we identified the known P_{II} interacting protein PipX and the Amt1 ammonium permease, supporting our suggestion that Amt1 represents a P_{II} target in cyanobacteria (table 4 and 5, publication 7). Surprisingly, besides Amt1 we also observed an enrichment of the NrtABCD nitrate/nitrite transporter as well as of the UrtABCDE urea transporter (table 4 and 5, publication 7).

To further confirm these interactions, bacterial two-hybrid assays were performed using the wild-type P_{II} and $P_{II}(I86N)$ variant against Amt1, NrtC, NrtD, UrtD and UrtE. In agreement with our pull-down results, the wild-type P_{II} showed interaction with Amt1, while the $P_{II}(I86N)$ variant showed no interaction. Concerning the ABC-type transporter NrtABCD and UrtABCDE, we could confirm an interaction of the wild-type P_{II} with NrtC, NrtD and UrtE (table 6, publication 7). The $P_{II}(I86N)$ variant was unable to interact with NrtC or NrtD but showed interaction with UrtE.

1.3 P_{II} localization changes under different nitrogen supplementations

Since all these transporters are plasma membrane associated, we characterized P_{II} localization under different conditions of nitrogen supplementation. Nitrate-replete *Synechocystis* sp. cells showed P_{II} -Venus fluorescence heterogeneously distributed in the cell. The majority of cells exhibited a strong fluorescence signal in their center and the cell-periphery (figure 3, publication 7). The P_{II} -Venus fluorescence in the cell periphery co-localizes with the plasma membrane where Amt1, NrtABCD and UrtABCDE are located.

After one week of nitrogen starvation, the P_{II}-Venus signal was more evenly distributed in the whole cell and its localization on the plasma membrane was not as distinct as during nitrate supplemented growth (figure 4, publication 7). Immediately after the addition of a suitable nitrogen source a change in P_{II}-Venus localization became apparent. The majority of cells showed distinct plasma membrane localization of P_{II}-Venus, while the remaining cytosol showed homogenously distributed fluorescence. The migration of P_{II}-Venus to the plasma membrane appeared more clearly by the addition of ammonia compared to nitrate or urea (figure 4 and 5, publication 7). One hour after the addition of ammonium or two hours after the addition of nitrate, P_{II} started to dissociate from the plasma membrane and moved back to its cytoplasmic localization. In contrast, urea addition induced a constant migration of P_{II} towards the plasma membrane without dissociation in the first four hours (figure 5, publication 7).

1.4 P_{II}(I86N) and the NrtABCD nitrate/nitrite transporter

In the last decades, several physiological studies suggested an involvement of P_{II} in regulation of nitrate/nitrite uptake [92, 192-194]. Our pull down experiments and bacterial two-hybrid assays supported the suggestion that P_{II} regulates the NrtABCD nitrate/nitrite transporter by interacting with the NrtC and NrtD subunits (table 4, 5 and 6, publication 7). A characteristic phenotype, which has been described for a P_{II} deletion mutant grown in the presence of nitrate, is the excretion of nitrite in the medium [194, 195]. The reduction of nitrate requires two electrons whereas six electrons are needed for the reduction of nitrite to ammonium. Due to the lower costs of nitrate reduction, the nitrite reduction becomes limiting in case of an uncontrolled nitrate influx. In consequence nitrite accumulates and gets excreted. Since the P_{II}(I86N) variant showed no interaction with NrtC and NrtD in the bacterial two-hybrid assay we asked if strain BW86 also excretes nitrite when nitrate is provided.

By measuring the nitrate consumption rate of the P_{II}-signaling mutants we could confirm that a P_{II} deletion or a replacement with the P_{II}(I86N) variant caused an uncontrolled nitrate influx. The uncontrolled nitrate influx indeed led to nitrite excretion (figure 6 and 7, publication 7).

In wild type cells active nitrate uptake requires photosynthetic CO₂ fixation as well as the absence of ammonium [92, 196]. We tested if our P_{II} signaling mutants still display the ammonium- and light-induced nitrate uptake inhibition by measuring the nitrate consumption in presence of ammonium and in absence of light. *Synechocystis* sp. wild-type and the P_{II}-Venus complementation strain inhibited nitrate uptake in an ammonium- and light-dependent manner. However, the P_{II} deletion mutant and strain BW86 were impaired

in ammonium- and light- promoted nitrate uptake inhibition (figure 7, publication 7). Accordingly, we conclude that NrtABCD is directly regulated by the interaction of P_{II} with the NrtC and NrtD subunits and its interaction is T-loop dependent. The interaction of P_{II} with the NrtC and NrtD subunits also mediate the ammonium and light dependent nitrate uptake inhibition.

1.5 P_{II}(I86N) and the UrtABCDE urea transporter

Our pull down experiments and bacterial two-hybrid assays indicated a regulation of the urea transporter UrtABCDE by the interaction of P_{II} with the UrtE subunit. In order to analyze the biological significance of this interaction, we monitored the urea utilization abilities of our P_{II} signaling mutants under different conditions.

By measuring the urea consumption of the P_{II}-signaling mutants, we observed that a P_{II} deletion caused an uncontrolled urea influx (figure 8, publication 7). In cyanobacteria, urea is hydrolyzed to CO₂ and two molecules of ammonium by the enzyme urease [197]. Due to the uncontrolled urea influx in the Δ P_{II} strain, we observed an excretion of ammonium in the medium (figure 8, publication 7). The addition of ammonium causes an inhibition of the urea uptake. However, in the Δ P_{II} mutant the ammonium-induced urea uptake inhibition is impaired (figure 8, publication 7).

The interaction of P_{II} and the UrtE is likely independent of a flexible T-loop, since our bacterial two-hybrid assay showed interaction between the P_{II}(I86N) variant and UrtE. In agreement, *Synechocystis* sp. harboring the P_{II}(I86N) variant behaved like the wild-type regarding the urea utilization properties (figure 8, publication 7). In contrast, *Synechocystis* sp. harboring the P_{II}-Venus fusion exhibited an impaired regulation of the urea utilization. The Δ P_{II} + P_{II}-Venus strain showed an elevated urea uptake and a slightly impaired ammonium induced urea uptake inhibition (figure 8, publication 7). However, the Δ P_{II} + P_{II}-Venus strain excreted no ammonium when urea was provided as only nitrogen source. The Venus fusion on the C-terminus of P_{II} could lead to a steric hindrance of the B- and C-loop while the T-loop remains unaffected. According to this data we strongly suggested an involvement of the B- or C-loop in the interaction of P_{II} with the UrtE subunit.

1.6 Additional research

1.6.1 P_{II}(I86N) and PipX

Since P_{II}(I86N) mimics the structure of P_{II} in the NAGK complex, we previously suggested that this variant is unable to interact with other P_{II} interaction partners. In a bacterial two-hybrid assay, the P_{II}(I86N) variant, thought to be a negative control, showed surprisingly

interaction with the PipX protein [198], therefore we analyzed the formation of P_{II}-PipX complexes by SPR spectroscopy, using an indirect assay, as described previously [96]. Monomeric His₆-PipX showed a weak transient binding to a Ni-NTA sensor chip due to low affinity of the single His₆-tag. Therefore, the response units (RUs) upon binding of PipX alone rapidly reached a plateau and after the end of the injection phase, they decreased due to dissociation of the protein from the sensor chip surface (figure 7 A, red curve). When PipX was incubated with P_{II} in the absence of effector molecules, wild-type P_{II} increased the binding of His₆-PipX to the sensor chip by approximately 17 %, due to complex formation (figure 7 A, black dotted line). Strikingly, the addition of the P_{II}(I86N) variant [119] led to a much stronger increase of PipX binding and to less dissociation during the dissociation phase (figure 7 A, straight black line). To compare the effect of P_{II} proteins on the dissociation of the complexes from the sensor chip (which is a good indicator of the efficiency of P_{II}-PipX interaction), the dissociation curves were normalized to the RUs at the end of the injection phase (taken as 100 %) (figure 7 B). The percent RUs remaining bound to the chip after 400 s of dissociation were then taken as a proxy for P_{II}-PipX interaction and used to quantify the effect of different effector molecules (figure 7 B-E).

The result from the first experiment, performed in the absence of effector molecules, showed that under these conditions, P_{II}(I86N) very strongly interacted with PipX, clearly much more than wild-type P_{II}. In the following experiments, the effect of different effector molecules on P_{II}-PipX complex stability was analyzed. Previous studies showed a strong positive effect of ADP on the interaction of wild-type P_{II} with PipX, due to a stabilization of the PipX-interacting conformation of P_{II} by ADP [96]. The same result was obtained here (figure 7 D,E). In comparison to wild-type P_{II}, binding of the P_{II}(I86N) variant to PipX was negatively affected by ADP (figure 7 C,E). As expected from previous analyses, ATP showed for the wild-type P_{II} protein a slightly lower stability of the complex than in the ADP-complexed state. By contrast the P_{II}(I86N) variant interacted more stably with PipX in the ATP state than with ADP (figure 7 C,D,E). As expected, in the presence of ATP, 2-OG was a strong inhibitor of wild-type P_{II}-PipX complex formation [96] (figure 7 D). An inhibitory effect of ATP and 2-OG on the P_{II}-PipX complex was also visible with the P_{II}(I86N) variant, however, not as strong as in the case of wild-type P_{II} protein (figure 7 C,D,E). This is in agreement with the impaired ability of the P_{II}(I86N) variant to bind 2-OG [101].

Taken together, this study demonstrated that the P_{II}(I86N) variant is very efficient in complex formation with PipX and that this binding does not require positive stimulation by ADP as is the case with wild-type P_{II}. Therefore, the P_{II}(I86N) might tune down PipX-mediated NtcA response *in vivo*.

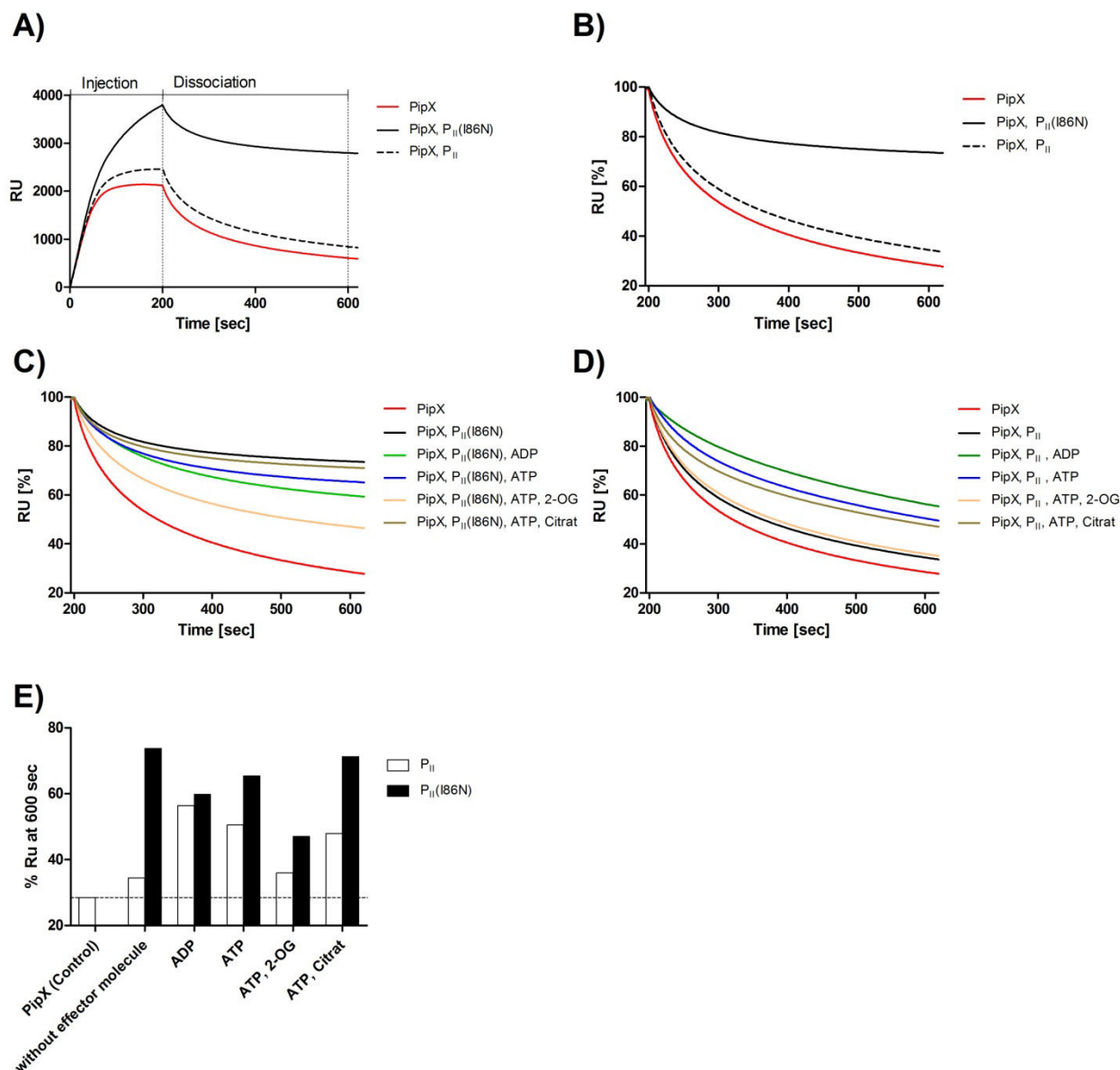


Figure 7 P_{II}-PipX complex formation and dissociation in presence and absence of effector molecules. (A) His₆-PipX (500 nM) was injected to the chip in absence of P_{II} (red line) and in presence of 100 nM Strep-P_{II} wild-type (black dashed line) or 100 nM P_{II}(I86N) (black line), without effectors. Injection phase takes 200 s, followed by 400 s dissociation. (B) shows the dissociation of His₆-PipX (red line) alone and in presence of Strep-P_{II} wild-type (black dashed line) and P_{II}(I86N) (black line). The response signal at the end of the injection at $t: 200$ s is normalized to 100%. (C) and (D) show the dissociation of P_{II}-PipX complex in presence of effectors, there for response signal at the end of the injection at $t: 200$ s is normalized to 100%. In (C) P_{II}(I86N) and in (D) P_{II} wild-type was pre-incubated without effectors (black line), 1 mM ADP (green line), 1 mM ATP (blue line) and 1 mM ATP/ 1 mM 2-OG (orange line). PipX without P_{II}, was used as control (red line). (E) shows the response signal in % at $t:600$ s

(400s after the end of the injection) of PipX in complex with P_{II} wild-type and P_{II}(I86N) in presence and absents of effectors. The residual signal at *t*:600s is an indicator for the stability of the complex.

1.6.2 P_{II}(I86N) and nitrogen starvation response

Our previous SPR spectroscopy study demonstrated a strong complex formation of the P_{II}(I86N) variant with PipX. Under insufficient nitrogen supplementation, the P_{II}-PipX complex dissociates, due to the elevated presence of ATP and 2-OG [95]. Free PipX can bind and activate NtcA, which leads to an activation of the NtcA regulon. A stronger sequestration of PipX by P_{II}(I86N), also in presence of elevated 2-OG levels, could lead to a delayed activation of the NtcA regulon. Therefore, we suggested a slowed down nitrogen starvation response in *Synechocystis* sp. harboring the P_{II}(I86N) variant. To investigate a possible delayed nitrogen starvation response, *Synechocystis* sp. wild-type and strain BW86 cells were grown to an OD₇₅₀ of 0.4 to 0.6, washed, and resuspended in BG-11 lacking a nitrogen source. This treatment induces nitrogen chlorosis, which gets visible due to the degradation of the photosynthetic apparatus (figure 8 A). Here both strains *Synechocystis* sp. wild-type and BW86 behaved similarly during chlorosis and no differences in the degradation of pigments became apparent (figure 8 A). After 8 days both strains completed the chlorosis process and appeared yellowish.

Dormant *Synechocystis* sp. cells are able to survive long periods of nitrogen starvation. After the addition of a nitrogen source, they can re-green and resume growth [25]. To test the viability of the chlorotic cells we performed a drop plate method every week. For the drop plate method, chlorotic *Synechocystis* sp. cultures were adjusted to an OD₇₅₀ of 1. Subsequently the cultures were diluted 10-fold in series. Drops of five dilutions (10⁰ to 10⁻⁴) were placed on BG-11 agar plates containing standard nitrate concentrations. In the first three weeks of chlorosis, *Synechocystis* sp. wild-type and strain BW86 showed the same viability according to the number of colony forming units (figure 8 A). After the fourth week, the number colony forming units of strain BW86 was reduced compared to the wild-type. This difference became more apparent when the nitrogen starvation was prolonged to six weeks. Here strain BW86 showed a clear lower number of colony forming units, indicating a decreased viability under long term nitrogen starvation (≥ 4 weeks).

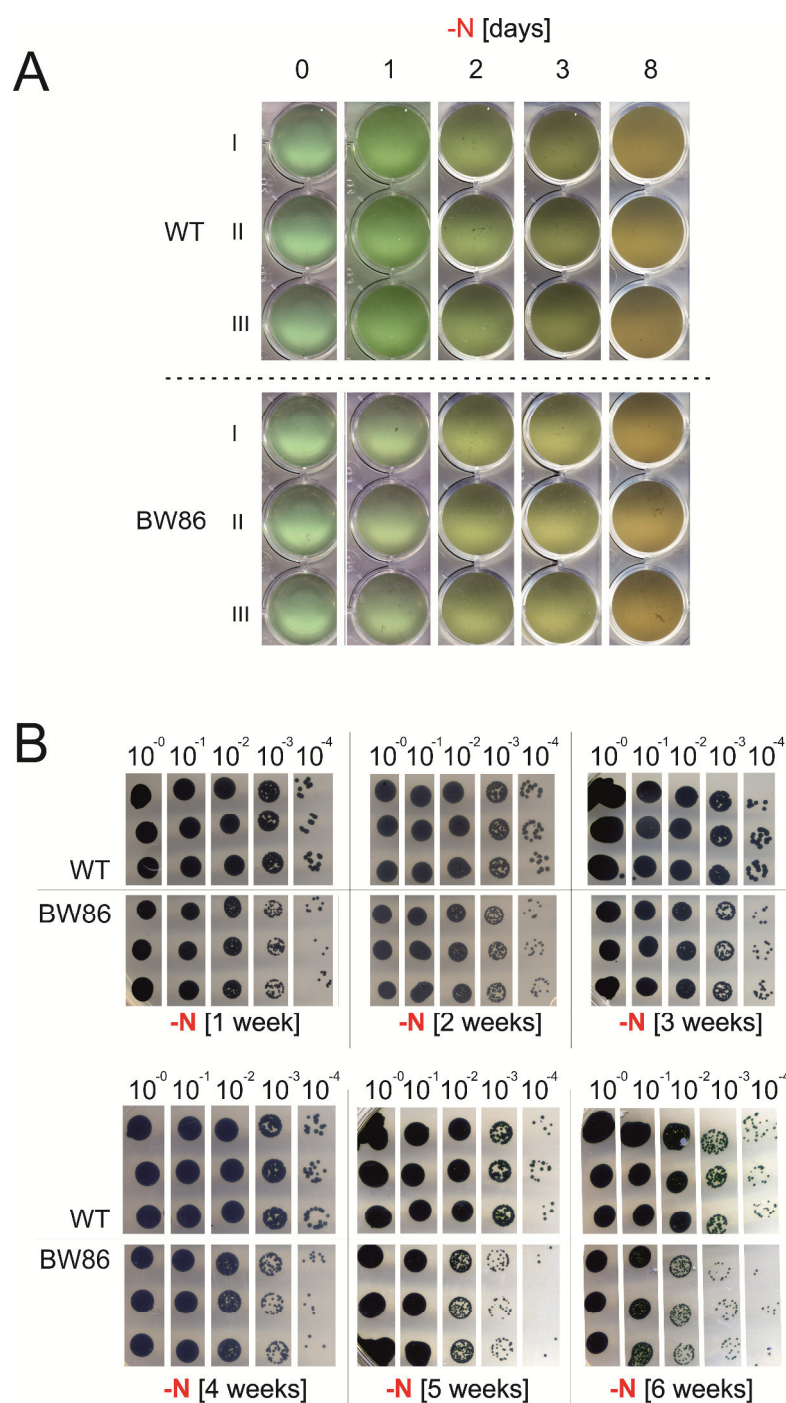


Figure 8 Nitrogen starvation and resuscitation of *Synechocystis* sp. wild type and strain BW86. (A) Changes in pigmentation during nitrogen starvation of *Synechocystis* sp. wild type and strain BW86. Nitrogen starvation was induced by resuspending washed, exponentially growing cells in BG-11 medium lacking nitrogen to an OD₇₅₀ of 0.5. Shown is the change in pigmentation of three independent cultures within 8 days of nitrogen starvation. (B) Drop plate method of resuscitating wild-type and P_{II}(I86N) mutant cells on BG-11 agar plates containing 17.3 mM nitrate. Cultures were adjusted to an OD₇₅₀ of 1.0, diluted in a 10-fold dilution series, and dropped on agar plates. Cultures were previously starved for nitrogen between 1 and 6 weeks. Assays were performed using three biological replicates per strain.

1.6.3 P_{II}(I86N) causes decreased PHB accumulation

P_{II} regulates a multitude of carbon and nitrogen metabolism associated processes and thereby controls the cellular carbon/nitrogen ratio. The accumulation of the carbon-storage polymer PHB depends heavily on the carbon/nitrogen ratio [199]. Previous studies documented a relation between P_{II} signaling and PHB accumulation [200, 201]. A P_{II} deletion mutant contains a significantly reduced acetyl-CoA level due to the derepression of the acetyl-CoA carboxylase activity [88]. This reduced acetyl-CoA level leads to an impaired accumulation of PHB [200, 201]. Phosphorylation of P_{II} is not a major factor regulating PHB accumulation, since phosphorylation mimicking mutants of P_{II} could complement the low PHB phenotype. We wondered if the *Synechocystis* sp. strain BW86, harboring the P_{II}(I86N) variant, also shows an impaired PHB accumulation.

Since PHB accumulation takes place under growth limiting starvation conditions, we tested the PHB accumulation properties under phosphate and potassium starvation. For this purpose, *Synechocystis* sp. wild-type and strain BW86 were grown to an OD₇₅₀ of 0.4 to 0.6, washed, and subsequently resuspended in BG-11 medium, lacking either phosphate or potassium. Under phosphate starvation, the strain BW86 accumulates significantly lower amounts of PHB than the wild-type. Here only residual amounts of PHB below 0.5 % to the CDM could be detected in the BW86 strain (figure 9 A). In contrast *Synechocystis* sp. wild-type accumulated up to 3 % to the CDM at the same condition. Surprisingly, under potassium starvation the PHB accumulation of strain BW86 was similar to the wild-type (figure 9 B).

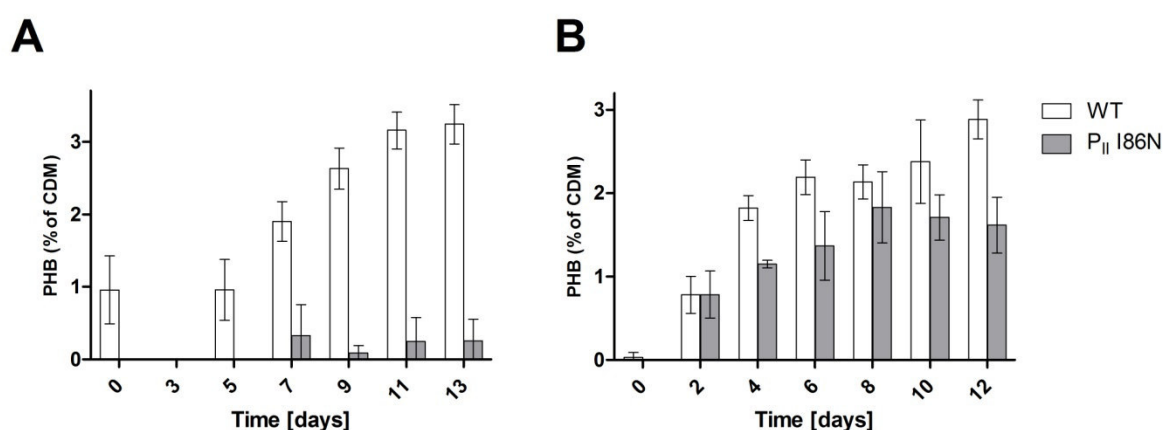


Figure 9 PHB accumulation under phosphate starvation (A) and potassium starvation (B) in *Synechocystis* sp. wild-type (*white bars*) and strain BW86 (*gray bars*). Phosphate starvation was induced by resuspending washed exponentially growing cells in BG-11 medium lacking a phosphate source to an OD₇₅₀ of 0.5. After 3 days, the cultures were diluted with fresh phosphate-free medium to an OD₇₅₀ of 0.2. For potassium starvation, exponentially growing

cells were washed and resuspended into potassium-free medium. Values are means of three biological replicates. The PHB amount is plotted against the cell dry mass (CDM). Note the different scales on the axes.

2. Cell biology of the nitrogen storage polymer cyanophycin

2.1 CphA localization changes during cyanophycin accumulation and degradation

To investigate the intracellular localization of CphA, we fused *cphA* to the gene encoding enhanced green fluorescent protein (eGFP) (yielding GFP fused to the C terminus of CphA) and inserted *cphA*-eGFP under the control of the native *cphA* promoter into the *Synechocystis* sp. shuttle vector pVZ322. The resulting pVZ322-*cphA*-eGFP plasmid was transformed into *Synechocystis* sp. This strain, termed *Synechocystis* sp. strain CphA-eGFP, was used to investigate the cellular localization of CphA using comprehensive statistical analysis of microscopy images.

In the mid-exponential growth phase, when no cyanophycin accumulation occurs, the majority of cells ($87\% \pm 3\%$) showed GFP signal uniformly distributed in the cytoplasm. The remaining cells ($13\% \pm 3\%$) contained distinct foci (figure 1, publication 6). Accordingly, the cyanophycin content during exponential growth is usually less than 1 % of the CDM, and visible cyanophycin granules were absent [71, 119, 202].

The *cphA* gene is constitutively expressed in different nitrogen regimes [25]. To reveal the localization of CphA during periods of cyanophycin accumulation or degradation, we monitored CphA-eGFP localization after the addition of nitrate to *Synechocystis* sp. cells which were nitrogen starved for 4 days. These conditions are known to induce transient cyanophycin accumulation [25, 120]. In nitrogen-starved cells, the GFP signal was almost exclusively found as a diffuse signal in the cytoplasm ($98\% \pm 2\%$ of the cells) (supplementary figure 1 publication 6). Immediately after the induction of cyanophycin synthesis by adding nitrogen to the starved cells, CphA aggregated in foci that were randomly distributed in the cell (figure 2, publication 6). Compared to the appearance of CphA-eGFP foci, the appearance of the cyanophycin granules was delayed. Six hours after nitrate addition, the number of cells containing cyanophycin granules increased drastically, reaching a plateau of $87.8\% \pm 4.2\%$ of the cells. Eighteen hours after the addition of nitrate, both, the number of cells with visible cyanophycin granules and the diameter of the foci decreased (figure 2, supplementary figure 2, publication 6). As the cyanophycin granules degraded, the cells simultaneously started to grow.

During recovery from nitrogen starvation, cyanophycin is produced transiently, and the maximal level of cyanophycin is relatively low compared to other conditions that trigger cyanophycin accumulation. Potassium starvation subjects an intense and immediate stress, which results in massive cyanophycin production [119]. This motivated us to analyze CphA localization under potassium starvation. Upon induction of potassium starvation, CphA re-localized from an initial diffuse cytoplasmic localization into distinct foci and later clearly localized on the surface of the cyanophycin granules, forming a halo-like structure (supplementary figure 3, publication 6). As cyanophycin accumulates, the numbers of foci and granules per cell continuously decreased, possibly as initial granules fuse to form larger aggregates (supplementary figure 5, publication 6). This behavior would explain the amorphous structure of large granules that we observed when the cellular cyanophycin content was high (supplementary figure 3, publication 6) and which we also observed previously in electron micrographs of the cyanophycin-overproducer strain BW86 (figure 8, publication 1).

Transferring the potassium-starved cells back to BG-11 medium containing a potassium source restored the growth within approximately 24 h, concomitantly with the degradation of the cyanophycin granules. During cyanophycin degradation, it appeared in some cases that CphA-eGFP no longer co-localized with the cyanophycin granule surface (supplementary figure 3, publication 6). The proportion of cells with cyanophycin granules and CphA-eGFP foci decreased accordingly, while the proportion of cells with exclusively cytoplasmic distributed CphA-eGFP signal increased (supplementary figure 4, publication 6). Furthermore, the average size of the granules decreased, while the number of granules per cell increased (supplementary figure 5, publication 6), indicating that the granules disaggregated into smaller particles.

2.2 Physiological function of cyanophycin in non-diazotrophic cyanobacteria

2.2.1 Cyanophycin-deficient mutant has a growth advantage under standard laboratory conditions

The ability to synthesize cyanophycin is widespread among cyanobacteria and other eubacteria. With a carbon/nitrogen ratio of 2:1, cyanophycin is perfectly suited as a nitrogen storage compound. However, the physiological significance of cyanophycin for non-diazotrophic cyanobacteria remained largely unknown. To analyze the physiological role of cyanophycin in the non-diazotrophic cyanobacterium *Synechocystis* sp., we generated a *cphA* deletion mutant by replacing the *slr2002* (*cphA*) open reading frame with a kanamycin resistance gene. The resulting *Synechocystis* sp. Δ *cphA* strain and the wild-type responded to nitrogen starvation similarly. The only difference that becomes apparent was a reproducible,

slightly higher residual pigment content in the chlorotic state of the $\Delta cphA$ mutant. However, the reason for the higher residual chlorophyll amount remains unknown (figure 4, publication 6).

To investigate the physiological role of cyanophycin, we focused on transient accumulation of cyanophycin during resuscitation from nitrogen starvation. To determine whether cyanophycin synthesis influences the resuscitation, we first compared the resuscitation of *Synechocystis* sp. wild-type and the $\Delta cphA$ mutant under standard laboratory conditions (nitrogen-rich medium and continuous light). Surprisingly, under standard laboratory conditions with continuous light and nitrogen excess, the $\Delta cphA$ mutant showed a clear growth advantage over the wild-type both in liquid medium and on agar plates (figure 5, publication 6).

2.2.2 Cyanophycin accumulation is beneficial under natural conditions

The growth advantage of the cyanophycin-deficient $\Delta cphA$ cells during resuscitation from nitrogen chlorosis was puzzling. We questioned whether this disadvantage was due to artificial laboratory conditions (nitrogen-rich medium and continuous light). Therefore, we nitrogen-starved *Synechocystis* sp. wild-type and $\Delta cphA$ mutant and compared their resuscitation with fluctuating and/or limiting nitrogen supplementation by using a modified drop plate method. To enable fluctuating nitrogen supplementation, cell suspensions of *Synechocystis* sp. wild-type and $\Delta cphA$ mutant were dropped onto a transfer membrane, which was periodically moved to another plate containing a different nitrogen concentration. This method allows changing nitrogen supplementations without imposing additional stress to the cells that occur with harvesting, washing, and resuspending cells in another medium.

The modified drop plate method of *Synechocystis* sp. wild-type and the $\Delta cphA$ mutant confirmed our hypothesis that the unnatural laboratory conditions caused the growth disadvantage of the cyanophycin accumulating wild-type cells. The ability to store nitrogen in the form of cyanophycin was beneficial during resuscitation under fluctuating or limiting nitrogen supplementation and the cells showed a growth advantage over the cyanophycin-deficient mutant (figure 6, publication 6). When nitrogen fluctuation and limitation are combined, the cyanophycin-deficient mutant was not able to fully recover from chlorosis and remained in a semi-chlorotic state. To determine whether the growth advantage under fluctuating nitrogen concentrations of wild-type cells over the $\Delta cphA$ mutant could also be observed in liquid culture, we provided nitrogen-starved liquid cultures of *Synechocystis* sp. wild-type and the $\Delta cphA$ mutant with nitrate for 4 h per day. In agreement to our modified drop plate method, *Synechocystis* sp. wild-type obtained a clear growth advantage against the $\Delta cphA$ mutant (figure 7, publication 6).

To further mimic natural conditions, we tested the impact of day/night cycles in addition to a fluctuating and/or limiting nitrogen supply. Nitrogen-starved liquid cultures of *Synechocystis* sp. wild-type and the $\Delta cphA$ mutant were exposed to nitrate but no light. After this dark and nitrogen supplemented period, the cells were washed and resuspended into fresh medium containing a small amount of nitrate and exposed to light. Under this condition the resuscitation of *Synechocystis* sp. wild-type cells proceeded as fast as in continuous light, with growth restoration after 48 h. In contrast, the cyanophycin deficient $\Delta cphA$ mutant was not able to resuscitate in this time period (figure 8, publication 6). We further analyzed the growth behavior with a modified version of the drop plate method, in which nitrogen starved *Synechocystis* sp. wild-type and $\Delta cphA$ mutant cells were grown on plates with fluctuating nitrogen supply and with day/night cycles. A small amount of nitrate was provided only during the night phase. In agreement with our observations in liquid culture the wild-type also showed a clear growth advantage over the $\Delta cphA$ mutant (figure 8 publication 6).

2.3 Additional research

2.3.1 Extraction of an unidentified polymer from a cyanophycin-deficient mutant

CphA is the only known enzyme involved in the synthesis of cyanophycin in *Synechocystis* sp.. Therefore, a deletion of the *cphA* gene causes the inability to synthesize cyanophycin. However, the elongation reaction of CphA requires cyanophycin primer, provided by the non-identified cyanophycin primase. We hypothesize an enrichment of cyanophycin primers if we delete *cphA* in the arginine-overproducing strain BW86. To test this hypothesis, we replaced the *slr2002* (*cphA*) open reading frame with a kanamycin resistance gene in *Synechocystis* sp. strain BW86, harboring the P_{II}(I86N) variant.

The inability of the mutant to build cyanophycin granules was confirmed by microscopy (data not shown). However, by using the common cyanophycin extraction method, we extracted a substance from the *Synechocystis* sp. BW86 $\Delta cphA$ strain. Extraction of cyanophycin is based on its solubility at low pH and insolubility at neutral pH. By applying this acid treatment, cyanophycin can be extracted with high purity with only residual amounts of proteins or other cell components [135].

The amount of this unknown substance was quantified by measuring the dry weight under different growth conditions. During exponential growth (OD₇₅₀ 0.7 - 0.9) with nitrate as sole nitrogen source *Synechocystis* sp. BW86 $\Delta cphA$ accumulated up to 20.8 % \pm 6.9 % of this substance relative to the CDM. As the cells entered the stationary phase (OD₇₅₀ 1.1 - 1.3) the amount decreased to 12.4 % \pm 1.4 % of the CDM (figure 10 A). As comparison we also

quantified the amount of cyanophycin of strain BW86 under the same conditions. Remarkably, the quantified cyanophycin amounts of the strain BW86 was similar to the amounts of the unknown substance produced by *Synechocystis* sp. BW86 $\Delta cphA$ (figure 10 A).

Cyanophycin accumulation is triggered by conditions of reduced growth rates, such as entry into stationary phase or unbalanced cultivation conditions. To test the effect of growth limitation on the accumulation of the unknown substance of the *Synechocystis* sp. BW86 $\Delta cphA$ strain, we starved cells for potassium. The substance content in potassium-starved *Synechocystis* sp. BW86 $\Delta cphA$ cells rapidly increased in the first 2 days and reached a peak of $39.8 \% \pm 12.9 \%$ of the CDM (figure 10 A). In course of the potassium starvation the amount decreases over time, probably as consequence of a stress response in the decaying cells, caused by the harmful lack of potassium. In comparison, the cyanophycin amount of *Synechocystis* sp. BW86 behaved similar. Here the maximum amount of cyanophycin reaches $46.9 \% \pm 15.8 \%$ of the CDM after 2 days of potassium starvation (figure 10 A).

To gain further insights in the nature of the cyanophycin-like substance, the isolated polymers were solubilized in SDS sample buffer and analyzed by SDS-PAGE. Cyanophycin isolated from *Synechocystis* sp. BW86 showed its typical polydispersity with a size range of 25 to well above 100 kDa (figure 10 B). However, the extracted cyanophycin-like substance showed distinct bands mainly ranging from below 10 to 20 kDa.

Cyanophycin is resistant against hydrolytic cleavage by several proteases. This resistance is due to the unique structure of cyanophycin. The arginine side-chains, which are linked by isopeptide-bonds to every aspartyl moiety, permit the resistance against several proteases. To test if the cyanophycin-like substance shows the same resistance against proteases, we incubated the isolated polymers with proteinase K and analyze the resulting degradation products. Since our SDS-PAGE analyses showed distinct bands mainly ranging from below 10 to 20 kDa we changed to a tricine-PAGE to gain higher resolution in the area of low molecular weight. As expected, the incubation with proteinase K didn't led to a degradation of cyanophycin. In contrast the distinct bands of the cyanophycin-like substance completely disappeared, indicating susceptibility against proteases (figure 10 C).

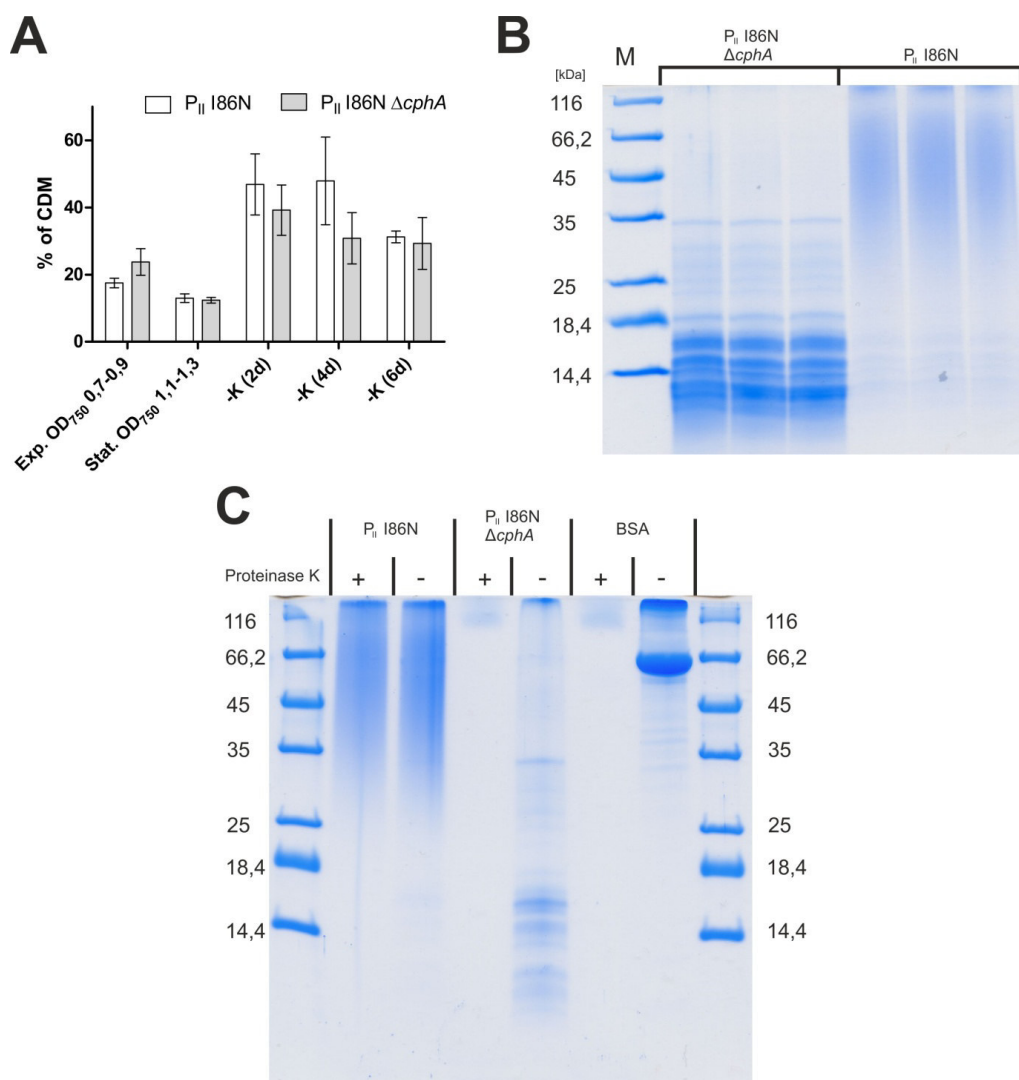


Figure 10 (A) Quantification of cyanophycin and the cyanophycin-like polymer from *Synechocystis* sp. BW86 and *Synechocystis* sp. BW86 $\Delta cphA$ under different growth conditions. Cells were cultivated with nitrate as nitrogen source. The quantification occurs at the exponential growth phase (Exp.) and in the stationary growth phase (Sat.). For potassium starvation (-K), exponentially growing cells were washed and resuspended into potassium-free medium. Values are means of three biological replicates. Amounts of cyanophycin and the cyanophycin-like polymer are plotted against the cell dry mass (CDM). (B) SDS-PAGE determination of the molecular weight of cyanophycin and the cyanophycin-like polymer isolated from *Synechocystis* sp. BW86 and *Synechocystis* sp. BW86 $\Delta cphA$, respectively. Shown are three biological replicates of each strain. Per lane, 40 μ g cyanophycin or cyanophycin-like polymer was loaded. (C) Tricine-PAGE of cyanophycin and the cyanophycin-like polymer in presence (+) and absence (-) of proteinase K. Isolated polymers were incubated with proteinase K overnight. Bovine serum albumin (BSA) was used as a control to confirm the functionality of the assay. Per lane, 40 μ g cyanophycin or cyanophycin-like polymer while 10 μ g BSA was loaded.

VII. Discussion

1. Metabolic engineering using custom- tailored P_{II} signaling proteins

In the last six decades several bacterial strains have been generated to improve the biotechnological production of arginine and its derivatives. Model organisms such as *Corynebacterium glutamicum*, *Escherichia coli* or *Bacillus subtilis* were used as production hosts [203]. A common metabolic engineering strategy to improve the production of arginine is the reduction of the feedback inhibitory effect of arginine to NAGK. By using site-directed mutagenesis, it was previously possible to create a feedback-resistant NAGK variant. Introduction of this modified NAGK variant led to a strongly increased arginine production [204].

In this thesis we present an alternative way to improve NAGK activity in unicellular cyanobacteria by manipulating the P_{II} signal. Complex formation of P_{II} with NAGK enhances its catalytic efficiency, with the V_{max} increasing fourfold and the K_m for N-acetylglutamate decreasing by a factor of 10 [89]. Furthermore, feedback inhibition of NAGK by arginine is strongly decreased in complex with P_{II} [89]. The P_{II}(I86N) variant is a structural mimic of P_{II} in the NAGK complex. As a consequence of this special T-loop folding, this variant has a high affinity for NAGK and responds no longer to 2-OG *in vitro* [101]. Due to the increased arginine content, strain BW86 accumulated almost six-fold more cyanophycin than the wild-type under balanced growth conditions with nitrate as nitrogen source. *Synechocystis* sp. BW86 is the cyanophycin producer strain with the highest abundance of cyanophycin described in literature. The large amount of cyanophycin with high molecular weight gives the opportunity for investigations regarding the material properties of this polymer.

Furthermore, engineered variants of the P_{II} signaling protein could also be used for other metabolic engineering strategies in bacteria. P_{II} controls a multitude of other cellular activities in various autotrophic and heterotrophic bacteria. A possible target for metabolic engineering is the interaction of P_{II} with the biotin carboxyl carrier protein (BCCP) of the acetyl-CoA carboxylase (ACC) [88]. The reaction of the acetyl-CoA carboxylase represents the first and committed step in fatty acid and PHB biosynthesis. A P_{II} deletion mutant obtains a significant reduced acetyl-CoA level due to the deregulation of the acetyl-CoA carboxylase [88]. The reduced acetyl-CoA level leads to an impaired production of PHB [200, 201]. P_{II} variants which permit an activation of the acetyl-CoA carboxylase could lead to an increased acetyl-CoA level. High availability of acetyl-CoA is a requirement for fatty acid and PHB biosynthesis.

1.1 Is the *Synechocystis* sp. BW86 an economical alternative to heterotrophic cyanophycin production?

Compared to other biotechnologically established bacteria, cyanobacteria possess a relative low growth rate. The slow growth represents the main bottleneck for the use of cyanobacteria in biotechnological industry. Conventional cultivation methods of cyanobacteria reach a biomass of roughly 1 g CDM per liter culture. The growth limitation is mainly due to insufficient light and CO₂ supplementation, especially at high cell densities [205] (figure 2, publication 3). Recently, a new cultivation method was developed to overcome this limitation, by using a two-tier vessel with membrane-mediated CO₂ supply. This cultivation method enabled rapid growth of *Synechocystis* sp. and *Synechococcus* sp. PCC 7002, with a final cell density up to 30 g CDM per liter [206]. Most recently, Lippi *et al.* used *Synechocystis* sp. wild-type and strain BW86 in this high-density cultivation system. During this study, a cyanophycin amount of 1 g per liter was reached in 96 h [207]. This is approximately four times more compared to the maximum cyanophycin yield observed by Trautmann *et al.* (publication 3) after 12 days cultivation.

¹ In comparison, the recombinant *E. coli* strain DH1 harboring *cphA* from *Synechocystis* sp. produces between 6.7 and 8.3 g CDM per liter culture in 16 h. The cyanophycin amounts during fed-batch fermentations using this production strain, were between 21 % and 24 % of the CDM [135], resulting in a cyanophycin production rate of 87.9 to 124.5 mg per liter and hour. This exceeds the production rate of strain BW86 according to Lippi *et al.* by a factor of 10. However the recombinant *E.coli* requires terrific broth complex medium, while *Synechocystis* sp. strain BW86 is cultivated in simple mineral medium and additionally sequesters the hazardous greenhouse-gas CO₂. Considering these super ordinate factors, the production of cyanophycin with cyanobacteria may in fact become an alternative to heterotrophic bacteria.

1.2 Further physiological impact by the P_{II}(I86N)

1.2.1 P_{II}(I86N) and the NtcA co-activator PipX

The crystal structure of P_{II}(I86N) shows an almost identical backbone as wild-type P_{II}. However, the T-loop adopts a compact conformation, which is a structural mimic of P_{II} in NAGK complex [100, 101]. Therefore we previously suggested that this variant is unable to interact with other P_{II} interaction partners. However, our results indicate a more complex influence of the P_{II}(I86N) variant to the physiology of *Synechocystis* sp.

¹ Paragraph adapted from Watzer, B. & Forchhammer, K. (2018) Cyanophycin, a nitrogen-rich reserve polymer. *Cyanobacteria*, ISBN: 978-953-51-6243-8

SPR spectroscopy studies confirmed that the P_{II}(I86N) variant can bind PipX. Moreover, in absence of effector molecules, the P_{II}(I86N) variant showed stronger interaction with PipX than wild-type P_{II}. Furthermore, the P_{II}(I86N) variant did not require positive stimulation by ADP to form a stable complex. It was previously shown that the P_{II}(I86N) variant did not respond to 2-OG in complex with NAGK [100]. However, an inhibitory effect of ATP and 2-OG on the P_{II}-PipX complex was also observed for the P_{II}(I86N) variant, although not as strong as in the case of the wild-type P_{II} protein.

Taken together, the interaction of P_{II}(I86N) and PipX is deregulated, but the complex stability is generally higher compared to wild-type P_{II} with PipX. Due to the stronger sequestration of PipX by P_{II}(I86N) we suggested a delayed nitrogen starvation response in a *Synechocystis* sp. harboring the P_{II}(I86N) variant. However, *Synechocystis* sp. wild-type and strain BW86 behaved similar during chlorosis. The only observable difference was a decreased viability of the BW86 strain when the nitrogen starvation was prolonged for more than four weeks.

As a future perspective, a transcriptome study could confirm an influence on the NtcA regulon by the P_{II}(I86N) variant. Moreover, resuscitation experiments could be performed to further investigate the influence of the P_{II}(I86N) variant.

1.2.2 P_{II}(I86N) influences PHB accumulation

Synechocystis sp strain BW86 accumulated significantly less PHB under phosphate starvation and slightly less PHB under potassium starvation compared to the wild-type. The P_{II}(I86N) variant causes an imbalanced metabolism, with a more than tenfold higher arginine content and slightly reduced pools of citrate/isocitrate, succinate and glycerate-3-P. During our metabolom study of *Synechocystis* sp. BW86 we were not able to detect acetyl-CoA; however it is most likely that the accelerated flux into arginine could drain the acetyl-CoA pool. PHB accumulation depends on the availability of acetyl-CoA.

Another explanation of the reduced acetyl-CoA level is the altered signaling of the P_{II}(I86N) variant. Previous studies document an relation between P_{II} and PHB accumulation [200, 201]. P_{II} can interact with the biotin carboxyl carrier protein (BCCP) of acetyl-CoA carboxylase (ACC) [88]. The reaction of the acetyl-CoA carboxylase represents the first and committed step in fatty acid and PHB synthesis. Due to the deregulated acetyl-CoA carboxylase, a P_{II} deletion mutant exhibits a reduced acetyl-CoA level [88]. The reduced acetyl-CoA level leads to an impaired accumulation of PHB [200, 201]. The P_{II}(I86N) variant could be also impaired in regulation of the acetyl-CoA carboxylase.

2. The signal transduction protein P_{II} controls nitrogen uptake

2.1 P_{II} regulate ammonium uptake

Binding of the P_{II} homolog GlnK to AmtB homologues represents a widely conserved function of P_{II} proteins in prokaryotes [49]. Our results revealed a similar involvement of GlnB in regulation of the Amt1 permease in the unicellular and non-diazotrophic cyanobacterium *Synechocystis* sp.

Pull-down and bacterial two-hybrid assays identified Amt1 as an interaction partner of P_{II} in *Synechocystis* sp. Examination of the binding properties of P_{II}-signaling mutants by bacterial two-hybrid assays gave strong evidences that the P_{II} interaction with the Amt1 permease is T-loop dependent, similar to the GlnK - AmtB interaction. The bended T-loop conformation of the P_{II}(I86N) variant led to an impaired interaction with Amt1. In agreement, *Synechocystis* sp. BW86 showed a similar impaired regulation of the ammonium uptake as a P_{II} deletion mutant. However, *Synechocystis* sp. BW86 showed a higher ammonium tolerance than the ΔP_{II} mutant. In a P_{II} deletion mutant, NAGK remains in a low activity state [90]. The high NAGK activity of *Synechocystis* sp. BW86 could promote faster ammonium assimilation and therefore protect the cell from an intracellular accumulation of toxic ammonium [119].

The GlnK - AmtB interaction in *E.coli* strongly responds to the ATP/ADP ratio. While ADP promotes a complex stabilization, ATP and synergistic bound 2-OG leads to its dissociation [107-109]. Nitrogen depletion induced dormancy is marked by a high 2-OG and low ATP level [208]. Under nitrogen starvation P_{II} is normally highly phosphorylated, however the C-terminal Venus fusion of the P_{II}-Venus variant could lead to an impaired phosphorylation [ref. Philipp Spät personal communication]. Providing ammonium to nitrogen starved cells induced a rapid drop in the 2-OG level and induced the translocation of P_{II}-Venus towards the plasma membrane. When the Amt1-channels are closed, no further ammonium can enter. In consequence the 2-OG level increased, which led to a dissociation of the P_{II}-Venus-Amt1 complex. This would explain the dissociation of P_{II}-Venus from the plasma membrane. (Figure 11 provides a hypothetical overview of the nitrate transporter regulation by P_{II})

2.2 P_{II} regulates nitrate uptake

Several previous studies documented an involvement of P_{II} in regulation of nitrate/nitrite uptake [92, 192-194]. Our data showed a direct regulation of NrtABCD by the interaction of P_{II} with the NrtC and NrtD subunits. This interaction appears to be T-loop dependent, since the P_{II}(I86N) variant could not complement the impaired nitrate utilization phenotype of a P_{II}

deletion mutant. A P_{II} deletion or changed T-loop conformation led to the inability to control the nitrate influx. In consequence, those mutants excreted nitrite into the medium.

Previous studies already showed the dependence of P_{II} and the C-terminal domain of NrtC on ammonium-induced inhibition of NrtABCD [92, 193]. The NrtC and NrtD subunits show the typical sequence motifs of the ATP-binding components of ABC-transporters [193, 209]. Our bacterial two-hybrid assays showed an interaction of P_{II} with both, NrtC and NrtD. Although bacterial two-hybrid assays allow only qualitative statements, the very weak interaction of P_{II} with NrtC and strong interaction with NrtD could indicate that NrtD represents the primary P_{II} target. Since the C-terminal domain of NrtC and P_{II} are necessary for regulation, Kloft *et al.* 2005 performed SPR spectroscopy to test if P_{II} interacts with NrtC *in vitro*. However, no interaction could be observed, supporting the suggestion that NrtD represents the primary P_{II} interaction partner [210].

P_{II} interaction with NrtC and NrtD mediates the ammonium and light dependent inhibition of nitrate uptake. The ammonium induced inhibition of nitrate utilization occurs independently from the P_{II} phosphorylation status [192, 194]. Therefore, we suggest that the rapid decreasing 2-OG level, which occurs due to the addition of ammonium, induces the nitrate uptake inhibition (figure 11). In agreement, the presence of L-methionine-d,l-sulfoximine (MSX) or azaserine (both inhibitors of the GS/GOGAT pathway) lead to an accumulation of 2-OG which causes an impaired ammonium dependent nitrate uptake inhibition [211].

Next to the ammonium dependent nitrate uptake inhibition, nitrogen assimilation is also tightly regulated by light/dark transitions [92, 196]. A transition from light to dark causes an immediate inhibition of nitrate uptake and an inhibition of the ammonium assimilating GS [196, 212]. Therefore, the increased ADP level, which is caused due to a low photosynthetic activity in the dark, could mediate the light dependent nitrate uptake inhibition. Accordingly it can be suggested that ADP stabilizes the interaction of non-phosphorylated P_{II} with NrtC and NrtD. However, nitrogen starved cells can utilize nitrate also in the absence of light (figure 8, publication 6). This could indicate that non-phosphorylated P_{II} interacts with NrtC and NrtD in higher affinity than phosphorylated P_{II}. Light-dependent nitrate uptake inhibition is only permitted by non-phosphorylated P_{II}, therefore the P_{II} phosphatase PphA plays an important role in this regulatory network. PphA permits the transition from phosphorylated to no-phosphorylated P_{II} which is required for light-dependent nitrate uptake inhibition (figure 11).

2.3 P_{II} regulate urea uptake

The cyanobacterial P_{II} protein is involved in the regulation of different ABC-type transporters like the bispecific nitrate/nitrite transporter NrtABCD and the bispecific cyanate/nitrite transporter CynABC [213]. Next to this known P_{II} targets, our data identified the UrtE subunit of the ABC-type UrtABCDE transporter as a novel P_{II} interaction partner.

According to sequence homologies, *urtA* encodes the periplasmic binding protein, *urtB* and *urtC* the transmembrane protein and *urtD* and *urtE* the ATP-binding protein [214]. P_{II} regulates the UrtABCDE transporter by interacting with the UrtE subunit. Since bacterial two-hybrid assays showed interaction of the P_{II}(I86N) variant with the UrtE subunit, this interaction is most likely T-loop independent. The P_{II}(I86N) variant enables a tightly bend T-loop conformation, which influences the T-loop dependent interactions with the Amt1 permease or the NrtC and NrtD subunits. However, the P_{II}(I86N) variant possess an almost identical backbone to that of the wild-type P_{II} [101]. In agreement, *Synechocystis* sp. harboring the P_{II}(I86N) variant showed the same urea utilization properties as the wild-type. In contrast, *Synechocystis* sp. harboring the P_{II}-Venus fusion-protein showed the same impaired regulation of the urea utilization as a P_{II} deletion mutant. The Venus fusion to the C-terminus of P_{II} could lead to a steric hindrance of the B- and C-loop while the T-loop remains unaffected. This observation further supports the suggestion that the interaction of P_{II} with UrtE appears T-loop independent, while the B- and C-loop play an important role.

Surprisingly, we could observe ammonium excretion of the P_{II} deletion mutant in response to the uncontrolled urea uptake. This ammonium excretion could be causal to limited ammonium assimilation by the GS/GOGAT cycle. The Δ P_{II} + P_{II}-Venus complementation strain also obtained an impaired urea uptake regulation, but showed no ammonium excretion. A possible explanation for this behavior is the deregulated Amt1 ammonium permease, which can operate in both directions [106]. The P_{II}-Venus variant interacts with Amt1 and could therefore avoid the ammonium excretion, while the P_{II} deletion mutant is unable to seal the Amt1 permease.

Urea is hydrolyzed by the enzyme urease to CO₂ and two molecules ammonium [93, 197]. The absence of ammonium excretion of the P_{II}-Venus complementation strain could also indicate a lower urease activity. Several unpublished pull down experiments with P_{II} as bait identified the urease as possible interaction partner of P_{II} in cyanobacteria [ref. Philipp Spät personal communication]. A high urease activity in the P_{II} deletion mutant could lead to an accumulation of ammonium and therefore causes an excretion. The P_{II}-Venus variant could regulate the urease. If this would be the case, a lowered urease activity would prevent an accumulation of ammonium.

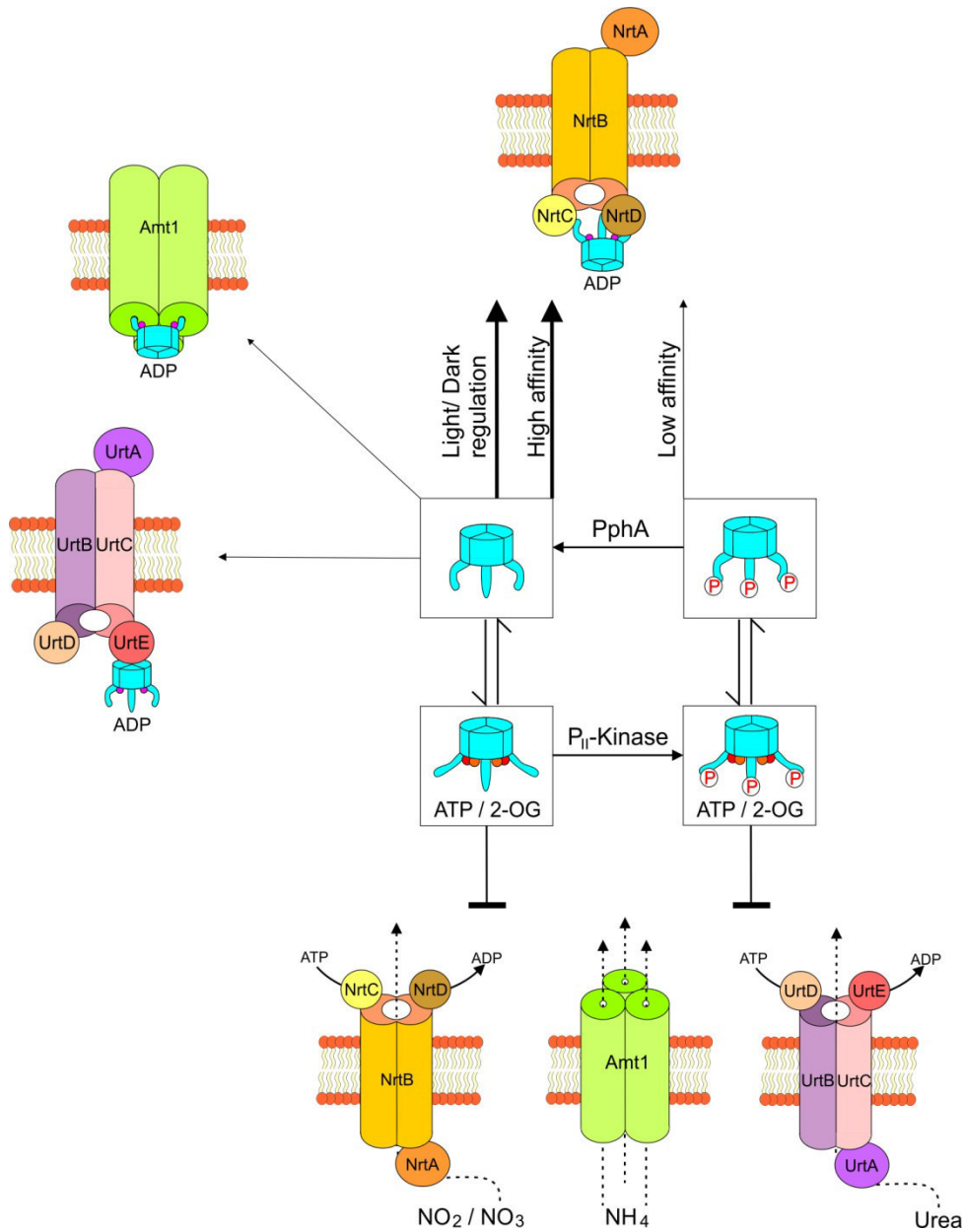


Figure 11 Hypothetical model of Amt1, NrtABCD and UrtABCDE regulation by P_{II} in *Synechocystis* sp. P_{II} can be present in four different forms: non-phosphorylated, phosphorylated, non-phosphorylated with ATP/2-OG and phosphorylated with ATP/2-OG. According to our data, we could confirm that non-phosphorylated can interact with Amt1 and the UrtE subunit, the latter in a T-loop independent manner. NrtABCD is regulated by both, non-phosphorylated and phosphorylated P_{II}. Non-phosphorylated P_{II} has a higher affinity towards NrtC and NrtD and allow the light dependent nitrate uptake inhibition. Phosphorylated P_{II} shows a lower affinity towards NrtC and NrtD and do not permit light mediated nitrate uptake inhibition. ADP probably stabilizes the complex of P_{II} with Amt1, NrtC/NrtD and UrtE. Binding of ATP/2-OG leads to a dissociation of P_{II} with Amt1, NrtC/NrtD and UrtE independently of its phosphorylation status.

3. Cell biology of the nitrogen storage polymer cyanophycin

3.1 CphA localization change indicates active and inactive forms

In order to gain new insight in the synthesis of cyanophycin we monitored the localization of CphA under cyanophycin accumulating and degrading conditions. Cyanophycin is a highly dynamic nitrogen storage component. The *cphA* gene is constitutively expressed under different nitrogen regimes to allow short term accumulation of cyanophycin [25]. In agreement, a quantitative proteomics study of resuscitating nitrogen-starved *Synechocystis* sp. cells showed only minor changes in the abundance of CphA [215]. We observed upcoming cyanophycin granules only six hours after the addition of nitrogen to fully chlorotic cells, supporting the results that CphA available remains sufficient even under non-cyanophycin accumulating conditions.

According to our microscopical observations regarding the CphA localization, we designed a model how cyanophycin accumulation occurs (figure 12). Under conditions without cyanophycin synthesis, such as exponential growth or nitrogen starvation, CphA is inactive and mainly located in the cytoplasm. Immediately after the induction of cyanophycin synthesis, CphA aggregated in foci that were randomly distributed in the cell. The location of these foci could be determined by providing agglomerations of cyanophycin-primers by the still unknown cyanophycin-primase. CphA, in its cyanophycin bound active form starts to elongate the primers. During this elongation process, the CphA foci increase their size and become visible as granules. During cyanophycin accumulation the number of foci and granules per cell continuously decreased. This effect could be explained by fusion of growing cyanophycin granules to larger aggregates. This behavior would also explain the amorphous structure of big granules, which can be found under conditions of high cellular cyanophycin content. The ring-like appearance of the fluorescence signal around the granules suggests that during cyanophycin accumulation, CphA-eGFP covers the surface of the granule. During cyanophycin degradation, CphA-eGFP changes from the granule surface localization to a cytoplasmic localization. This indicates that CphA dissociates from the granule surface during degradation and switches to the inactive cytoplasmic localized form.

3.2 CphA biochemical properties

CphA requires cyanophycin-primers, arginine, aspartate, MgCl₂, KCl, ATP and sulfdryl reagent for activity *in vitro* [143]. A removal of one of these components results in a strong decreased enzymatic activity. By immunoblot detection of CphA, we could show that Mg²⁺ is strictly required for the localization on the cyanophycin granule surface. Accordingly, Mg²⁺ may stabilize the active conformation of CphA which is able to bind the C-terminus of the

cyanophycin substrate. In absence of Mg^{2+} , CphA cannot maintain its enzymatic activity, which leads to a release from the granule surface.

The synthesis of cyanophycin is induced by the high cellular arginine level, which increases under growth-limiting conditions due to a lowered protein biosynthesis. High concentrations of arginine surpass the K_m of CphA for arginine and could trigger cyanophycin biosynthesis [90].

Whether CphA is subjected to additional activity control remains unclear. A phosphor-proteomic study of *Synechocystis* sp. grown in presence of nitrate, found evidences for a phosphorylation event of CphA near the C-terminus at Ser808 [216]. This phosphorylation event could be responsible for the CphA activation and inactivation. However, a later phosphor-proteomic study of resuscitating *Synechocystis* sp. could not confirm this phosphorylation event [215]. Therefore, whether CphA is subjected to additional activity control by phosphorylation remains to be elucidated.

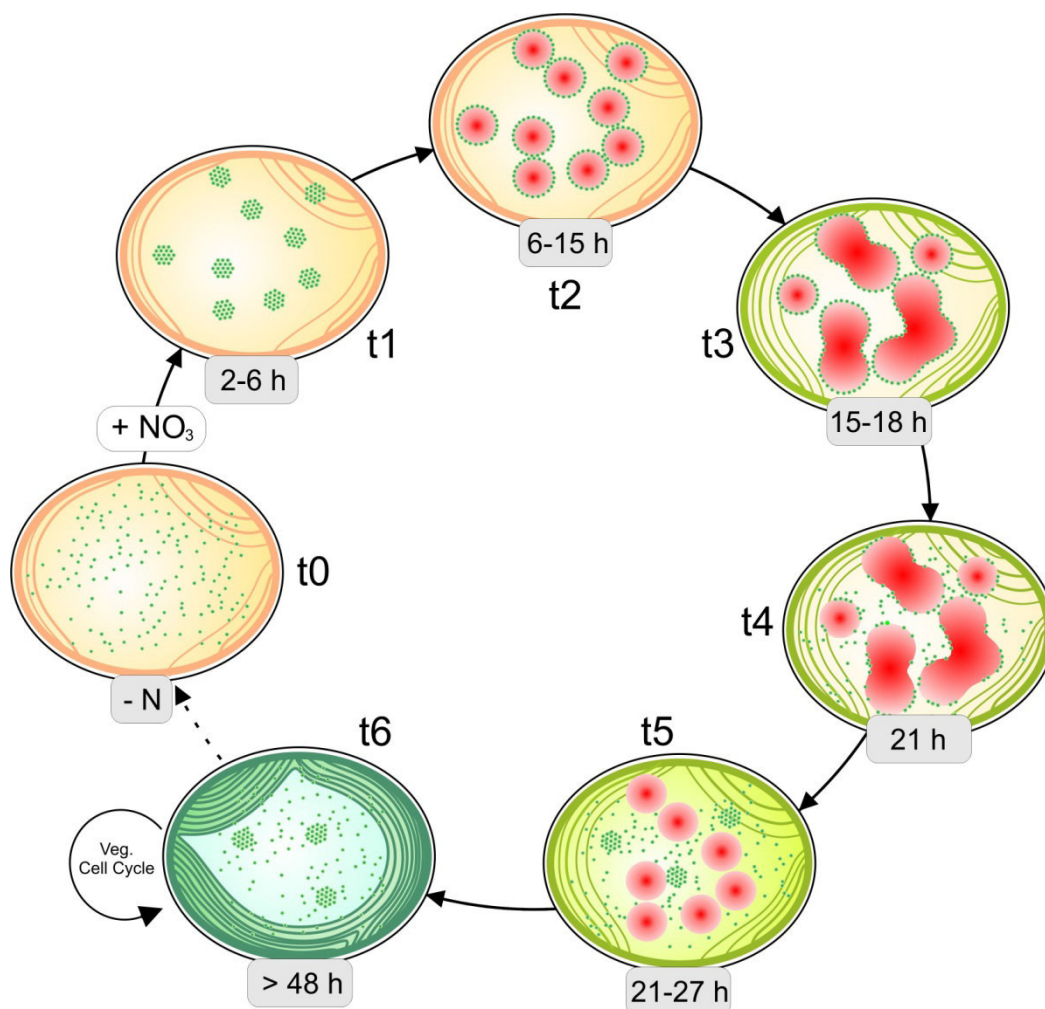


Figure 11 Hypothetical cycle of transient cyanophycin accumulation during resuscitation from nitrogen starvation. t0, when cyanophycin does not accumulate, CphA (green dots) is equally distributed in the cytoplasm; t1 2 to 6 h after the addition of a nitrogen source, CphA aggregates in foci; t2, 6 to 15 h after the addition of nitrogen, the first cyanophycin granules (red dots) appear, with CphA localized on their surface; t3, 15 to 18 h after nitrogen addition, adjacent growing granules merge when they collide, building amorphous granules with CphA on their surface; t4, 21 h after nitrogen addition, when cyanophycin starts to degrade, CphA dissociates from the granule surface; t5, 21 to 27 h after nitrogen addition, the granules become smaller, and CphA pass over in a cytoplasmic localization; t6, after the cell completes the resuscitation process after more than 48 h, they start to divide, with CphA mainly distributed in the cytoplasm but still forming a few foci. Veg, vegetative. (Figure taken from Watzer *et al.* 2018 (Publication 6))

3.3 Physiological role of cyanophycin in cyanobacteria

The ability to synthesize cyanophycin is wide spread among cyanobacteria and other prokaryotes. With a carbon/nitrogen ratio of 2:1, cyanophycin is perfectly suited as nitrogen storage.

In filamentous and diazotrophic cyanobacteria, cyanophycin has the function to increase the efficiency of nitrogen fixation [124]. In *Anabaena* sp. PCC 7120, all genes involved in cyanophycin metabolism are expressed in heterocysts and vegetative cells but at different expression levels. CphA and CphB are much higher expressed in heterocysts than in vegetative cells [165]. However, the expression of the isoaspartyl dipeptidases All3922 is significantly lower in heterocysts [124]. Cyanophycin deficiency in the filamentous cyanobacteria *Anabaena variabilis* ATCC 29413 shows no disadvantage in growth in presence of combined nitrogen or under diazotrophic and low light conditions. Only in combination of high light and diazotrophic conditions, the cyanophycin-deficient mutant shows a reduced growth [123]. Deletions of either CphB or the asparaginase All3922 in *Anabaena* sp. PCC 7120 showed a similarly impaired diazotrophic growth [124, 126].

These observations imply that the first step of cyanophycin catabolism, catalyzed by CphB, is localized in the heterocyst. The released β -Asp-Arg dipeptides are transported to the adjacent vegetative cells. Isoaspartyl dipeptidase All3922, present in the vegetative cells, cleave the β -Asp-Arg dipeptides and thereby releases aspartate and arginine [124]. When cyanophycin synthesis is impaired, due to a deletion of CphA, arginine and aspartate might be transported directly from heterocysts, which explain the normal growth of a CphA deletion mutant under standard diazotrophic growth.

Cyanophycin synthetase of group II (CphA2), present in filamentous nitrogen-fixing cyanobacteria, uses β -Asp-Arg dipeptides to synthesize cyanophycin [153]. Under diazotrophic growth in presence of high light, a CphA2-deficient mutant showed similar growth defects as a CphA1 mutant, although the overall cyanophycin content in this mutant was only slightly lowered [153]. This suggests the operation of a futile cycle, in which cyanophycin hydrolysis and immediate re-polymerization is probably of physiological significance in the context of high light and nitrogen fixing conditions [125].

3.3.1 Growth advantage of cyanophycin-deficient mutant under standard laboratory conditions

We showed that the deletion of CphA, which goes along with the inability to produce cyanophycin, has no impact on the nitrogen starvation response in *Synechocystis* sp. Both, wild-type and the Δ cphA strain behaved similar during chlorosis. However, the Δ cphA

mutant retains slightly higher residual pigment content in the final chlorotic state. Merritt *et al.* reported a cyanophycin-like polymer containing glutamic acid instead of arginine in nitrogen limited cells of *Synechocystis* sp. [217]. The bulk of proteins are degraded during chlorosis, which releases free amino acids. The cyanophycin-like polymer could act as a temporary storage compound for sequestration of the released amino acids. CphA could be involved in the biosynthesis of this polymer, since CphA shows a broad substrate spectrum next to arginine and aspartate in recombinant bacteria and yeast [182-184]. In the absence of this cyanophycin-like polymer, the chlorosis reaction in the $\Delta cphA$ mutant might be slowed down. The remaining pigments could assume the storage function of the cyanophycin-like polymer.

Since cyanophycin transiently accumulates during resuscitation from nitrogen starvation [25, 120], we focused on this process to investigate the physiological role of cyanophycin in *Synechocystis* sp. Surprisingly, under standard laboratory conditions, meaning continuous of light and nitrogen excess, the $\Delta cphA$ showed a clear growth advantage over the wild-type in liquid medium or on agar-plates. This result can be explained by the energy consuming cyanophycin synthesis. CphA from *Synechocystis* sp. converts 1.3 ± 0.1 mol ATP to ADP per mol incorporated amino acid into cyanophycin *in vitro* [152]. Without need of cyanophycin as a nitrogen storage compound, the synthesis of cyanophycin is only a burden to the cells, and consequently, the cyanophycin-deficient $\Delta cphA$ mutant has an advantage over the wild-type.

3.3.2 Cyanophycin accumulation provides fitness advantage under natural conditions

We hypothesized cyanophycin accumulation to be a cellular strategy to overcome temporary environmental nitrogen limitations. Our growth and resuscitation experiments of *Synechocystis* sp. wild-type and $\Delta cphA$ confirmed this suggestion. The ability to store nitrogen in form of cyanophycin provided a fitness advantage during resuscitation under fluctuating or limiting nitrogen supplementation. When nitrogen fluctuation and limitation was combined, the cyanophycin deficient mutant is not able to fully resuscitate from chlorosis.

The unicellular diazotrophic cyanobacterium *Cyanothece* sp. ATCC 51142 and the filamentous cyanobacterium *Trichodesmium* sp. use cyanophycin as temporary nitrogen storage to enable the coexistence of nitrogen fixation and photosynthesis in the same cell [121, 122]. These cyanobacteria perform nitrogen fixation in the night and store the fixed nitrogen in cyanophycin. During the day, when photosynthesis is performed, the cyanophycin is degraded to mobilize the stored nitrogen. Based on this behavior in

diazotrophic cyanobacteria we hypothesized a similar role of cyanophycin in non-diazotrophic cyanobacteria. When we combined fluctuating nitrogen supplementation and day/night cycles, the resuscitation of *Synechocystis* sp. wild-type cells proceeded as fast as in continuous light, with growth restoration after 48 h. In contrast, the cyanophycin deficient mutant was not able to resuscitate.

Interestingly, artificial laboratory conditions are not providing any fitness advantage for cyanophycin accumulating cells, whereas in a fluctuating environment, cyanophycin accumulation becomes beneficial. CphA is constitutively expressed in *Synechocystis* sp. and therefore, the cells are programmed to overcome fluctuating nitrogen supply and transient periods of starvation.

4. Final conclusions

Cyanophycin is a highly dynamic nitrogen storage polymer, whose metabolism is regulated by the P_{II} protein. The constitutive expression of CphA allows an immediate cyanophycin synthesis to overcome transient periods of starvation in a constantly changing environment. Thereby, CphA is most probably regulated by the intracellular arginine level. High concentrations of arginine surpass the K_m of CphA and could trigger cyanophycin biosynthesis. Accordingly cyanophycin could act as a sink for arginine to optimize nitrogen utilization.

The P_{II} protein controls the committed step in the arginine biosynthesis and is therefore significantly involved in the regulation of cyanophycin. The P_{II}(I86N) variant represents a highly potent NAGK activator, causing a strongly increased arginine level. The high arginine content of *Synechocystis* sp. BW86, harboring the P_{II}(I86N) variant, leads to a strongly enhanced cyanophycin synthesis. *Synechocystis* sp. BW86 is the cyanophycin producer strain with the highest abundance of cyanophycin described so far. This exemplifies the possibilities of using custom-tailed P_{II} proteins as a novel approach of metabolic engineering.

In summary, the P_{II}(I86N) variant simulates the situation of high energy and nitrogen supply. Additionally, we could confirm that the P_{II}(I86N) variant binds PipX. Moreover, the complex formation of P_{II}(I86N) and PipX is more stable compared to the complex of wild-type P_{II} with PipX. However, this deregulation has only minor effects on the nitrogen starvation response. Furthermore, we observed a reduced PHB accumulation of *Synechocystis* sp. strain BW86, which can be explained by the accelerated carbon flux into the arginine biosynthesis. The impaired ammonium utilization of *Synechocystis* sp. harboring the P_{II}(I86N) variant implied a relation between P_{II} signaling and ammonium uptake in cyanobacteria. In order to analyze a possible regulation of the cyanobacterial Amt1 permease by P_{II} we found further evidences for an involvement of P_{II} in regulation of the nitrate/ nitrite transporter NrtABCD and the urea transporter UrtABCDE.

VIII. References

1. Soo, R.M., Hemp, J., Parks, D.H., Fischer, W.W., and Hugenholtz, P. (2017). On the origins of oxygenic photosynthesis and aerobic respiration in cyanobacteria. *Science* 355, 1436-1439.
2. Whitton, B.A. (2012). *Ecology of cyanobacteria II : their diversity in space and time*, (New York: Springer).
3. Blankenship, R.E. (2014). *Molecular mechanisms of photosynthesis*, Second edition. Edition, (Chichester, West Sussex: Wiley/Blackwell).
4. Herrero, A., and Flores, E. (2008). *The cyanobacteria : molecular biology, genomics, and evolution*, (Norfolk, UK: Caister Academic Press).
5. Rippka, R., Deruelles, J., Waterbury, J.B., Herdman, M., and Stanier, R.Y. (1979). Generic assignments, strain histories and properties of pure cultures of cyanobacteria. *Journal of General Microbiology* 111, 1-61.
6. Bassham, J.A. (1979). The reductive pentose phosphate cycle and its regulation. In *Photosynthesis II: Photosynthetic Carbon Metabolism and Related Processes*, M. Gibbs and E. Latzko, eds. (Berlin, Heidelberg: Springer Berlin Heidelberg), pp. 9-30.
7. Bauwe, H., Hagemann, M., and Fernie, A.R. (2010). Photorespiration: players, partners and origin. *Trends in Plant Science* 15, 330-336.
8. Kaplan, A., Schwarz, R., Lieman-Hurwitz, J., Ronen-Tarazi, M., and Reinhold, L. (1994). Physiological and molecular studies on the response of cyanobacteria to changes in the ambient inorganic carbon concentration. In *The Molecular Biology of Cyanobacteria*, D.A. Bryant, ed. (Dordrecht: Springer Netherlands), pp. 469-485.
9. Price, G.D., Badger, M.R., Woodger, F.J., and Long, B.M. (2008). Advances in understanding the cyanobacterial CO₂-concentrating-mechanism (CCM): functional components, Ci transporters, diversity, genetic regulation and prospects for engineering into plants. *Journal of Experimental Botany* 59, 1441-1461.
10. Zhang, S.Y., and Bryant, D.A. (2011). The tricarboxylic acid cycle in cyanobacteria. *Science* 334, 1551-1553.
11. Smith, A.J., London, J., and Stanier, R.Y. (1967). Biochemical basis of obligate autotrophy in blue-green algae and Thiobacilli. *Journal of Bacteriology* 94, 972-983.
12. Pearce, J., and Carr, N.G. (1967). An incomplete tricarboxylic acid cycle in blue-green alga *Anabaena variabilis*. *Biochemical Journal* 105, 45.
13. Steinhauser, D., Fernie, A.R., and Araujo, W.L. (2012). Unusual cyanobacterial TCA cycles: not broken just different. *Trends in Plant Science* 17, 503-509.
14. Damrow, R., Maldener, I., and Zilliges, Y. (2016). The multiple functions of common microbial carbon polymers, glycogen and PHB, during stress responses in the non-diazotrophic cyanobacterium *Synechocystis* sp PCC 6803. *Frontiers in Microbiology* 7.
15. Preiss, J., and Romeo, T. (1994). Molecular-biology and regulatory aspects of glycogen biosynthesis in bacteria. *Progress in Nucleic Acid Research and Molecular Biology* 47, 299-329.
16. Cifuentes, J.O., Comino, N., Madariaga-Marcos, J., Lopez-Fernandez, S., Garcia-Alija, M., Agirre, J., Albesa-Jove, D., and Guerin, M.E. (2016). Structural basis of glycogen biosynthesis regulation in bacteria. *Structure* 24, 1613-1622.

17. Shearer, J., and Graham, T.E. (2002). New perspectives on the storage and organization of muscle glycogen. *Canadian Journal of Applied Physiology-Revue Canadienne De Physiologie Appliquee* 27, 179-203.
18. Buschiazzo, A., Ugalde, J.E., Guerin, M.E., Shepard, W., Ugalde, R.A., and Alzari, P.M. (2004). Crystal structure of glycogen synthase: homologous enzymes catalyze glycogen synthesis and degradation. *Embo Journal* 23, 3196-3205.
19. Yoo, S.H., Spalding, M.H., and Jane, J.L. (2002). Characterization of cyanobacterial glycogen isolated from the wild type and from a mutant lacking of branching enzyme. *Carbohydrate Research* 337, 2195-2203.
20. Fu, J., and Xu, X.D. (2006). The functional divergence of two *glgP* homologues in *Synechocystis* sp PCC 6803. *Fems Microbiology Letters* 260, 201-209.
21. Ball, S.G., and Morell, M.K. (2003). From bacterial glycogen to starch: Understanding the biogenesis of the plant starch granule. *Annual Review of Plant Biology* 54, 207-233.
22. Grundel, M., Scheunemann, R., Lockau, W., and Zilliges, Y. (2012). Impaired glycogen synthesis causes metabolic overflow reactions and affects stress responses in the cyanobacterium *Synechocystis* sp PCC 6803. *Microbiology-Sgm* 158, 3032-3043.
23. Wilson, W.A., Roach, P.J., Montero, M., Baroja-Fernandez, E., Munoz, F.J., Eydallin, G., Viale, A.M., and Pozueta-Romero, J. (2010). Regulation of glycogen metabolism in yeast and bacteria. *Fems Microbiology Reviews* 34, 952-985.
24. Beck, C., Knoop, H., Axmann, I.M., and Steuer, R. (2012). The diversity of cyanobacterial metabolism: genome analysis of multiple phototrophic microorganisms. *BMC Genomics* 13, 56.
25. Klotz, A., Georg, J., Budinska, L., Watanabe, S., Reimann, V., Januszewski, W., Sobotka, R., Jendrossek, D., Hess, W.R., and Forchhammer, K. (2016). Awakening of a dormant cyanobacterium from nitrogen chlorosis reveals a genetically determined program. *Current Biology* 26, 2862-2872.
26. Klotz, A., and Forchhammer, K. (2017). Glycogen, a major player for bacterial survival and awakening from dormancy. *Future Microbiology* 12, 101-104.
27. Dawes, E.A. (1988). Polyhydroxybutyrate: an intriguing biopolymer. *Bioscience Reports* 8, 537-547.
28. Lopez, N.I., Pettinari, M.J., Nickel, P.I., and Mendez, B.S. (2015). Polyhydroxyalkanoates: Much more than biodegradable plastics. *Advances in applied microbiology* 93, 73-106.
29. Stal, L.J. (1992). Poly(Hydroxyalkanoate) in cyanobacteria - an overview. *Fems Microbiology Letters* 103, 169-180.
30. Panda, B., Jain, P., Sharma, L., and Mallick, N. (2006). Optimization of cultural and nutritional conditions for accumulation of poly-beta-hydroxybutyrate in *Synechocystis* sp. PCC 6803. *Bioresource Technology* 97, 1296-1301.
31. Hauf, W., Schlebusch, M., Hüge, J., Kopka, J., Hagemann, M., and Forchhammer, K. (2013). Metabolic changes in *Synechocystis* PCC 6803 upon nitrogen-starvation: Excess NADPH sustains polyhydroxybutyrate accumulation. *Metabolites* 3, 101-118.
32. Taroncher-Oldenberg, G., Nishina, K., and Stephanopoulos, G. (2000). Identification and analysis of the polyhydroxyalkanoate-specific beta-ketothiolase and acetoacetyl coenzyme A reductase genes in the cyanobacterium *Synechocystis* sp. strain PCC6803. *Applied and Environmental Microbiology* 66, 4440-4448.

33. Rehm, B. (2006). *Microbial bionanotechnology : biological self-assembly systems and biopolymer-based nanostructures*, (Wymondham, Norfolk, U.K.: Horizon Bioscience).
34. Hein, S., Tran, H., and Steinbuchel, A. (1998). *Synechocystis* sp. PCC 6803 possesses a two-component polyhydroxyalkanoic acid synthase similar to that of anoxygenic purple sulfur bacteria. *Archives of Microbiology* 170, 162-170.
35. Jendrossek, D. (2009). Polyhydroxyalkanoate granules are complex subcellular organelles (Carbonosomes). *Journal of Bacteriology* 191, 3195-3202.
36. Bresan, S., Sznajder, A., Hauf, W., Forchhammer, K., Pfeiffer, D., and Jendrossek, D. (2016). Polyhydroxyalkanoate (PHA) granules have no phospholipids. *Scientific Reports* 6.
37. Wieczorek, R., Pries, A., Steinbuchel, A., and Mayer, F. (1995). Analysis of a 24-kilodalton protein associated with the polyhydroxyalkanoic acid granules in *Alcaligenes eutrophus*. *Journal of Bacteriology* 177, 2425-2435.
38. Pfeiffer, D., Wahl, A., and Jendrossek, D. (2011). Identification of a multifunctional protein, PhaM, that determines number, surface to volume ratio, subcellular localization and distribution to daughter cells of poly(3-hydroxybutyrate), PHB, granules in *Ralstonia eutropha* H16. *Molecular Microbiology* 82, 936-951.
39. Jendrossek, D., and Pfeiffer, D. (2014). New insights in the formation of polyhydroxyalkanoate granules (Carbonosomes) and novel functions of poly(3-hydroxybutyrate). *Environmental Microbiology* 16, 2357-2373.
40. Flores, E., and Herrero, A. (2005). Nitrogen assimilation and nitrogen control in cyanobacteria. *Biochemical Society Transactions* 33, 164-167.
41. Muro-Pastor, M.I., Reyes, J.C., and Florencio, F.J. (2005). Ammonium assimilation in cyanobacteria. *Photosynthesis Research* 83.
42. Muro-Pastor, M.I., Reyes, J.C., and Florencio, F.J. (2001). Cyanobacteria perceive nitrogen status by sensing intracellular 2-oxoglutarate levels. *Journal of Biological Chemistry* 276, 38320-38328.
43. Forchhammer, K. (2004). Global carbon/nitrogen control by P_{II} signal transduction in cyanobacteria: from signals to targets. *Fems Microbiology Reviews* 28, 319-333.
44. Yuan, J., Doucette, C.D., Fowler, W.U., Feng, X.J., Piazza, M., Rabitz, H.A., Wingreen, N.S., and Rabinowitz, J.D. (2009). Metabolomics-driven quantitative analysis of ammonia assimilation in *E. coli*. *Molecular Systems Biology* 5, 302.
45. Dodsworth, J.A., Cady, N.C., and Leigh, J.A. (2005). 2-oxoglutarate and the P_{II} homologues NifI(1) and NifI(2) regulate nitrogenase activity in cell extracts of *Methanococcus maripaludis*. *Molecular Microbiology* 56, 1527-1538.
46. Brauer, M.J., Yuan, J., Bennett, B.D., Lu, W.Y., Kimball, E., Botstein, D., and Rabinowitz, J.D. (2006). Conservation of the metabolomic response to starvation across two divergent microbes. *Proceedings of the National Academy of Sciences of the United States of America* 103, 19302-19307.
47. Senior, P.J. (1975). Regulation of nitrogen-metabolism in *Escherichia coli* and *Klebsiella aerogenes* - Studies with continuous culture technique. *Journal of Bacteriology* 123, 407-418.
48. Yan, D.L., Lenz, P., and Hwa, T. (2011). Overcoming fluctuation and leakage problems in the quantification of intracellular 2-oxoglutarate levels in *Escherichia coli*. *Applied and Environmental Microbiology* 77, 6763-6771.

49. Forchhammer, K. (2008). P_{II} signal transducers: novel functional and structural insights. *Trends Microbiology* 16, 65-72.
50. Fokina, O., Chellamuthu, V.R., Forchhammer, K., and Zeth, K. (2010). Mechanism of 2-oxoglutarate signaling by the *Synechococcus elongatus* P_{II} signal transduction protein. *Proceedings of the National Academy of Sciences of the United States of America* 107, 19760-19765.
51. Tanigawa, R., Shirokane, M., Maeda, S., Omata, T., Tanaka, K., Takahashi, H., and Takahashi, H. (2002). Transcriptional activation of NtcA-dependent promoters of *Synechococcus* sp PCC 7942 by 2-oxoglutarate *in vitro*. *Proceedings of the National Academy of Sciences of the United States of America* 99, 4251-4255.
52. Cases, I., Velazquez, F., and de Lorenzo, V. (2007). The ancestral role of the phosphoenolpyruvate-carbohydrate phosphotransferase system (PTS) as exposed by comparative genomics. *Research in Microbiology* 158, 666-670.
53. Doucette, C.D., Schwab, D.J., Wingreen, N.S., and Rabinowitz, J.D. (2011). Alpha-ketoglutarate coordinates carbon and nitrogen utilization via enzyme I inhibition. *Nature Chemical Biology* 7, 894-901.
54. Bettenbrock, K., Sauter, T., Jahreis, K., Kremling, A., Lengeler, J.W., and Gilles, E.D. (2007). Correlation between growth rates, EIIA(Crr) phosphorylation, and intracellular cyclic AMP levels in *Escherichia coli* K-12. *Journal of Bacteriology* 189, 6891-6900.
55. Botsford, J.L., and Harman, J.G. (1992). Cyclic-AMP in prokaryotes. *Microbiological Reviews* 56, 100-122.
56. Gorke, B., and Stulke, J. (2008). Carbon catabolite repression in bacteria: many ways to make the most out of nutrients. *Nature Reviews Microbiology* 6, 613-624.
57. Huergo, L.F., and Dixon, R. (2015). The emergence of 2-oxoglutarate as a master regulator metabolite. *Microbiology and Molecular Biology Reviews* 79, 419-435.
58. Vitousek, P.M., and Howarth, R.W. (1991). Nitrogen limitation on land and in the sea - how can it occur. *Biogeochemistry* 13, 87-115.
59. Flores, E., and Herrero, A. (1994). Assimilatory nitrogen metabolism and its regulation. In *The Molecular Biology of Cyanobacteria*, D.A. Bryant, ed. (Dordrecht: Springer Netherlands), pp. 487-517.
60. Labarre, J., Thuriaux, P., and Chauvat, F. (1987). Genetic-analysis of amino-acid-transport in the facultatively heterotrophic cyanobacterium *Synechocystis* sp PCC 6803. *Journal of Bacteriology* 169, 4668-4673.
61. Schwarz, R., and Forchhammer, K. (2005). Acclimation of unicellular cyanobacteria to macronutrient deficiency: emergence of a complex network of cellular responses. *Microbiology-Sgm* 151, 2503-2514.
62. Giner-Lamia, J., Robles-Rengel, R., Hernandez-Prieto, M.A., Muro-Pastor, M.I., Florencio, F.J., and Futschik, M.E. (2017). Identification of the direct regulon of NtcA during early acclimation to nitrogen starvation in the cyanobacterium *Synechocystis* sp. PCC 6803. *Nucleic Acids Research* 45, 11800-11820.
63. Vegapalas, M.A., Flores, E., and Herrero, A. (1992). NtcA, a global nitrogen regulator from the cyanobacterium *Synechococcus* that belongs to the Crp family of bacterial regulators. *Molecular Microbiology* 6, 1853-1859.
64. Grossman, A.R., Schaefer, M.R., Chiang, G.G., and Collier, J.L. (1993). The phycobilisome, a light-harvesting complex responsive to environmental-conditions. *Microbiological Reviews* 57, 725-749.

65. Collier, J.L., and Grossman, A.R. (1994). A small polypeptide triggers complete degradation of light-harvesting phycobiliproteins in nutrient-deprived cyanobacteria. *Embo Journal* 13, 1039-1047.
66. Klotz, A., Reinhold, E., Doello, S., and Forchhammer, K. (2015). Nitrogen starvation acclimation in *Synechococcus elongatus*: Redox-control and the role of nitrate reduction as an electron sink. *Life (Basel)* 5, 888-904.
67. van Waasbergen, L.G., Dolganov, N., and Grossman, A.R. (2002). NblS, a gene involved in controlling photosynthesis-related gene expression during high light and nutrient stress in *Synechococcus elongatus* PCC 7942. *Journal of Bacteriology* 184, 2481-2490.
68. Ruiz, D., Salinas, P., Lopez-Redondo, M.L., Cayuela, M.L., Marina, A., and Contreras, A. (2008). Phosphorylation-independent activation of the atypical response regulator NblR. *Microbiology-Sgm* 154, 3002-3015.
69. Kato, H., Kubo, T., Hayashi, M., Kobayashi, I., Yagasaki, T., Chibazakura, T., Watanabe, S., and Yoshikawa, H. (2011). Interactions between histidine kinase NblS and the response regulators RpaB and SrrA are involved in the bleaching process of the cyanobacterium *Synechococcus elongatus* PCC 7942. *Plant and Cell Physiology* 52, 2115-2122.
70. Sauer, J., Gorl, M., and Forchhammer, K. (1999). Nitrogen starvation in *Synechococcus* PCC 7942: involvement of glutamine synthetase and NtcA in phycobiliprotein degradation and survival. *Archives of Microbiology* 172, 247-255.
71. Allen, M.M. (1984). Cyanobacterial cell inclusions. *Annual Review of Microbiology* 38, 1-25.
72. Bryant, D. (1986). The cyanobacterial photosynthetic apparatus: comparison to those of higher plants and photosynthetic bacteria. *Canadian Bulletin of Fisheries and Aquatic Sciences* 214, 423-500.
73. Wanner, G., Henkelmann, G., Schmidt, A., and Kost, H.P. (1986). Nitrogen and sulfur starvation of the cyanobacterium *Synechococcus* sp. PCC 6301 - an ultrastructural, morphometrical, and biochemical-comparison. *Zeitschrift für Naturforschung C* 41, 741-750.
74. Sauer, J., Schreiber, U., Schmid, R., Volker, U., and Forchhammer, K. (2001). Nitrogen starvation-induced chlorosis in *Synechococcus* PCC 7942. Low-level photosynthesis as a mechanism of long-term survival. *Plant Physiology* 126, 233-243.
75. Forchhammer, K., and Luddecke, J. (2016). Sensory properties of the P_{II} signalling protein family. *FEBS Journal* 283, 425-437.
76. Arcondeguy, T., Jack, R., and Merrick, M. (2001). P_{II} signal transduction proteins, pivotal players in microbial nitrogen control. *Microbiology and Molecular Biology Reviews* 65, 80-105.
77. Zeth, K., Fokina, O., and Forchhammer, K. (2014). Structural basis and target-specific modulation of ADP sensing by the *Synechococcus elongatus* P_{II} signaling protein. *Journal of Biological Chemistry* 289, 8960-8972.
78. Cheah, E., Carr, P.D., Suffolk, P.M., Vasudevan, S.G., Dixon, N.E., and Ollis, D.L. (1994). Structure of the *Escherichia coli* signal transducing protein P_{II}. *Structure* 2, 981-990.
79. Xu, Y.B., Carr, P.D., Clancy, P., Garcia-Dominguez, M., Forchhammer, K., Florencio, F., de Marsac, N.T., Vasudevan, S.G., and Ollis, D.L. (2003). The structures of the P_{II}

- proteins from the cyanobacteria *Synechococcus* sp PCC 7942 and *Synechocystis* sp PCC 6803. *Acta Crystallographica Section D-Biological Crystallography* 59, 2183-2190.
80. Llacer, J.L., Contreras, A., Forchhammer, K., Marco-Marin, C., Gil-Ortiz, F., Maldonado, R., Fita, I., and Rubio, V. (2007). The crystal structure of the complex of P_{II} and acetylglutamate kinase reveals how P_{II} controls the storage of nitrogen as arginine. *Proceedings of the National Academy of Sciences of the United States of America* 104, 17644-17649.
 81. Zhao, M.X., Jiang, Y.L., Xu, B.Y., Chen, Y., Zhang, C.C., and Zhou, C.Z. (2010). Crystal structure of the cyanobacterial signal transduction protein P_{II} in complex with PipX. *Journal of Molecular Biology* 402, 552-559.
 82. Forchhammer, K., and Tandeau de Marsac, N. (1995). Phosphorylation of the P_{II} protein (*glnB* gene product) in the cyanobacterium *Synechococcus* sp. strain PCC 7942: analysis of in vitro kinase activity. *Journal of Bacteriology* 177, 5812-5817.
 83. Forchhammer, K., and Hedler, A. (1997). Phosphoprotein P_{II} from cyanobacteria—analysis of functional conservation with the P_{II} signal-transduction protein from *Escherichia coli*. *European Journal of Biochemistry* 244, 869-875.
 84. Jiang, P., Peliska, J.A., and Ninfa, A.J. (1998). Enzymological characterization of the signal-transducing uridylyltransferase/uridylyl-removing enzyme (EC 2.7.7.59) of *Escherichia coli* and its interaction with the P_{II} protein. *Biochemistry* 37, 12782-12794.
 85. Hesketh, A., Fink, D., Gust, B., Rexer, H.U., Scheel, B., Chater, K., Wohlleben, W., and Engels, A. (2002). The GlnD and GlnK homologues of *Streptomyces coelicolor* A3(2) are functionally dissimilar to their nitrogen regulatory system counterparts from enteric bacteria. *Molecular Microbiology* 46, 319-330.
 86. Radchenko, M., and Merrick, M. (2011). The role of effector molecules in signal transduction by P_{II} proteins. *Biochemical Society Transactions* 39, 189-194.
 87. Espinosa, J., Forchhammer, K., and Contreras, A. (2007). Role of the *Synechococcus* PCC 7942 nitrogen regulator protein PipX in NtcA-controlled processes. *Microbiology-Sgm* 153, 711-718.
 88. Hauf, W., Schmid, K., Gerhardt, E.C., Huergo, L.F., and Forchhammer, K. (2016). Interaction of the nitrogen regulatory protein GlnB (P_{II}) with biotin carboxyl carrier protein (BCCP) controls acetyl-CoA levels in the cyanobacterium *Synechocystis* sp. PCC 6803. *Frontiers in Microbiology* 7, 1700.
 89. Maheswaran, M., Urbanke, C., and Forchhammer, K. (2004). Complex formation and catalytic activation by the P_{II} signaling protein of N-acetyl-L-glutamate kinase from *Synechococcus elongatus* strain PCC 7942. *Journal of Biological Chemistry* 279, 55202-55210.
 90. Maheswaran, M., Ziegler, K., Lockau, W., Hagemann, M., and Forchhammer, K. (2006). P_{II}-regulated arginine synthesis controls accumulation of cyanophycin in *Synechocystis* sp strain PCC 6803. *Journal of Bacteriology* 188, 2730-2734.
 91. Heinrich, A., Maheswaran, M., Ruppert, U., and Forchhammer, K. (2004). The *Synechococcus elongatus* P_{II} signal transduction protein controls arginine synthesis by complex formation with N-acetyl-L-glutamate kinase. *Molecular Microbiology* 52, 1303-1314.
 92. Lee, H.M., Flores, E., Herrero, A., Houmard, J., and de Marsac, N.T. (1998). A role for the signal transduction protein P_{II} in the control of nitrate/nitrite uptake in a cyanobacterium. *Febs Letters* 427, 291-295.

93. Esteves-Ferreira, A.A., Inaba, M., Fort, A., Araújo, W.L., and Sulpice, R. (2018). Nitrogen metabolism in cyanobacteria: metabolic and molecular control, growth consequences and biotechnological applications. *Critical Reviews in Microbiology*, 1-20.
94. Espinosa, J., Rodriguez-Mateos, F., Salinas, P., Lanza, V.F., Dixon, R., de la Cruz, F., and Contreras, A. (2014). PipX, the coactivator of NtcA, is a global regulator in cyanobacteria. *Proceedings of the National Academy of Sciences of the United States of America* 111, E2423-2430.
95. Llacer, J.L., Espinosa, J., Castells, M.A., Contreras, A., Forchhammer, K., and Rubio, V. (2010). Structural basis for the regulation of NtcA-dependent transcription by proteins PipX and P_{II}. *Proceedings of the National Academy of Sciences of the United States of America* 107, 15397-15402.
96. Fokina, O., Herrmann, C., and Forchhammer, K. (2011). Signal-transduction protein P_{II} from *Synechococcus elongatus* PCC 7942 senses low adenylate energy charge *in vitro*. *Biochemical Journal* 440, 147-156.
97. Espinosa, J., Forchhammer, K., Burillo, S., and Contreras, A. (2006). Interaction network in cyanobacterial nitrogen regulation: PipX, a protein that interacts in a 2-oxoglutarate dependent manner with P_{II} and NtcA. *Molecular Microbiology* 61, 457-469.
98. Cunin, R., Glansdorff, N., Pierard, A., and Stalon, V. (1986). Biosynthesis and metabolism of arginine in bacteria. *Microbiological Reviews* 50, 314-352.
99. Caldovic, L., and Tuchman, M. (2003). N-acetylglutamate and its changing role through evolution. *Biochemical Journal* 372, 279-290.
100. Fokina, O., Chellamuthu, V.R., Zeth, K., and Forchhammer, K. (2010). A novel signal transduction protein P_{II} variant from *Synechococcus elongatus* PCC 7942 indicates a two-step process for NAGK-P_{II} complex formation. *Journal of Molecular Biology* 399, 410-421.
101. Zeth, K., Fokina, O., and Forchhammer, K. (2012). An engineered P_{II} protein variant that senses a novel ligand: atomic resolution structure of the complex with citrate. *Acta Crystallographica Section D-Biological Crystallography* 68, 901-908.
102. Wirén, N.v., and Merrick, M. (2004). Regulation and function of ammonium carriers in bacteria, fungi, and plants. In *Molecular Mechanisms Controlling Transmembrane Transport*. (Berlin, Heidelberg: Springer Berlin Heidelberg), pp. 95-120.
103. Conroy, M.J., Durand, A., Lupo, D., Li, X.D., Bullough, P.A., Winkler, F.K., and Merrick, M. (2007). The crystal structure of the *Escherichia coli* AmtB-GlnK complex reveals how GlnK regulates the ammonia channel. *Proceedings of the National Academy of Sciences of the United States of America* 104, 1213-1218.
104. Khademi, S., O'Connell, J., Remis, J., Robles-Colmenares, Y., Miericke, L.J.W., and Stroud, R.M. (2004). Mechanism of ammonia transport by Amt/MEP/Rh: Structure of AmtB at 1.35 angstrom. *Science* 305, 1587-1594.
105. Zheng, L., Kostrewa, D., Berneche, S., Winkler, F.K., and Li, X.D. (2004). The mechanism of ammonia transport based on the crystal structure of AmtB of *Escherichia coli*. *Proceedings of the National Academy of Sciences of the United States of America* 101, 17090-17095.
106. Soupene, E., Lee, H., and Kustu, S. (2002). Ammonium/methylammonium transport (Amt) proteins facilitate diffusion of NH₃ bidirectionally. *Proceedings of the National Academy of Sciences of the United States of America* 99, 3926-3931.

107. Gruswitz, F., O'Connell, J., and Stroud, R.M. (2007). Inhibitory complex of the transmembrane ammonia channel, AmtB, and the cytosolic regulatory protein, GlnK, at 1.96 Å. *Proceedings of the National Academy of Sciences of the United States of America* 104, 42-47.
108. Durand, A., and Merrick, M. (2006). *In vitro* analysis of the *Escherichia coli* AmtB-GlnK complex reveals a stoichiometric interaction and sensitivity to ATP and 2-oxoglutarate. *Journal of Biological Chemistry* 281, 29558-29567.
109. Rodrigues, T.E., Souza, V.E.P., Monteiro, R.A., Gerhardt, E.C.M., Araujo, L.M., Chubatsu, L.S., Souza, E.M., Pedrosa, F.O., and Huergo, L.F. (2011). *In vitro* interaction between the ammonium transport protein AmtB and partially uridylylated forms of the P_{II} protein GlnZ. *Biochimica et Biophysica Acta - Proteins and Proteomics* 1814, 1203-1209.
110. Feng, S., and ZhiNan, X. (2007). Microbial production of natural poly amino acid. *Science in China Series B-Chemistry* 50, 291-303.
111. Simon, R.D., and Weathers, P. (1976). Determination of the structure of the novel polypeptide containing aspartic acid and arginine which is found in cyanobacteria. *Biochimica et Biophysica Acta* 420, 165-176.
112. Borzi, A. (1887). Le comunicazioni intracellulari delle *Nostochinee*. *Malpighia* 1, 28-74.
113. Wood, P., Peat, A., and Whitton, B.A. (1986). Influence of phosphorus status on fine-structure of the cyanobacterium (blue-green-alga) *Calothrix parietina*. *Cytobios* 47, 89-99.
114. Lang, N.J. (1968). The fine structure of blue-green algae. *Annual Review of Microbiology* 22, 15-46.
115. Lang, N.J., Simon, R.D., and Wolk, C.P. (1972). Correspondence of cyanophycin granules with structured granules in *Anabaena cylindrica*. *Archiv Fur Mikrobiologie* 83, 313-&.
116. Allen, M.M., and Weathers, P.J. (1980). Structure and composition of cyanophycin granules in the cyanobacterium *Aphanocapsa* sp. PCC 6308. *Journal of Bacteriology* 141, 959-962.
117. Weathers, P.J., Chee, H.L., and Allen, M.M. (1978). Arginine catabolism in *Aphanocapsa* sp. PCC 6308. *Archives of Microbiology* 118, 1-6.
118. Allen, M.M., Hutchison, F., and Weathers, P.J. (1980). Cyanophycin granule polypeptide formation and degradation in the cyanobacterium *Aphanocapsa* sp. PCC 6308. *Journal of Bacteriology* 141, 687-693.
119. Watzel, B., Engelbrecht, A., Hauf, W., Stahl, M., Maldener, I., and Forchhammer, K. (2015). Metabolic pathway engineering using the central signal processor P_{II}. *Microbial Cell Factories* 14, 192.
120. Allen, M.M., and Hutchison, F. (1980). Nitrogen limitation and recovery in the cyanobacterium *Aphanocapsa* sp. PCC 6308. *Archives of Microbiology* 128, 1-7.
121. Sherman, L.A., Meunier, P., and Colon-Lopez, M.S. (1998). Diurnal rhythms in metabolism: A day in the life of a unicellular, diazotrophic cyanobacterium. *Photosynthesis Research* 58, 25-42.
122. Finzi-Hart, J.A., Pett-Ridge, J., Weber, P.K., Popa, R., Fallon, S.J., Gunderson, T., Hutcheon, I.D., Neelson, K.H., and Capone, D.G. (2009). Fixation and fate of C and N in the cyanobacterium *Trichodesmium* using nanometer-scale secondary ion mass

- spectrometry Proceedings of the National Academy of Sciences of the United States of America 106, 9931-9931.
123. Ziegler, K., Stephan, D.P., Pistorius, E.K., Ruppel, H.G., and Lockau, W. (2001). A mutant of the cyanobacterium *Anabaena variabilis* ATCC 29413 lacking cyanophycin synthetase: growth properties and ultrastructural aspects. *Fems Microbiology Letters* 196, 13-18.
 124. Burnat, M., Herrero, A., and Flores, E. (2014). Compartmentalized cyanophycin metabolism in the diazotrophic filaments of a heterocyst-forming cyanobacterium. *Proceedings of the National Academy of Sciences of the United States of America* 111, 3823-3828.
 125. Forchhammer, K., and Watzler, B. (2016). Closing a gap in cyanophycin metabolism. *Microbiology-Sgm* 162, 727-729.
 126. Picossi, S., Valladares, A., Flores, E., and Herrero, A. (2004). Nitrogen-regulated genes for the metabolism of cyanophycin, a bacterial nitrogen reserve polymer - Expression and mutational analysis of two cyanophycin synthetase and cyanophycinase gene clusters in the heterocyst-forming cyanobacterium *Anabaena* sp. PCC 7120. *Journal of Biological Chemistry* 279, 11582-11592.
 127. Sukenik, A., Maldener, I., Delhaye, T., Viner-Mozzini, Y., Sela, D., and Bormans, M. (2015). Carbon assimilation and accumulation of cyanophycin during the development of dormant cells (akinetes) in the cyanobacterium *Aphanizomenon ovalisporum*. *Frontiers in Microbiology* 6, 1067.
 128. Perez, R., Forchhammer, K., Salerno, G., and Maldener, I. (2016). Clear differences in metabolic and morphological adaptations of akinetes of two *Nostocales* living in different habitats. *Microbiology-Sgm* 162, 214-223.
 129. Perez, R., Wormer, L., Sass, P., and Maldener, I. (2018). A highly asynchronous developmental program triggered during germination of dormant akinetes of filamentous diazotrophic cyanobacteria. *FEMS Microbiology Ecology* 94.
 130. Sutherland, J.M., Reaston, J., Stewart, W.D.P., and Herdman, M. (1985). Akinetes of the cyanobacterium *Nostoc* PCC 7524 - Macromolecular and biochemical-changes during synchronous germination. *Journal of General Microbiology* 131, 2855-2863.
 131. Krehenbrink, M., Oppermann-Sanio, F.B., and Steinbuchel, A. (2002). Evaluation of non-cyanobacterial genome sequences for occurrence of genes encoding proteins homologous to cyanophycin synthetase and cloning of an active cyanophycin synthetase from *Acinetobacter* sp. strain DSM 587. *Archives of Microbiology* 177, 371-380.
 132. Ziegler, K., Deutzmann, R., and Lockau, W. (2002). Cyanophycin synthetase-like enzymes of non-cyanobacterial eubacteria: characterization of the polymer produced by a recombinant synthetase of *Desulfitobacterium hafniense*. *Zeitschrift für Naturforschung C* 57, 522-529.
 133. Fuser, G., and Steinbuchel, A. (2007). Analysis of genome sequences for genes of cyanophycin metabolism: identifying putative cyanophycin metabolizing prokaryotes. *Macromolecular Bioscience* 7, 278-296.
 134. Simon, R.D. (1971). Cyanophycin granules from the blue-green alga *Anabaena cylindrica*: A reserve material consisting of copolymers of aspartic acid and arginine. *Proceedings of the National Academy of Sciences of the United States of America* 68, 265-267.

135. Frey, K.M., Oppermann-Sanio, F.B., Schmidt, H., and Steinbuchel, A. (2002). Technical-scale production of cyanophycin with recombinant strains of *Escherichia coli*. *Applied and Environmental Microbiology* 68, 3377-3384.
136. Richter, R., Hejazi, M., Kraft, R., Ziegler, K., and Lockau, W. (1999). Cyanophycinase, a peptidase degrading the cyanobacterial reserve material multi-L-arginyl-poly-L-aspartic acid (cyanophycin) - Molecular cloning of the gene of *Synechocystis* sp PCC 6803, expression in *Escherichia coli*, and biochemical characterization of the purified enzyme. *European Journal of Biochemistry* 263, 163-169.
137. Simon, R.D., Lawry, N.H., and McLendon, G.L. (1980). Structural characterization of the cyanophycin granule polypeptide of *Anabaena cylindrica* by circular dichroism and Raman spectroscopy. *Biochimica et Biophysica Acta* 626, 277-281.
138. Elbahloul, Y., Krehenbrink, M., Reichelt, R., and Steinbuchel, A. (2005). Physiological conditions conducive to high cyanophycin content in biomass of *Acinetobacter calcoaceticus* strain ADP1. *Applied and Environmental Microbiology* 71, 858-866.
139. Steinle, A., Oppermann-Sanio, F.B., Reichelt, R., and Steinbuchel, A. (2008). Synthesis and accumulation of cyanophycin in transgenic strains of *Saccharomyces cerevisiae*. *Applied and Environmental Microbiology* 74, 3410-3418.
140. Nausch, H., Huckauf, J., and Broer, I. (2016). Peculiarities and impacts of expression of bacterial cyanophycin synthetases in plants. *Applied Microbiology and Biotechnology* 100, 1559-1565.
141. Ziegler, K., Diener, A., Herpin, C., Richter, R., Deutzmann, R., and Lockau, W. (1998). Molecular characterization of cyanophycin synthetase, the enzyme catalyzing the biosynthesis of the cyanobacterial reserve material multi-L-arginyl-poly-L-aspartate (cyanophycin). *European Journal of Biochemistry* 254, 154-159.
142. Wiefel, L., and Steinbuchel, A. (2014). Solubility behavior of cyanophycin depending on lysine content. *Applied and Environmental Microbiology* 80, 1091-1096.
143. Simon, R.D. (1976). The biosynthesis of multi-L-arginyl-poly(L-aspartic acid) in the filamentous cyanobacterium *Anabaena cylindrica*. *Biochimica et Biophysica Acta* 422, 407-418.
144. Berg, H., Ziegler, K., Piotukh, K., Baier, K., Lockau, W., and Volkmer-Engert, R. (2000). Biosynthesis of the cyanobacterial reserve polymer multi-L-arginyl-poly-L-aspartic acid (cyanophycin) - Mechanism of the cyanophycin synthetase reaction studied with synthetic primers. *European Journal of Biochemistry* 267, 5561-5570.
145. Hai, T., Oppermann-Sanio, F.B., and Steinbuchel, A. (2002). Molecular characterization of a thermostable cyanophycin synthetase from the thermophilic cyanobacterium *Synechococcus* sp strain MA19 and *in vitro* synthesis of cyanophycin and related polyamides. *Applied and Environmental Microbiology* 68, 93-101.
146. Shively, J.M. (2006). *Inclusions in prokaryotes*, (Berlin ; New York: Springer).
147. Arai, T., and Kino, K. (2008). A cyanophycin synthetase from *Thermosynechococcus elongatus* BP-1 catalyzes primer-independent cyanophycin synthesis. *Applied Microbiology and Biotechnology* 81, 69-78.
148. Hai, T., Oppermann-Sanio, F.B., and Steinbuchel, A. (1999). Purification and characterization of cyanophycin and cyanophycin synthetase from the thermophilic *Synechococcus* sp. MA19. *Fems Microbiology Letters* 181, 229-236.
149. Aboulmagd, E., Sanio, F.B.O., and Steinbuchel, A. (2001). Purification of *Synechocystis* sp strain PCC 6308 cyanophycin synthetase and its characterization with respect to

- substrate and primer specificity. *Applied and Environmental Microbiology* 67, 2176-2182.
150. Krehenbrink, M., and Steinbuchel, A. (2004). Partial purification and characterization of a non-cyanobacterial cyanophycin synthetase from *Acinetobacter calcoaceticus* strain ADP1 with regard to substrate specificity, substrate affinity and binding to cyanophycin. *Microbiology* 150, 2599-2608.
151. Berg, H. (2003). Untersuchungen zu Funktion und Struktur der Cyanophycin-Synthetase von *Anabaena variabilis* ATCC 29413. Dissertation. Humboldt-Universität zu Berlin, Germany.
152. Aboulmagd, E., Oppermann-Sanio, F.B., and Steinbuchel, A. (2000). Molecular characterization of the cyanophycin synthetase from *Synechocystis* sp strain PCC 6308. *Archives of Microbiology* 174, 297-306.
153. Klemke, F., Nurnberg, D.J., Ziegler, K., Beyer, G., Kahmann, U., Lockau, W., and Volkmer, T. (2016). CphA2 is a novel type of cyanophycin synthetase in N₂-fixing cyanobacteria. *Microbiology-Sgm* 162, 526-536.
154. Simon, R.D. (1987). Inclusion bodies in the cyanobacteria: cyanophycin, polyphosphate, polyhedral bodies. In *The Cyanobacteria.*, P. Fay and C. Van Baalen, eds. (Elsevier Science Publishers B.V.), pp. 199-225.
155. Law, A.M., Lai, S.W., Tavares, J., and Kimber, M.S. (2009). The structural basis of beta-peptide-specific cleavage by the serine protease cyanophycinase. *Journal of Molecular Biology* 392, 393-404.
156. Obst, M., Oppermann-Sanio, F.B., Luftmann, H., and Steinbuchel, A. (2002). Isolation of cyanophycin-degrading bacteria, cloning and characterization of an extracellular cyanophycinase gene (*cphE*) from *Pseudomonas anguilliseptica* strain BI. The *cphE* gene from *P. anguilliseptica* BI encodes a cyanophycin hydrolyzing enzyme. *Journal of Biological Chemistry* 277, 25096-25105.
157. Rehm, B. (2009). *Microbial production of biopolymers and polymer precursors : applications and perspectives*, (Wymondham: Caister Academic).
158. Obst, M., Sallam, A., Luftmann, H., and Steinbuchel, A. (2004). Isolation and characterization of gram-positive cyanophycin-degrading bacteria - Kinetic studies on cyanophycin depolymerase activity in aerobic bacteria. *Biomacromolecules* 5, 153-161.
159. Obst, M., and Steinbuchel, A. (2004). Microbial degradation of poly(amino acid)s. *Biomacromolecules* 5, 1166-1176.
160. Obst, M., Krug, A., Luftmann, H., and Steinbuchel, A. (2005). Degradation of cyanophycin by *Sedimentibacter hongkongensis* strain KI and *Citrobacter amalonaticus* strain G isolated from an anaerobic bacterial consortium. *Applied and Environmental Microbiology* 71, 3642-3652.
161. Sallam, A., and Steinbuchel, A. (2008). Anaerobic and aerobic degradation of cyanophycin by the denitrifying bacterium *Pseudomonas alcaligenes* strain DIP1 and role of three other coisolates in a mixed bacterial consortium. *Applied and Environmental Microbiology* 74, 3434-3443.
162. Sallam, A., and Steinbuchel, A. (2009). Cyanophycin-degrading bacteria in digestive tracts of mammals, birds and fish and consequences for possible applications of cyanophycin and its dipeptides in nutrition and therapy. *Journal of Applied Microbiology* 107, 474-484.

163. Lough, T.J., Reddington, B.D., Grant, M.R., Hill, D.F., Reynolds, P.H.S., and Farnden, K.J.F. (1992). The isolation and characterization of a cDNA clone encoding L-asparaginase from developing seeds of Lupin (*Lupinus arboreus*). *Plant Molecular Biology* 19, 391-399.
164. Hejazi, M., Piotukh, K., Mattow, J., Deutzmann, R., Volkmer-Engert, R., and Lockau, W. (2002). Isoaspartyl dipeptidase activity of plant-type asparaginases. *Biochemical Journal* 364, 129-136.
165. Gupta, M., and Carr, N.G. (1981). Enzyme-activities related to cyanophycin metabolism in heterocysts and vegetative cells of *Anabaena* sp. *Journal of General Microbiology* 125, 17-23.
166. Wolk, C.P., Austin, S.M., Bortins, J., and Galonsky, A. (1974). Autoradiographic localization of N-13 after fixation of N-13-labeled nitrogen gas by a heterocyst-forming blue-green-alga. *Journal of Cell Biology* 61, 440-453.
167. Thomas, J., Meeks, J.C., Wolk, C.P., Shaffer, P.W., Austin, S.M., and Chien, W.S. (1977). Formation of glutamine from [ammonia-N-13], [dinitrogen-N-13], and [glutamate-C-14] by heterocysts isolated from *Anabaena cylindrica*. *Journal of Bacteriology* 129, 1545-1555.
168. Mitschke, J., Georg, J., Scholz, I., Sharma, C.M., Dienst, D., Bantscheff, J., Voss, B., Steglich, C., Wilde, A., Vogel, J., et al. (2011). An experimentally anchored map of transcriptional start sites in the model cyanobacterium *Synechocystis* sp PCC 6803. *Proceedings of the National Academy of Sciences of the United States of America* 108, 2124-2129.
169. Simon, R.D. (1973). The effect of chloramphenicol on the production of cyanophycin granule polypeptide in the blue green alga *Anabaena cylindrica*. *Archives of Microbiology* 92, 115-122.
170. Liotenberg, S., Campbell, D., Rippka, R., Houmard, J., and deMarsac, N.T. (1996). Effect of the nitrogen source on phycobiliprotein synthesis and cell reserves in a chromatically adapting filamentous cyanobacterium. *Microbiology* 142, 611-622.
171. Sarma, T.A., and Khatrar, J.I.S. (1986). Accumulation of cyanophycin and glycogen during sporulation in the blue-green-alga *Anabaena torulosa*. *Biochemie Und Physiologie Der Pflanzen* 181, 155-164.
172. Leganes, F., Fernandez-Pinas, F., and Wolk, C.P. (1998). A transposition-induced mutant of *Nostoc ellipsosporum* implicates an arginine-biosynthetic gene in the formation of cyanophycin granules and of functional heterocysts and akinetes. *Microbiology* 144, 1799-1805.
173. Elbahloul, Y., and Steinbuchel, A. (2006). Engineering the genotype of *Acinetobacter* sp strain ADP1 to enhance biosynthesis of cyanophycin. *Applied and Environmental Microbiology* 72, 1410-1419.
174. Liu, D., and Yang, C. (2014). The nitrogen-regulated response regulator NrrA controls cyanophycin synthesis and glycogen catabolism in the cyanobacterium *Synechocystis* sp. PCC 6803. *Journal of Biological Chemistry* 289, 2055-2071.
175. Khlystov, N.A., Chan, W.Y., Kunjapur, A.M., Shi, W.C., Prather, K.U., and Olsen, B.D. (2017). Material properties of the cyanobacterial reserve polymer multi-L- arginyl-poly-L-aspartate (cyanophycin). *Polymer* 109, 238-245.
176. Sallam, A., and Steinbuchel, A. (2010). Dipeptides in nutrition and therapy: cyanophycin-derived dipeptides as natural alternatives and their biotechnological production. *Applied Microbiology and Biotechnology* 87, 815-828.

177. Aboulmagd, E., Voss, I., Oppermann-Sanio, F.B., and Steinbuchel, A. (2001). Heterologous expression of cyanophycin synthetase and cyanophycin synthesis in the industrial relevant bacteria *Corynebacterium glutamicum* and *Ralstonia eutropha* and in *Pseudomonas putida*. *Biomacromolecules* 2, 1338-1342.
178. Hai, T., Frey, K.M., and Steinbuchel, A. (2006). Engineered cyanophycin synthetase (CphA) from *Nostoc ellipsosporum* confers enhanced CphA activity and cyanophycin accumulation to *Escherichia coli*. *Applied and Environmental Microbiology* 72, 7652-7660.
179. Diniz, S.C., Voss, I., and Steinbuchel, A. (2006). Optimization of cyanophycin production in recombinant strains of *Pseudomonas putida* and *Ralstonia eutropha* employing elementary mode analysis and statistical experimental design. *Biotechnology and Bioengineering* 93, 698-717.
180. Voss, I., Diniz, S.C., Aboulmagd, E., and Steinbuchel, A. (2004). Identification of the *Anabaena* sp. strain PCC 7120 cyanophycin synthetase as suitable enzyme for production of cyanophycin in gram-negative bacteria like *Pseudomonas putida* and *Ralstonia eutropha*. *Biomacromolecules* 5, 1588-1595.
181. Voss, I., and Steinbuchel, A. (2006). Application of a KDPG-aldolase gene-dependent addition system for enhanced production of cyanophycin in *Ralstonia eutropha* strain H16. *Metabolic Engineering* 8, 66-78.
182. Steinle, A., Bergander, K., and Steinbuchel, A. (2009). Metabolic engineering of *Saccharomyces cerevisiae* for production of novel cyanophycins with an extended range of constituent amino acids. *Applied and Environmental Microbiology* 75, 3437-3446.
183. Wiefel, L., Broker, A., and Steinbuchel, A. (2011). Synthesis of a citrulline-rich cyanophycin by use of *Pseudomonas putida* ATCC 4359. *Applied Microbiology and Biotechnology* 90, 1755-1762.
184. Steinle, A., Witthoff, S., Krause, J.P., and Steinbuchel, A. (2010). Establishment of cyanophycin biosynthesis in *Pichia pastoris* and optimization by use of engineered cyanophycin synthetases. *Applied and Environmental Microbiology* 76, 1062-1070.
185. Sallam, A., Kast, A., Przybilla, S., Meiswinkel, T., and Steinbuchel, A. (2009). Biotechnological process for production of beta-dipeptides from cyanophycin on a technical scale and its optimization. *Applied and Environmental Microbiology* 75, 29-38.
186. Huhns, M., Neumann, K., Hausmann, T., Ziegler, K., Klemke, F., Kahmann, U., Staiger, D., Lockau, W., Pistorius, E.K., and Broer, I. (2008). Plastid targeting strategies for cyanophycin synthetase to achieve high-level polymer accumulation in *Nicotiana tabacum*. *Plant Biotechnology Journal* 6, 321-336.
187. Huhns, M., Neumann, K., Hausmann, T., Klemke, F., Lockau, W., Kahmann, U., Kopertekh, L., Staiger, D., Pistorius, E.K., Reuther, J., et al. (2009). Tuber-specific *cphA* expression to enhance cyanophycin production in potatoes. *Plant Biotechnology Journal* 7, 883-898.
188. Dillschneider, R., Steinweg, C., Rosello-Sastre, R., and Posten, C. (2013). Biofuels from microalgae: Photoconversion efficiency during lipid accumulation. *Bioresource Technology* 142, 647-654.
189. Jacobi, A., Steinweg, C., Sastre, R.R., and Posten, C. (2012). Advanced photobioreactor LED illumination system: Scale-down approach to study microalgal growth kinetics. *Engineering in Life Sciences* 12, 621-630.

190. Hisbergues, M., Jeanjean, R., Joset, F., de Marsac, N.T., and Bedu, S. (1999). Protein P_{II} regulates both inorganic carbon and nitrate uptake and is modified by a redox signal in *Synechocystis* PCC 6803. *Febs Letters* 463, 216-220.
191. Montesinos, M.L., Muro-Pastor, A.M., Herrero, A., and Flores, E. (1998). Ammonium/methylammonium permeases of a cyanobacterium. Identification and analysis of three nitrogen-regulated amt genes in *Synechocystis* sp. PCC 6803. *Journal of Biological Chemistry* 273, 31463-31470.
192. Lee, H.M., Flores, E., Forchhammer, K., Herrero, A., and de Marsac, N.T. (2000). Phosphorylation of the signal transducer P_{II} protein and an additional effector are required for the P_{II}-mediated regulation of nitrate and nitrite uptake in the cyanobacterium *Synechococcus* sp. PCC 7942. *European Journal of Biochemistry* 267, 591-600.
193. Kobayashi, M., Rodriguez, R., Lara, C., and Omata, T. (1997). Involvement of the C-terminal domain of an ATP-binding subunit in the regulation of the ABC-type nitrate/nitrite transporter of the cyanobacterium *Synechococcus* sp. strain PCC 7942. *Journal of Biological Chemistry* 272, 27197-27201.
194. Kloft, N., and Forchhammer, K. (2005). Signal transduction protein P_{II} phosphatase PphA is required for light-dependent control of nitrate utilization in *Synechocystis* sp. strain PCC 6803. *Journal of Bacteriology* 187, 6683-6690.
195. Forchhammer, K., and Demarsac, N.T. (1995). Functional-analysis of the phosphoprotein P_{II} (*glnB* gene-product) in the cyanobacterium *Synechococcus* sp. strain PCC 7942. *Journal of Bacteriology* 177, 2033-2040.
196. Romero, J.M., Lara, C., and Guerrero, M.G. (1985). Dependence of nitrate utilization upon active CO₂ fixation in *Anacystis Nidulans* - a regulatory aspect of the interaction between photosynthetic carbon and nitrogen-metabolism. *Archives of Biochemistry and Biophysics* 237, 396-401.
197. Mobley, H.L.T., and Hausinger, R.P. (1989). Microbial ureases - Significance, regulation, and molecular characterization. *Microbiological Reviews* 53, 85-108.
198. Koch, M. (2016). Establishing a bacterial-two-hybrid assay as a high throughput method for verifying interactions between PII-mutants and putative interaction candidates., Volume Master of Science. (Universität Tübingen).
199. Miyake, M., Kataoka, K., Shirai, M., and Asada, Y. (1997). Control of poly-beta-hydroxybutyrate synthase mediated by acetyl phosphate in cyanobacteria. *Journal of Bacteriology* 179, 5009-5013.
200. Koch, M. (2012). Analysis of the Sll0783 function in PHB synthesis in *Synechocystis* PCC 6803: A crucial role of NADPH in N-starvation. (Universität Tübingen).
201. Hauf, W. (2016). Regulation of carbon polymer accumulation in *Synechocystis* sp. PCC 6803. (Universität Tübingen).
202. Simon, R.D. (1973). Measurement of the cyanophycin granule polypeptide contained in the blue-green alga *Anabaena cylindrica*. *Journal of Bacteriology* 114, 1213-1216.
203. Shin, J.H., and Lee, S.Y. (2014). Metabolic engineering of microorganisms for the production of L-arginine and its derivatives. *Microbial Cell Factories* 13, 166.
204. Xu, M.J., Rao, Z.M., Dou, W.F., Yang, J., Jin, J., and Xu, Z.H. (2012). Site-directed mutagenesis and feedback-resistant N-acetyl-L-glutamate kinase (NAGK) increase *Corynebacterium crenatum* L-arginine production. *Amino Acids* 43, 255-266.

205. Beardall, J., and Raven, J.A. (2013). Limits to phototrophic growth in dense culture: CO₂ supply and light. In *Algae for Biofuels and Energy*, M.A. Borowitzka and N.R. Moheimani, eds. (Dordrecht: Springer Netherlands), pp. 91-97.
206. Bahr, L., Wustenberg, A., and Ehwald, R. (2016). Two-tier vessel for photoautotrophic high-density cultures. *Journal of Applied Phycology* 28, 783-793.
207. Lippi, L., Bähr, L., Wüstenberg, A., Wilde, A., and Steuer, R. (2018). Exploring the potential of high-density cultivation of cyanobacteria for the production of cyanophycin. *Algal Research* 31, 363-366.
208. Doello, S., Klotz, A., Makowka, A., Gutekunst, K., and Forchhammer, K. (2018). A specific glycogen mobilization strategy enables awakening of dormant cyanobacteria from chlorosis. *Journal of Plant Physiology* pp-00297.
209. Omata, T., Andriese, X., and Hirano, A. (1993). Identification and characterization of a gene-cluster involved in nitrate transport in the cyanobacterium *Synechococcus* sp. PCC 7942. *Molecular & General Genetics* 236, 193-202.
210. Kloft, N. (2005). Dephosphorylierung des signalproteins P_{II} in *Synechocystis* sp. PCC 6803: Rolle der protein phosphatase PphA und kontrolle des stickstoffmetabolismus. (Justus-Liebig-Universität Gießen).
211. Flores, E., Guerrero, M.G., and Losada, M. (1980). Short-term ammonium inhibition of nitrate utilization by *Anacystis nidulans* and other cyanobacteria. *Archives of Microbiology* 128, 137-144.
212. Marques, S., Merida, A., Candau, P., and Florencio, F.J. (1992). Light-mediated regulation of glutamine-synthetase activity in the unicellular cyanobacterium *Synechococcus* sp PCC 6301. *Planta* 187, 247-253.
213. Chang, Y.J., Takatani, N., Aichi, M., Maeda, S., and Omata, T. (2013). Evaluation of the effects of P_{II} deficiency and the toxicity of PipX on growth characteristics of the P_{II}-less mutant of the cyanobacterium *Synechococcus elongatus*. *Plant and Cell Physiology* 54, 1504-1514.
214. Valladares, A., Montesinos, M.L., Herrero, A., and Flores, E. (2002). An ABC-type, high-affinity urea permease identified in cyanobacteria. *Molecular Microbiology* 43, 703-715.
215. Spät, P., Klotz, A., Rexroth, S., Maček, B., and Forchhammer, K. (2018). Chlorosis as a developmental program in cyanobacteria: the proteomic fundament for survival and awakening. *Molecular & Cellular Proteomics*.
216. Spät, P., Macek, B., and Forchhammer, K. (2015). Phosphoproteome of the cyanobacterium *Synechocystis* sp PCC 6803 and its dynamics during nitrogen starvation. *Frontiers in Microbiology* 6.
217. Merritt, M.V., Sid, S.S., Mesh, L., and Allen, M.M. (1994). Variations in the amino acid composition of cyanophycin in the cyanobacterium *Synechocystis* sp. PCC 6308 as a function of growth conditions. *Archives of Microbiology* 162, 158-166.

IX. Appendix

1. Accepted publication

Wutzer, B., Engelbrecht, A., Hauf, W., Stahl, M., Maldener, I. & Forchhammer, K.
(2015).

Metabolic pathway engineering using the central signal processor P_{II}.

Microbial cell factories, 14(1), 192.

RESEARCH

Open Access



Metabolic pathway engineering using the central signal processor P_{II}

Björn Watzer¹, Alicia Engelbrecht¹, Waldemar Hauf¹, Mark Stahl², Iris Maldener¹ and Karl Forchhammer^{1*}

Abstract

Background: P_{II} signal processor proteins are wide spread in prokaryotes and plants where they control a multitude of anabolic reactions. Efficient overproduction of metabolites requires relaxing the tight cellular control circuits. Here we demonstrate that a single point mutation in the P_{II} signaling protein from the cyanobacterium *Synechocystis* sp. PCC 6803 is sufficient to unlock the arginine pathway causing over accumulation of the biopolymer cyanophycin (multi-L-arginyl-poly-L-aspartate). This product is of biotechnological interest as a source of amino acids and polyaspartic acid. This work exemplifies a novel approach of pathway engineering by designing custom-tailored P_{II} signaling proteins. Here, the engineered *Synechocystis* sp. PCC6803 strain with a P_{II}-I86N mutation over-accumulated arginine through constitutive activation of the key enzyme *N*-acetylglutamate kinase (NAGK).

Results: In the engineered strain BW86, in vivo NAGK activity was strongly increased and led to a more than tenfold higher arginine content than in the wild-type. As a consequence, strain BW86 accumulated up to 57 % cyanophycin per cell dry mass under the tested conditions, which is the highest yield of cyanophycin reported to date. Strain BW86 produced cyanophycin in a molecular mass range of 25 to >100 kDa; the wild-type produced the polymer in a range of 30 to >100 kDa.

Conclusions: The high yield and high molecular mass of cyanophycin produced by strain BW86 along with the low nutrient requirements of cyanobacteria make it a promising means for the biotechnological production of cyanophycin. This study furthermore demonstrates the feasibility of metabolic pathway engineering using the P_{II} signaling protein, which occurs in numerous bacterial species.

Keywords: Cyanophycin, Cyanobacteria, L-Arginine, P_{II} protein

Background

Cyanophycin (multi-L-arginyl-poly-L-aspartate) is a nitrogen/carbon reserve polymer present in most cyanobacteria [1, 2] and in a few heterotrophic bacteria [3, 4]. It consists of a polyaspartic backbone with arginine residues linked via isopeptide bonds at the free carboxylate groups of the aspartic backbone [5, 6]. Cyanophycin is nonribosomally synthesized from arginine and aspartate by cyanophycinsynthetase (CphA) in an ATP-dependent elongation reaction using unidentified primers [6–8]. Cyanophycin accumulates in the cytoplasmic space as

opaque, membrane-less granules [9]. Isolated cyanophycin has a molecular weight widely ranging from 25 to 100 kDa [5] and is insoluble at physiological pH, but soluble in diluted acids or bases [10].

In cyanobacteria, the amount of cyanophycin is usually less than 1 % of the cell dry mass during exponential growth. When cells experience certain unfavorable conditions other than nitrogen starvation, such as stationary phase or unbalanced growth conditions owing to nutrient limitation, e.g., sulfate or phosphate starvation [11], light stress, low temperature [12], or presence of chloramphenicol [13], the cyanophycin content may increase to 18 % of the cell dry mass. Cyanophycin also can accumulate transiently during the recovery of nitrogen-starved, non-diazotrophic cyanobacteria upon addition of a usable nitrogen source [14]. Furthermore,

*Correspondence: karl.forchhammer@uni-tuebingen.de

¹ Interfaculty Institute of Microbiology and Infection Medicine Tübingen, Eberhard-Karls-Universität Tübingen, Auf der Morgenstelle 28, 72076 Tübingen, Germany

Full list of author information is available at the end of the article

in heterocysts (specialized cells for nitrogen fixation) of cyanobacteria of the order *Nostocales*, polar nodules consisting of cyanophycin are deposited at the contact site to adjacent vegetative cells [15].

The cyanobacterial P_{II} protein is a member of the widely distributed family of P_{II} signal transduction proteins present in bacteria, plants, and some archaea [16]. P_{II} proteins are largely involved in the regulation of nitrogen assimilatory metabolism. For this purpose, P_{II} senses the cellular energy level by binding ATP or ADP competitively [17] and senses the state of central carbon/nitrogen metabolism by binding or lack of binding of the status reporter molecule 2-oxoglutarate (2-OG) [18, 19]. Effector molecule binding results in structural rearrangements of the large surface-exposed T-loops of P_{II} , its major protein-interaction determinant. In the unicellular freshwater cyanobacteria *Synechococcus elongatus* PCC 7942 and *Synechocystis* sp. PCC 6803 during nitrogen starvation, which corresponds with high 2-OG levels, the P_{II} protein binds 2-OG and is phosphorylated at the apex of the T-loop at position Ser49; when nitrogen is in excess, which corresponds to 2-OG paucity and therefore no binding of the P_{II} protein to 2-OG, Ser49 is dephosphorylated [16, 20].

Depending on the bound effector molecules and the phosphorylation status, P_{II} interacts and influences many target proteins, including enzymes, channels, and regulatory proteins [18, 21, 22]. One of the major P_{II} target proteins is the enzyme *N*-acetylglutamate kinase (NAGK) [23], which catalyzes the committed step in the cyclic arginine biosynthesis pathway [24]. Under nitrogen excess, P_{II} in its non-phosphorylated form binds to NAGK [25], thereby strongly enhancing its biosynthetic activity as well as relieving the feedback inhibitory effect of arginine on NAGK activity [18]. In a screening for P_{II} variants with altered NAGK binding properties, our laboratory previously identified a variant of the *S. elongatus* PCC 7942 P_{II} protein with a single amino acid replacement, Ile86 to Asp86, hereafter referred to as $P_{II}(I86N)$, that constitutively binds NAGK in vitro [26]. The variant is a structural mimic of P_{II} in the NAGK complex, with its T-loops in a kinked conformation; as a consequence of this special T-loop folding, this variant has a high affinity for NAGK and no longer responds to 2-OG but can bind citrate in vitro [27].

For in vivo studies of the role of P_{II} in arginine metabolism, strain *Synechocystis* sp. PCC 6803 offers the advantage over *S. elongatus* that it produces cyanophycin. In a P_{II} -deficient mutant of *Synechocystis* sp. PCC 6803, not only does NAGK remain in a low activity state, but also the transient accumulation of cyanophycin that normally occurs after exposing a nitrogen-starved culture to excess

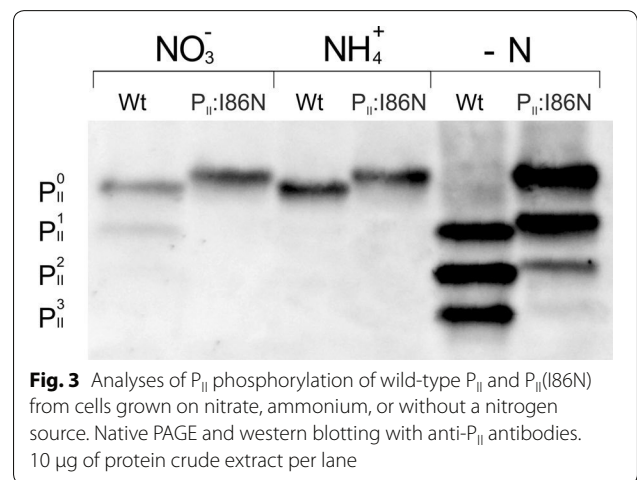
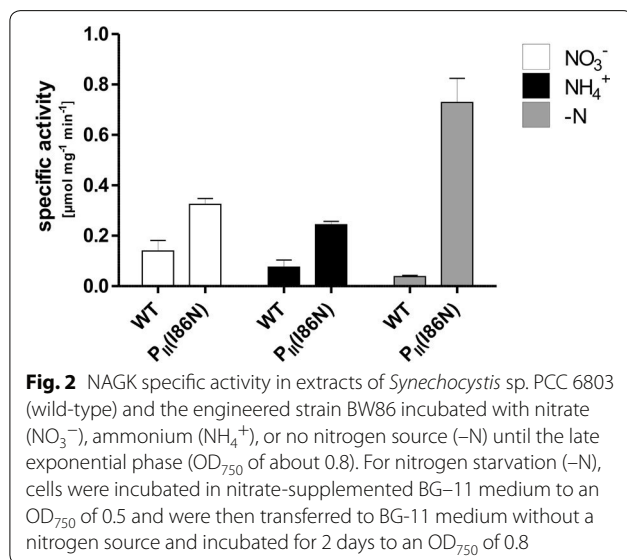
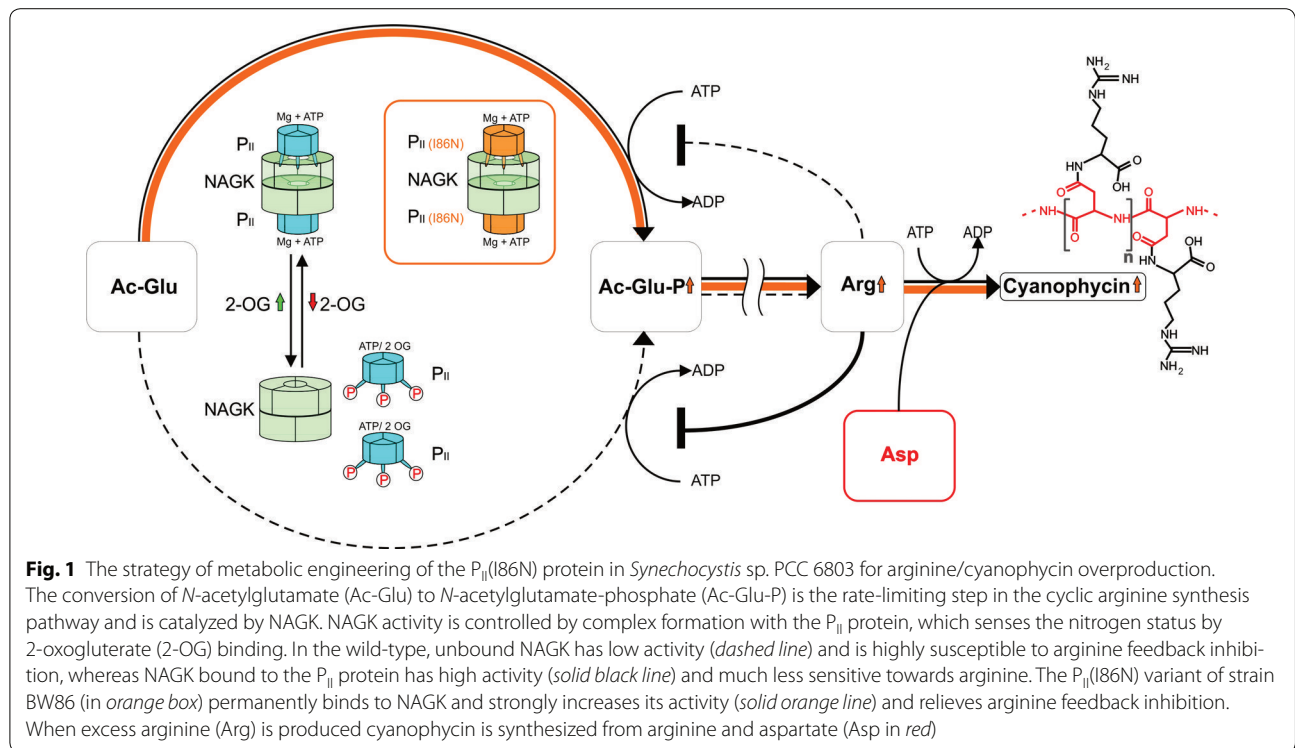
ammonia is impaired [23]. We tested whether the opposite phenotype in *Synechocystis* sp. PCC 6803 would be possible if we replaced the wild-type *glnB* gene (encoding P_{II}) with a *glnB* variant with codon alteration Ile86 to Asp, thereby generating a P_{II} variant that constitutively activates NAGK, which could lead to the accumulation of cyanophycin not just transiently, but in high amounts. This metabolic pathway engineering via manipulation of the P_{II} signal indeed resulted in a strain that excessively overproduces cyanophycin (Fig. 1).

Results and discussion

Expression of the $P_{II}(I86N)$ variant in *Synechocystis* sp. PCC 6803 causes a strong in vivo activation of NAGK

Previous biochemical studies have shown that the $P_{II}(I86N)$ variant of *S. elongatus* PCC 7942 constitutively binds to NAGK in vitro [26]. To test whether this P_{II} variant affects the in vivo activity of NAGK, we constructed a genomic mutant of *Synechocystis* sp. PCC 6803 in which the *glnB* gene was replaced by a *glnB* gene carrying the mutation for I86N together with a spectinomycin resistance cassette via homologous recombination. Complete segregation of the mutation in the polyploidy *Synechocystis* sp. strain, named strain BW86, was confirmed via PCR (Additional file 1: Figure S1).

To determine in vivo NAGK activity during growth with different nitrogen sources, we cultivated the wild-type *Synechocystis* sp. PCC 6803 and strain BW86 in BG-11 medium containing either nitrate, ammonia, or no nitrogen source (Fig. 2). NAGK activity was higher in strain BW86 than in the wild-type in all cases; the activity was 2.3-fold higher after growth with nitrate and 3.2-fold higher after growth with ammonium. The nitrogen source, i.e., nitrate or ammonium, did not strongly affect NAGK activity. However, under nitrogen starvation, NAGK activity strongly increased in strain BW86 and decreased in the wild-type, such that the activity was 19.2-fold higher in strain BW86. The low activity of NAGK in the wild-type under nitrogen starvation could be explained by the full phosphorylation of P_{II} under these conditions [28] since this prevents P_{II} -NAGK interaction and thus, the NAGK enzyme would be in an inactive state [25]. Transcriptome studies of *Synechocystis* show an induced expression of the *glnB* and *argB* (encoding NAGK) genes under nitrogen starvation [29]. Such an induced expression would lead to increased levels of $P_{II}(I86N)$ and NAGK. Provided that phosphorylation of $P_{II}(I86N)$ is impaired, this could be the cause of the high NAGK activity shown in Fig. 2, since P_{II} in its non-phosphorylated state interacts with NAGK and strongly enhances its activity [25].



The P_{II}(I86N) variant has a reduced phosphorylation

To test the assumption that the high activity of NAGK in strain BW86 is due to impaired phosphorylation of P_{II}(I86N), we analyzed its phosphorylation status using non-denaturing PAGE followed by immunoblotting using P_{II} specific antibodies [30] (Fig. 3). Each phosphorylation event increases the negative charge of the P_{II} protein and, therefore, leads to three isoforms of increasing

electrophoretic mobility corresponding to one- two- and threefold phosphorylated forms (P_{II}¹, P_{II}², P_{II}³). The mobility of non-phosphorylated P_{II}(I86N) and wild-type P_{II} slightly differed due to the replacement of isoleucine with asparagine at position 86. In nitrate-grown cells, wild-type P_{II} was in the non-phosphorylated state (P_{II}⁰) and in the mono-phosphorylated state (P_{II}¹), whereas P_{II}(I86N) was only in the non-phosphorylated state. As expected, both P_{II} proteins were non-phosphorylated when the cells were grown with ammonium as nitrogen source. Under conditions of nitrogen starvation, P_{II}

in wild-type cells was strongly phosphorylated with the two- and three-fold phosphorylated forms (P_{II}^2 , P_{II}^3) prevailing. By contrast, phosphorylation of $P_{II}(186N)$ was severely impaired, with absence of the fully phosphorylated form P_{II}^3 but dominance of the non-phosphorylated (P_{II}^0) and mono-phosphorylated form of P_{II} . Furthermore, due to the induced expression of *glnB* during nitrogen starvation [21], the bands of wild-type P_{II} and $P_{II}(186N)$ from nitrogen-starved cell are more intensive compared to non-starved cells (Fig. 3). These data confirm that the strikingly high activity of NAGK under nitrogen starvation in strain BW86 (Fig. 2) is due to impaired phosphorylation of $P_{II}(186N)$.

The high NAGK activity of the $P_{II}(186N)$ variant leads to a high intracellular arginine level

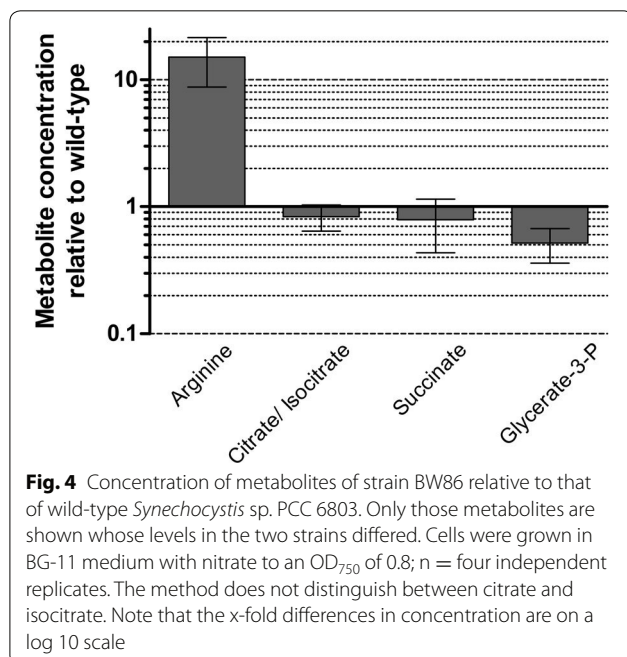
NAGK represents a key enzyme in the regulation of arginine biosynthesis and as such its activity is feedback-controlled by the cellular arginine levels, the final product of the pathway. Importantly, in vitro analysis demonstrated that complex formation of NAGK with P_{II} not only activates the enzyme, but strongly relieves feedback-inhibition by arginine [26]. To reveal the metabolic changes that are caused by the replacement of wild-type P_{II} by the $P_{II}(186N)$ variant in vivo, we determined the metabolome of the two strains with a focus on metabolites of primary metabolism, i.e., of the TCA cycle, CO_2 fixation, amino acid biosynthesis, and glycolysis (Fig. 4). For the comparison an untargeted metabolomics approach was chosen. According to PCA and OPLS-DA analysis (see

“Methods”), the only changing metabolites are arginine, citrate/isocitrate, succinate and glycerate-3-P. Remarkably, strain BW86 accumulated on average 15-fold more arginine than the wild-type. This increase reflects the constant activation of NAGK by the $P_{II}(186N)$ variant, which maintains NAGK in a state that is highly insensitive towards arginine-feedback inhibition. On the other hand, the pools of citrate/isocitrate, succinate and glycerate-3-P were decreased. The pools of citrate/isocitrate and succinate were just slightly (p value >0.05) lower in strain BW86 whereas the amount of glycerate-3-P was significantly lower in strain BW86 (p value 0.0107). The reason for the decreased level of glycerate-3-P is not known, but it indicates a yet to be explored connection to the increased metabolite flow into the arginine pool, e.g. by accelerated glycolytic flux that could drain the glycerate-3-P pool.

The $P_{II}(186N)$ mutation leads to cyanophycin accumulation

Previous studies have shown a relationship between a lack of P_{II} -dependent NAGK activation and a lack of cyanophycin accumulation. It has been suggested that the lack of P_{II} -induced arginine accumulation disables the accumulation of cyanophycin [23]. As shown above, strain BW86 displays enhanced NAGK activity due to constant NAGK activation by the $P_{II}(186N)$ variant and in consequence, over produces arginine. It was, therefore, intriguing to elucidate how this affects the accumulation of cyanophycin. Preliminary analysis indicated, that indeed the cellular cyanophycin content was strongly increased. Next, we systematically determined the relationship between nutritional conditions and cyanophycin production (Fig. 5). With nitrate as nitrogen source (Fig. 5a), wild-type cells accumulated about 1.1 ± 0.5 % cyanophycin relative to the cell dry mass (CDM) in the first 4 days. As the cells entered stationary phase on day 6 up to day 12 (Fig. 5Aⁱ), cyanophycin slightly increased up to 3.6 ± 0.8 % of the CDM. By contrast, strain BW86 accumulated up to 15.6 ± 5.4 % cyanophycin relative to the CDM, i.e., on average almost six fold more than the wild-type. Remarkably, upon inoculation of a fresh BW86 culture with stationary cells, the cyanophycin content was initially very high, but the level transiently decreased in the following days, corresponding to the exponential growth phase. After entry into stationary phase, the cyanophycin content increased again.

With ammonium as nitrogen source (Fig. 5b), wild-type cells accumulated cyanophycin similarly as with nitrate as nitrogen source, whereas strain BW86 produced less cyanophycin than in nitrate-supplemented medium, but still considerably more than the wild-type. The cyanophycin level increased up to 9.6 ± 1.7 % of the CDM in the first 4 days but began to slightly decrease on



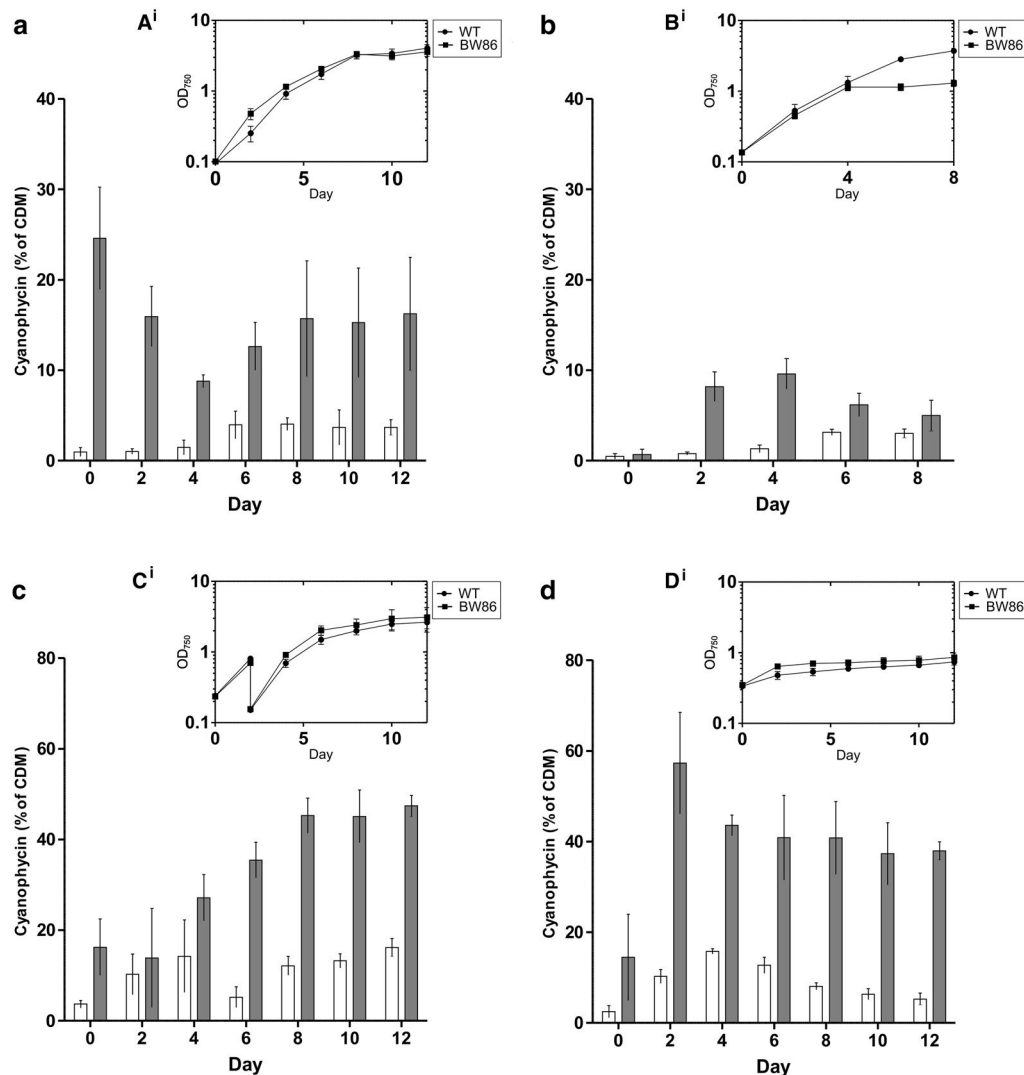


Fig. 5 Cyanophycin accumulation in *Synechocystis* sp. PCC 6803 wild-type (white bars) and strain BW86 (gray bars) cultivated **a** with nitrate, **b** with ammonium, **c** under phosphate starvation, and **d** under potassium starvation. **Aⁱ-Dⁱ** Growth curve of *Synechocystis* sp. PCC 6803 (WT) (circles) and strain BW86 (squares). Y-axes in log₁₀ shows the OD₇₅₀. Cells of each strain exponentially growing in BG-11 medium were inoculated into 800 ml of the respective BG-11 medium and incubated with an influx of 2 % CO₂ in air. For phosphate starvation, washed cells were grown in phosphate-free medium and were diluted with fresh phosphate-free medium after 2 days of cultivation; this time point was day 2. For potassium starvation, the cells of the inoculum were washed and inoculated into potassium-free medium. In **c** and **d**, the nitrogen source was nitrate. Cyanophycin was quantified every second day; the concentration is plotted against the cell dry mass (CDM). Note the different scales on the y-axes

day 6. Quantification of the amount of ammonium in the medium supernatant of the two strains indicated that strain BW86 consumed ammonia more slowly than the wild-type (Additional file 2: Figure S2). In the first 2 days of cultivation, ammonia consumption of the wild-type and the BW86 strain was similar (Additional file 2: Figure S2). Subsequently, ammonia consumption in strain BW86 ceased. It is conceivable that the initial uptake of ammonium allowed initial cyanophycin accumulation, resulting in a peak of cyanophycin amount at day 2 and 4 (Fig. 5b).

However, since after 4 days the strain BW86 stopped to consume ammonia and to grow (Fig. 5Bⁱ), the cells might have degraded their cyanophycin reserves and used them as internal nitrogen source. The impaired ammonia consumption of strain BW86 could indicate a possible role of P_{II} in ammonium utilization, which might be affected in the P_{II}(I86N) variant. In *Escherichia coli* and many other heterotrophic bacteria, the P_{II} homologue GlnK regulates the membrane-localized ammonia transporter AmtB [18]. Although an involvement of cyanobacterial

P_{II} in the regulation of Amt homologues has not yet been clearly demonstrated, such a function seems possible [28]. The phenotype of impaired ammonia utilization observed here could indicate a direct involvement of P_{II} in ammonia uptake in *Synechocystis* sp. as well.

As nitrate-grown cells had higher cyanophycin contents than ammonium-grown cells, we used nitrate as the nitrogen source in the following studies. In some cyanobacterial species, the cyanophycin content can increase up to 18 % of the CDM [11–13, 31] under certain stress-conditions. Generally, cyanophycin accumulation is triggered by conditions of reduced growth rate, such as entry into stationary phase or unbalanced cultivation conditions, whereas during exponential growth, the amino acids arginine and aspartate are mostly used for protein biosynthesis. To test the effect of growth limitation on cyanophycin accumulation, we starved cells for phosphate or potassium (Fig. 5c, d, respectively).

To induce phosphate starvation cells were washed and inoculated in phosphate free BG-11 medium. Since the internal phosphate pools are only slowly depleted, the cell growth in phosphate free medium is initially not affected. In order to avoid growth into stationary phase without full induction of phosphate starvation, after 2 days, the cultures were again diluted 1:5 in phosphate free medium. After two more days, growth ceases due to phosphate starvation. Accordingly, the cyanophycin content of both strains on day 0 and day 2 (Fig. 5c) is comparable to that of non-starved cells (Fig. 5a). In agreement, the growth rate at this early stage was not affected because of a sufficient internal phosphate pool (Fig. 5Cⁱ) [32]. On day 4, the cyanophycin content in both the wild-type and strain BW86 strongly increased, correlating to the onset of the phosphate starvation. After 12 days, the accumulation of cyanophycin was maximal, with the wild-type exhibiting 16.2 ± 1.9 % of the CDM and strain BW86 47.4 ± 2.3 % of the CDM.

Potassium starvation is a very strong and immediate stress for cyanobacterial cells [33] because it is not buffered by internal pools and stringently affects the growth. In the absence of potassium, the growth rate of both strains was nearly zero [33] (Fig. 5Dⁱ). To test the effect of potassium starvation on cyanophycin production, exponentially growing cells of both strains were washed and inoculated into potassium-free BG-11 medium (Fig. 5d). In contrast to phosphate starvation, the cyanophycin content in potassium-starved cells rapidly increased in the first 2 days, due to the rapid arrest of growth. As long as the metabolism is in an active state, growth arrest allows the efficient synthesis of reserve materials. In agreement, cyanophycin accumulation in the wild-type reached a peak of 15.8 ± 0.5 % of the CDM after 4 days. In strain BW86, a peak of 57.3 ± 11.1 % cyanophycin per

CDM was already reached on day 2. Thereafter, the cyanophycin content of both strains slowly decreased, probably a consequence of a stress response in the decaying cells, caused by the harmful lack of potassium.

Strain BW86 produces cyanophycin of high molecular mass

To test the influence of the P_{II} (I86N) mutation on the cyanophycin polymer length, we isolated cyanophycin granules from cells during the course of a phosphate starvation experiment. We used an extraction method that prevents hydrolyzation of the polymer that normally occurs during the usual acid extraction protocol (see “Methods”). The isolated polymer was solubilized in SDS sample buffer and analyzed by SDS-PAGE (Fig. 6). Cyanophycin isolated from strain BW86 had a size range of 25 to well above 100 kDa; the lowest molecular mass was slightly lower than that of the wild-type (range 30 to >100 kDa). Like in the wild-type, the time point at which samples were taken had no influence on the size distribution of the polymer. The high molecular weight of cyanophycin produced in strain BW86 is one of the main differences to other recombinant cyanophycin productions strains using heterologous expression systems with heterotrophic bacteria or genetically engineered yeast or plants harboring a cyanobacterial cyanophycin synthetase gene [34–36]. Those strains produce cyanophycin with a size range of only 25–45 kDa, but why they fail to produce higher molecular mass cyanophycin has not been elucidated so far. A possible explanation would be that cyanophycin synthesis in the native *Synechocystis* PCC 6803 background (as is provided in the presently engineered strain BW86) involves additional factors contributing to the polymer length. Further work on the molecular biology of cyanophycin granule synthesis is required to solve this question.

Microscopic examination of cyanophycin production in strain BW86

The above experiments showed that cells of strain BW86 massively overproduced cyanophycin during exponential growth and even more, under growth-limited conditions, whereas wild-type cells under both conditions produced very little amounts of cyanophycin. To gain insight into the distribution of cyanophycin production in the population of cells of strain BW86, we attempted to microscopically visualize cyanophycin. In previous studies, cyanophycin granules have been recognized by their appearance as light dense granules in bright-field images. Consequently, clear identification of granules is difficult and only large granules could be recognized. The Sakaguchi reaction is a colorimetric reaction for identifying and quantifying arginine [37]. To use the Sakaguchi reaction

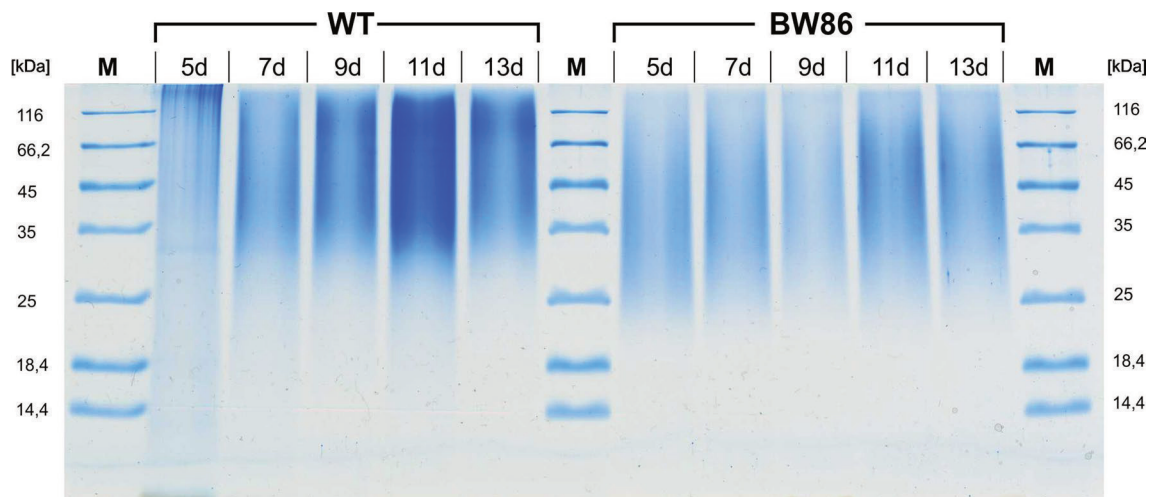


Fig. 6 SDS-PAGE determination of the molecular weight of cyanophycin isolated from *Synechocystis* sp. PCC 6803 wild-type (WT) and strain BW86 at the indicated time points (in days) from phosphate-starved cultures. Per lane, 40 µg cyanophycin was loaded

in unicellular cyanobacteria, we developed a fixation protocol that maintained the structure of cells and cyanophycin granules (Fig. 7).

The cytoplasm of exponentially growing wild-type cells stained light red due to the arginine content of cellular proteins. Dark red dots were visible only in very

few cells. The intense color of these particles arises presumably from the high arginine content, and they would thus correspond to cyanophycin granules (Fig. 7a). Accordingly, the cytoplasm of cells of strain BW86 was clearly stained darker red due to the higher arginine content as well as more and larger cyanophycin granules, and the granules were heterogeneously distributed. During phosphate starvation, almost all cells, both from the wild-type and strain BW86, produced cyanophycin granules recognizable as dark red dots (Fig. 7b). The granules in strain BW86 were clearly larger than those in the wild-type; i.e., strain BW86 accumulated a few large cyanophycin granules compared to the small granules in the wild-type. We resolved the granule size in greater detail by examining phosphate-starved cells of wild-type and strain BW86 by transmission electron microscopy (Fig. 8). Cells of strain BW86 contained huge ovoid granules with a scar-like sub-structure (Fig. 8b). To our knowledge, these are the largest cyanophycin granules observed to date. In agreement with the above results, the cyanophycin granules of the wild-type were considerably smaller.

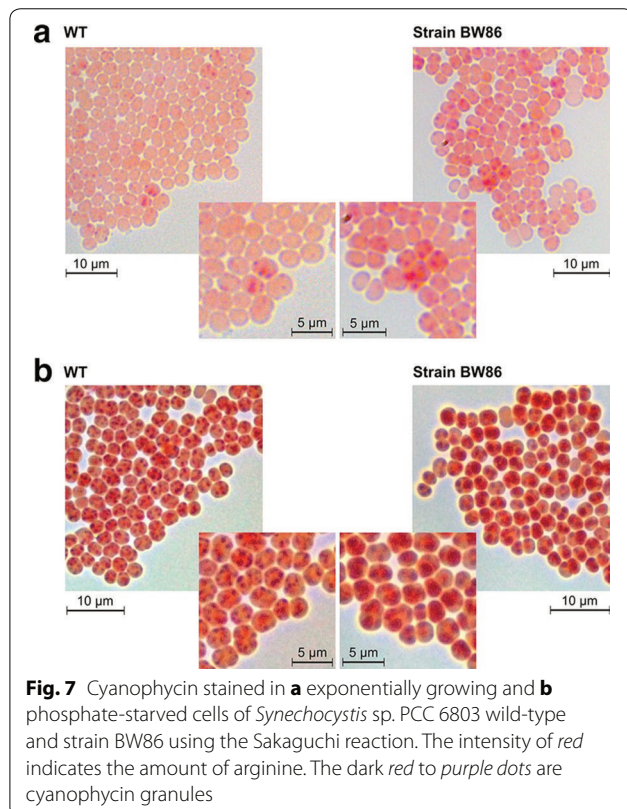


Fig. 7 Cyanophycin stained in **a** exponentially growing and **b** phosphate-starved cells of *Synechocystis* sp. PCC 6803 wild-type and strain BW86 using the Sakaguchi reaction. The intensity of red indicates the amount of arginine. The dark red to purple dots are cyanophycin granules

Conclusions

This work demonstrated the possibility of metabolic engineering using the P_{II}(I86N) variant of the P_{II} signal transduction protein to strongly increase arginine levels due to the P_{II} dependence of the key enzyme of arginine biosynthesis, NAGK. As a consequence, cells of the engineered strain, strain BW86, overproduced arginine and over-accumulated cyanophycin of high molecular weight. This direct link further supports our previous assumption that cyanophycin synthesis is primarily controlled

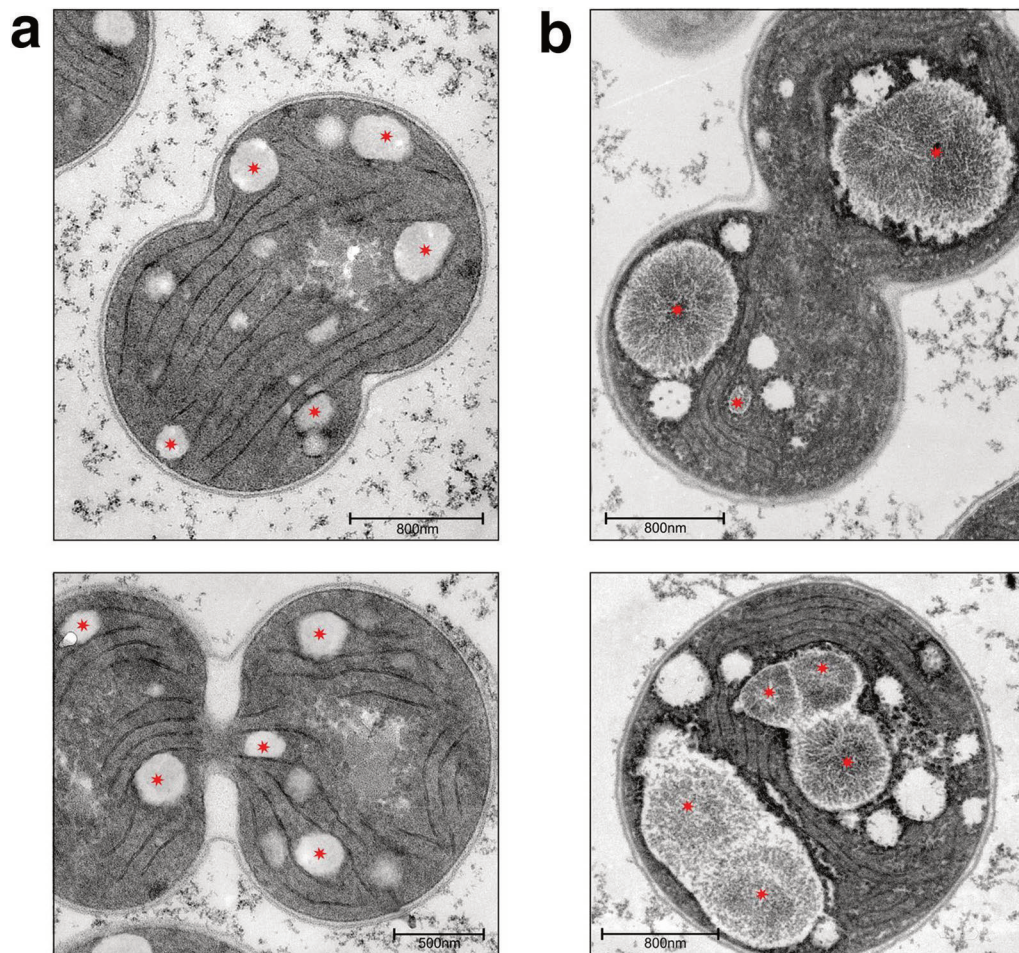


Fig. 8 Transmission electron micrographs of ultrathin sections of phosphate-starved **a** *Synechocystis* sp. PCC 6803 wild-type and **b** strain BW86. Red asterisks indicate cyanophycin granules

by cellular arginine levels [23]. Taken together, the *Synechocystis* sp. strain described in this study, strain BW86, is the most potent cyanophycin producer described to date and is, therefore, a promising option for photoautotrophic production of arginine as well as cyanophycin. The large amount of cyanophycin of high molecular weight that can be produced with this strain opens the possibility of investigating novel applications of this polymer for biotechnological purposes.

In addition to the specific benefit of arginine and cyanophycin production obtained with the P_{II} (I86N) variant, this study demonstrated the feasibility of using engineered variants of the P_{II} signaling protein for metabolic engineering in bacteria. In addition to arginine synthesis, P_{II} controls a multitude of other cellular activities in various autotrophic and heterotrophic bacteria. Therefore, metabolic pathways that are under control of this versatile regulatory protein could similarly be engineered.

Methods

Cultivation of bacteria

Standard cloning procedures were done in *E. coli* XL1-Blue (Stratagene) grown in Luria–Bertani medium at 37 °C with constant shaking at 300 rpm.

Cyanobacterial stains were grown photoautotrophically in BG-11 medium [38] containing nitrate or ammonium as nitrogen source and supplemented with 5 mM NaHCO_3 . Cultures were incubated in 50 or 200 ml medium in 100 or 500 ml Erlenmeyer flasks, respectively, at 28 °C with constant shaking at 120 rpm and illuminated with 50 $\mu\text{mol photons m}^{-2} \text{s}^{-1}$. Larger cultures were grown in illuminated cylinders containing 800 ml medium supplemented with 5 mM NaHCO_3 , 5 mM TES/NaOH pH 8.2 (Roth). The cylinders were constantly aerated by bubbling 2 % CO_2 in air through the liquid without additional shaking. Antibiotics were added to the media when required. Growth rates were monitored by measuring the optical density of the cultures at 750 nm.

Starvation conditions were induced by harvesting, washing, and transferring exponentially growing cells (OD_{750} 0.4–0.5) into BG-11 media lacking a specific nutrient, i.e., no nitrogen source for nitrogen starvation; K_2HPO_4 replaced by KCl for phosphate starvation; and K_2HPO_4 replaced by Na_2HPO_4 for potassium starvation. In the case of phosphate starvation, after 2 days cultures were diluted again in phosphate-free BG-11 medium to an OD_{750} of 0.15 to avoid entry into stationary phase before cellular phosphate reserves were exhausted.

Construction of a P_{II} (I86N)mutant

To construct a genomic P_{II} (I86N) mutant of *Synechocystis* sp. PCC 6803, the P_{II} -encoding gene *glnB* was genetically modified with the I86N mutation [Ile (5'ATC) at codon position 86 to Asp (5'AAC)]. The entire cloning procedure is shown in Additional file 3: Figure S3. To incorporate the corresponding ATC to AAC mutation in the *glnB* gene, two amplicons of *glnB* were made using oligonucleotides P_{II} (I86N)_rev (containing the ATC to AAC mutation) and P_{II} _prom_for as well as P_{II} _ter_rev (containing *SacI* restriction site) and P_{II} (I86N)_for. Both *glnB* amplicons were fused by fusion PCR resulting in the mutated *glnB* amplicon. The genomic region downstream of *glnB* was amplified using *slr0402*_rev (containing *NdeI* restriction site) and *slr0402*_for primers. The mutated *glnB* amplicon was fused with the *slr0402* fragment by fusion PCR and the resulting product was cloned in pJet 1.2 (Fermentas). Subsequently, a spectinomycin resistance cassette and a terminator sequence were inserted between the mutated *glnB* gene and the *slr0402* fragment for later selection. A spectinomycin resistance cassette was first amplified using oligonucleotides *spec*'_for (containing *SacI* restriction site) and *spec*'_rev and was then fused with a terminator sequence that was, amplified using oligonucleotides *Ter*_rev (containing *NdeI* restriction site) and *Ter*_for. The product was inserted between the *SacI* and *NdeI* restriction sites of the *glnB*-*slr0402* fusion product, resulting in pJet P_{II} (I86N). See Additional file 4: Table S1 for a list of all oligonucleotides used to generate constructs.

Synechocystis sp. PCC 6803 was transformed with pJet P_{II} (I86N) via natural competence [39]; transformants were selected on BG-11 agar plates supplemented with 25 μ g/ml spectinomycin. Transformants were screened for complete segregation via PCR using oligonucleotides P_{II} _prom_for and *slr0402*_for (Additional file 1: Figure S1).

In vivo NAGK activity assay

Cells (20 ml of a 50-ml culture at an OD_{750} of 0.8) were rapidly harvested by centrifugation and resuspended in a buffer consisting of 50 mM Tris/HCl pH 7.4, 4 mM EDTA, 1 mM DTT, and 0.5 mM benzamidine. Cells were

lysed using FastPrep[®]-24 (MP biomedical) with 0.1 mm glass beads at a speed of 6.0 m/s for 20 s five times. The lysate was separated into soluble and insoluble fractions by centrifugation at 25,000 \times g for 25 min at 4 °C. The protein concentration of the soluble fraction was determined using the Bradford assay [40]. NAGK activity of cell-free extract was measured according to Heinrich et al. [25] using 100 μ g/ml protein for each measurement.

Determination of P_{II} phosphorylation via western blotting

For non-denaturing electrophoretic separation of proteins, a native Gel was used according to Forchhammer et al. [30]. Per lane, 10 μ g of crude protein extract was loaded; after electrophoretic separation, the gel was blotted onto a PVDF membrane [41]. The membrane was blocked with TBS blocking buffer (25 mM Tris/HCl pH 7.4, 75 mM NaCl) containing 1 % (v/v) Tween 20 overnight at 4 °C. The membrane was washed three times with TBS containing 0.1 % (v/v) Tween 20 (TBS-T) and afterwards incubated in TBS-T containing the anti- P_{II} antibody [20] for 1 h at ambient temperature. Unbound antibody was removed by washing three times with TBS-T. Anti-rabbit IgG secondary antibody conjugated to horseradish peroxidase (α -rabbit polyclonal goat antibody, Sigma-Aldrich) diluted 1:10,000 in TBS-T was applied to the membrane and incubated for 30 min at ambient temperature. Unbound antibodies were removed by three washes with TBS-T. Bound antibodies were visualized using the Lumi Light detection system (Roche Diagnostics). Luminograms were taken with the Gel Logic 1500 imaging system (Kodak) with the associated software.

Metabolite extraction and quantification

For the extraction of metabolites, cells in 50 ml of culture at an OD_{750} of 0.8 were shock-cooled by mixing with crushed ice, rapidly harvested by centrifugation, and immediately frozen in liquid nitrogen. After freeze-drying, 5.0 mg lyophilized cells were homogenized with tungsten carbide beads in a Retsch Mill MM 200 (Retsch). Metabolites were extracted with 400 μ l methanol, followed by a second extraction of the cells with 400 μ l 20 % methanol with 0.1 % formic acid. The two supernatants were combined; solvents were removed using a vacuum concentrator. Metabolites were re-dissolved in 60 μ l 20 % methanol with 0.1 % formic acid. A 5 μ l aliquot was injected on a Waters UPLC/Synapt G2 LC/MS system equipped with a Waters Acquity 2.1 mm \times 100 mm, 1.8 μ m particle size HSS T3 reversed phase column. Metabolites were separated in a gradient from 20 % methanol with 0.1 % formic acid to 100 % methanol with 0.1 % formic acid in 10 min. The mass spectrometer was operated in ESI-positive and -negative modes with a scan range from m/z 50 to 2000 and a dwell time of 0.5 s. Data

were evaluated using the MarkerLynx Software (Waters Cooperation, Milford, MA, USA) in combination with Simca-P (Umetrics AB Umea, Sweden). Compounds (based on formula and MS^E fragmentation pattern) that differed between the different samples were identified by principal component analysis (PCA) and Orthogonal projections to latent structures (OPLS)—discriminant analysis (DA). From the entire metabolome, this procedure therefore identifies only those compounds, whose abundance differs between the two analyzed samples.

Cyanophycin extraction and quantification

Cyanophycin was extracted as described by Elbahloul et al. [42] with some modifications. Briefly, cells in 20–50 ml of culture at an OD₇₅₀ of 0, 1–4 were harvested by centrifugation, resuspended in 100 % acetone, and incubated for 30 min with constant shaking at 1400 rpm. Cells were collected by centrifugation at 25,000×g for 15 min. The pellet was resuspended in 1.5 ml 0.1 M HCl and incubated for 1 h with constant shaking at 1400 rpm at 60 °C to solubilize cyanophycin. To remove debris, the sample was centrifuged at 25,000×g for 15 min. Cyanophycin in the clear supernatant was precipitated by adding 300 µl 1 M Tris/HCl pH 8.0 and incubating the mixture for 40 min at 4 °C. The mixture was then centrifuged at 25,000×g for 15 min at 4 °C. The supernatant was discarded, and the pelleted cyanophycin was dissolved in 500 µl 0.1 M HCl. Cyanophycin was quantified by determining arginine using the Sakaguchi reaction according to Messineo [43].

Cyanophycin isolation and determination of molecular mass

To determine the molecular mass of native cyanophycin, we modified the procedure of Ziegler et al. [3] to avoid hydrolyzation of cyanophycin by acid extraction. Cells were harvested and washed three times in buffer consisting of 50 mM Tris/HCl pH 7.4, 150 mM NaCl, and 5 mM EDTA. The cell pellet was resuspended in B-PerTM buffer supplemented with 100 µg/ml lysozyme and 5 U/ml DNase I. Cells were lysed using FastPrep[®]-24 (MP biomedical) with 0.1 mm glass beads at a speed of 6.0 m/s for 20 s five times. The lysate was separated into soluble and insoluble fractions by centrifugation at 25,000×g for 25 min at 4 °C. The insoluble fraction was washed three times with the same buffer and resuspended in B-PerTM buffer supplemented with 200 µg/ml proteinase K, which does not degrade cyanophycin, and incubated at 50 °C overnight. Cyanophycin granules were collected by centrifugation at 25,000×g for 25 min at 4 °C and washed three times with water. Cyanophycin was quantified as described above. To determine the molecular mass, cyanophycin granules were solubilized in SDS-loading buffer and separated by SDS-PAGE on a 12 % polyacrylamide gel according to Sambrook and Russell [44].

Microscopy and cyanophycin staining

Cyanophycin granules in bacterial cells were visualized microscopically using a newly developed staining method based on the Sakaguchi reaction. Cells of a 500 µl culture at an OD₇₅₀ of 0.1–1.0 were collected via centrifugation and washed with 2.7 mM KCl, 1.5 mM KH₂PO₄, 137 mM NaCl, 8.1 mM Na₂HPO₄, pH 6.5 (PBS buffer). The cells were fixed by resuspending them in 500 µl PBS buffer containing 2.5 % (v/v) glutardialdehyde and incubated for 30 min at 4 °C. After fixation, the cells were washed with PBS and collected by centrifugation at 3000×g for 8 min at 4 °C. Then, cells were gently resuspended in 80 µl 5 M KOH and 10 µl of 1 % (w/v) 2,4-dichloro-1-naphthol dissolved in absolute ethanol was added; the mixture was incubated for 2 min at ambient temperature. Subsequently, 10 µl of 4–6 % (v/v) NaClO was added, and the mixture was incubated for 2 min. Finally, the cells were collected by centrifugation at 3000×g for 5 min, resuspended in 100 µl PBS buffer, and viewed under a Leica DM2500 microscope with a 100 ×/1.3 oil objective. Photographs were taken with a Leica DFC420C color camera.

Transmission electron microscopy

Samples for transmission electron microscopy were prepared as described in Fiedler et al. [45]. Briefly, samples were fixed and post-fixed using glutaraldehyde and potassium permanganate. The samples were embedded in EPON, and ultrathin sections were stained with uranyl acetate and lead citrate. The samples were examined with a Philips Tecnai electron microscope at 80 kV.

Additional files

Additional file 1: Figure S1. Complete segregation of the mutation in the polyploidy *Synechocystis* sp. BW86. The replacement of all genomic copies of *glnB* (*ssl0707*) confirmed via PCR with isolated genomic DNA of *Synechocystis* sp. BW86, and, as controls, the wild-type *Synechocystis* PCC 6803 and the pJet 1.2 pJet P_{II}(I86N) construct. Wild-type *glnB* produces a PCR fragment of approximately 1,300 bp, whereas the *glnB* (I86N) construct in both pJet 1.2 and strain BW86 produces a PCR fragment of approximately 2,600 bp with no observable wild-type background fragment.

Additional file 2: Figure S2. Ammonium concentration in culture supernatants of the wild-type *Synechocystis* sp. PCC 6803 (WT) and strain BW86 grown in BG-11 medium with ammonium.

Additional file 3: Figure S3. Cloning schemes for generation of the gene encoding P_{II}(I86N) in *Synechocystis* sp. PCC 6803 showing all primer binding positions and restriction sites used in the construction. A) Spectinomycin resistance cassette (*spec*) fused with a terminator sequence (*Ter*). B) P_{II}-encoding gene *glnB* and downstream open reading frame *slr0402*. C) Engineered construct encoding P_{II}(I86N) with spectinomycin resistance cassette inserted downstream of the variant *glnB* gene.

Additional file 4: Table S1. Oligonucleotides used in this study.

37. Deitch AD. An improved Sakaguchi reaction for microspectrophotometric use. *J Histochem Cytochem*. 1961;9:477–83.
38. Rippka R, Deruelles J, Waterbury JB, Herdman M, Stanier RY. Generic assignments, strain histories and properties of pure cultures of cyanobacteria. *J Gen Microbiol*. 1979;111:1–61.
39. Grigorieva G, Shestakov S. Transformation in the cyanobacterium *Synechocystis* sp. 6803. *FEMS Microbiol Lett*. 1982;13:367–70.
40. Bradford MM. A rapid and sensitive method for the quantitation of microgram quantities of protein utilizing the principle of protein-dye binding. *Anal Biochem*. 1976;72:248–54.
41. Towbin H, Staehelin T, Gordon J. Electrophoretic transfer of proteins from polyacrylamide gels to nitrocellulose sheets: procedure and some applications. *Proc Natl Acad Sci USA*. 1979;76:4350–4.
42. Elbahloul Y, Krehenbrink M, Reichelt R, Steinbuechel A. Physiological conditions conducive to high cyanophycin content in biomass of *Acinetobacter calcoaceticus* strain ADP1. *Appl Environ Microbiol*. 2005;71:858–66.
43. Messineo L. Modification of Sakaguchi reaction—spectrophotometric determination of arginine in proteins without previous hydrolysis. *Arch Biochem Biophys*. 1966;117:534–40.
44. Sambrook J, Russell D. *Molecular cloning: a laboratory manual*. 3rd ed. New York: Cold Spring Harbor Laboratory Press; 2001.
45. Fiedler G, Arnold M, Hannus S, Maldener I. The DevBCA exporter is essential for envelope formation in heterocysts of the cyanobacterium *Anabaena* sp. strain PCC 7120. *Mol Microbiol*. 1998;27:1193–202.

Submit your next manuscript to BioMed Central
and we will help you at every step:

- We accept pre-submission inquiries
- Our selector tool helps you to find the most relevant journal
- We provide round the clock customer support
- Convenient online submission
- Thorough peer review
- Inclusion in PubMed and all major indexing services
- Maximum visibility for your research

Submit your manuscript at
www.biomedcentral.com/submit



2. Accepted publication

Forchhammer, K. & **Wutzer, B.** (2016).

Closing a gap in cyanophycin metabolism (Microbiology Comment).

Microbiology, 162(5), 727-729.

Closing a gap in cyanophycin metabolism

Cyanophycin is a bacterial polymer that consists of the two amino acids aspartate and arginine, forming a poly-L-aspartic acid backbone with each carboxyl group linked to an arginine residue (multi-L-arginyl-poly-L-aspartic acid) (Simon, 1971). Cyanophycin was identified as a constituent of granular inclusions in cyanobacteria (Allen *et al.*, 1980) and was therefore referred to as cyanophycin granule polypeptide (CGP). CGP is synthesized by a single enzyme, cyanophycin synthetase, CphA1, in a two-step reaction from L-aspartate and L-arginine, with one ATP used per step. The first step in cyanophycin formation is an aspartate ligase reaction, where the C terminus of the growing chain is phosphorylated and then an aspartate residue is attached via peptide bond formation. Second, the β -carboxyl group of the newly added aspartate residue is phosphorylated and then ligated to the α -amino group of an L-arginine residue (Berg, 2003; Ziegler *et al.*, 1998). By these consecutive reactions, an Asp-Arg co-polymer is formed with a chain length of 100–500 Asp-Arg building units. With a C/N ratio of 2 : 1, this polymer is extremely rich in nitrogen and an excellent nitrogen storage compound (Carr, 1988; Obst & Steinbüchel, 2006). In agreement, CGP accumulates in many cyanobacteria under conditions of unbalanced growth (Allen *et al.*, 1980), when nitrogen is still available in abundance. The ability to form CGP is widespread among cyanobacteria and is found in both non-diazotrophic and diazotrophic strains. Meanwhile, CphA homologues were also identified in some heterotrophic bacteria (Krehenbrink *et al.*, 2002; Ziegler *et al.*, 2002).

As shown in the non-diazotrophic strain *Synechocystis* sp. PCC 6803, the accumulation of CGP depends on the cellular arginine level, which itself is controlled by the P_{II} signal transduction protein in response to the cellular nitrogen supply and energy supply (Maheswaran

et al., 2006; Watzer *et al.*, 2015). This ensures that CGP is produced only when nitrogen and energy are in abundance. Under conditions of nitrogen limitation, CGP can be rapidly metabolized and used as an internal nitrogen source. For this, CGP is first hydrolysed by cyanophycinase CphB, releasing the dipeptide β -aspartyl-arginine, which is subsequently cleaved by isoaspartyl dipeptidase, yielding the free amino acids Asp and Arg for further metabolic use (Fig. 1). In unicellular nitrogen-fixing cyanobacteria, CGP serves as a transient depository of fixed nitrogen that accumulates during active nitrogen fixation in the dark and is consumed during the day, when nitrogenase is switched off (Li *et al.*, 2001). In heterocystous filamentous cyanobacteria (order *Nostocales*), CGP appears to play an additional role. Heterocysts, specialized cells for nitrogen fixation, contain at their contact sites with the adjacent vegetative cells large CGP bodies, so-called polar nodules. This heterocystous CGP seems to be intimately involved in transfer of fixed nitrogen from heterocysts to the photosynthetically active vegetative cells (Burnat *et al.*, 2014). CGP is synthesized from the Asp and Arg pools of the heterocyst as a result of active nitrogen fixation, and simultaneously CGP is degraded by CphB to yield the β -aspartyl-arginine dipeptide, which is transported to the neighbouring cells and provides them with fixed nitrogen. At the same time, CGP could serve as a sink for fixed nitrogen in the heterocysts to prevent potential inhibitory feedback effects from soluble products of nitrogen fixation (Burnat *et al.*, 2014). However, *Anabaena* PCC 7120 mutants deficient in CGP synthesis showed no

diazotrophic growth defect (Picossi *et al.*, 2004), whereas diazotrophic growth of an *Anabaena variabilis* CphA1 mutant was impaired at high light intensities (Ziegler *et al.*, 2001).

In many nitrogen-fixing cyanobacteria, a truncated version of CphA1 is present, termed CphA2, whose function was enigmatic up to now. A deletion of the *cphA2* gene resulted only in a minor loss of total CGP and thus CphA2 was considered to be of minor importance (Picossi *et al.*, 2004). In the paper by Klemke *et al.* (2016), the authors identified a distinct function for CphA2 that closes an unrecognized gap in cyanophycin metabolism. They demonstrate that CphA2 acts as a cyanophycin synthetase that uses the β -aspartyl-arginine dipeptide as substrate, consuming one molecule of ATP per reaction. Thus, CphA2 enables a direct recycling of the β -aspartyl-arginine dipeptide into CGP (see Fig. 1). Although a loss of CphA2 results in only a minor decrease of the overall cellular CGP content, the reaction performed by CphA2 could be of considerable physiological relevance. The CphA2-deficient mutant displays a similar diazotrophic growth defect under high light conditions as compared to the CGP-free CphA1 mutant. This implies that the apparent 'futile cycling' of CGP by hydrolysis and immediate re-polymerization (Fig. 1) has functional importance. Despite the fact that CGP is present in CphA2 mutants, this polymer, in the absence of CphA2 function, seems to provide no benefit to the nitrogen-

Microbiology Comment provides a forum for discussion of scientific issues arising directly from papers published in the journal. The authors of papers under discussion will be offered an opportunity to respond.

Guidelines on how to submit a *Microbiology Comment* article can be found in the Instructions for Authors at <http://mic.microbiologyresearch.org>

It should be noted that the Editors of *Microbiology* do not necessarily agree with the views expressed in *Microbiology Comment*.

Tanya Parish, Editor-in-Chief

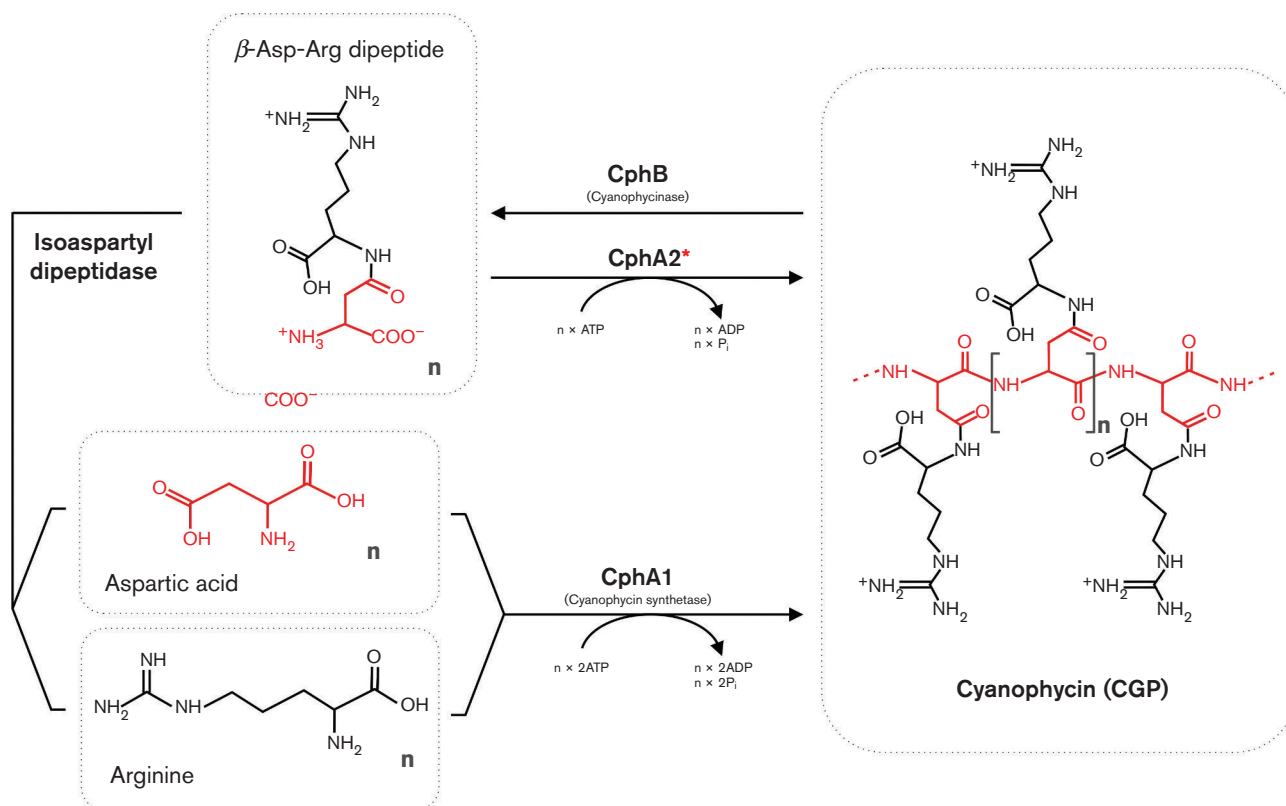


Fig. 1. Schematic illustration of CGP metabolism in N_2 -fixing cyanobacteria. The newly identified reaction of CphA2 (Klemke *et al.*, 2016) is indicated by the red asterisk.

fixing heterocystous filaments under high light conditions. Recycling CGP via CphA2 consumes less ATP than recycling via *de novo* synthesis from arginine and aspartate. However, if energy saving were the reason for the observed phenotype, as suggested by Klemke *et al.* (2016), an even stronger impairment would be expected under low light conditions, where the cells are really energy-limited. As this is not the case, the observation of Klemke and colleagues points towards another, as yet unknown requirement for dynamic remodelling of CGP in filamentous cyanobacteria. CphA2-mediated re-polymerization of the dipeptide could, for example, set an upper limit to the cellular concentration of β -aspartyl-arginine and thereby control its cleavage by isoaspartyl dipeptidase. Such a mechanism could enable different cells in the multicellular cyanobacteria to optimize and fine-tune their arginine or aspartate budget, depending on their position in the filament. Intriguingly, CphA2 homologues

are only present in cyanobacteria that fix nitrogen, including unicellular strains. In non-diazotrophic strains, where CGP functions only as a transient nitrogen reservoir, CphA2 is dispensable. The CphA2-mediated recycling of the β -aspartyl-arginine dipeptide seems, therefore, to be related to a specific function of CGP in unicellular and filamentous nitrogen-fixing cells, which deserves further investigation.

Karl Forchhammer and Björn Watzler

Department of Microbiology/Organismic Interactions, University of Tübingen, Auf der Morgenstelle 28, D-72076 Tübingen, Germany

Correspondence: Karl Forchhammer
karl.forchhammer@uni-tuebingen.de

Abbreviation: CGP, cyanophycin granule polypeptide.

References

- Allen, M. M., Hutchison, F. & Weathers, P. J. (1980). Cyanophycin granule polypeptide formation and degradation in the cyanobacterium *Aphanocapsa* 6308. *J Bacteriol* **141**, 687–693.
- Berg, H. (2003). *Untersuchungen zu Funktion und Struktur der Cyanophycin-Synthetase von Anabaena variabilis ATCC 29413*. Humboldt-Universität zu Berlin.
- Burnat, M., Herrero, A. & Flores, E. (2014). Compartmentalized cyanophycin metabolism in the diazotrophic filaments of a heterocyst-forming cyanobacterium. *Proc Natl Acad Sci U S A* **111**, 3823–3828.
- Carr, N. G. (1988). Nitrogen reserves and dynamic reservoirs in cyanobacteria. In *Biochemistry of the Algae and Cyanobacteria. Annual Proceedings of the Phytochemical Society of Europe*, pp. 13–21. Edited by L. J. Rogers & J. R. Gallon. Oxford: Clarendon Press.
- Klemke, F., Nürnberg, D. J., Ziegler, K., Beyer, G., Kahrmann, U., Lockau, W. & Volkmer, T. (2016). CphA2 is a novel type of cyanophycin synthetase in N_2 -fixing cyanobacteria. *Microbiology* **162**, 526–536.

- Krehenbrink, M., Oppermann-Sanio, F. B. & Steinbüchel, A. (2002). Evaluation of non-cyanobacterial genome sequences for occurrence of genes encoding proteins homologous to cyanophycin synthetase and cloning of an active cyanophycin synthetase from *Acinetobacter* sp. strain DSM 587. *Arch Microbiol* **177**, 371–380.
- Li, H., Sherman, D. M., Bao, S. & Sherman, L. A. (2001). Pattern of cyanophycin accumulation in nitrogen-fixing and non-nitrogen-fixing cyanobacteria. *Arch Microbiol* **176**, 9–18.
- Maheswaran, M., Ziegler, K., Lockau, W., Hagemann, M. & Forchhammer, K. (2006). P_{II}-regulated arginine synthesis controls accumulation of cyanophycin in *Synechocystis* sp. strain PCC 6803. *J Bacteriol* **188**, 2730–2734.
- Obst, M. & Steinbüchel, A. (2006). Cyanophycin—an ideal bacterial nitrogen storage material with unique chemical properties. In *Inclusions in Prokaryotes*, pp. 167–193. Edited by J. M. Shively. Berlin: Springer.
- Picossi, S., Valladares, A., Flores, E. & Herrero, A. (2004). Nitrogen-regulated genes for the metabolism of cyanophycin, a bacterial nitrogen reserve polymer: expression and mutational analysis of two cyanophycin synthetase and cyanophycinase gene clusters in heterocyst-forming cyanobacterium *Anabaena* sp. PCC 7120. *J Biol Chem* **279**, 11582–11592.
- Simon, R. D. (1971). Cyanophycin granules from the blue-green alga *Anabaena cylindrica*: a reserve material consisting of copolymers of aspartic acid and arginine. *Proc Natl Acad Sci U S A* **68**, 265–267.
- Watzer, B., Engelbrecht, A., Hauf, W., Stahl, M., Maldener, I. & Forchhammer, K. (2015). Metabolic pathway engineering using the central signal processor P_{II}. *Microb Cell Fact* **14**, 192.
- Ziegler, K., Diener, A., Herpin, C., Richter, R., Deutzmann, R. & Lockau, W. (1998). Molecular characterization of cyanophycin synthetase, the enzyme catalyzing the biosynthesis of the cyanobacterial reserve material multi-L-arginyl-poly-L-aspartate (cyanophycin). *Eur J Biochem* **254**, 154–159.
- Ziegler, K., Stephan, D. P., Pistorius, E. K., Ruppel, H. G. & Lockau, W. (2001). A mutant of the cyanobacterium *Anabaena variabilis* ATCC 29413 lacking cyanophycin synthetase: growth properties and ultrastructural aspects. *FEMS Microbiol Lett* **196**, 13–18.
- Ziegler, K., Deutzmann, R. & Lockau, W. (2002). Cyanophycin synthetase-like enzymes of non-cyanobacterial eubacteria: characterization of the polymer produced by a recombinant synthetase of *Desulfitobacterium hafniense*. *Z Naturforsch C* **57**, 522–529.

DOI 10.1099/mic.0.000260

3. Accepted publication

Trautmann, A., Watzer, B., Wilde, A., Forchhammer, K. & Posten, C. (2016).

Effect of phosphate availability on cyanophycin accumulation in *Synechocystis* sp. PCC 6803 and the production strain BW86.

Algal research, 20, 189-196.



Effect of phosphate availability on cyanophycin accumulation in *Synechocystis* sp. PCC 6803 and the production strain BW86



Andreas Trautmann^{a,*}, Björn Watzler^b, Annegret Wilde^c, Karl Forchhammer^b, Clemens Posten^a

^a Karlsruhe Institute of Technology (KIT), Institute of Process Engineering in Life Sciences, Section III: Bioprocess Engineering, Fritz-Haber-Weg 2, 76131 Karlsruhe, Germany

^b Interfaculty Institute of Microbiology and Infection Medicine Tübingen, Eberhard-Karls-Universität Tübingen, Auf der Morgenstelle 28, 72076 Tübingen, Germany

^c Institute of Biology III, University of Freiburg, 79104 Freiburg, Germany

ARTICLE INFO

Article history:

Received 1 August 2016

Received in revised form 28 September 2016

Accepted 16 October 2016

Available online 20 October 2016

Keywords:

Cyanophycin
Cyanobacteria
Phosphate starvation
Photobioreactor

ABSTRACT

The cyanobacterial wild-type strain *Synechocystis* sp. PCC 6803 and its engineered strain BW86 were cultivated under defined conditions in photobioreactors to investigate the effect of phosphate availability on cyanophycin accumulation. Cyanophycin, multi-L-arginyl-poly-L-aspartate, can be deployed as amino acid source or can be chemically converted into polyaspartic acid, a biodegradable polymer. In previous studies it was demonstrated that a single point mutation in the PII signaling protein from the *Synechocystis* wild type is sufficient to unlock the arginine pathway causing an over accumulation of the biopolymer cyanophycin in BW86. One process strategy to evoke cyanophycin synthesis in *Synechocystis* is nutrient starvation. Therefore, different phosphate concentrations from 17.5 to 175 μM were tested. Progressive phosphate starvation resulted in an increased cyanophycin accumulation. The highest obtained cyanophycin amounts in g cyanophycin per g cell dry mass were 18% and 40% for *Synechocystis* sp. PCC 6803 wild type and BW86 respectively, demonstrating that phosphate starvation is an effective route for biotechnological cyanophycin production. By evaluating cyanophycin and phosphorus quotas per cell dry mass, it was possible to determine the specific required amount of phosphorus to accumulate cyanophycin and to initialize stationary growth phase. Phosphorus quotas in the range of 4 to 1 mg phosphorus per g cell dry mass triggered cyanophycin biosynthesis while *Synechocystis* entered the stationary phase at phosphorus quotas of 1 mg phosphorus per g cell dry mass or less. Additionally, light kinetics was determined. Photon flux densities exceeding $46 \mu\text{mol photons m}^{-2} \text{s}^{-1}$ result in a maximum growth rate of 1.32 d^{-1} .

© 2016 The Authors. Published by Elsevier B.V. This is an open access article under the CC BY-NC-ND license (<http://creativecommons.org/licenses/by-nc-nd/4.0/>).

1. Introduction

Cyanobacteria are photosynthetic gram-negative prokaryotes. Besides their ability to obtain energy by oxygenic photosynthesis, they are known to synthesize reserve substances like cyanophycin, polyhydroxybutyrate (PHB) [1] and glycogen [2]. The accumulation of cyanophycin or multi-L-arginyl-poly-L-aspartate, a nitrogen and carbon reserve polymer, is unique for cyanobacterial metabolism and a few other heterotrophic bacteria [3–7].

Extracted cyanophycin can be chemically converted to polyaspartic acid, a biodegradable substitute for polyacrylic acid which can be used for many technical and medical applications [8,9]. Furthermore, cyanophycin could be used as a possible amino acid source for arginine and asparagine. Cyanophycin-derived dipeptides as natural alternatives to the widely applied amino acid mixtures are under discussion [10].

Cyanophycin consists of a polyaspartic acid backbone, its β -carboxyl groups are linked via amid bonds to the α -amino group of L-arginine. Aspartic acid and arginine are usually present in equimolar amounts in cyanophycin. The molecular masses of the polymer range from 25 to 100 kDa [11–14]. Cyanophycin is located in the cytoplasm in form of optically opaque granules. It is soluble under acidic, $\text{pH} < 2$, or alkaline, $\text{pH} > 9$, conditions and insoluble at physiological pH [15,16]. Cyanophycin is non-ribosomally synthesized by the cyanophycin synthetase (CphA) and can be degraded by the enzyme cyanophycinase within the cell (CphB) or extracellularly by the cyanophycin hydrolyzing enzyme CphE, which is excreted by other bacteria like *Pseudomonas anguilliseptica* [17]. It has to be mentioned that other proteases like pepsin, leucine aminopeptidase, chymotrypsin or α - and β -carboxypeptidases are not able to degrade cyanophycin [18–21].

The cyanophycin content of *Synechocystis* sp. PCC 6803 (from now on *Synechocystis* 6803) and other cyanobacteria varies depending on the growth phase and environmental conditions. During exponential growth, a cyanophycin content of roughly 1% per cell dry mass (CDM) is reported while higher contents up to 18% per CDM are synthesized under unbalanced conditions, as there are nutrient starvation e.g. of phosphate or sulfate, adverse light intensities and low temperature

* Corresponding author at: Institute of Process Engineering in Life Sciences, Section III: Bioprocess Engineering, Karlsruhe Institute of Technology (KIT), Fritz-Haber-Weg 2, 76131 Karlsruhe, Germany.

E-mail address: andreas.trautmann@kit.edu (A. Trautmann).

[22,23]. Simon [5] showed that chloramphenicol, a broad-spectrum antibiotic which inhibits protein synthesis, stimulates cyanophycin synthesis in *Anabaena cylindrica*. Cyanophycin contents up to 46% (w/w) were achieved in cultivations of *Acinetobacter calcoaceticus* by using a phosphate-limited medium spiked with arginine and chloramphenicol [24]. Generally, cyanophycin accumulation is depending on the availability of arginine [25].

It is also possible to obtain increased cyanophycin concentrations by genetic engineering. The key enzyme of the arginine pathway, acetyl glutamate kinase (NAGK), is controlled by the global carbon-nitrogen-energy-status sensing PII signaling protein, which is a member of the widely distributed family of PII signal transduction proteins, present in bacteria, plants and archaea [26]. PII proteins are involved in the regulation of nitrogen assimilation. Therefore PII senses the cellular energy level by binding ATP or ADP, as well as the carbon/nitrogen availability by 2-oxoglutarate [27–29]. Depending on the bound effector molecules and phosphorylation status, PII changes its conformation leading to a structural rearrangement of the T-loops, which are the major protein interaction structures [30]. Under nitrogen excess conditions, PII binds to NAGK [31] and strongly enhances its activity. A PII variant with a single amino acid replacement, Ile86 to Asp86, is responsible for a constitutively in vivo activation of NAGK, which leads to the accumulation of cyanophycin in high amounts in this strain, named BW86. Under phosphate-limited conditions this engineered strain accumulated an extremely high cyanophycin content per CDM, which is 57% [32]. To our knowledge this is the highest cellular cyanophycin content in a bacterial cell reported so far.

Here the engineered strain *Synechocystis* BW86 is used to investigate the quantitative effect of phosphate availability on cyanophycin accumulation. Experiments were carried out in photobioreactors under defined cultivation conditions. The wild-type strain *Synechocystis* 6803 was cultivated using the same process parameters as benchmark. Furthermore, light kinetics were determined for the wild type.

2. Materials and methods

2.1. Strain, medium and culture conditions

Liquid cultures of the strains *Synechocystis* 6803 and BW86 [32] were cultivated for 2 weeks in shaking flasks and incubated at 25 °C, 100 rpm, pH 7.5 and a photon flux density (PFD) of 135 $\mu\text{mol m}^{-2} \text{s}^{-1}$ (PAR photons, photosynthetic active radiation) supplied by warm-white LED illumination. The culture medium was BG-11 [33]. In shaking flask cultures, 10 mM HEPES buffer was added to the medium. Phosphate concentrations in the photobioreactor experiments varied from 16.65, 8.32, 4.16, 3.33 and 2.08 to 1.66 mg L^{-1} . Reduced phosphate concentrations were achieved by using lower amounts of K_2HPO_4 in the culture medium. To prevent potassium starvation, KCl was added in equimolar amounts. To attain equal starting conditions for the respective experiments, the inoculum volumes were slightly adjusted depending on the optical densities of the precultures. All chemicals used were of analytical grade (p.a.) and purchased from Carl Roth, Sigma Aldrich, VWR Chemicals and Merck.

2.2. Photobioreactor system

Experiments to investigate cyanophycin accumulation were carried out in flat plate photobioreactors (Midiplate reactor, Fig. S2 in the supplementary material) with a working volume of 1 L and a temperature of 28 °C. This reactor system was described earlier by Dillschneider et al. [34]. Light kinetics were determined in flat plate photobioreactors (Miniplate reactor) with a working volume of 0.2 L. The basic design is analogous to the Midiplate reactor with inner reactor dimensions for height, width, depth of 140, 100, 20 mm. Gas flow was adjusted to 0.33 and 0.25 vvm for Midi- and Miniplate reactors, respectively. Prior to inoculation the reactor system was saturated with 2 to 5% CO_2 for

24 h. In Miniplate reactors temperature was controlled by a climate chamber (25 °C, MKK1200, Flohr Instruments) and pH was buffered with 10 mM HEPES, while 1 M NaOH was used for pH adjustment in Midiplate reactors. The pH value was set to 7.5. For experiments in Midiplate reactors, the amount of CO_2 and O_2 in the exhaust gas was measured by the gas analyzer M610, Maihak AG. PFD (PAR photons) was adjusted with a planar light sensor (Li-250, Li-Cor) by measuring the PFD directly behind the first glass plate where photons enter the liquid suspension. The amount of transmitted photons was measured behind the second glass plate. Illumination was supplied using warm-white LEDs.

2.3. Cyanophycin extraction and quantification

Cyanophycin extraction was carried out as described in the protocol from Elbahloul et al. [24] with some modifications. A sample volume of 15 mL was centrifuged (Rotina 420R, Hettich Zentrifugen) for 15 min with 11,000 rpm and 4 °C and supernatant discarded. The remaining pellet was dissolved in 1 mL absolute acetone and incubated at room temperature for 30 min at 900 rpm (orbital shaker KS 501 digital, IKA). After a second centrifugation step (10 min, 11,000 rpm, 4 °C) the acetone supernatant was discarded again, the pellet was resuspended in 1.2 mL 0.1 M HCl and incubated for 60 min at 60 °C and 900 rpm. A third centrifugation step (10 min, 11,000 rpm, 4 °C) was performed to remove cell debris as pellet. The supernatant contains the solubilized cyanophycin. Addition of 720 μL 0.1 M Tris/HCl, pH 8.0, to the supernatant and following incubation at 4 °C for 40 min leads to precipitation of cyanophycin. A further centrifugation step (15 min, 11,000 rpm, 4 °C) was carried out to obtain a cyanophycin pellet. The described precipitation step was repeated once more with the obtained pellet to ensure a higher purity of the product. After disposal of the supernatant, the pellet was resuspended in 500 μL 0.1 M HCl. Cyanophycin quantification was carried out according to Messineo [35] by using the Sakaguchi reaction, a detection method for arginine. L-arginine was used to generate a calibration curve. Each cyanophycin sample was measured in duplicates.

2.4. Ion chromatography

Concentrations of nitrate (NO_3^-), phosphate (PO_4^{3-}) and sulfate (SO_4^{2-}) were determined by ion chromatography (Metrohm 882 Compact IC plus) equipped with a Metrosep A Supp 5 column 150/4.0, filling material polyvinyl-alcohol with quaternary ammonium groups, as stationary phase and a conductivity detector (Metrohm). The limit of quantification was 1.0 mg L^{-1} . Mobile phase was an elution buffer consisting of 3.2 mM Na_2CO_3 , 1.0 mM NaHCO_3 and 12.5% (v/v) acetonitrile in water. Cyanobacterial samples were centrifuged (10 min, 11,000 rpm, 4 °C) and the supernatant was used for subsequent analyses. An autosampler unit (Metrohm Professional Sample Processor 858) diluted and injected the samples automatically. The phosphor concentration was calculated through the determined phosphate concentration by the particular molar mass of phosphor and phosphate, 30.97 g mol^{-1} and 94.97 g mol^{-1} .

2.5. Determination of cell dry mass concentration and cell density

For CDM determination, duplicates of 20 mL cyanobacterial samples were taken, centrifuged (15 min, 6000 rpm, 4 °C, Rotina 420R, Heraeus), washed and incubated in a drying chamber (48 h, 80 °C). The resulting pellets were cooled down to room temperature and weighed on an analytical balance (Kern & Sohn GmbH ABJ 320-4). A synchronous measurement of the optical density at 750 nm (spectrophotometer Lambda 35, Perkin Elmer) enabled the generation of individual calibration curves for each experiment. A reproducible correlation factor of 0.179 g CDM L^{-1} per $\text{OD}_{750\text{nm}}$ for wild type ($R^2 = 0.997$) and 0.177 g CDM L^{-1} per $\text{OD}_{750\text{nm}}$ for BW86 ($R^2 = 0.999$) was determined. Cell density was measured via flow cytometry (Guava EasyCyte 6–2 L,

Merck Millipore). Cyanobacterial cells were counted by gating RED/RED2 fluorescence; RED = red laser, filter bandpass 690/50; RED2 = red laser, filter bandpass 661/19. The cell density of each sample was measured in triplicates.

2.6. Calculation of specific growth rate

The specific growth rate μ in d^{-1} was determined from the initial exponential phase according to eq. (1) where $c_{X,2}$ is the cell concentration on time point t_2 and $c_{X,1}$ the cell concentration on time point t_1 . Using the optical density at 750 nm instead of c_X would also be applicable.

$$\mu = \ln\left(\frac{c_{X,2}}{c_{X,1}}\right) \cdot \frac{1}{t_2 - t_1} \quad (1)$$

2.7. Calculation of photo conversion efficiency

Photo conversion efficiency (PCE) was calculated as the quotient of E_X , the captured biomass energy, divided by $E_{abs,light}$, the absorbed light energy (Eq. (2)).

$$PCE = \frac{E_X}{E_{abs,light}} \cdot 100 \quad (2)$$

According to Dillschneider et al. [34], by assuming an average photon energy E_{photon} of $210.48 \text{ kJ mol}^{-1}$ for the illumination device and an combustion enthalpy of cyanobacterial biomass ΔH_X of 22 kJ g^{-1} [36], E_X and $E_{abs,light}$ can be defined as follows (eq. (3)):

$$PCE = \frac{P_X \cdot \Delta H_X}{E_{photon} \cdot \frac{A_F}{V_R} \cdot (I_0 - I_{trans}) \cdot \Delta t} \cdot 100\% \quad (3)$$

with P_X as the volumetric CDM productivity in $\text{g L}^{-1} \text{ d}^{-1}$, A_F in m^2 the illuminated surface area of the liquid reactor volume V_R in L, I_0 and I_{trans} in $\text{mol m}^{-2} \text{ d}^{-1}$ represents the incident and transmitted PFD. Start and end time of the PCE calculation interval is defined as Δt [d]. It has to be mentioned that ΔH_X can change with biomass composition [34]. The measurements for I_0 and I_{trans} were performed in triplicates using a planar light sensor (Li-250, Li-Cor).

2.8. Calculation of cyanophycin and phosphor quota

The calculations of cyanophycin and phosphor quota are given in Eq. (4). Either cyanophycin c_{CP} (w/v) or phosphor concentration c_P (w/v) is used for c_i with reference to the measured CDM concentration c_X (w/v).

$$q_{i,X} = \frac{c_i}{c_X} \quad (4)$$

By the evaluation of quotas (w/w), it is possible to determine the specific content of the investigated substance within the produced biomass. Quotas can be seen as an expression for theoretical balance boundary of cells.

2.9. Statistical analysis

One representative photobioreactor experiment was performed for each initial phosphate concentration and light intensity. The measurement of cyanophycin, optical density and cell density were conducted in duplicates, while PFD was measured in triplicates. A correlation curve enabled the determination of CDM in triplicates from optical density measurements. The software Microsoft Excel 2013 was used to calculate average and standard deviation values as well as one-way analysis of variance (ANOVA) with a statistical significance of $p = 0.05$. For IC analysis, an absolute analytical error of 10% was applied.

3. Results

3.1. Growth rates in dependency of photon flux densities

A light kinetics curve for the strain *Synechocystis* 6803 was determined in Miniplate photobioreactors to identify the reasonable irradiance for maximum growth (Fig. 1). Therefore, PFD were adjusted to 15, 25, 50, 100, 160, 250 and $450 \mu\text{mol m}^{-2} \text{ s}^{-1}$. For each irradiance used, one batch experiment was performed and specific growth rate μ in d^{-1} was determined according to Eq. (1). The particular growth curve for each light intensity applied can be found in Fig. S2 in the supplementary material. Since low biomass concentrations $<0.125 \text{ g CDM L}^{-1}$ were used to study the effect of PFD on growth rate, the formation of a light gradient can be neglected. In our experiments the maximum growth rate was $1.32 d^{-1}$, resulting in a generation time of $0.52 d^{-1}$ ($= \ln(2)/1.32 d^{-1}$) or a cell division rate of $1.91 d^{-1}$ ($= 1.32 d^{-1}/\ln(2)$). We observed that growth rate increased strongly when PFDs in the range of 15 to $50 \mu\text{mol m}^{-2} \text{ s}^{-1}$ were applied, while in the range of 100 to $450 \mu\text{mol m}^{-2} \text{ s}^{-1}$ μ showed only a slight increase. The point of intersection between the dashed lines in Fig. 1 represents I_k , the transition from photo-limited to the photo-saturated region. I_k was determined to be $46 \mu\text{mol m}^{-2} \text{ s}^{-1}$. This means that in the light-limited region, lower than $46 \mu\text{mol m}^{-2} \text{ s}^{-1}$, growth rate is directly proportional to irradiance whereas in the light-saturated region, above $46 \mu\text{mol m}^{-2} \text{ s}^{-1}$ this relation is no longer valid and the growth rate reaches its maximum at around $150 \mu\text{mol m}^{-2} \text{ s}^{-1}$. However, for future experiments it would be reasonable to use a PFD slightly higher than I_k to achieve high growth rates with the lowest possible light intensity supplied.

3.2. Cultivation of *Synechocystis* BW86 under phosphate starvation

Batch experiments in Midiplate reactors were performed with different concentrations of phosphate in the culture medium in order to investigate the potential of *Synechocystis* BW86 to accumulate the biopolymer cyanophycin. Initial phosphate concentrations varied from 16.65, 8.32, 4.16, 3.33 and 2.08 to 1.66 mg L^{-1} (corresponding to 5.43, 2.71, 1.36, 1.09 and $0.68 \text{ to } 0.54 \text{ mg L}^{-1}$ phosphor). Furthermore, the wild-type strain *Synechocystis* 6803 was cultivated under same conditions as benchmark. Since the phosphate availability affects both cyanophycin accumulation and metabolism maintenance, we were able to evaluate how the concentration of the internal cellular

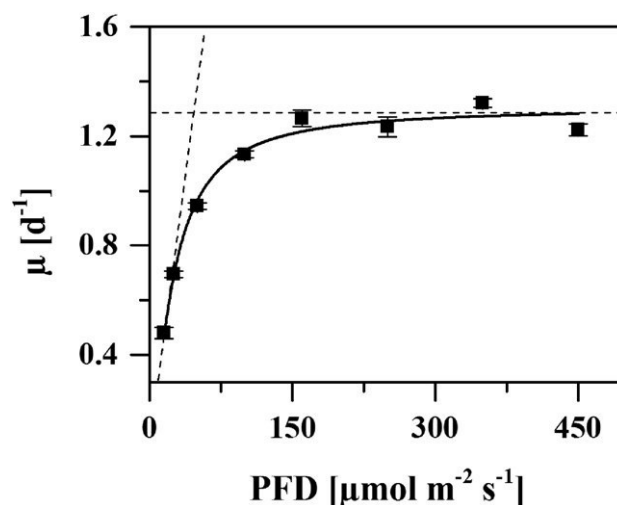


Fig. 1. Growth rate of *Synechocystis* 6803 in dependence on light intensity (photon flux density, PFD) at 25°C , pH 7.5 and 5% CO_2 . The point of intersection of the dashed lines represents the transition from the photo-limited to the photo-saturated range, $I_k = 46 \mu\text{mol m}^{-2} \text{ s}^{-1}$; maximum growth rate was $1.32 d^{-1}$. Error bars represent the standard deviation of one representative batch cultivation.

phosphate, i.e. the phosphor quota $q_{P,X}$ (in mg initial phosphor per g CDM), specifically influences the cyanophycin concentration, i.e. the cyanophycin quota $q_{CP,X}$ (in g cyanophycin per g CDM), as well as the transition to stationary growth phase. I_0 was manually adjusted to $70 \mu\text{mol m}^{-2} \text{s}^{-1}$ prior to each experiment in accordance to I_k (Fig. 1) and in order to facilitate the comparability with Watzer et al. [32]. The initial biomass concentration (CDM) for all experiments was 0.03 g L^{-1} .

Fig. 2 shows exemplarily a batch cultivation with an initial phosphate concentration of 3.33 mg L^{-1} (corresponding to 1.09 mg L^{-1} phosphor). Concentration gradients of CDM c_X , phosphor c_P , cyanophycin c_{CP} and the PFD of transmitted photons I_{trans} are given in Fig. 2A. Fig. 2A can be defined as the balance boundary “cell suspension”, showing volumetric quantities. Fig. 2B shows the cell concentration c_{cells} , phosphor quota $q_{P,X}$ and cyanophycin quota $q_{CP,X}$ and therefore can be defined as the balance boundary “cells”, showing specific quantities. During the first 4 days cells were growing exponentially while I_{trans} decreased to $19 \mu\text{mol m}^{-2} \text{s}^{-1}$, corresponding to a decrease of 67%. From day 4 to 8 growth extends linearly and merges into the stationary phase from day 8 to 9. Due to the increasing biomass concentration, I_{trans} decreased below $6 \mu\text{mol m}^{-2} \text{s}^{-1}$ until cultivation day 13. The cultivation was finished at day 13 with a maximum biomass concentration

of 1.1 g L^{-1} . Concerning the low amount of transmitted light at the end of this experiment, the cells are light limited at this point. As can be seen in Fig. 2 light limitation usually leads to linear growth. Hence, with phosphate as the only depleted nutrient, stationary growth phase was induced due to phosphate limitation. The predetermined amount of phosphor was consumed within the first 24 h of cultivation as confirmed by ion chromatography (Fig. 3). Incident and transmitted PFD were measured to calculate the photo conversion efficiency (PCE, Table 1). The calculation of PCE was performed according to chapter 2.7 and yielded a value of 5.5% for this exemplary batch cultivation.

Cyanophycin concentration increased 8.5fold from 40 to 340 mg L^{-1} , resulting in a cyanophycin quota $q_{CP,X}$ of 0.14 and 0.34 g cyanophycin per g CDM, respectively. After entering the stationary phase, c_{CP} did not increase anymore. By considering the progression of $q_{CP,X}$ in Fig. 2B an increase in cyanophycin content was observed during the linear phase. During the stationary phase, $q_{CP,X}$ decreased slightly from 0.34 to $0.32 \text{ g cyanophycin per g CDM}$. This decline can be attributed to the increase in c_X from 1.0 to 1.1 g L^{-1} despite steady cell concentrations c_{cells} , which indicates that cyanobacterial cells increase their weight, probably by accumulating proteins or storage compounds like lipids, PHB or glycogen. The amount of initial phosphor per CDM $q_{P,X}$

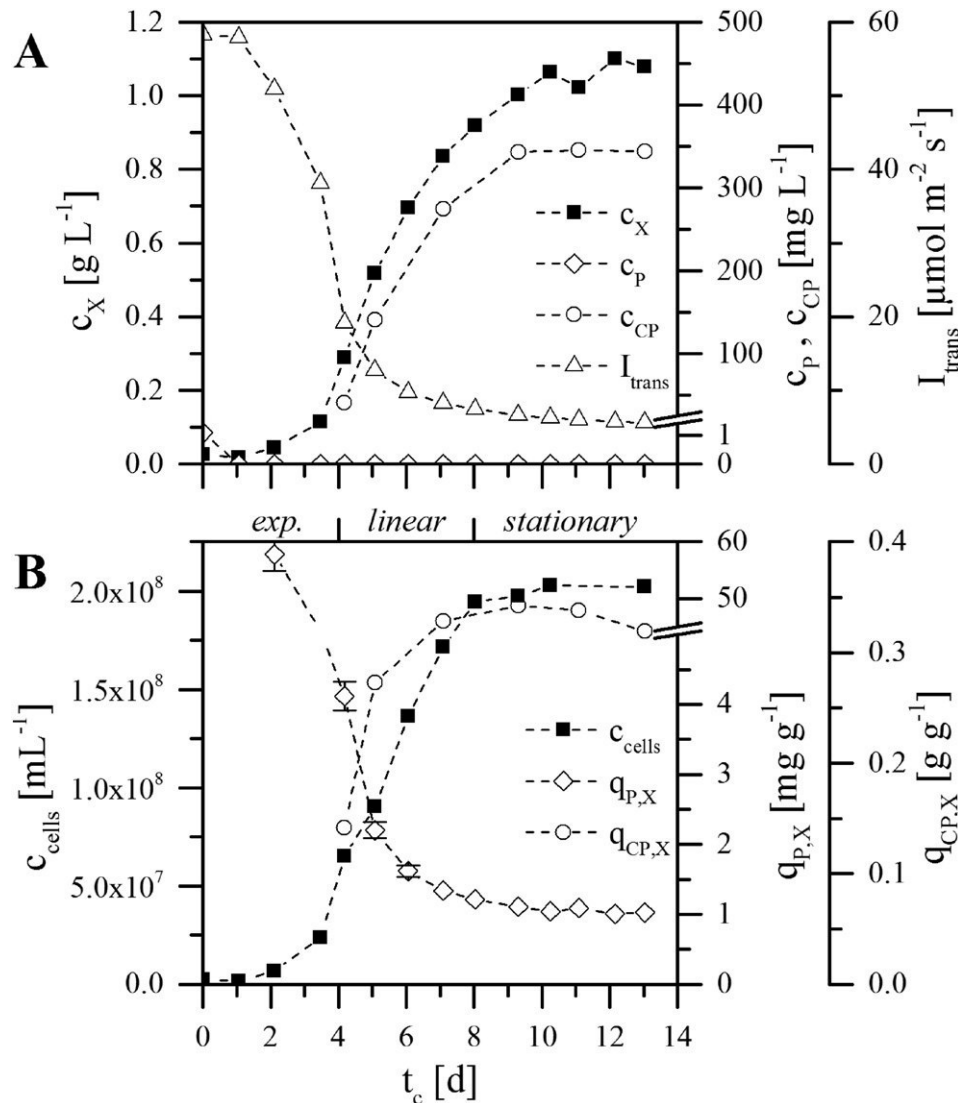


Fig. 2. Batch cultivation of *Synechocystis* BW86 under phosphate starvation in dependence of cultivation time t_c . A: cell dry mass (CDM) concentration c_X , media phosphor concentration c_P , cyanophycin concentration c_{CP} and PFD of transmitted photons I_{trans} . B: cell concentration c_{cells} , phosphor quota $q_{P,X}$ [mg initial phosphor per g CDM] and cyanophycin quota $q_{CP,X}$ [g cyanophycin per g CDM]. Cultivation parameters: I_0 $70 \mu\text{mol m}^{-2} \text{s}^{-1}$, 28°C , pH 7.5–8.0, 2% CO_2 . Except for $q_{P,X}$ no error bars are given since no significant difference regarding the standard deviation ($<1\%$) was observed.

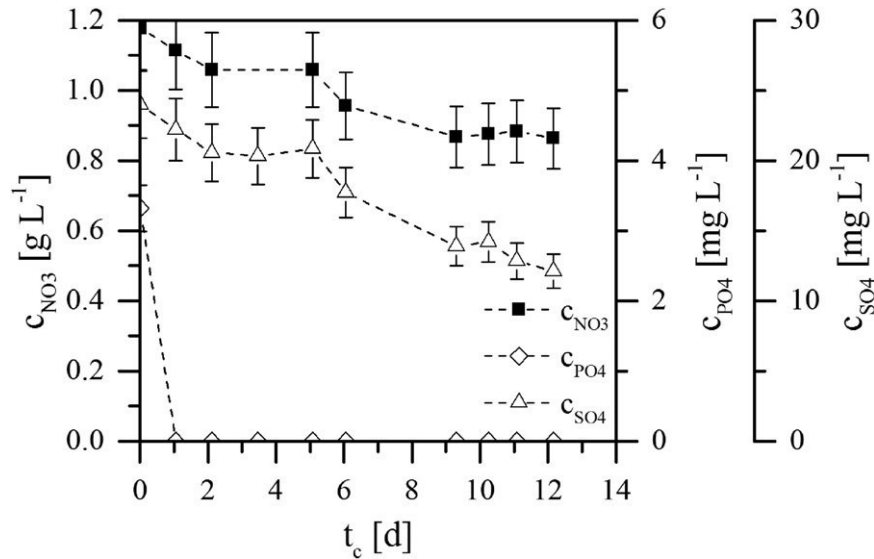


Fig. 3. Nutrient consumption during *Synechocystis* BW86 batch cultivation under phosphate starvation in dependence of cultivation time t_c . The nutrient concentrations of nitrate (c_{NO_3}), phosphate (c_{PO_4}) and sulfate (c_{SO_4}) were determined. Error bars mark an absolute analytical error of 10%.

showed a reverse progression compared to c_{cells} . At the end of exponential phase, $q_{P,X}$ was already reduced to 4.1 mg/g and reduced further to 1.2 and 1.0 mg/g at the end of linear and stationary phase, respectively. The data presented in Fig. 2B show that the highest increase in cyanophycin content occurred in the range of 4.1 to 1.2 mg phosphor per g CDM and that the stationary phase was initiated at 1.0 mg phosphor per g CDM. This value corresponds to a phosphor content of 5.5 ng phosphor per cell. Thus, according to the determined values for $q_{P,X}$ and under consideration of the growth curves, the entry to the stationary phase presumably occurs at phosphor quotas of 1.0 mg phosphor per g CDM or 5.5 ng phosphor per cell. The accumulation of cyanophycin occurs between 4.1 and 1.2 mg phosphor per g cell or 16.6 to 6.0 ng phosphor per cell. The nutrients nitrate and sulfate were sufficiently available since their final concentrations at the end of the cultivation were estimated as 0.86 g nitrate L^{-1} and 12.1 mg sulfate L^{-1} (Fig. 3).

It was furthermore possible to evaluate the specific cyanophycin formation rate r_{CP} in d^{-1} , and the specific growth rate μ in d^{-1} . r_{CP} was calculated according to Eq. (5) where $c_{i,2}$ is the cell concentration on time point t_2 and $c_{i,1}$ the cell concentration on time point t_1 .

$$r_{CP} = \frac{c_{CP,2} - c_{CP,1}}{t_2 - t_1} \cdot \frac{1}{c_{X,2}} \quad (5)$$

A linear stoichiometric correlation between r_{CP} and μ was observed. The slope of the estimated specific rates was determined to be 0.33 (correlation coefficient $R^2 = 0.999$, Fig. 4).

3.3. Cyanophycin accumulation of *Synechocystis* 6803 and BW86 under phosphate starvation

The engineered strain *Synechocystis* BW86 and the wild-type strain were used to investigate the effect of phosphate availability regarding cyanophycin accumulation. Therefore, several cultivations with different initial phosphate concentrations in BG-11 medium were performed, using Midiplate photobioreactors. A representative batch process for *Synechocystis* BW86 is illustrated in chapter 3.2. The combined results of all performed batch cultivations regarding the cyanophycin quota $q_{CP,X}$ in dependence of initial phosphor concentration $c_{P,initial}$ (applied as K_2HPO_4 in the medium) and in dependence of phosphor quota $q_{P,X}$ are shown in Fig. 5. With the reduction of the initial phosphate concentration in the medium ($c_{P,initial} \sim 2.71 \text{ mg L}^{-1}$), an increased cyanophycin quota was observed in the stationary phase ($q_{CP,end,X}$). From 2.71 to 0.54 mg L^{-1} a linear increase in $q_{CP,end,X}$ for both *Synechocystis* 6803 and BW86 was detected. A maximum of 0.40 and 0.18 g cyanophycin per g CDM was achieved for mutant and wild-type cultures, respectively (Fig. 5A).

The diagram in Fig. 5B, representing phosphor quotas to corresponding cyanophycin quotas for *Synechocystis* BW86 and 6803, reveals that a certain amount of phosphor should not be exceeded to induce cyanophycin accumulation. For phosphor quotas higher than 4 mg per g, no increase in $q_{CP,X}$ was found. In contrast, as soon as $q_{P,X}$ falls below 4 mg phosphor per g CDM, cyanophycin accumulation occurs. For $q_{P,X}$ values < 1 mg phosphor per g CDM no further increase of $q_{CP,X}$ was observed because the stationary phase was usually reached at this point, most likely due to the ongoing decrease in $q_{P,X}$ and the related

Table 1

Initial phosphor concentrations $c_{P,initial}$, calculated from applied K_2HPO_4 , and corresponding final biomass concentrations $c_{X,end}$, cell densities $c_{cells,end}$, cyanophycin quotas $q_{CP,end,X}$ and photosynthetic conversion efficiencies (PCE) for the photoautotrophic cultivation of *Synechocystis* BW86 and 6803. Data are means of at least two measurements. Standard deviation for $c_{P,initial}$ and $q_{CP,end,X}$ represents an absolute analytical error of 10%. The respective columns for BW86 and 6803 are significantly different ($p < 0,05$) according to $c_{P,initial}$.

$c_{P,initial}$ [mg L^{-1}]	$c_{X,end}$ [g L^{-1}]		$c_{cells,end}$ [mL^{-1}]		$q_{CP,end,X}$ [g g^{-1}]		PCE [%]	
	BW86	6803	BW86	6803	BW86	6803	BW86	6803
5.43 ± 0.54	2.1	2.3	4.0×10^8	4.3×10^8	0.156 ± 0.016	0.002 ± 0.000	5.8	7.3
2.71 ± 0.27	2.2	2.4	n.a.	4.5×10^8	0.159 ± 0.016	0.016 ± 0.002	5.7	7.1
1.36 ± 0.14	1.6	2.0	n.a.	3.4×10^8	0.250 ± 0.025	0.110 ± 0.011	5.7	6.6
1.09 ± 0.11	1.1	1.7	2.0×10^8	2.9×10^8	0.331 ± 0.033	0.135 ± 0.014	5.5	7.0
0.68 ± 0.07	0.7	1.1	1.5×10^8	1.9×10^8	0.360 ± 0.036	0.156 ± 0.016	3.1	4.9
0.54 ± 0.05	0.7	0.6	1.5×10^8	8.2×10^7	0.402 ± 0.040	0.180 ± 0.018	2.8	2.6

n.a. = not available

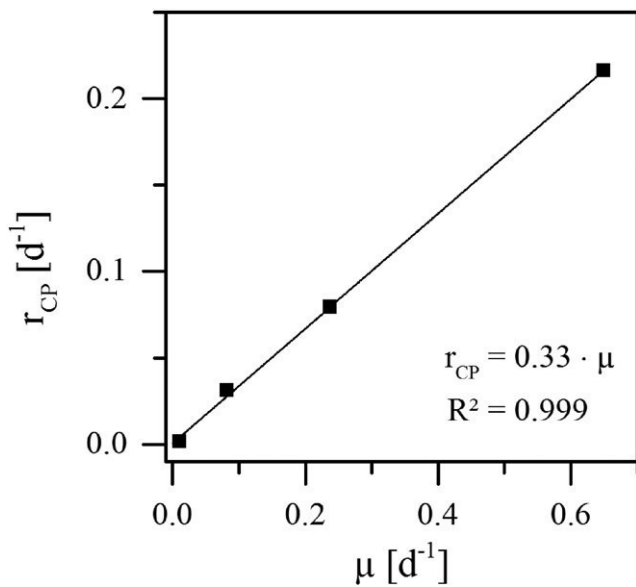


Fig. 4. Stoichiometric correlation between the specific cyanophycin formation rate r_{CP} and the specific growth rate μ of *Synechocystis* BW86 cultivated under phosphate starvation. No error bars are given since no significant difference regarding the standard deviation (<1%) was observed.

inability of synthesizing nucleic acids. The breakdown of the cell metabolism is attributable solely to phosphate limitation, not to light deficiency, as confirmed by the PCE data presented in Table 1. By reducing $C_{P,initial}$ lower than 1 mg phosphor L^{-1} , PCE is reduced as well. Therefore, based on the data presented here, it is assumed that firstly, cell growth of *Synechocystis* enters the stationary phase at phosphor quotas below 1 mg phosphor per g CDM and secondly, cyanophycin accumulation is triggered at phosphor quotas between 4 and 1 mg phosphor per g CDM.

The volumetric cyanophycin productivity P_{CP} in Fig. 5D follows an analogue pattern compared to the cyanophycin quotas of Fig. 5B. For phosphor quotas higher than 4 mg per g, no increase in P_{CP} was found whereas lower values for $q_{P,X}$ result in higher productivities up to 38.7 mg cyanophycin per L per day for *Synechocystis* BW86. However, low initial phosphor concentrations can lead to a reduction of the volumetric cyanophycin productivity in batch mode as shown in Fig. 5C.

A summary of the batch experiments from Fig. 5 regarding final biomass concentrations $C_{X,end}$, cell densities $C_{cells,end}$, final cyanophycin quotas $q_{CP,end,X}$ as well as PCE to the corresponding initial phosphor concentrations C_P is given in Table 1. $C_{X,end}$ was determined gravimetric as indicated in chapter 2.5. Phosphor concentrations were calculated based on applied K_2HPO_4 in the culture medium. The wild type *Synechocystis* 6803 generally showed higher values for $C_{X,end}$ and $C_{cells,end}$, indicating a higher conversion of incorporated phosphor to biomass. In return, $q_{CP,end,X}$ in the wild type was lower compared to the strain BW86, suggesting that the engineered strain preferably uses the available resources for cyanophycin synthesis with a negative effect on biomass production. By considering the calculated PCE results, it is obvious that the wild-type strain is more efficient in converting absorbed energy to biomass. Except for the two lowest phosphor concentrations, the maximum PCE was between 6.6 and 7.3% for the wild type and between 5.5 and 5.8% for the mutant, indicating that *Synechocystis* BW86 is less effective in the conversion of photons, probably due to the introduced mutation. The calculation of PCE is given in chapter 2.6.

4. Discussion

The growth rate of *Synechocystis* 6803 in dependence on PFD was investigated in Miniplate photobioreactors (Fig. 1). Maximum growth rate was determined as $1.32 d^{-1}$. A former study investigated the

growth rate of *Synechocystis minima* at different PFD in light/dark cycles and different temperatures. Cultivation conditions of $32^\circ C$ and $125 \mu mol m^{-2} s^{-1}$ resulted in a similar maximum growth rate of $1.32 d^{-1}$ [37]. Though *Synechocystis minima* and *Synechocystis* 6803 belong to the same genus, the maximum growth rates are not directly comparable. Bland and Angenent [38] cultivated *Synechocystis* 6803 at different light regimes and room temperature. White light did not induce photoinhibition even at high PFD up to $1000 \mu mol m^{-2} s^{-1}$. Photo-saturation occurred at $200 \mu mol m^{-2} s^{-1}$ with growth rates between $1.2 d^{-1}$ and $1.44 d^{-1}$ [38]. Hence, the data presented here confirm previous studies since maximum growth rates and the photo-saturated area are in the same order of magnitude although different temperatures, i.e. $25^\circ C$ and $32^\circ C$, were applied. Since temperature presumably affects the growth rate, it would be worthwhile to investigate this impact on light kinetics in future studies.

To investigate the ratio of the energy output that can be obtained from the produced biomass to the supplied light energy, PCE was calculated for batch cultivations with Midiplate photobioreactors, using different initial phosphate concentrations (Table 1). A theoretical maximum PCE value of 12.4% is described in literature. In real cultures the PCE is lower depending on the photobioreactor system or cultivation environment. Values between 1.5 and 5.0% are cited although higher PCEs can be reached by means of favorable light distribution [39]. Touloupakis et al. [36] reported PCE values between 7.7 and 11.9% by growing *Synechocystis* 6803 in continuous cultures. The comparably high PCE levels were achieved in particular by applying high dilution rates, indicating that the reduction or avoidance of dark zone formation in the reactor can lead to an increased PCE. Regarding the PCE information from literature, we assume that the utilized photobioreactor system is adequate for the cultivation of *Synechocystis*. PCE values between 5.5 and 7.3% as achieved in this study for initial phosphor concentrations between 16.65 and $3.33 mg L^{-1}$ (corresponding to 5.43 and $1.09 mg L^{-1}$ phosphor) are common and have no adverse effect on phototrophic cells. In order to achieve higher PCE values continuous grown cultures might be an option.

In chapter 3.2 an exemplary growth curve was shown for a batch cultivation of *Synechocystis* BW86 under phosphate starvation (Fig. 2). We observed that cell growth proceeds despite phosphor depletion. For that reason we assume that polyphosphate granules were enriched within the first 24 h and supplied the organism with phosphor until the stationary phase was reached. Moreover, it is likely that the cells degraded their phycobilisomes. Bleaching of the culture from a blue-green to a yellowish color was observed during process time (unpublished data). This effect was already described earlier for *Synechococcus* sp. PCC 7942 grown under nitrogen, sulfur and phosphor deprivation in 50 mL culture tubes, bubbled with 3% CO_2 in air [40]. Nutrient deprivation of cyanobacterial cells leads to degradation of phycobilisomes after sulfur or nitrogen deprivation. Collier and Grossman [40] also reported a partial degradation of light-harvesting phycobiliproteins in cyanobacteria after phosphor deprivation. Hence, it is reasonable to run a cyanophycin production process at phosphor quotas $q_{P,X}$ in which a high PCE value is reached despite the fact that phycobilisomes are degraded, i.e. between 1 and 3 mg phosphor per g CDM (see Table 1 or Fig. 5B). Of course, nitrogen and sulfur deprivations have to be avoided. A further degradation of phycobilisomes due to nutrient deprivation would result in lower PCE values.

Nutrient consumption of *Synechocystis* BW86 revealed a linear decrease of NO_3^- and SO_4^{2-} concentrations (Fig. 3) until stationary growth phase was reached. In terms of cultivating this strain under phosphate starvation, the use of lower amounts of these nutrients in the medium would be feasible regarding the fact that only 26% of the available NO_3^- and 50% of the available SO_4^{2-} in the BG-11 medium were consumed. The linear correlation between r_{CP} and μ in Fig. 4 point out that considered phosphate depletion has no adverse effect on the growth efficiency of cells as additionally confirmed by the comparably high PCE (Table 1). Progressing phosphate starvation force the cell to

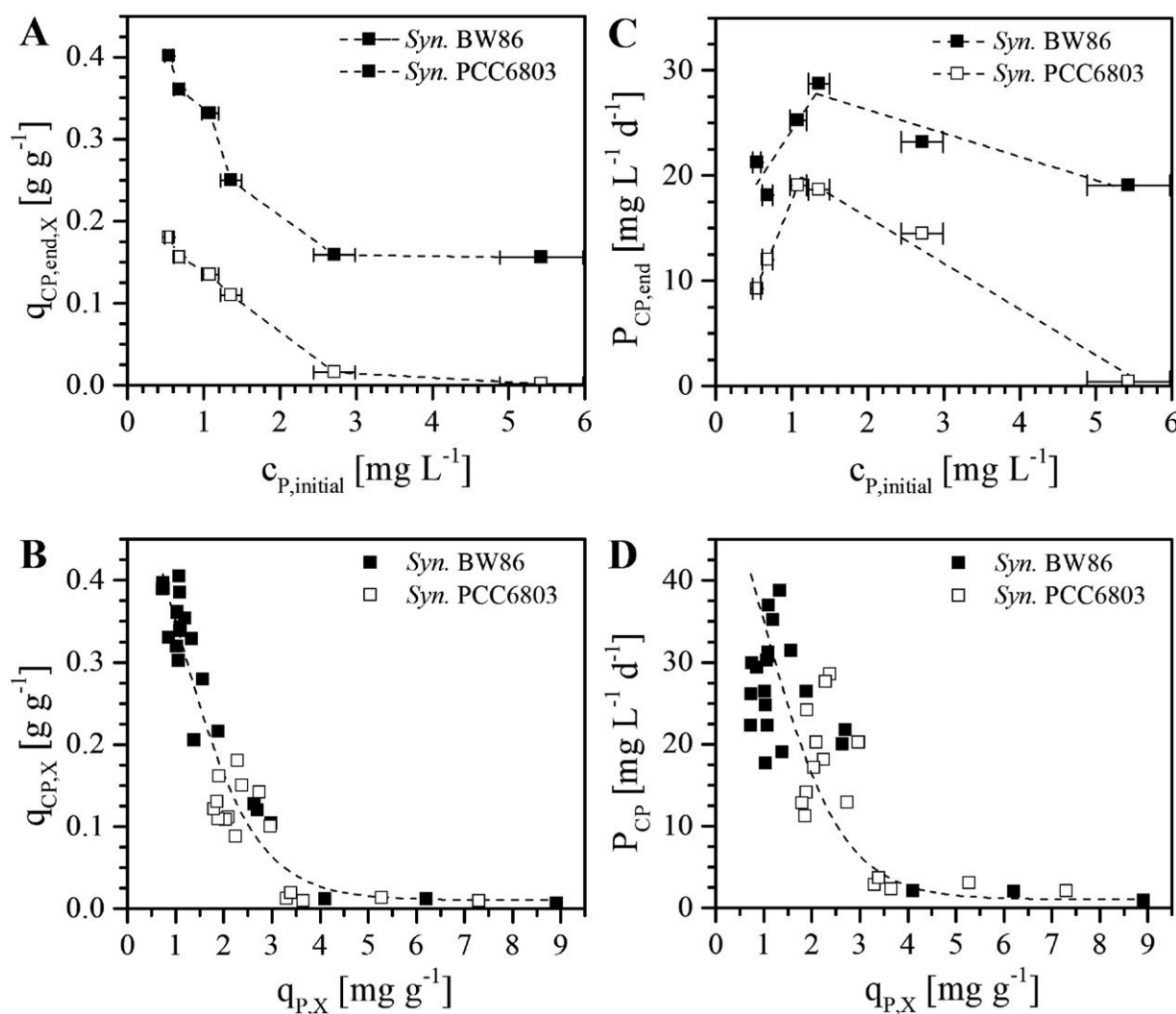


Fig. 5. Effect of phosphate availability on cyanophycin accumulation and productivity in *Synechocystis* 6803 and BW86; A: cyanophycin quota in the stationary phase $q_{CP,end,X}$ [g cyanophycin per g cell dry mass] in dependence of initial phosphor concentration $c_{P,initial}$ [mg L⁻¹]; B: cyanophycin quota $q_{CP,X}$ in dependence of phosphor quota $q_{P,X}$ [mg phosphor per g cell dry mass]; C: volumetric cyanophycin productivity in the stationary phase $P_{CP,end}$ [mg cyanophycin per L per day]; D: volumetric cyanophycin productivity P_{CP} [mg cyanophycin per L per day]. The dashed line shows the trend of the respective quota and productivity. Cultivation parameters: I_0 70 $\mu\text{mol m}^{-2} \text{s}^{-1}$, 28 °C, pH 7.5–8.0, 2% CO₂. For reasons of clarity no error bars are shown in 4B and 4D, the absolute analytical error in 4A and 4C is 10%.

cease nucleic acid synthesis. Consequently, cell division stops (see Fig. 2). The subsequent increase in CDM indicates that the remaining nutrients are used to form proteins or storage compounds.

The main focus of this research was to understand how phosphate availability affects the production of cyanophycin. Previous studies already described a relation between phosphate concentration and cyanophycin accumulation [24,32,41]. However, there was a lack of quantitative information regarding the suitable phosphate concentration, phosphor quota as well as corresponding PCE so far. The engineering approach and quantitative data of this work can consequently contribute to improve cyanophycin production with *Synechocystis*. Elbahloul et al. [24] characterized phosphate limitation as the most effective nutrient limitation for promoting cyanophycin biosynthesis and accumulation in *Acinetobacter calcoaceticus*. For small phosphate amounts of 42 μM , which corresponds to a phosphor concentration of 1.30 mg L⁻¹, higher cyanophycin contents were reported. This value corresponds to our results for *Synechocystis* (Fig. 5A). Stevens and Paone [41] describe the accumulation of cyanophycin granules as a result of phosphate limitation in *Agmenellum quadruplicatum* (now renamed as *Synechococcus* sp. PCC 7002). So far, heterologous expression systems like heterotrophic bacteria, genetically engineered yeast or plants harboring a cyanobacterial cyanophycin synthetase gene

(CphA) were used for cyanophycin production in bench scale [3]. The resulting heterologous cyanophycin differs from native cyanophycin in the length of the polymer, amino acid composition and solubility. The unicellular cyanobacterium *Synechocystis* 6803 can accumulate native cyanophycin in response to unbalanced growth conditions.

The work of Watzer et al. [32] and the results presented here confirm an enhanced cyanophycin accumulation in cyanobacteria due to deficiency of the element phosphor, in particular for *Synechocystis* 6803 and the engineered strain BW86. Therefore, phosphate starvation can be an effective strategy to produce cyanophycin in high yields using photobioreactors. The flat plate reactors we used are geometrical similar to larger flat plate production systems and allow a scale-up to higher volumes. For open pond or bag systems the geometric differences should be considered. In terms of productivity, the applied phosphate concentration and production strategy such as batch or fed-batch is important to achieve a sufficient volumetric cyanophycin productivity (fig. 5C and fig. 5D).

Based on the data of this work it is furthermore possible to develop a cultivation process, preferably a fed-batch or continuous process, where the phosphate availability is controlled to induce an ongoing cyanophycin production with high cyanophycin yields. Genetic stabilization of the engineered production strain BW86 might be an issue in

biotechnological applications, especially for continuous processes. Although Guerrero et al. [42] reported that an engineered *Synechocystis* 6803 strain for ethylene production was stable for >6 months in liquid culture, it has to be considered that the BW86 strain harbors solely a point mutation in the PII gene.

5. Conclusion

A quantitative regulation of phosphate availability in terms of different initial phosphate concentrations affect the cyanophycin accumulation. The engineered strain *Synechocystis* BW86 showed higher cyanophycin yields compared to the wild type due to the increased NAGK activity. However, the total produced biomass and PCE values were lower compared to cultivations of the wild type, indicating a less effective conversion of absorbed photons. The essential amount to induce cyanophycin accumulation is between 1 and 4 mg phosphor per g CDM, while stationary growth phase was reached around 1 mg phosphor per g CDM. To our knowledge, this is the first study analyzing the specific necessary phosphor quota to trigger cyanophycin accumulation and to initialize stationary growth phase of *Synechocystis*. A maximum growth rate of 1.32 d^{-1} was found by applying a photon flux density of $150 \mu\text{mol m}^{-2} \text{ s}^{-1}$ whereby the transition from photo-limited to photo-saturated region already occurred at $46 \mu\text{mol m}^{-2} \text{ s}^{-1}$. The quantitative statements of this work allow a scale-up to larger production systems.

Acknowledgements

This work of A. Trautmann was supported by grants (7533-10-5-88 to C. Posten; 7533-10-5-92 to K. Forchhammer and A. Wilde) from the Ministry of Science, Research and the Arts of Baden-Württemberg, Germany as part of the BBW ForWerts Graduate Program. Special thanks go to Lara Stelsmaszyk B.Sc. and Eva Heymann B.Sc. for their contributions to the experimental work.

Appendix A. Supplementary data

Supplementary data to this article can be found online at doi:10.1016/j.algal.2016.10.009.

References

- [1] G. Wu, Q. Wu, Z. Shen, Accumulation of poly- β -hydroxybutyrate in cyanobacterium *Synechocystis* sp. PCC6803, *Bioresour. Technol.* 76 (2) (2001) 85–90.
- [2] C. Beck, H. Knoop, I.M. Axmann, R. Steuer, The diversity of cyanobacterial metabolism: genome analysis of multiple phototrophic microorganisms, *BMC Genomics* 13 (2012).
- [3] K. Ziegler, R. Deutzmann, W. Lockau, Cyanophycin synthetase-like enzymes of non-cyanobacterial eubacteria: characterization of the polymer produced by a recombinant synthetase of *Desulfotobacterium hafniense*, *Zeitschrift für Naturforschung Section C-A Journal of Biosciences* 57 (5–6) (2002) 522–529.
- [4] M.M. Allen, [19] Inclusions: Cyanophycin, *Methods Enzymol.* 167 (C) (1988) 207–213.
- [5] R.D. Simon, The effect of chloramphenicol on the production of cyanophycin granule polypeptide in the blue-green alga *Anabaena cylindrica*, *Arch. Mikrobiol.* 92 (2) (1973) 115–122.
- [6] M.M. Allen, M.A. Hawley, Protein degradation and synthesis of cyanophycin granule polypeptide in *Aphanocapsa* sp. *J. Bacteriol.* 154 (3) (1983) 1480–1484.
- [7] N.H. Lawry, R.D. Simon, The normal and induced occurrence of cyanophycin inclusion-bodies in several blue-green-algae, *J. Phycol.* 18 (3) (1982) 391–399.
- [8] M. Schwamborn, Chemical synthesis of polyaspartates: a biodegradable alternative to currently used polycarboxylate homo- and copolymers, *Polym. Degrad. Stab.* 59 (1) (1998) 39–45.
- [9] D.D. Alford, A.P. Wheeler, C.A. Pettigrew, Biodegradation of thermally synthesized polyaspartate, *J. Environ. Polymer Degrad.* 2 (4) (1994) 225–236.
- [10] A. Sallam, A. Steinbüchel, Dipeptides in nutrition and therapy: cyanophycin-derived dipeptides as natural alternatives and their biotechnological production, *Appl. Microbiol. Biotechnol.* 87 (3) (2010) 815–828.
- [11] M.M. Allen, A. Smith, Nitrogen chlorosis in blue-green algae, *Arch. Mikrobiol.* 69 (2) (1969) 114–120.
- [12] M.M. Allen, Cyanobacterial cell inclusions, *Annu. Rev. Microbiol.* 38 (1984) 1–25.
- [13] R.D. Simon, Cyanophycin granules from the blue-green alga *Anabaena cylindrica*: a reserve material consisting of copolymers of aspartic acid and arginine, *Proc. Natl. Acad. Sci.* 68.2 (1971) 265–267.
- [14] R.D. Simon, P. Weathers, Determination of the structure of the novel polypeptide containing aspartic acid and arginine which is found in cyanobacteria, *Biochim. Biophys. Acta, Protein Struct.* 420 (1) (1976) 165–176.
- [15] N.J. Lang, R.D. Simon, C.P. Wolk, Correspondence of cyanophycin granules with structured granules in *Anabaena cylindrica*, *Arch. Mikrobiol.* 83 (4) (1972) 313–320.
- [16] M.M. Allen, P.J. Weathers, Structure and composition of cyanophycin granules in the cyanobacterium *Aphanocapsa* 6308, *J. Bacteriol.* 141 (2) (1980) 959–962.
- [17] M. Obst, F.B. Oppermann-Sanio, H. Luftmann, A. Steinbüchel, Isolation of cyanophycin-degrading bacteria, cloning and characterization of an extracellular cyanophycinase gene (*cphE*) from *Pseudomonas anguilliseptica* strain BI - The *cphE* gene from *P. anguilliseptica* BI encodes a cyanophycin-hydrolyzing enzyme, *J. Biol. Chem.* 277 (28) (2002) 25096–25105.
- [18] H. Li, D. Sherman, S. Bao, L. Sherman, Pattern of cyanophycin accumulation in nitrogen-fixing and non-nitrogen-fixing cyanobacteria, *Arch. Mikrobiol.* 176 (1–2) (2001) 9–18.
- [19] S. Picossi, A. Valladares, E. Flores, A. Herrero, Nitrogen-regulated genes for the metabolism of cyanophycin, a bacterial nitrogen reserve polymer - Expression and mutational analysis of two cyanophycin synthetase and cyanophycinase gene clusters in the heterocyst-forming cyanobacterium *Anabaena* sp. PCC 7120, *J. Biol. Chem.* 279 (12) (2004) 11582–11592.
- [20] M. Obst, A. Sallam, H. Luftmann, A. Steinbüchel, Isolation and characterization of gram-positive cyanophycin-degrading bacteria - Kinetic studies on cyanophycin depolymerase activity in aerobic bacteria, *Biomacromolecules* 5 (1) (2003) 153–161.
- [21] R. Richter, M. Hejazi, R. Kraft, K. Ziegler, W. Lockau, Cyanophycinase, a peptidase degrading the cyanobacterial reserve material multi-L-arginyl-poly-L-aspartic acid (cyanophycin). Molecular cloning of the gene of *Synechocystis* sp. PCC 6803, expression in *Escherichia coli*, and biochemical characterization of the purified enzyme, *Eur. J. Biochem.* 263 (1) (1999) 163–169.
- [22] M. Obst, A. Steinbüchel, Microbial degradation of poly(amino acid)s, *Biomacromolecules* 5 (4) (2004) 1166–1176.
- [23] R.D. Simon, Measurement of the cyanophycin granule polypeptide contained in the blue-green alga *Anabaena cylindrica*, *J. Bacteriol.* 114 (3) (1973) 1213–1216.
- [24] Y. Elbahloul, M. Krehenbrink, R. Reichelt, A. Steinbüchel, Physiological conditions conducive to high cyanophycin content in biomass of *Acinetobacter calcoaceticus* strain ADP1, *Appl. Environ. Microbiol.* 71.2 (2005) 858–866.
- [25] M. Maheswaran, K. Ziegler, W. Lockau, M. Hagemann, K. Forchhammer, PII-regulated arginine synthesis controls accumulation of cyanophycin in *Synechocystis* sp. strain PCC 6803, *J. Bacteriol.* 188 (7) (2006) 2730–2734.
- [26] K. Forchhammer, Global carbon/nitrogen control by PII signal transduction in cyanobacteria: from signals to targets, *FEMS Microbiol. Rev.* 28 (3) (2004) 319–333.
- [27] K. Zeth, O. Fokinas, K. Forchhammers, Structural basis and target-specific modulation of ADP sensing by the *Synechococcus elongatus* PII signaling protein, *J. Biol. Chem.* 289 (13) (2014) 8960–8972.
- [28] K. Forchhammer, PII signal transducers: novel functional and structural insights, *Trends Microbiol.* 16 (2) (2008) 65–72.
- [29] O. Fokina, V.-R. Chellamuthu, K. Forchhammer, K. Zeth, Mechanism of 2-oxoglutarate signaling by the *Synechococcus elongatus* P-II signal transduction protein, *Proc. Natl. Acad. Sci.* 107 (46) (2010) 19760–19765.
- [30] K. Zeth, O. Fokina, K. Forchhammer, An engineered PII protein variant that senses a novel ligand, *Acta Crystallogr. Sect. D* 68 (8) (2012) 901–908.
- [31] A. Heinrich, M. Maheswaran, U. Ruppert, K. Forchhammer, The *Synechococcus elongatus* PII signal transduction protein controls arginine synthesis by complex formation with N-acetyl-L-glutamate kinase, *Mol. Microbiol.* 52 (5) (2004) 1303–1314.
- [32] B. Watzler, A. Engelbrecht, W. Hauf, M. Stahl, I. Maldener, K. Forchhammer, Metabolic pathway engineering using the central signal processor PII, *Microb. Cell Factories* 14 (1) (2015) 192.
- [33] R. Rippka, J. Deruelles, J.B. Waterbury, M. Herdman, R.Y. Stanier, Generic assignments, strain histories and properties of pure cultures of cyanobacteria, *J. Gen. Microbiol.* 111 (1) (1979) 1–61.
- [34] R. Dillschneider, C. Steinweg, R. Rosello-Sastre, C. Posten, Biofuels from microalgae: Photoconversion efficiency during lipid accumulation, *Bioresour. Technol.* 142 (2013) 647–654.
- [35] L. Messineo, Modification of the Sakaguchi reaction: Spectrophotometric determination of arginine in proteins without previous hydrolysis, *Arch. Biochem. Biophys.* 117 (3) (1966) 534–540.
- [36] E. Touloupakis, B. Cicchi, G. Torzillo, A bioenergetic assessment of photosynthetic growth of *Synechocystis* sp. PCC 6803 in continuous cultures, *Biotechnol. Biofuels* 8 (2015) 133.
- [37] A. Dauta, J. Devaux, F. Piquemal, L. Boumnick, Growth rate of four freshwater algae in relation to light and temperature, *Hydrobiologia* 207 (1) (1990) 221–226.
- [38] E. Bland, L.T. Angenent, Pigment-targeted light wavelength and intensity promotes efficient photoautotrophic growth of Cyanobacteria, *Bioresour. Technol.* 216 (2016) 579–586.
- [39] P. Schlagermann, G. Göttlicher, R. Dillschneider, R. Rosello-Sastre, C. Posten, Composition of algal oil and its potential as biofuel, *J. Comb.* (2012).
- [40] J.L. Collier, A.R. Grossman, A small polypeptide triggers complete degradation of light-harvesting phycobiliproteins in nutrient-deprived cyanobacteria, *EMBO J.* 13 (5) (1994) 1039–1047.
- [41] S.E. Stevens, D.A. Paone, Accumulation of cyanophycin granules as a result of phosphate limitation in *Agmenellum quadruplicatum*, *Plant Physiol.* 67 (4) (1981) 716–719.
- [42] F. Guerrero, V. Carbonell, M. Cossu, D. Correddu, P.R. Jones, Ethylene synthesis and regulated expression of recombinant protein in *Synechocystis* sp. PCC 6803, *PLoS One* 7 (11) (2012), e50470.


4. Accepted publication

Lüddecke, J., Francois, L., Spät, P., **Watzer, B.**, Chilczuk, T., Poschet, G., Hell, R., Radlwimmer, B. & Forchhammer, K. (2017).

P_{II} protein-derived FRET sensors for quantification and live-cell imaging of 2-oxoglutarate.

Scientific reports, 7(1), 1437

SCIENTIFIC REPORTS



OPEN

P_{II} Protein-Derived FRET Sensors for Quantification and Live-Cell Imaging of 2-Oxoglutarate

Jan Lüddecke¹, Liliana Francois², Philipp Spät¹, Björn Watzer¹, Tomasz Chilczuk¹, Gernot Poschet³, Rüdiger Hell³, Bernhard Radlwimmer² & Karl Forchhammer¹ 

The citric acid cycle intermediate 2-oxoglutarate (2-OG, a.k.a. alpha-ketoglutarate) links the carbon and nitrogen metabolic pathways and can provide information on the metabolic status of cells. In recent years, it has become exceedingly clear that 2-OG also acts as a master regulator of diverse biologic processes in all domains of life. Consequently, there is a great demand for time-resolved data on 2-OG fluctuations that can't be adequately addressed using established methods like mass spectrometry-based metabolomics analysis. Therefore, we set out to develop a novel intramolecular 2-OG FRET sensor based on the signal transduction protein P_{II} from *Synechococcus elongatus* PCC 7942. We created two variants of the sensor, with a dynamic range for 2-OG from 0.1 μM to 0.1 mM or from 10 μM to 10 mM. As proof of concept, we applied the sensors to determine *in situ* glutamine:2-oxoglutarate aminotransferase (GOGAT) activity in *Synechococcus elongatus* PCC 7942 cells and measured 2-OG concentrations in cell extracts from *Escherichia coli* *in vitro*. Finally, we could show the sensors' functionality in living human cell lines, demonstrating their potential in the context of mechanistic studies and drug screening.

The emerging field of metabolomics has the potential to accurately describe the physiological state of a cell at the time of measurement^{1,2}. Technological improvements during the last decade have led to more rapid and precise metabolite identification³; however, state of the art HPLC-MS based analyses require extraction of the metabolites from the cells, making the study of detailed temporal metabolite fluctuations a challenging task. Additionally, certain metabolites are not stable under commonly used extraction conditions or their recovery rates are low⁴. To overcome these drawbacks, a variety of genetically encoded, protein-based sensors were developed. These *in vivo/ex vivo* sensors allow real-time measurements of high temporal resolution without disrupting the cell. To date, there are hundreds of sensors available, not only for metabolites, but also for cellular aspects like ion concentration, mechanical stress, enzyme and kinase activity, redox potential, etc. (<http://biosensor.dpb.carnegiescience.edu/>)⁵. The majority of these sensors utilize the growing number of optimized fluorescence proteins (FPs) to create a Förster resonance energy transfer (FRET) readout^{6,7}. FRET occurs when donor and acceptor fluorophores with overlapping emission and excitation spectra come in close proximity. Following excitation of the donor, energy is transmitted to the acceptor in a non-radiative manner by means of intermolecular long-range dipole-dipole coupling and emitted by the acceptor. Ligand-binding-induced conformational changes in the sensors containing both, donor and acceptor fluorophores, results in altered FRET efficiency, which can be monitored under a fluorescence microscope or in a fluorimeter⁸.

One central metabolite of high interest is 2-oxoglutarate (2-OG), which links the carbon and nitrogen metabolic pathways in all domains of life. 2-OG is used as the carbon skeleton for nitrogen assimilatory reactions and has been proposed as a master regulatory metabolite⁹. It has been shown that the 2-OG pool reacts to changes in extracellular nitrogen availability within minutes and its half-life has been estimated as 0.5 s¹⁰⁻¹³. Apart from the regulatory P_{II} proteins (see below) 2-OG is sensed by a number of transcription factors⁹. Furthermore, 2-OG acts as a starvation signal in eukaryotes like *S. cerevisiae* or the metazoa *C. elegans*^{14,15}. Competitive inhibition of 2-OG-dependent DNA and histone demethylases by the oncometabolite and 2-OG analogue 2-hydroxyglutarate

¹Interfaculty Institute for Microbiology and Infection Medicine, Division Organismic Interactions, University of Tübingen, Tübingen, Germany. ²Division of Molecular Genetics, German Cancer Research Center (DKFZ), Heidelberg, Germany. ³Centre for Organismal Studies Heidelberg, Rupprecht-Karls-Universität Heidelberg, Heidelberg, Germany. Jan Lüddecke and Liliana Francois contributed equally to this work. Correspondence and requests for materials should be addressed to K.F. (email: karl.forchhammer@uni-tuebingen.de)

have been shown to be the cause of cancer-specific epigenome and gene expression alterations in glioma and acute myelogenous leukemia^{16–18}. Furthermore, 2-OG levels were proposed to regulate the epigenome of differentiating human pluripotent stem cells¹⁹ and embryonic stem cells^{20,21}. In mice it has recently been shown, that 2-OG acts as a systemic signal providing protection from cardiac ischemia²². In bacteria, the sugar-uptake phosphotransferase system (PTS) in *E. coli* is regulated by the 2-OG/phosphoenolpyruvate ratio^{23,24}. The PTS not only promotes sugar transport but is also responsible for activation or inhibition of the adenylate cyclase which produces cyclic AMP, a very important signaling molecule that affects the expression of a vast range of genes^{25,26}. These examples demonstrate the importance of 2-OG as a regulatory metabolite and underline the need for a functional sensor in living cells, which allows investigations of 2-OG fluctuations with high spatial and temporal resolution.

The small trimeric regulatory protein P_{II}, which is widely distributed in prokaryotes and chloroplasts, is known as a sensor of cellular 2-OG levels²⁷. Binding of 2-OG leads to conformational changes in the protein structure in a concentration dependent manner^{27–30}. These conformational changes modulate the interaction of P_{II} with its regulatory targets³¹. In previous studies, these interactions have been utilized to create inter-molecular FRET sensors employing cyanobacterial P_{II} proteins and their targets N-acetyl-L-glutamate kinase (NAGK) and PipX. These sensors have successfully been used to expand the knowledge about the 2-OG dependent mode of interaction between P_{II} and its targets^{32–34}. However, FRET sensors using protein-protein interactions have disadvantages, especially for applications in living cells, where different expression rates and protein half-lives have to be taken into account, as well as the increased chance of unwanted side reactions, e.g. by NAGK enzymatic activity. Berg *et al.* have constructed a P_{II}-based intramolecular FRET sensor to read out fluctuations in ATP/ADP levels, after having inactivated the 2-OG binding site in P_{II}³⁵. This motivated us to create an enhanced intra-molecular 2-OG FRET sensor making use of the high specificity of P_{II} proteins towards 2-OG.

As a first application we used the 2-OG sensor for an *in situ* glutamine:2-oxoglutarate aminotransferase (GOGAT) assay. GOGAT catalyzes the reductive transfer of the amide group from glutamine to the carbon backbone of 2-OG, which yields two molecules of glutamate. This is a key reaction in nitrogen assimilation in bacteria and plants³⁶, but studies on GOGAT activity regulation are scarce³⁷, due to the lack of a simple assay. Using the P_{II}-based 2-OG specific FRET sensors, we present here the determination of the *in situ* fdGOGAT activity in the unicellular cyanobacteria *Synechococcus elongatus* PCC 7942 (hereafter designated as *S. elongatus*). Furthermore, we used the sensor to determine 2-OG concentrations in cell extracts from *E. coli*. Finally, we conducted the first application of a real-time 2-OG sensor in mammalian cells to measure 2-OG fluctuations in human glioblastoma brain-cancer cells and other cell lines. These experiments provide the proof of principle that P_{II}-based 2-OG specific FRET sensors could become useful tools for studying cancer patho-mechanisms and as functional readouts in metabolic-drug screening.

Results and Discussion

Development of the FRET Sensor. On our attempt to construct a 2-OG sensor that employs the conformational change of P_{II} upon 2-OG binding, we made use of the knowledge gained during the development of the P_{II}-NAGK FRET sensor³² and crystal structures of *S. elongatus* P_{II}²⁸. Different sensor variants were constructed, most of which use the monomeric (m) cyan FP mCerulean as the FRET donor and the yellow FP Venus as acceptor. The simplest approach was to fuse these FPs to the N and C-terminus of P_{II}. Crystal structures of P_{II} with Mg²⁺-ATP + 2-OG bound display a conformational change in the C-terminus²⁸: in the ligand free state (PDB: 1QY7) or while interacting with NAGK (PDB: 2V5H), the P_{II} C-terminus adopts a stretched conformation, pointing away from the trimer. By contrast, upon binding of Mg²⁺-ATP + 2-OG, the C-terminus retracts and folds over the metabolite binding site of the inter-subunit cleft (PDB: 2XUL). With the first variants, we aimed to assess if this conformational change in the C-terminus could be used to create a change in FRET.

To achieve this goal, we had to overcome a problem associated with modifying the N-terminus of bacterial P_{II} proteins. The N-terminus of *S. elongatus* P_{II} is hidden within the protein and a direct fusion to the buried end leads to misfolding and degradation (data not shown). To solve this problem, we used the non-conserved extended N-terminus of *Chlamydomonas reinhardtii* P_{II} that protrudes from the protein³⁸ and fused these six N-terminal amino acids (S-A-F-P-G-V) to the N-terminus of *S. elongatus* P_{II}. This indeed led to a stably expressed protein. On top of that, we added flexible (FL; L[SGGGG]_nSAAA) or stiff helical (HL; A[EAAA]_n) linkers of 20 or 25 amino acids (Fig. 1, P_{II}-NC1 to 4)³⁹. The Venus FP was fused to the C-terminus of P_{II} via the 12 amino acid long streptavidin affinity tag (Strep-tag), as has been done previously³². The Strep-tag should enable the transfer of the proposed C-terminal movement to the FP and was also used for protein purification. While P_{II}-NC1 and NC3 could be purified in good quantity and quality, P_{II}-NC2 and NC4 were not expressed in *E. coli*. Probably the helical linker led to misfolding and degradation of these proteins.

In other variants, we aimed to use the conformational change of the T-loop upon Mg²⁺-ATP + 2-OG binding to obtain a change in FRET. As shown in the crystal structures mentioned above, the stretched T-loops of ligand-free P_{II} are retracted and folded upon binding of Mg²⁺-ATP + 2-OG. This folding also prevents the interaction of P_{II} with other receptor proteins like NAGK or PipX³⁰. We devised eight variants to test this approach. In the first two variants (Fig. 1, P_{II}-TC1 and TC2) we inserted mCerulean with its natural C- and N-terminus into the tip of P_{II}'s T-loop between amino acids 44 and 45. Venus was again placed at the C-terminus using either the Strep-tag, or a four amino acid linker (LAAA). FRET is not only influenced by the distance between donor and acceptor, but also by their angle towards each other⁴⁰. With that in mind, we also used circularly permuted (cp) versions of mCerulean, by connecting its native C- and N-terminus with a short flexible linker (GSGGTG) and using other positions for the fusion into the T-loop, similar to the approach described by Berg *et al.* for the construction of a P_{II}-based ATP/ADP sensor³⁵. Topell *et al.* showed that circular permutations of GFP to positions Y145-N144, K158-Q157 as well as G174-D173 yielded correctly folded FPs⁴¹. We used these locations for fusion with the T-loop and again varied the linker between the P_{II} C-terminus and Venus (Fig. 1, P_{II}-TC3 to 8).

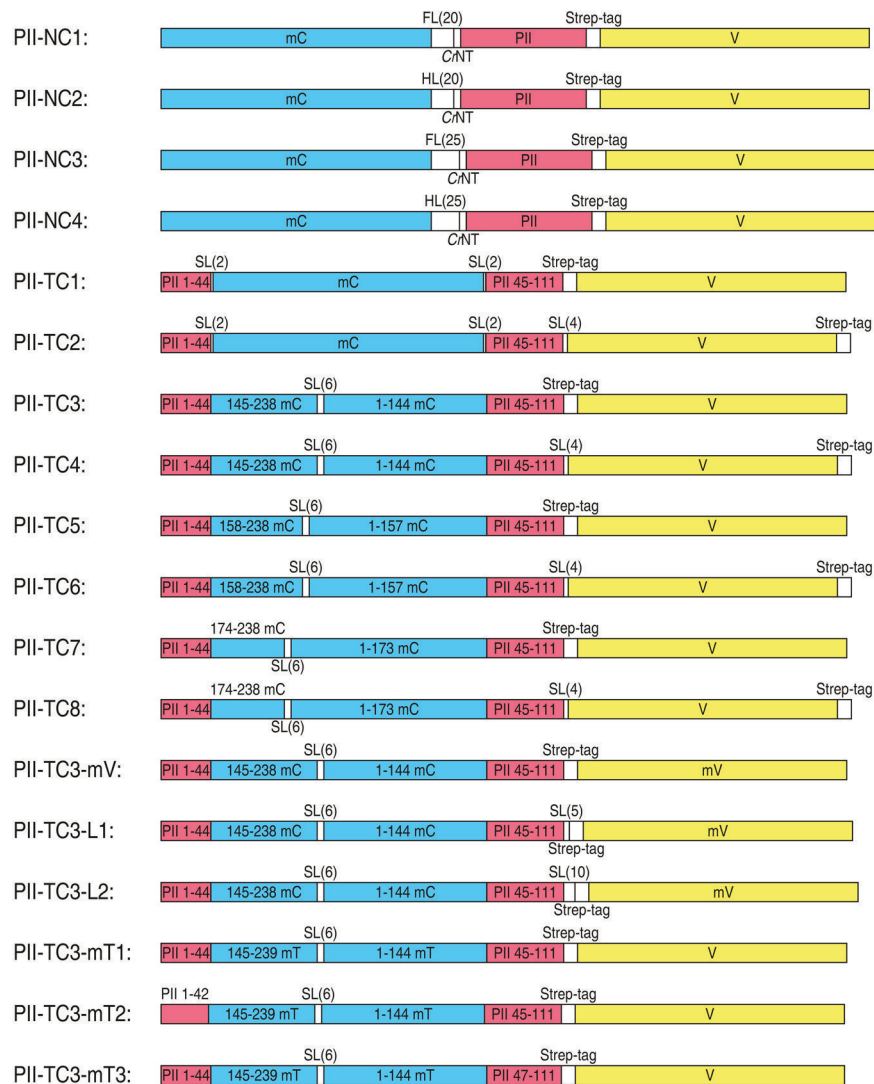


Figure 1. Schematic representation of the FRET-sensor constructs. Red: P_{II}; Blue: mCerulean; Yellow: mVenus; White: linker regions. Flexible (FL) or stiff helical (HL) linkers or short linkers (SL) of different length, *Chlamydomonas reinhardtii* P_{II} N-terminus (CrNT) or streptavidin affinity tag (Strep-tag). All Domains are presented to scale.

All tested variants showed strong initial FRET signals, indicating that the FPs were correctly folded and in close proximity. Subsequently 0.1 mM ADP, 0.1 mM ATP or 0.1 mM ATP together with 1 mM 2-OG were added to the solution and the FRET change was measured (Table 1). Most variants showed only small FRET changes, either slightly increasing or decreasing the FRET upon effector molecule addition. Only P_{II}-TC3 showed an 18% drop in FRET. The decreased FRET indicates that the FPs move away from each other, which is consistent with the crystal structures, where the T-loop folds downward upon 2-OG binding, away from the C-terminus.

Since P_{II}-TC3 showed the strongest FRET change so far, we tried further modifications of the P_{II}-TC3 variant. GFPs have the tendency to dimerize. To allow the C-terminally attached Venus more flexibility in movement, we added the monomer mutation A206K⁴² and also elongated the linker between P_{II} and mVenus by five or ten amino acids (Fig. 1, P_{II}-TC3-mV, -L1 and -L2). Even though P_{II}-TC3-mV showed a higher initial FRET value, the relative FRET drop upon addition of ATP + 2-OG was lower compared to P_{II}-TC3. Also the modified linkers did not increase the sensors signal (Table 1). Next, we tried to enhance the TC3 sensor by replacing mCerulean by the advanced mTurquoise2, which shows exceptional quantum yield, brightness, photostability and a fast maturation rate and is thus proposed as an optimal donor for FRET systems⁴³. Additionally, we created two versions with partially deleted T-loops (P_{II}-TC3-mT1 to 3). P_{II}-TC3-mT1 and -mT3 showed lower signal changes than P_{II}-TC3. Interestingly, P_{II}-TC3-mT2, with T-loop amino acids 43 and 44 deleted, showed increased FRET upon addition of ATP + 2-OG. This indicates that the small deletion in the T-loop alters the orientation of the attached FP, demonstrating once again that subtle changes can have a dramatic and unpredictable impact on the signal output of a FRET sensor. A detailed analysis showed that P_{II}-TC3-mT2 was only reacting to high 2-OG concentrations and was not as sensitively responding towards 2-OG as P_{II}-TC3 (data not shown).

Sensor	% FRET change after addition of		
	ADP	ATP	ATP + 2-OG
P _{II} -NC1	n. d.	0.3	4.4
P _{II} -NC3	n. d.	3.1	3.1
P _{II} -TC1	-2.0	-1.1	-1.7
P _{II} -TC2	-1.1	1.0	5.7
P _{II} -TC3	0.8	-0.8	-18.3
P _{II} -TC4	-0.4	0.8	-2.5
P _{II} -TC5	-6.1	-0.1	-3.1
P _{II} -TC6	1.0	0.2	3.4
P _{II} -TC7	-0.6	-0.8	-2.3
P _{II} -TC8	6.2	0.8	0.9
P _{II} -TC3-mV	n. d.	n. d.	-15.1
P _{II} -TC3-L1	n. d.	n. d.	-15.4
P _{II} -TC3-L2	n. d.	n. d.	-15.6
P _{II} -TC3-mT1	n. d.	n. d.	-8.3
P _{II} -TC3-mT2	n. d.	n. d.	25.8
P _{II} -TC3-mT3	n. d.	n. d.	-13.3

Table 1. FRET change after addition of metabolites. FRET of the purified sensor proteins was measured before and after addition of 0.1 mM ADP, 0.1 mM ATP or 0.1 mM ATP + 1 mM 2-OG and the relative FRET change was calculated. (n. d., not determined).

After all, P_{II}-TC3 appeared to be the most promising sensor variant for sensitive 2-OG detection. To biochemically characterize P_{II}-TC3, the affinity-tag isolated protein was further purified by size-exclusion chromatography to remove degradation products containing only one of the two FPs. We also optimized the buffer conditions and the workflow to improve TC3's signal to noise ratio and to be able to use a 96-well plate setup and a small reaction volume. As previously described for P_{II}-NAGK interactions, the proteins can be unstable when buffer conditions are quickly changed³². When the sensor, stored in a 50% glycerol buffer at -20 °C, was quickly mixed with the measurement buffer, it showed a lower signal to noise ratio and sensitivity, possibly due to dissociation of the trimer. To circumvent this problem, we tested a variety of reaction-buffer setups and came up with a mixture containing 15% glycerol, which not only stabilized the sensor and enabled easy preparation of a master mix for 96-well plate application, but also lead to a increase of the signal-to-noise ratio to 25%. Figure 2A shows the 2-OG induced FRET change under these optimized conditions. P_{II}-TC3 displayed a K_d for 2-OG of approximately 3 μM. This is close to the binding constant of the high affinity 2-OG binding site in wild-type P_{II} protein, showing that, despite the insertion of mCerulean into the T-loop, P_{II}-TC3 acts similar to P_{II}-wildtype. However, for possible *in vivo* applications, where one- to two orders of magnitude higher 2-OG concentrations are expected, this response is too sensitive. Therefore, we constructed a variant of P_{II}-TC3 with a mutation in the vicinity of the 2-OG binding site. Previously, it was shown that mutation of Arg9 reduces the affinity of 2-oxoglutarate binding²⁸. Here, a mutation of arginine 9 to proline (R9P) decreased the affinity of P_{II} for 2-OG 35 times, resulting in a K_d of 91 μM (Fig. 2A). With a dynamic range of the FRET response from 10 μM to 10 mM, this sensor seems to be ideally suited to span the physiological relevant range of 2-OG concentrations. Because ATP and ADP compete for the same binding site on the P_{II} protein, but only ATP enables the binding of 2-OG, we also measured the competitive effect of ADP on the signal output. As shown in Fig. 2B, physiological ATP/ADP ratios (ATP > ADP) do not influence 2-OG sensing.

In the next step, we tested the sensitivity and specificity of TC3 and TC3-R9P. All metabolites of the tricarboxylic acid (TCA) cycle and the 2-OG analog dimethyl-2-OG (dm2-OG) were tested. As shown in Fig. 2C, TC3 is about 460 times more sensitive for 2-OG than for dm2-OG, which gave the second strongest signal. The third strongest signal was induced by oxaloacetate, with a 900 times reduced sensitivity. All other tested metabolites were even less interfering than oxaloacetate, demonstrating the high specificity of the sensor towards 2-OG. Interestingly, increasing NaCl concentrations also lead to a decrease in FRET. Most of the tested compounds were sodium salts or had to be titrated with NaOH to adjust the pH, and therefore might give a stronger response than pure compounds. Similarly, TC3-R9P was also highly specific for 2-OG. It showed an 85 times decreased sensitivity for dm2-OG and responded to other metabolites only at non-physiologically high concentrations (Fig. 2D).

Establishing an *in situ* fdGOGAT assay using the 2-OG FRET-sensor. One possible application of a 2-OG FRET-sensor is the *in situ* determination of GOGAT activity. In contrast to previously described approaches, in which the formation of glutamate or consumption of glutamine were measured using HPLC-based amino acid quantification methods⁴⁴, the FRET sensor based 2-OG quantification is much faster and cost efficient.

The *in situ* GOGAT assay was established for *S. elongatus*, which only possesses a ferredoxin-dependent GOGAT. The method developed in the present study is based on experiments from Marqués *et al.* and Kameya *et al.*^{44–46}. In short, the cells were permeabilized by toluene, the GOGAT substrates 2-OG, glutamine and reductant were added and the mixture incubated at 32 °C. The efficiency of cell permeabilization was tested via fluorescence

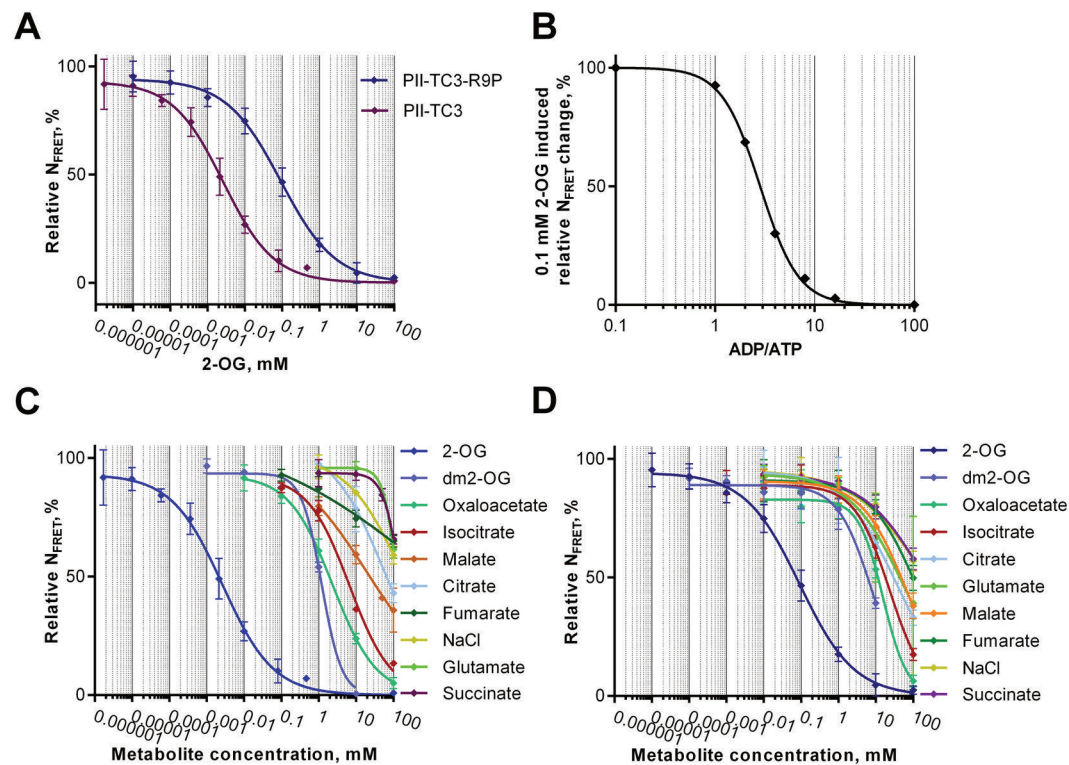


Figure 2. Properties of FRET-sensor $P_{\text{II}}\text{-TC3}$. (A) Relative N_{FRET} response of $P_{\text{II}}\text{-TC3}$ and $P_{\text{II}}\text{-TC3-R9P}$ to increasing 2-OG concentrations. (B) Influence of different ADP/ATP ratios on the N_{FRET} response of $P_{\text{II}}\text{-TC3}$ upon addition of 0.1 mM 2-OG. (C and D) Relative N_{FRET} response of $P_{\text{II}}\text{-TC3}$ (C) and $P_{\text{II}}\text{-TC3-R9P}$ (D), to different metabolites of the TCA cycle. Error bars: \pm s.e.m., $n = 4$.

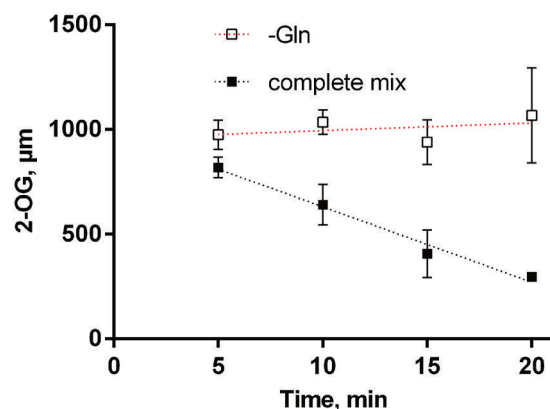


Figure 3. fdGOGAT assay with complete and incomplete reaction mix. *S. elongatus* cells were grown to an OD_{750} of 0.3 in nitrate-supplemented medium. The 2-OG concentrations in the reaction mixture were determined by FRET over time. Results are shown for a complete reaction mix (black squares and black dashed line) and the blank mix lacking glutamine (white squares and red dashed line). Error bars: \pm s.e.m., $n = 3$.

microscopy using a live/dead staining kit for bacteria, revealing a very efficient permeabilization (Fig. S1). In our experimental setup, the natural reductant ferredoxin was substituted by methyl viologen as electron donor, which was reduced by addition of sodium dithionite. To avoid air-oxidation of the dithionite, we covered the reaction mix with paraffin oil. Samples were taken in 5 to 10 minutes intervals and the reaction was stopped by aeration through intense vortexing and cooling on ice, which is quick and easy to apply. Afterwards, the cells were separated by centrifugation and the supernatant was used for 2-OG quantification via FRET measurements. The components of the GOGAT-reaction mixture itself had no influence on the FRET measurement, since addition of the reaction mix to a 2-OG standard curve did not affect the read-out (Fig. S2).

When all components, including permeabilized cells, glutamine, 2-OG and the electron donor were present in the reaction mix, a decrease of the 2-OG concentration over time could be detected (Fig. 3). Preliminary

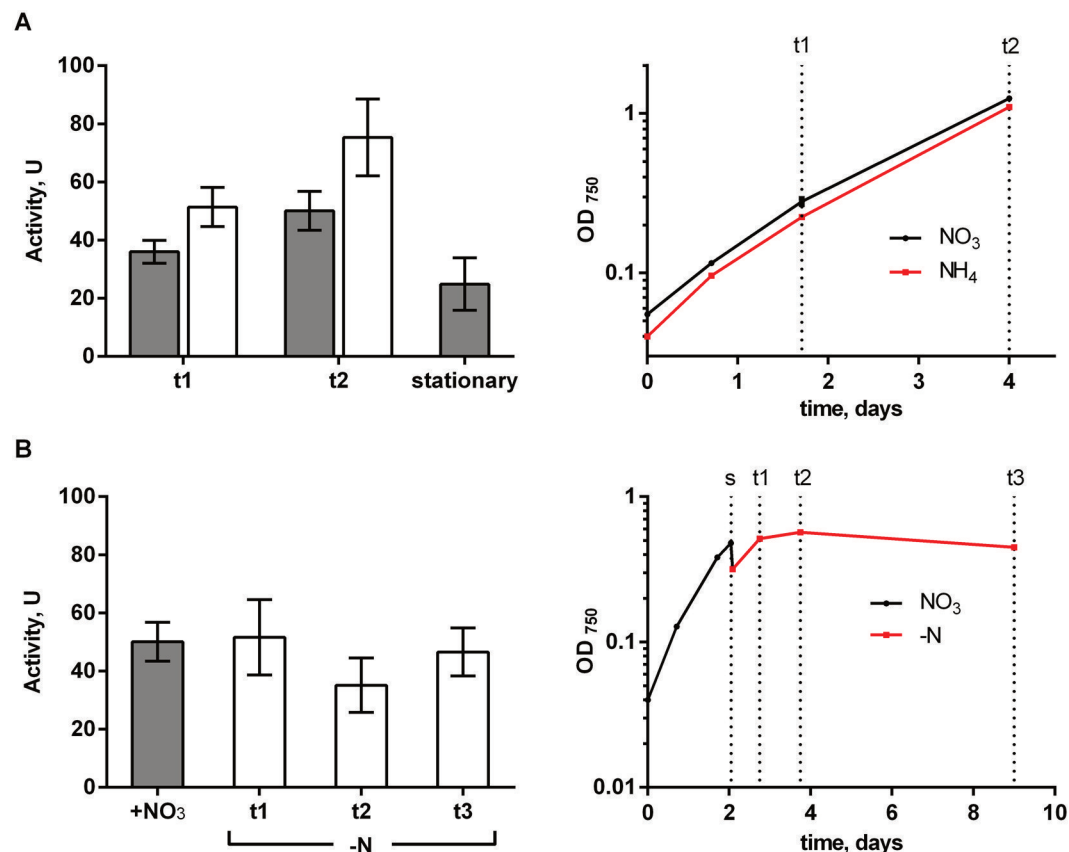


Figure 4. *In situ* fdGOGAT activity with different nitrogen sources. **(A)** *In situ* fdGOGAT activity of *S. elongatus* cultivated with nitrate (grey bars) or ammonium (white bars). Corresponding growth curves are shown on the right. Stationary cells were cultivated for 9 days to an OD₇₅₀ of 5.5 to 6.0. **(B)** fdGOGAT activity of *S. elongatus* cultivated with nitrate and after shift (s) into nitrogen free medium (t1-3) with corresponding growth curve on the right. Error bars: \pm s.e.m., n = 4.

experiments indicated a linear decline in the first 20 min of the reaction (data not shown) when using 4×10^8 cells (± 6.7 mL of culture at OD₇₅₀ = 0.3). When glutamine was omitted from the reaction mix, the concentration of 2-OG remained constant (Fig. 3), which indicates the absence of background 2-OG consuming side reactions.

Characterization of fdGOGAT in *S. elongatus* using the *in situ* fdGOGAT Assay. The glutamine synthetase (GS) - GOGAT cycle represents the connection between the carbon and nitrogen metabolism in bacteria and plants. Whereas GS activity is easy to measure, established GOGAT activity assays are highly elaborate. To determine the fdGOGAT activity with the newly developed FRET-based assay *in situ*, we used, as a test case, *S. elongatus* cells grown in presence of nitrate or ammonia and cells that had been shifted to medium without nitrogen sources (Fig. 4). Samples were taken at three different phases of growth.

With nitrate as nitrogen source, the *in situ* fdGOGAT activity increased by approximately 40% from the early exponential (t1) to the late exponential growth phase (t2, Fig. 4A). After the cells entered the stationary phase, fdGOGAT activity decreased to approx. 70% of the initial value, probably in response to the reduced growth rate and declining metabolic activity in the stationary phase. Under ammonium supplemented growth conditions, the fdGOGAT activity was generally 40–50% higher as compared to nitrate conditions (Fig. 4A). Like in the nitrate-supplemented medium, a 47% increase in activity occurred from early exponential to late exponential growth phase.

The higher *in situ* fdGOGAT activity under ammonium-supplemented growth shows that fdGOGAT is regulated differently to GS. In cyanobacteria and many other prokaryotes, GS is subjected to tight regulation³⁶. In *Synechocystis* sp. PCC 6803, GS activity is tuned down by addition of ammonia, both at the transcriptional level via the NtcA regulatory system⁴⁷ as well as post-translationally by interaction with two inactivation factors IF7 and IF17³⁶. Inhibition is reversed by ammonia depletion within 10–20 min. The ammonium-triggered short-term GS inactivation is essential for maintenance of glutamate homeostasis⁴⁸. When ammonium is in abundance, although GS activity is decreased, more glutamate can be converted to glutamine. Under these conditions, a higher fdGOGAT activity could keep the glutamine/glutamate balance in equilibrium.

Under nitrogen starvation conditions (Fig. 4B), the fdGOGAT activity remains at a constant level. This level is kept constant even after 8 days of starvation, when the cells became chlorotic. This basal activity could ensure

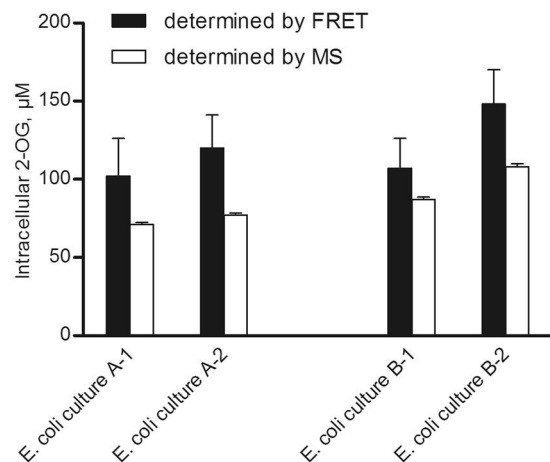


Figure 5. Intracellular 2-OG concentrations of *E. coli* 20 mL of exponentially growing *E. coli* culture were rapidly cooled to 0 °C and harvested by centrifugation. Two *E. coli* cultures (A,B) were used and two samples were taken per culture (1, 2). 2-OG was extracted and intracellular concentrations determined by FRET-sensor (grey; error bars: \pm s.e.m. with $n = 4$) or GC-MS measurements (white; error bar denotes the standard error of the 2-OG calibration curve).

sufficiently high nitrogen assimilation capacity via the GS-GOGAT cycle, enabling the chlorotic cells to immediately assimilate any ammonia that becomes available in the environment.

Determination of 2-OG Concentrations in Cell Extracts. Another possibility to use our sensor is to estimate the concentrations of 2-OG in cell-extracts. Metabolite concentrations in living cells are prone to fluctuations and can change very quickly during cell treatments, such as cell harvesting. To extract physiologically relevant quantities of metabolites from cells, the quenching of cellular activity before metabolite extraction is required²⁷. There are several established metabolic inactivation methods. The use of -40 °C cooled 70% methanol rapidly freezes the cells, but also leads to metabolite loss⁴⁹. Fast centrifugation and subsequent freezing works for heterotrophically growing cells, but is problematic for autotrophically growing cyanobacteria, which quickly adapt their metabolism to darkness. Fast filtration with illumination can solve this problem⁵⁰. After quenching of enzymatic activities, the metabolites are immediately extracted from the cells. There are several established methods, but not all of them are suitable for 2-OG⁴: classical methods use mixtures of chloroform, methanol and buffer with 53% 2-OG recovery⁵¹, boiling ethanol with 58% recovery⁵² or pure -40 °C methanol with 82% recovery⁴. These protocols all include lyophilization of the extracts.

Our first approach was to rapidly filter the cells and immediately freeze the filters in liquid nitrogen. For this purpose, we used 2.5 cm diameter polyether sulfone (PES) membrane filters with a 0.45 μ m pore size. The filters were immediately frozen in liquid nitrogen and afterwards briefly grounded. 2-OG was extracted with pure -40 °C methanol or with a mixture of methanol, chloroform and buffer. However, the organic solvents extracted unidentified compounds which interfered with the fluorescence measurements, showing high background fluorescence of more than 50% of the signal. Therefore, we used toluene to permeabilize the cells, after filtration and freezing as above, and measured 2-OG directly in the supernatant using P_{II}-TC3. The cells were vortexed with 1400 rpm for 8 min at 25 °C in the presence of 1% toluene and 4% EtOH (v/v), similar to the protocol described above⁴⁶. However, the standard deviations were still high. Therefore, we tried an even milder approach without freezing, by sampling the cultures into ice-cooled medium and thus immediately cooling the cells to 0 °C. The cells were then harvested by centrifugation and thereafter quickly permeabilized by toluene/EtOH, yielding reproducible results. The calculated intracellular 2-OG concentrations are shown in Fig. 5. In parallel to the FRET measurements, we determined the 2-OG concentrations by gas chromatography - mass spectrometry (GC-MS), revealing in general 20–30% lower values (for technical detail see Supplementary Information). This is likely due to losses during lyophilization and sample preparation for the GC-MS analyses. The measured intracellular 2-OG concentrations for *E. coli* cells are around 100 μ M, using M9 medium with 19 mM NH₄Cl (Fig. 5). These concentrations are in the same range as reported earlier for *E. coli* growing with high nitrogen supply^{10, 11}. Despite this progress, quantification of cellular 2-OG levels from cell extracts remains problematic due to uncertainties in the extraction method¹³. The ultimate goal is therefore *in vivo* detection of cellular 2-OG levels in single cells. For this purpose, the TC3-R9L variant seemed promising and in the following, we applied this sensor to human cell lines, for which microscopic detection of metabolite FRET sensors is documented⁵³.

Ex vivo Measurements of 2-OG Fluctuations in Human Cell Lines. As a proof of concept, we tested the TC3-R9P sensor (with a dynamic range between 10 μ M – 10 mM) in the human glioblastoma cell line U87-MG. Deregulation of 2-OG metabolism in glioblastoma and other gliomas previously has been shown to be responsible for the aberrant epigenetic gene regulation that characterizes many of these tumors¹⁶. While healthy brain cells show 2-OG concentrations in the range of 1–3 mM, brain cancer cells contain drastically reduced concentrations ranging from 100–300 μ M^{16, 54}. Accordingly, we transiently transfected these cells with plasmids expressing TC3-R9P under the control of the cytomegalovirus (CMV) promoter. We measured the FRET change

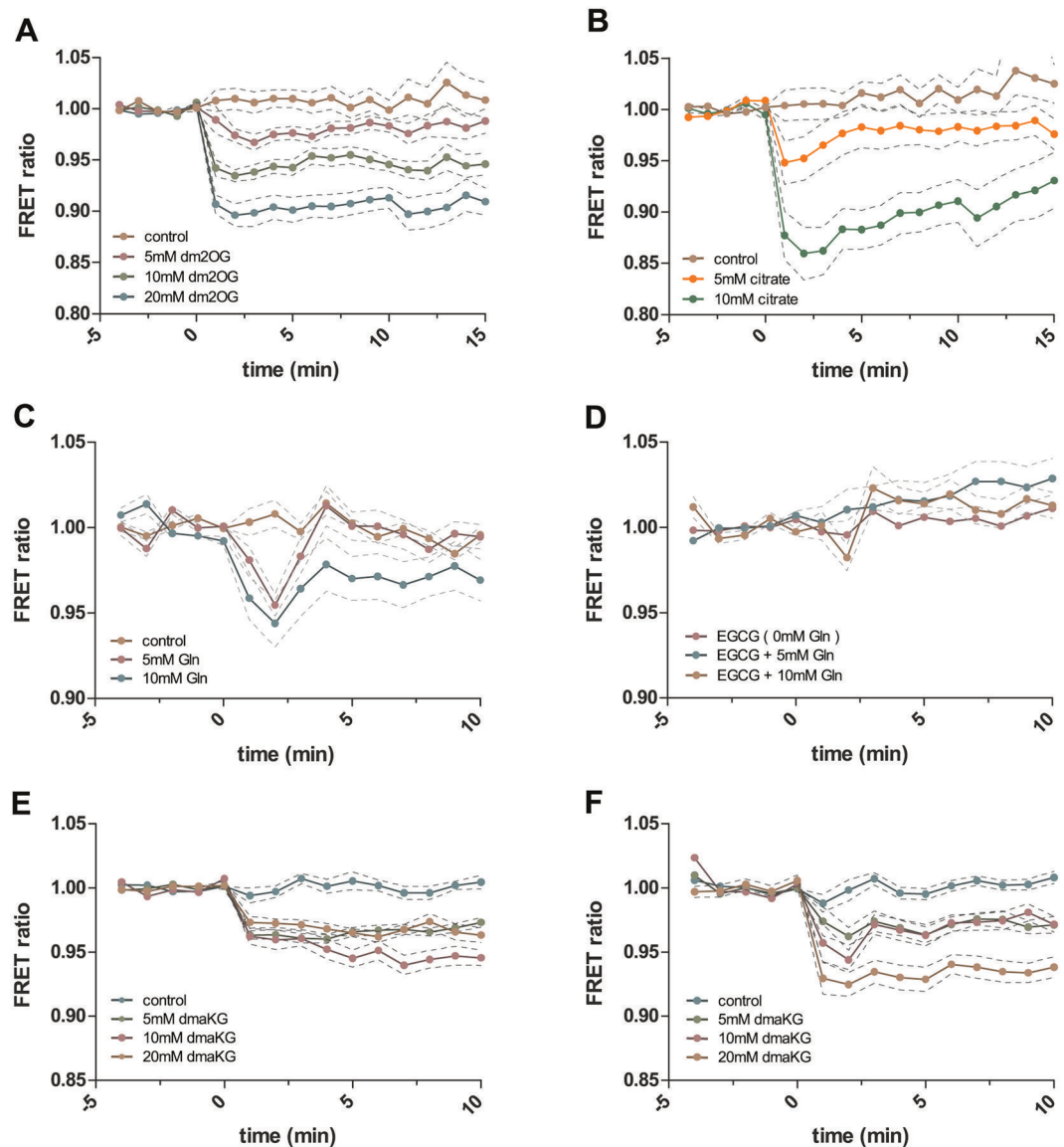


Figure 6. Effect of TCA-cycle metabolites on the FRET signal of TC3-R9P in cultured human cells. (A–D) Various concentrations of the compounds were added to the cell culture media of U87-MG glioblastoma cancer cells at time point zero. 10 to 50 cells were evaluated in each experiment. Average values \pm s.e.m. are shown. (A) 2-OG analogue dm2-OG; (B) Citrate; (C) Glutamine; (D) Glutamine following pre-incubation with 100 μ M of the glutaminolysis inhibitor epigallocatechin gallate (EGCG). (E) Embryonic kidney cells (HEK293T) treated with dm2-OG. (F) Retinal pigment epithelium cells (RPE1) treated with dm2-OG.

after adding either dm2-OG, citrate or glutamine in different concentrations to the cells. The cell-permeable compound dm2-OG is converted into 2-OG inside the cells⁵⁵. As shown in Fig. 6, the FRET dropped within minutes after addition of the compounds, in a concentration-dependent manner. For example, with 20 mM dm2-OG, a 10% drop in FRET was observed (Fig. 6A; Supplementary Video 1 and 2). Theoretically, this drop could be explained by the direct effect of dm2-OG on the sensor; however, since TC3-R9P has an almost two orders of magnitude lower affinity for dm2-OG than 2-OG (Fig. 2D), and dm2-OG furthermore is rapidly demethylated by esterases in the cell, this FRET change likely represents the accumulation of 2-OG in the cells.

Even more pronounced than dm2-OG, addition of citrate rapidly induced a 15% FRET drop, which is close to the maximal observable FRET change (Fig. 6B). As the sensor is 3600 times less sensitive for citrate than for 2-OG, the strong drop in FRET can only be generated by the fast conversion of citrate to 2-OG by the TCA cycle. To estimate the absolute changes in 2-OG, we harvested cells 5 minutes after addition of citrate and determined 2-OG amounts by ultra-performance liquid chromatography. Relative to control cells which contained 56.12 ± 4.08 pmol/ 10^5 cells (mean \pm s.e.m.), addition of 5 mM and 10 mM citrate increased the 2-OG contents to 59.84 ± 1.95 (7%) and 67.77 ± 1.28 pmol/ 10^5 cells (21%), respectively. In contrast to dm2-OG addition, the response towards citrate is more dynamic: addition of 10 mM citrate results in a rapid but transient FRET response. This indicates that citrate is actively taken up and rapidly metabolized to 2-OG leading to a peak in

intracellular 2-OG levels. Subsequently, the 2-OG concentrations inside the cells return back to equilibrium, as revealed by the sensor. By contrast, in the case of dm2-OG, the FRET signal remains at a decreased steady state level over the measuring time. This indicates that the diffusion of dm2-OG into the cells and subsequent demethylation to 2-OG leads to increased 2-OG levels, which remain constant, since passive dm2-OG diffusion maintains the novel steady state level of 2-OG.

The growth of glioblastoma and many other cancer cell lines is dependent on the uptake of glutamine, which is converted to 2-OG by glutaminolysis. This process involves the enzyme glutamate dehydrogenase 1 (GLUD1), a potential target for anti-cancer therapy, whose activity can be suppressed by the small molecule inhibitor epigallocatechin gallate (EGCG)⁵⁶. To test whether the TC3-R9P sensor could detect the intracellular increase of 2-OG level due to increased glutamine uptake and conversion to 2-OG by glutaminolysis, we added 5 mM or 10 mM glutamine to U87 MG cells that were cultured in low-glutamine conditions (0.5 mM instead of 2 mM). Immediately following glutamine supplementation we observed a concentration-dependent drop of the FRET ratios suggesting elevated uptake of glutamine by the cells and its conversion to 2-OG (Fig. 6C). After an initial transient over-accumulation, 2-OG levels returned to a new steady state within a few minutes. When glutaminolysis was blocked by pre-incubation with 100 μ M EGCG for three hours, no change in FRET was observed (Fig. 6D) indicating that the additional intracellular 2-OG that accumulated in the inhibitor-free condition (Fig. 6C) indeed was derived from glutamine. These data show that our P_{II}-protein-derived FRET sensors potentially could be used to detect phenotype-relevant changes of 2-OG concentrations in cancer cells, making them useful tools to monitor readout during metabolic drug screening. To test whether the 2-OG sensor also could be used in other types of cells, we measured FRET changes in cell lines that have been derived from embryonic (human embryonic kidney; HEK293T) and differentiated (retinal pigment epithelium; RPE1) tissues. In both cell lines FRET ratios decreased following the addition of dm2-OG (Fig. 6E and F) suggesting that the TC3-R9P sensor can be used to analyze 2-OG changes in various types of cells.

In summary, with these various applications we could demonstrate the functionality of our FRET based 2-OG sensor for different applications. The TC3 sensor performed very well for *in situ* GOGAT activity determination. For determining cellular 2-OG concentrations, the final goal was to create a sensor that sensitively reports fluctuating 2-OG concentration in living cells. For this purpose, the R9P variant of the TC3 sensor seems to be a very good starting point. This sensor variant allowed real-time live-cell imaging of 2-OG in cancer, embryonic and differentiated cells, and potentially could also be used as a readout assay in high-throughput drug screening.

For even more sensitive *in vivo* experiments, the maximal signal change of 25% upon 2-OG addition should be further improved by protein engineering of the FRET sensor, to achieve a more robust signal. As seen in the sensor development, small alterations can have a drastic, unpredictable influence on the FRET output. Accordingly, we suggest a directed evolutionary approach to further improve the FRET sensor. It has been shown before, that a random mutagenesis approach with a well-designed selection mechanism can strongly enhance the capabilities of a FRET sensor^{57,58}. In view of the emerging importance of 2-OG as effector molecule for central cellular processes, monitoring *in vivo* fluctuations of 2-OG will lead to a deeper understanding on the role of the metabolism on cell functions.

Material and Method

Cultivation of bacterial and human cell lines. Cyanobacterial strains were cultivated photoautotrophically at a constant illumination of 50 μ mol photons $m^{-2} s^{-1}$ in BG-11 medium⁵⁹ supplemented with 5 mM NaHCO₃ at 28 °C in flasks shaking at 120 rpm. As nitrogen source, either 17.65 mM NaNO₃ or 5 mM NH₄Cl, with 5 mM TES/NaOH; pH 8.2 (Roth), was added.

Escherichia coli K-12 substrain MG1655 cells were cultivated in M9 minimal medium containing: 48 mM Na₂HPO₄, 22 mM KH₂PO₄, 8.5 mM NaCl, 19 mM NH₄Cl, 2 mM MgSO₄, 0.1 mM CaCl₂, 0.4% (w/v) glucose, 0.0001% (w/v) thiamin. Cultures of 100–200 mL volume were grown in 1 L wide-neck flasks at 180 rpm, using silicone sponge closures to ensure aerobic growth. Optical density was measured at 600 nm.

Human glioma cell line U87-MG was cultured at 37 °C, 90% air/10% CO₂ in Dulbecco's Modified Eagle's medium (DMEM Sigma D5921) without phenol-red, 1000 mg/L glucose, supplemented with 10% FCS (Biochrom #S0115), 2 mM glutamine and 1% penicillin/streptomycin mix. HEK293T cells were cultured in RPMI 1640 Medium, 4500 mg/L glucose, supplemented with 10% FCS, 2 mM glutamine and 1% penicillin/streptomycin mix. hTERT-RPE1 cells were cultured in DMEM/F12 Medium, 4500 mg/L glucose, supplemented with 10% FCS and additional 1% glutamine. All cell lines were transfected with 0.8 μ g/mL plasmid DNA using TransIt-LT1 reagent (Mirus). Dimethyl-2-oxoglutarate (dm-2OG, Sigma), citric acid (AppliChem) and glutamine (Gibco 25030) were diluted in DMEM buffered with HEPES solution. For GDH inhibition, cells were pre-incubated 3 h with 100 μ M (–)-Epigallocatechin gallate (Sigma E4143).

Cloning and Protein purification. Plasmids were constructed by PCR amplification of P_{II} and FP genes with primers containing overlapping regions. The PCR products were fused with an XbaI and HindIII double digested pASK-IBA3 vector (IBA GmbH, Göttingen, Germany) via isothermal, single-reaction DNA assembly following the protocol by Gibson *et al.*⁶⁰. The sensor genes were amplified by standard PCR and cloned into the mammalian expression vector pcDNA3.1 using the BamHI and HindIII restriction sites. The complete sequences of the sensor genes are provided in the Supplementary Information.

P_{II} protein variants were overexpressed in *E. coli* RB9060 and purified as described earlier using Strep-tag affinity chromatography²⁸. To remove contaminating proteins and degradation products the sensor proteins were further purified by size exclusion chromatography, using an Äkta purifier and a HiLoad 26/600 Superdex 200 prep grade column (GE Healthcare GmbH, Solingen, Germany). The running buffer contained 30 mM Tris (pH 7.5) and 175 mM NaCl. The proteins were stored in a buffer containing 50 mM Tris-HCl pH 7.8, 100 mM KCl, 5 mM MgCl₂, 0.5 mM EDTA, 1 mM DTT and 50% glycerol (v/v) at –20 °C.

***In situ* fdGOGAT Assay.** *In situ* Fd-GOGAT activity was determined according to Marqués *et al.*⁴⁴ and Kameya *et al.*⁴⁵, with some modifications. For assaying the *in situ* Fd-GOGAT activity in *S. elongatus*, 4×10^8 cells were collected and washed twice with PBS buffer containing 2.7 mM KCl, 1.5 mM KH_2PO_4 , 137 mM NaCl, 8.1 mM Na_2HPO_4 , pH 7.5 at 4 °C. The cell pellet was resuspended in 200 μL reaction buffer containing 20 mM Na_3PO_4 pH 7.2, 10 mM glutamine, 1 mM 2-OG and 5 mM methyl viologen. Cells were permeabilized by addition of 4.4 μL toluene and constant vortexing at 1400 rpm for 5 min at 32 °C. To insulate the reaction from atmospheric oxygen, the reaction mixture was covered by 500 μL paraffin oil. The reaction was started by addition of 5 mM sodium dithionite, gently mixing and incubating at 32 °C. Reaction aliquots (30 μL) were removed in regular intervals and the reaction was stopped by intensive shaking until the blue color disappeared, indicating oxidation of the electron donor methyl viologen. Aliquots were then centrifuged at $15,000 \times g$ for 10 min at 4 °C and the 2-OG concentration in the supernatant was determined as described below. One unit of activity was defined as μmol 2-OG consumption per min.

Cell Extraction for FRET Measurements. *E. coli* cultures (20 ml aliquots) were harvested at an optical density (OD_{600}) of 0.5 by pipetting directly out of the shaking culture and mixing with 30 mL of the corresponding culture medium and 30 g ice for rapid quenching of the metabolism. Cells were pelleted by centrifugation at $15,000 \times g$ for 8 min at 0 °C. The cell pellet was resuspended on ice with 94 μL 20% (v/v) ethanol. The cell suspension was transferred into a 2 mL sample tube and 406 μL MilliQ water was added to a final volume of 500 μL with a final ethanol concentration of 3.75% (v/v), as well as 6.25 μL toluene for membrane permeabilization, as described by Gomez Casati *et al.*⁴⁶. The mixture was incubated for 8 min at 25 °C under shaking at 1,400 rpm and subsequently quickly cooled on ice and centrifuged at $14,000 \times g$ for 5 min at 0 °C. The clear supernatant was transferred into a fresh tube and centrifuged as before. The supernatant was either directly used for FRET measurements or stored at -20 °C.

Ultra Performance Liquid Chromatography (UPLC) analysis. For determination of intracellular 2-OG content in human glioblastoma cell line, 1×10^5 cells were extracted with 200 μL cold 1 M perchloric acid. Insoluble material was removed by centrifugation for 10 min at $25,000 \times g$. For derivatization with DMB (1,2-diamino-4,5-methylenedioxybenzene), 30 μL extract were mixed with 30 μL DMB derivatization reagent (5 mM DMB, 20 mM sodium hydrosulfite, 1 M 2-mercaptoethanol, 1.2 M HCl) and incubated at 100 °C for 45 min. After 10 min centrifugation, the reaction was diluted with 240 μL 10% acetonitrile. The derivatized ketoacids were separated by reversed phase chromatography on an Acquity HSS T3 column (100 mm \times 2.1 mm, 1.7 μm , Waters) connected to an Acquity H-class UPLC system. Prior separation, the column was heated to 40 °C and equilibrated with 5 column volumes of solvent A (0.1% formic acid in 10% acetonitrile) at a flow rate of 0.55 ml/min. Baseline separation of DMB derivates was achieved by increasing the concentration of acetonitrile (B) in buffer A as follows: 2 min 2% B, 4.5 min 15% B, 10.5 min 38% B, 10.6 min 90% B, hold for 2 min, and return to 2% B in 3.5 min. The separated derivates were detected by fluorescence (Acquity FLR detector, Waters; excitation: 367 nm; emission: 446 nm) and quantified using ultrapure standards (Sigma). Data acquisition and processing was performed with the Empower3 software suite (Waters). 2-OG data were globally normalized relative to the mean of all analyzed derivatized metabolites.

***In vitro* FRET Measurements.** FRET measurements were conducted in a buffer containing 50 mM imidazole (pH 7.5), 50 mM KCl, 20 mM MgCl_2 , 15% glycerol (v/v), 0.5 mM DTT and 5 mM ATP. The sensor protein was carefully added to a final concentration of 100 nM (monomer). For blank measurements the master mix was prepared by adding water instead of the sensor protein. Without mixing, the solution was incubated for 15 min on ice to allow the protein to adapt to the buffer. After that, the solution was mixed by inverting the tube several times and 70 μL (extract measurement) or 90 μL (GOGAT measurement) aliquots were dispensed onto a black non-binding 96-well plate (Greiner Bio-One, Frickenhausen, Germany). 30 μL of the cell extracts or 10 μL of the GOGAT assay supernatant and a 2-OG standard solution were added to the plate. The plate was sealed using an adhesive foil to prevent evaporation. Subsequently the plate was placed in a Tecan Spark 10 M microplate reader (Tecan, Männedorf, Switzerland) at 37 °C. The plate was shaken for 80 s and incubated for 20 min. After the incubation, the plate was again shaken for 20 s, the foil was removed and the FRET signal was measured. Each well was measured in three channels (each 20 nm bandwidth): Venus, excitation: 485 nm, emission: 530 nm; Cerulean: excitation: 435 nm, emission: 480 nm; FRET: excitation: 435 nm, emission: 530 nm. Blank values were subtracted from the measurements in each channel. Following the N_{FRET} formula developed by Xia and Liu⁶¹ corrected FRET values were calculated. The correction factors *a* and *b* were determined in separate measurements containing only Venus or Cerulean. Each plate contained a standard curve of known 2-OG concentrations and the samples. Using GaphPad Prism 6 (GraphPad Software, San Diego, USA) the unknown concentrations were interpolated from the standard curve. For the calculation of intracellular 2-OG concentrations the intracellular volume of glucose grown *E. coli* MG1655 was assumed to be 3.3 μL per mL of $\text{OD}_{600} = 1$ culture, as determined by Volkmer and Heinemann⁶².

Life-Cell Imaging. Fluorescence measurements were performed in a Leica TCS-SP5 laser scanning confocal microscope equipped with resonant scanners and hybrid photon detectors (HyD) and using a 40x objective (HCX PL APO, NA 1.25, oil-immersion). Cells were excited with a UV diode (405 nm) and emission was detected at 450–490 nm (CFP) and 520–590 nm (FRET). Pictures were acquired every 60 sec. After a baseline of 5 min, media containing metabolites or not were added and changes in fluorescence were recorded for 15 minutes. During imaging, cells were maintained at 37 °C and 5% CO_2 . Image processing was performed with ImageJ (<http://fiji.sc/>). After background subtraction and registration, single cells were segmented by threshold and mean intensity was measured for each channel at every time point. The ratio was calculated by dividing the mean intensity of

the acceptor (FRET) by the intensity of the donor (CFP). Ratios calculated from every cell were normalized to baseline measurements.

References

- Aretz, I. & Meierhofer, D. Advantages and Pitfalls of Mass Spectrometry Based Metabolome Profiling in Systems Biology. *Int J Mol Sci* **17**, doi:10.3390/ijms17050632 (2016).
- Schwarz, D., Orf, I., Kopka, J. & Hagemann, M. Recent applications of metabolomics toward cyanobacteria. *Metabolites* **3**, 72–100, doi:10.3390/metabo3010072 (2013).
- Bingol, K. *et al.* Metabolomics beyond spectroscopic databases: a combined MS/NMR strategy for the rapid identification of new metabolites in complex mixtures. *Anal Chem* **87**, 3864–3870, doi:10.1021/ac504633z (2015).
- Villas-Boas, S. G., Hojer-Pedersen, J., Akesson, M., Smedsgaard, J. & Nielsen, J. Global metabolite analysis of yeast: evaluation of sample preparation methods. *Yeast* **22**, 1155–1169, doi:10.1002/yea.1308 (2005).
- Jones, A. M. *et al.* In vivo biochemistry: applications for small molecule biosensors in plant biology. *Curr Opin Plant Biol* **16**, 389–395, doi:10.1016/j.pbi.2013.02.010 (2013).
- Newman, R. H., Fosbrink, M. D. & Zhang, J. Genetically encodable fluorescent biosensors for tracking signaling dynamics in living cells. *Chemical reviews* **111**, 3614–3666, doi:10.1021/cr100002u (2011).
- Hochreiter, B., Garcia, A. P. & Schmid, J. A. Fluorescent proteins as genetically encoded FRET biosensors in life sciences. *Sensors (Basel)* **15**, 26281–26314, doi:10.3390/s151026281 (2015).
- Kaper, T., Lager, I., Looger, L. L., Chermak, D. & Frommer, W. B. Fluorescence resonance energy transfer sensors for quantitative monitoring of pentose and disaccharide accumulation in bacteria. *Biotechnol Biofuels* **1**, 11, doi:10.1186/1754-6834-1-11 (2008).
- Huergo, L. F. & Dixon, R. The Emergence of 2-Oxoglutarate as a Master Regulator Metabolite. *Microbiol Mol Biol Rev* **79**, 419–435, doi:10.1128/MMBR.00038-15 (2015).
- Yuan, J. *et al.* Metabolomics-driven quantitative analysis of ammonia assimilation in *E. coli*. *Mol Syst Biol* **5**, 302, doi:10.1038/msb.2009.60 (2009).
- Radchenko, M. V., Thornton, J. & Merrick, M. Control of AmtB-GlnK complex formation by intracellular levels of ATP, ADP, and 2-oxoglutarate. *J Biol Chem* **285**, 31037–31045, doi:10.1074/jbc.M110.153908 (2010).
- Dodsworth, J. A., Cady, N. C. & Leigh, J. A. 2-Oxoglutarate and the PII homologues Nif1 and Nif2 regulate nitrogenase activity in cell extracts of *Methanococcus maripaludis*. *Mol Microbiol* **56**, 1527–1538, doi:10.1111/j.1365-2958.2005.04621.x (2005).
- Yan, D., Lenz, P. & Hwa, T. Overcoming Fluctuation and Leakage Problems in the Quantification of Intracellular 2-Oxoglutarate Levels in *Escherichia coli*. *Applied and Environmental Microbiology* **77**, 6763–6771, doi:10.1128/aem.05257-11 (2011).
- Brauer, M. J. *et al.* Conservation of the metabolomic response to starvation across two divergent microbes. *Proc Natl Acad Sci USA* **103**, 19302–19307, doi:10.1073/pnas.0609508103 (2006).
- Chin, R. M. *et al.* The metabolite alpha-ketoglutarate extends lifespan by inhibiting ATP synthase and TOR. *Nature* **510**, 397–401, doi:10.1038/nature13264 (2014).
- Dang, L. *et al.* Cancer-associated IDH1 mutations produce 2-hydroxyglutarate. *Nature* **462**, 739–744, doi:10.1038/nature08617 (2009).
- Gross, S. *et al.* Cancer-associated metabolite 2-hydroxyglutarate accumulates in acute myelogenous leukemia with isocitrate dehydrogenase 1 and 2 mutations. *J Exp Med* **207**, 339–344, doi:10.1084/jem.20092506 (2010).
- Cascella, B. & Mirica, L. M. Kinetic analysis of iron-dependent histone demethylases: alpha-ketoglutarate substrate inhibition and potential relevance to the regulation of histone demethylation in cancer cells. *Biochemistry* **51**, 8699–8701, doi:10.1021/bi3012466 (2012).
- TeSlaa, T. *et al.* α -Ketoglutarate Accelerates the Initial Differentiation of Primed Human Pluripotent Stem Cells. *Cell Metabolism* **24**, 485–493, doi:10.1016/j.cmet.2016.07.002 (2016).
- Carey, B. W., Finley, L. W. S., Cross, J. R., Allis, C. D. & Thompson, C. B. Intracellular α -ketoglutarate maintains the pluripotency of embryonic stem cells. *Nature* **518**, 413–416, doi:10.1038/nature13981 (2015).
- Hwang, I.-Y. *et al.* Psat1-Dependent Fluctuations in α -Ketoglutarate Affect the Timing of ESC Differentiation. *Cell Metabolism* **24**, 494–501, doi:10.1016/j.cmet.2016.06.014 (2016).
- Olenchock, B. A. *et al.* EGLN1 Inhibition and Rerouting of alpha-Ketoglutarate Suffice for Remote Ischemic Protection. *Cell* **165**, 497, doi:10.1016/j.cell.2016.03.037 (2016).
- Doucette, C. D., Schwab, D. J., Wingreen, N. S. & Rabinowitz, J. D. alpha-Ketoglutarate coordinates carbon and nitrogen utilization via enzyme I inhibition. *Nat Chem Biol* **7**, 894–901, doi:10.1038/nchembio.685 (2011).
- Venditti, V., Tugarinov, V., Schwieters, C. D., Grishaev, A. & Clore, G. M. Large interdomain rearrangement triggered by suppression of micro- to millisecond dynamics in bacterial Enzyme I. *Nat Commun* **6**, 5960, doi:10.1038/ncomms6960 (2015).
- Gorke, B. & Stulke, J. Carbon catabolite repression in bacteria: many ways to make the most out of nutrients. *Nat Rev Microbiol* **6**, 613–624, doi:10.1038/nrmicro1932 (2008).
- Park, Y. H., Lee, B. R., Seok, Y. J. & Peterkofsky, A. In vitro reconstitution of catabolite repression in *Escherichia coli*. *J Biol Chem* **281**, 6448–6454, doi:10.1074/jbc.M512672200 (2006).
- Huergo, L. F., Chandra, G. & Merrick, M. P_{II} signal transduction proteins: nitrogen regulation and beyond. *FEMS Microbiology Reviews* **37**, 251 (2013).
- Fokina, O., Chellamuthu, V.-R., Forchhammer, K. & Zeth, K. Mechanism of 2-oxoglutarate signaling by the *Synechococcus elongatus* P(II) signal transduction protein. *Proceedings of the National Academy of Sciences of the United States of America* **107**, 19760–19765, doi:10.1073/pnas.1007653107 (2010).
- Truan, D. *et al.* A New PII Protein Structure Identifies the 2-Oxoglutarate Binding Site. *Journal of Molecular Biology* **400**, 531–539, doi:10.1016/j.jmb.2010.05.036 (2010).
- Forchhammer, K. & Lüddecke, J. Sensory properties of the PII signalling protein family. *FEBS Journal* **283**, 425–437, doi:10.1111/febs.13584 (2016).
- Forchhammer, K. P. II Signal transducers: novel functional and structural insights. *Trends in microbiology* **16**, 65–72, doi:10.1016/j.tim.2007.11.004 (2008).
- Lüddecke, J. & Forchhammer, K. From PII Signaling to Metabolite Sensing: A Novel 2-Oxoglutarate Sensor That Details PII - NAGK Complex Formation. *PLoS ONE* **8**, e83181, doi:10.1371/journal.pone.0083181 (2013).
- Chen, H. L., Bernard, C. S., Hubert, P., My, L. & Zhang, C. C. Fluorescence resonance energy transfer based on interaction of PII and PipX proteins provides a robust and specific biosensor for 2-oxoglutarate, a central metabolite and a signalling molecule. *FEBS J* **281**, 1241–1255, doi:10.1111/febs.12702 (2014).
- Lüddecke, J. & Forchhammer, K. Energy Sensing versus 2-Oxoglutarate Dependent ATPase Switch in the Control of *Synechococcus* PII Interaction with Its Targets NAGK and PipX. *PLoS ONE* **10**, e0137114, doi:10.1371/journal.pone.0137114 (2015).
- Berg, J., Hung, Y. P. & Yellen, G. A genetically encoded fluorescent reporter of ATP:ADP ratio. *Nat Methods* **6**, 161–166, doi:10.1038/nmeth.1288 (2009).
- Muro-Pastor, M. I., Reyes, J. C. & Florencio, F. J. Ammonium assimilation in cyanobacteria. *Photosynth Res* **83**, 135–150, doi:10.1007/s11120-004-2082-7 (2005).

37. Luque, I. & Forchhammer, K. In *The Cyanobacteria: Molecular Biology, Genomics and Evolution* (eds A. Herrero & E. Flores) Ch. 13, (Caister Academic Press, 2008).
38. Ermilova, E. *et al.* PII signal transduction protein in *Chlamydomonas reinhardtii*: localization and expression pattern. *Protist* **164**, 49–59, doi:10.1016/j.protis.2012.04.002 (2013).
39. Arai, R., Ueda, H., Kitayama, A., Kamiya, N. & Nagamune, T. Design of the linkers which effectively separate domains of a bifunctional fusion protein. *Protein Engineering* **14**, 529–532, doi:10.1093/protein/14.8.529 (2001).
40. Muller, S. M., Galliardt, H., Schneider, J., Barisas, B. G. & Seidel, T. Quantification of Förster resonance energy transfer by monitoring sensitized emission in living plant cells. *Front Plant Sci* **4**, 413, doi:10.3389/fpls.2013.00413 (2013).
41. Topell, S., Hennecke, J. & Glockshuber, R. Circularly permuted variants of the green fluorescent protein. *FEBS Lett* **457**, 283–289 (1999).
42. Zacharias, D. A., Violin, J. D., Newton, A. C. & Tsien, R. Y. Partitioning of Lipid-Modified Monomeric GFPs into Membrane Microdomains of Live Cells. *Science* **296**, 913–916, doi:10.1126/science.1068539 (2002).
43. Goedhart, J. *et al.* Structure-guided evolution of cyan fluorescent proteins towards a quantum yield of 93%. *Nature Communications* **3**, 751, doi:10.1038/ncomms1738 (2012).
44. Marqués, S., Florencio, F. J. & Candau, P. Ammonia assimilating enzymes from cyanobacteria: *in situ* and *in vitro* assay using high-performance liquid chromatography. *Anal Biochem* **180**, 152–157 (1989).
45. Kameya, M. *et al.* A novel ferredoxin-dependent glutamate synthase from the hydrogen-oxidizing chemoautotrophic bacterium *Hydrogenobacter thermophilus* TK-6. *J Bacteriol* **189**, 2805–2812, doi:10.1128/JB.01360-06 (2007).
46. Gomez Casati, D. F., Aon, M. A., Cortassa, S. & Iglesias, A. A. Measurement of the glycogen synthetic pathway in permeabilized cells of cyanobacteria. *FEMS Microbiol Lett* **194**, 7–11 (2001).
47. Luque, I., Vazquez-Bermudez, M. F., Paz-Yepes, J., Flores, E. & Herrero, A. In vivo activity of the nitrogen control transcription factor NtcA is subjected to metabolic regulation in *Synechococcus* sp. strain PCC 7942. *FEMS Microbiol Lett* **236**, 47–52, doi:10.1016/j.femsle.2004.05.018 (2004).
48. Kustu, S., Hirschman, J., Burton, D., Jelesko, J. & Meeks, J. C. Covalent modification of bacterial glutamine synthetase: physiological significance. *Mol Gen Genet* **197**, 309–317 (1984).
49. Young, J. D., Shastri, A. A., Stephanopoulos, G. & Morgan, J. A. Mapping photoautotrophic metabolism with isotopically nonstationary (¹³C) flux analysis. *Metab Eng* **13**, 656–665, doi:10.1016/j.ymben.2011.08.002 (2011).
50. Krall, L., Huege, J., Catchpole, G., Steinhauser, D. & Willmitzer, L. Assessment of sampling strategies for gas chromatography-mass spectrometry (GC-MS) based metabolomics of cyanobacteria. *J Chromatogr B Analyt Technol Biomed Life Sci* **877**, 2952–2960, doi:10.1016/j.jchromb.2009.07.006 (2009).
51. de Koning, W. & van Dam, K. A method for the determination of changes of glycolytic metabolites in yeast on a subsecond time scale using extraction at neutral pH. *Anal Biochem* **204**, 118–123 (1992).
52. Gonzalez, B., Francois, J. & Renaud, M. A rapid and reliable method for metabolite extraction in yeast using boiling buffered ethanol. *Yeast* **13**, 1347–1355, doi:10.1002/(SICI)1097-0061(199711)13:14<1347::AID-YEA176>3.0.CO;2-O (1997).
53. San Martín, A. *et al.* A Genetically Encoded FRET Lactate Sensor and Its Use To Detect the Warburg Effect in Single Cancer Cells. *PLoS ONE* **8**, e57712, doi:10.1371/journal.pone.0057712 (2013).
54. Thirstrup, K. *et al.* Endogenous 2-oxoglutarate levels impact potencies of competitive HIF prolyl hydroxylase inhibitors. *Pharmacol Res* **64**, 268–273, doi:10.1016/j.phrs.2011.03.017 (2011).
55. Carey, B. W., Finley, L. W., Cross, J. R., Allis, C. D. & Thompson, C. B. Intracellular alpha-ketoglutarate maintains the pluripotency of embryonic stem cells. *Nature* **518**, 413–416, doi:10.1038/nature13981 (2015).
56. Lecumberri, E., Dupertuis, Y. M., Miralbell, R. & Pichard, C. Green tea polyphenol epigallocatechin-3-gallate (EGCG) as adjuvant in cancer therapy. *Clinical Nutrition* **32**, 894–903, doi:10.1016/j.clnu.2013.03.008 (2013).
57. Litzlbauer, J. *et al.* Large Scale Bacterial Colony Screening of Diversified FRET Biosensors. *PLoS ONE* **10**, e0119860, doi:10.1371/journal.pone.0119860 (2015).
58. Thestrup, T. *et al.* Optimized ratiometric calcium sensors for functional in vivo imaging of neurons and T lymphocytes. *Nat Methods* **11**, 175–182, doi:10.1038/nmeth.2773 (2014).
59. Rippka, R., Deruelles, J., Waterbury, J. B., Herdman, M. & Stanier, R. Y. Generic Assignments, Strain Histories and Properties of Pure Cultures of Cyanobacteria. *J Gen Microbiol* **111**, 1–61 (1979).
60. Gibson, D. G. *et al.* Enzymatic assembly of DNA molecules up to several hundred kilobases. *Nat Methods* **6**, 343–345, doi:10.1038/nmeth.1318 (2009).
61. Xia, Z. & Liu, Y. Reliable and global measurement of fluorescence resonance energy transfer using fluorescence microscopes. *Biophysical Journal* **81**, 2395–2402, doi:10.1016/S0006-3495(01)75886-9 (2001).
62. Volkmer, B. & Heinemann, M. Condition-dependent cell volume and concentration of *Escherichia coli* to facilitate data conversion for systems biology modeling. *PLoS ONE* **6**, e23126, doi:10.1371/journal.pone.0023126 (2011).

Acknowledgements

This work was funded by a grant from the Deutsche Forschungsgemeinschaft (Fo195/9-2) and in part by a grant to B.R., provided by the Heidelberg CellNetworks cluster within the framework of the German Excellence Initiative. We'd also like to give special thanks to the National Council for Science and Technology (CONACYT-Mexico) for the financial support provided to Liliana François (CVU 468797). We would like to thank Dr. Joachim Kilian for kind help in GC-MS analysis and to acknowledge the support of the German Cancer Research Center (DKFZ) Light Microscopy Facility.

Author Contributions

J.L. and T.C. developed the FRET sensor. J.L. and P.S. characterized the sensor variants and performed *in vitro* assays in bacteria. B.W. and J.L. performed *in situ* fdGOGAT assays. L.F. transfected human cell lines and performed live-cell imaging assays. G.P. and R.H. performed the UPLC analysis, B.R. and K.F. supervised the experiments. J.L., L.F., P.S. and K.F. prepared the manuscript.

Additional Information

Supplementary information accompanies this paper at doi:10.1038/s41598-017-01440-w

Competing Interests: The authors declare that they have no competing interests.

Publisher's note: Springer Nature remains neutral with regard to jurisdictional claims in published maps and institutional affiliations.



Open Access This article is licensed under a Creative Commons Attribution 4.0 International License, which permits use, sharing, adaptation, distribution and reproduction in any medium or format, as long as you give appropriate credit to the original author(s) and the source, provide a link to the Creative Commons license, and indicate if changes were made. The images or other third party material in this article are included in the article's Creative Commons license, unless indicated otherwise in a credit line to the material. If material is not included in the article's Creative Commons license and your intended use is not permitted by statutory regulation or exceeds the permitted use, you will need to obtain permission directly from the copyright holder. To view a copy of this license, visit <http://creativecommons.org/licenses/by/4.0/>.

© The Author(s) 2017

5. Accepted publication

Watzer, B. & Forchhammer, K. (2018).

Cyanophycin, a nitrogen-rich reserve polymer.

Cyanobacteria, ISBN: 978-953-51-6243-8

Cyanophycin: A Nitrogen-Rich Reserve Polymer

Björn Watzer and Karl Forchhammer

Additional information is available at the end of the chapter

<http://dx.doi.org/10.5772/intechopen.77049>

Abstract

Cyanophycin is a nitrogen/carbon reserve polymer present in most cyanobacteria as well as in a few heterotrophic bacteria. It is a non-ribosomally synthesized polyamide consisting of aspartate and arginine (multi-L-arginyl-poly-L-aspartic acid). The following chapter provides an overview of the characteristics and occurrence of cyanophycin in cyanobacteria. Information about the enzymes involved in cyanophycin metabolism and the regulation of cyanophycin accumulation is also summarized. Herein, we focus on the main regulator, the P_{II} signal transduction protein and its regulation of arginine biosynthesis. Since cyanophycin could be used in various medical or industrial applications, it is of high biotechnological interest. In the last few years, many studies were published aiming at the large-scale production of cyanophycin in different heterotrophic bacteria, yeasts and plants. Recently, a cyanobacterial production strain has been reported, which shows the highest so ever reported cyanophycin yield. The potential and possibilities of biotechnological cyanophycin production will be reviewed in this chapter.

Keywords: cyanophycin, cyanophycin synthetase, cyanophycinase, nitrogen reserve, polyamide, L-arginine, L-aspartate, P_{II} protein

1. Introduction

Cyanophycin, abbreviated CGP (cyanophycin granule peptide), is next to poly- γ -glutamic acid and poly- ϵ -lysine, the third polyamino acid known to occur in nature [1]. It serves as a nitrogen/carbon reserve polymer in many cyanobacterial strains as well as in a few heterotrophic bacteria. CGP consists of the two amino acids, aspartate and arginine, forming a poly-L-aspartic acid backbone with arginine side chains. The arginine residues are linked to the β -carboxyl group of every aspartyl moiety via isopeptide bond [2].

CGP was discovered in 1887 by the botanist Antonio Borzi during microscopic studies of filamentous cyanobacteria [3]. He observed opaque and light scattering inclusions by using light microscopy and created the name *cianoficina*. Early electron microscopic studies showed a strong structure variation of the CGP granules, depending on the fixatives and poststains used during electron microscopic examinations [4, 5]. This led to a controversy about the ultrastructure of these inclusions until the 1970s. Later, electron microscopic studies described CGP granules as membrane less, electron dense and highly structured cytoplasmic inclusions [6, 7].

With a C/N ratio of 2:1, CGP is extremely rich in nitrogen and consequently an excellent nitrogen storage compound. During the degradation of CGP and subsequent degradation of arginine, a function as energy source was also proposed [8].

2. CGP occurrence

Most cyanobacteria, including unicellular and filamentous, as well as diazotrophic and non-diazotrophic groups are able to accumulate CGP (**Figure 1**).

In non-diazotrophic cyanobacteria, the amount of CGP is usually less than 1% of the cell dry mass during exponential growth. CGP accumulates conspicuously under unbalanced growth conditions including stationary phase, light stress or nutrient limitation (sulfate, phosphate or potassium starvation) that do not involve nitrogen starvation [9, 10]. Under such unbalanced conditions, the amount of CGP may increase up to 18% of the cell dry mass [10]. During the recovery from nitrogen starvation by the addition of a usable nitrogen source, CGP is transiently accumulated [11, 12].

In the unicellular diazotrophic cyanobacterium *Cyanothece* sp. ATCC 51142, nitrogen fixation and photosynthesis can coexist in the same cell, but temporarily separated. The nitrogen-fixing enzyme, nitrogenase, is highly sensitive to oxygen. Nitrogen fixation occurs in dark periods and the fixed nitrogen is stored in CGP. In the light period, when photosynthesis is performed, the CGP is degraded to mobilize the fixed nitrogen [13]. Transient CPG accumulation during dark periods was also reported in the filamentous cyanobacterium *Trichodesmium* sp., which has a high abundance in tropical and subtropical seas and is an important contributor to global N and C cycling [14].

Furthermore, in heterocysts of diazotrophic cyanobacteria of the order *Nostocales*, polar nodules consisting of CGP are deposited at the contact site to adjacent vegetative cells [15] (**Figure 1**). The heterocystous CGP seems to be involved in transport of fixed nitrogen to the adjacent photosynthetically active vegetative cell. CGP catabolic enzymes are present at significantly higher levels in vegetative cells than in heterocysts. Moreover, CGP could serve as a sink for fixed nitrogen in the heterocyst to avoid feedback inhibition from soluble products of nitrogen fixation [16, 17]. In *Anabaena* sp. PCC 7120 and *Anabaena variabilis*, mutational studies have shown that strains lacking CGP synthetic genes are little affected in diazotrophic growth under standard laboratory conditions [15, 18]. However, a growth defect was observed under high light conditions [15]. Moreover, diazotrophic growth is significantly decreased in strains that are unable to degrade CGP [16, 18].

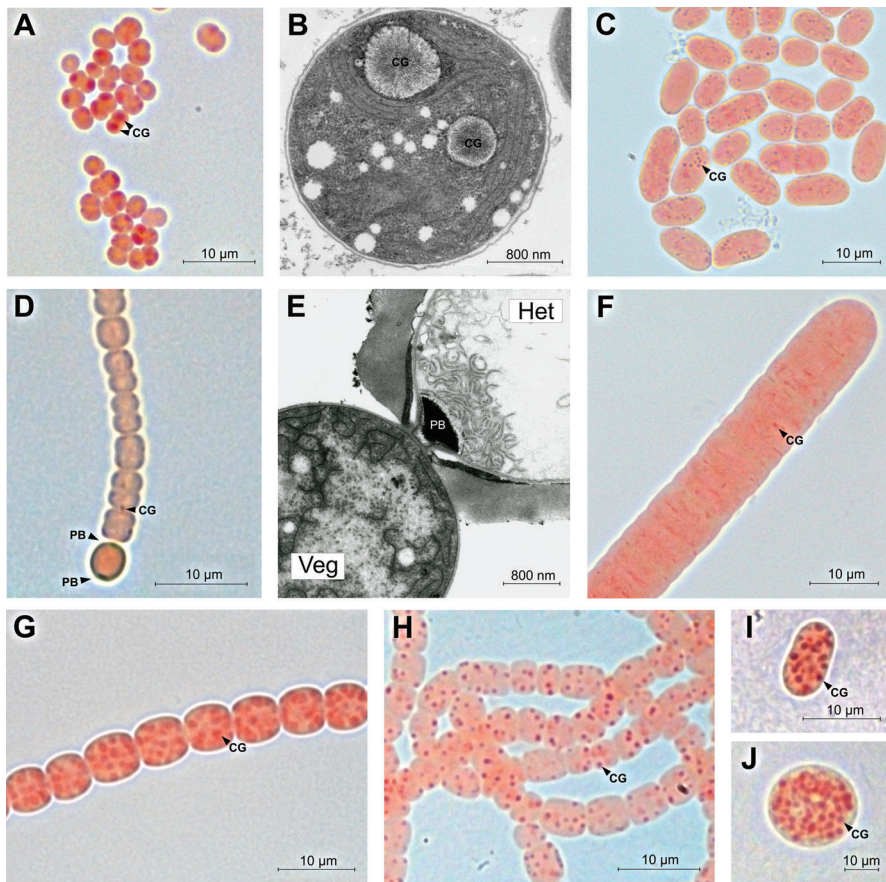


Figure 1. Light and electron microscopic pictures of CGP accumulating cyanobacteria. In light microscopic pictures, CGP was stained using the Sakaguchi reaction [10]. The intensity of the red color indicates the amount of arginine. Dark red to purple dots are CGP granules [CG]. (A) and (B) Phosphate starved *Synechocystis* sp. PCC 6803 in light and transmission electron microscopy, respectively. (C) *Cyanotheca* sp. PCC 7424 cultivated in presence of nitrate and continuous light. (D) Filament of diazotrophic growing *Anabaena* sp. PCC 7120 with terminal heterocyst containing polar bodies [PB]. (E) Transmission electron micrographs of a heterocyst and adjacent vegetative cell from *Anabaena* sp. PCC 7120, showing a GCP consisting polar body [PB]. (F) *Oscillatoria* sp. cultivated with nitrate supplementation, showing small CGP granules. (G) Phosphate starved *Anabaena variabilis* ATCC 29413 under nitrate supplemented growth. (H) *Nostoc punctiforme* ATCC 29133 under phosphate starvation and nitrate supplementation. (I) and (J) Mature akinetes of *Anabaena variabilis* ATCC 29413 and *Nostoc punctiforme* ATCC 29133, respectively.

Akinetes are resting spore-like cells of a subgroup of heterocyst-forming cyanobacteria for surviving long periods of unfavorable conditions. During akinete development, the cells transiently accumulate storage compounds, namely glycogen, lipid droplets and CGP [19, 20] (**Figure 1**). CGP granules also appear during germination of dormant akinetes [21]. *Anabaena variabilis* akinetes lacking CGP granules were also able to germinate. This behavior agrees with early observations that CGP is not the direct nitrogen source for protein biosynthesis and therefore not essential for akinete germination [21, 22].

CGP was formally thought to be unique in cyanobacteria. In 2002, Krehenbrink et al. and Ziegler et al. discovered through evaluation of obligate heterotrophic bacteria genomes that many heterotrophic bacteria possess CGP synthetase genes [23, 24]. Genes of CGP metabolism occur in a wide range of different phylogenetic taxa and not closely related to cyanobacteria [25].

3. CGP characteristics

In 1971, Robert Simon isolated CGP granules for the first time by using differential centrifugation. Along with this study, CGP has shown its special and unique solubility behavior [26]. CGP is insoluble at physiological ionic strength and at neutral pH, but soluble in solutions which are acidic, basic or highly ionic. In non-ionic detergents such as Triton X-100, CGP is insoluble; however, in ionic detergents like SDS, it is soluble [6]. Present-day CGP extraction methods are based on its solubility at low pH and insolubility at neutral pH [27].

The chemical structure of CGP was proposed in 1976 by Simon and Weathers [2]. According to this model, CGP has a polymer backbone consisting of α -linked aspartic acid residues. The α -amino group of arginine is linked via isopeptide bonds to the β -carboxylic group of every aspartyl moiety. Because every aspartate residue is linked to an arginine residue, CGP contains equimolar amounts of aspartate and arginine [2]. This structure has been confirmed via enzymatic degradation studies. CGP-degrading enzymes (see below) release β -Asp-Arg dipeptides [28]. CD spectroscopy data suggest that the acid-soluble and neutral insoluble forms of CGP have similar conformations. Both forms contain substantial fractions of β -pleated sheet structure [29].

Cyanobacterial CGP has a molecular weight and polydispersity ranging from 25 to 100 kDa [26]. In contrast, the native CGP producer *Acinetobacter* sp. ADP1 synthesizes CGP with a lower molecular weight ranging from 21 to 28 kDa [30]. Recombinant bacteria or genetically engineered yeast harboring heterologous expression of cyanobacterial CGP synthesis genes also show a lower molecular weight of 25–45 kDa [27, 31]. Transgenic plant-produced CGP also shows a reduced polydispersity between 20 and 35 kDa [32]. A possible explanation would be that cyanophycin synthesis in the native cyanobacterial background involves additional factors contributing the polymer length. These additional factors should also be absent in *Acinetobacter* sp. ADP1.

Native CGP is exclusively composed of aspartate and arginine. By contrast, in CGP isolated from recombinant *E. coli* expressing cyanophycin synthetase (see below) from *Synechocystis* sp. PCC 6803, besides aspartate and arginine, lysine has been found [33]. The amount of incorporated lysine in CGP influences its solubility behavior. Recombinant CGP with a high lysine amount (higher than 31 mol%) is soluble at neutral pH [34].

4. CGP metabolism

4.1. Cyanophycin synthetase

CGP is non-ribosomally synthesized from aspartate and arginine by cyanophycin synthetase (CphA1) (**Figure 2**). In 1976, CphA1 was enriched and characterized for the first time by

Simion [35]. The enzyme incorporates aspartate and arginine in an elongation reaction, which requires ATP, KCl, MgCl₂ and a sulfhydryl reagent (β-mercaptoethanol or DTT). For its activity, CphA1 needs a so far unknown CGP primer, as a starting point of the elongation reaction [35]. By using synthetically primers, Berg et al. could show that a single building block of CGP (β-Asp-Arg) does not serve as an efficient primer for CphA1 elongation reaction in vitro. The primers need to consist of at least three Asp-Arg building blocks (β-Asp-Arg)₃ to detect CphA1 activity [36]. Other peptides, like cell wall or other cellular components, have been suggested to serve as an alternative priming substance for the CphA1 reaction [37]. This could be an explanation for the functionality of CGP synthesis in recombinant bacteria, without the ability to produce native CGP primers [38]. Interestingly, the CphA1 of *Thermosynechococcus elongatus* strain BP-1 shows primer-independent CGP synthesis [39].

Today, CphA1 enzymes from several bacteria, including cyanobacteria and heterotrophic bacteria, have been purified and characterized [33, 39–42]. The molecular mass of the characterized CphA1 enzymes ranges from 90 to 130 kDa. The active form of CphA1s from *Synechocystis* sp. PCC6308 and *Anabaena variabilis* PCC7937 is most likely homodimeric [33, 41], while the primer-independent CphA1 from *Thermosynechococcus elongatus* strain BP-1 forms a homotetramer [39]. The primary structure of cyanobacterial CphA1 can be divided into two regions [33]. The C-terminal region shows sequence similarities to peptide ligases that include murein ligases and folyl poly-γ-glutamate ligase. The N-terminal part of CphA1 shows sequence similarities with another superfamily of ATP-dependent ligases that include carboxylate-thiol

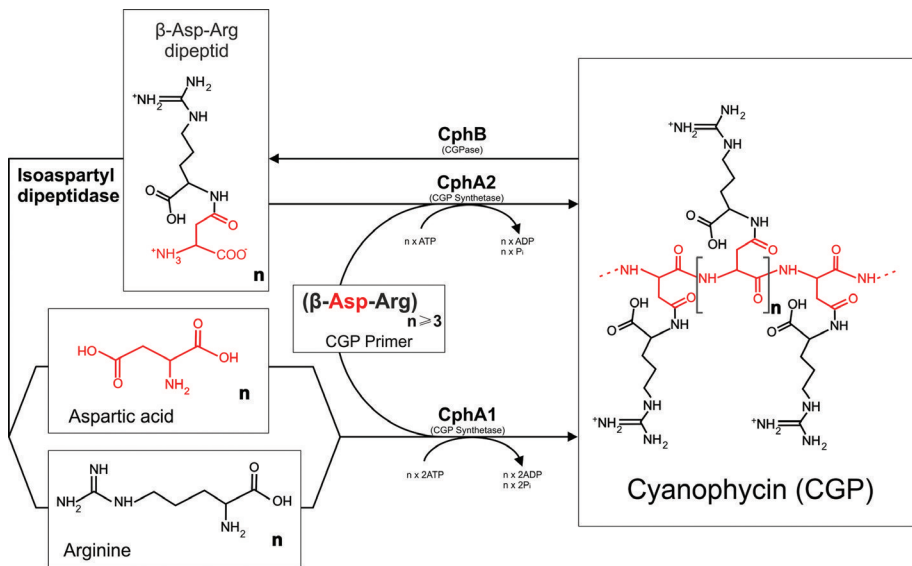


Figure 2. Schematic illustration of CGP metabolism in cyanobacteria. CGP is synthesized from aspartate and arginine by CGP synthetase (CphA1) in an ATP-depending elongation reaction using CGP primers, containing of at least three Asp-Arg building blocks. Intracellular CGP degradation is catalyzed by the CGPase (CphB). The β-Asp-Arg dipeptides resulting from cleavage of CGP are further hydrolyzed by isoaspartyl dipeptidase, releasing aspartate and arginine. In many nitrogen-fixing cyanobacteria, an additional CGP synthetase is present, termed CphA2. CphA2 can use β-aspartyl-arginine dipeptides to resynthesize CGP.

and carboxylate-amine ligase. Since the C- and N-terminal parts show similarity to different superfamilies of ATP-dependent ligases, two ATP-binding sites and two different active sites have been predicted [36]. In vitro experiments revealed that arginine is probably bound in the C-terminal and aspartate in the N-terminal active site [43].

The mechanism of CGP synthesis by CphA1 has been suggested by Berg et al. in 2000, by measuring the step-wise incorporation of amino acids to the C-terminus of the CGP primer. The putative CGP elongation cycle starts at the C-terminal end of the poly-aspartate backbone. First, the carboxylic acid group of the poly-aspartate backbone is activated by transfer of the γ -phosphoryl group of ATP. In the second step, one aspartate is bound at the C-terminus of the growing polymer by its amino group, forming a peptide bond. Subsequently, the intermediate (β -Asp-Arg)_n-Asp is transferred to the second active site of CphA1 and phosphorylated at the β -carboxyl group of the aspartate. Finally, the α -group of arginine is linked to the β -carboxyl group of aspartate, forming an isopeptide bond [36].

Various CphA1 enzymes have been characterized with respect to their substrate affinity and specificity. For CphA1 of *Synechocystis* sp. PCC 6308, apparent K_m values were determined to be 450 μ M for aspartate, 49 μ M for arginine, 200 μ M for ATP and 35 μ g/ml CGP as priming substance. The lower K_m of arginine compared to aspartate indicates a higher affinity of CphA1 towards arginine. During the in vitro reaction, CphA1 converts per mol incorporated amino acid 1.3 ± 0.1 mol ATP to ADP. The optimal reaction conditions of this enzyme were at pH 8.2 and 50°C [41].

CphA homologs are widely distributed in eubacteria. In silico analysis proposes 10 different groups of cyanophycin synthetases [25]. In cyanobacteria, cyanophycin synthetases of group I–III (CphA, CphA2 and CphA2') can be found.

Recently, the function of a cyanophycin synthetase of group II (CphA2) has been characterized. Most non-diazotrophic cyanobacteria use a single type of cyanophycin synthetase (CphA1). However, in many nitrogen-fixing cyanobacteria, an additional version of CphA is present, termed CphA2. In 2016, Klemke et al. resolved the function of CphA2 [44]. Compared to CphA1, CphA2 has a reduced size and just one ATP-binding site. CphA2 uses the product of CGP hydrolysis, β -aspartyl-arginine dipeptide as substrate to resynthesize cyanophycin, consuming one molecule of ATP per elongation. A mutant lacking CphA2 shows only a minor decrease in the overall CGP content. However, a CphA2-deficient mutant displays similar defects under diazotrophic and high light conditions than a CphA1 mutant [15, 44]. This observation suggests that the apparent “futile cycle” of CGP hydrolysis and immediate re-polymerization is probably of physiological significance in the context of nitrogen fixation [17].

4.2. Cyanophycinase

Since 1976, it is known that CGP is resistant against hydrolytic cleavage by several proteases or arginase [2, 45]. This resistance is probably due to the branched structure of CGP [38]. Therefore, the presence of a highly specified peptidase for CGP hydrolysis was suggested.

In 1999, Richter et al. reported a CGP hydrolyzing enzyme from the unicellular cyanobacterium *Synechocystis* sp. PCC 6803, called CphB [28] (Figure 2). During this study, CphB was purified

and studied in detail. CphB is a 29.4 kDa C-terminal exopeptidase, catalyzing the hydrolyzation of CGP to β -Asp-Arg dipeptides [28]. Based on sequence analysis and inhibitor sensitivity to serine protease inhibitors, CphB appears to be a serine-type exopeptidase related to dipeptidase E (PepE) [28]. According to its sequence, CphB contains a serine residue within a lipase box motive (Gly-Xaa-Ser-Xaa-Gly). The serine residue together with a glutamic acid residue and a histidine residue forms the catalytic triad, which is typical for serine-type peptidases [28]. In 2009, the crystal structure has been solved at a resolution of 1.5 Å, showing that CphB forms a dimer. Site-directed mutagenesis confirms that CphB is a serine-type peptidase, consisting of a conserved pocket with the catalytic Ser at position 132 [46]. Structure modeling indicates that the cleavage specificity occurs due to an extended conformation in the active site pocket. The unique conformation of the active site pocket requires β -linked aspartyl peptides for binding and catalysis, preventing CphB from non-specific cleavage of other polypeptides next to CGP [46].

In addition to CphB, which catalyzes the intracellular cleavage of CGP, other versions of cyanophycinase exist, catalyzing the extracellular hydrolysis of CGP. In 2002, Obst et al. isolated several Gram-negative bacteria from different habitats, which were able to utilize CGP as a source of carbon and energy [47, 48]. One isolate was affiliated as *Pseudomonas anguilliseptica* strain BI. In the supernatant of a *Pseudomonas anguilliseptica* culture, a cyanophycinase was found and purified, called CphE [47]. CphE exhibits a high specificity for CGP; however, proteins were not or only marginally hydrolyzed. Degradation products of CphE are β -Asp-Arg dipeptides. Inhibitor sensitivity studies indicated that the catalytic mechanism of CphE is related to serine-type proteases. CphE from *Pseudomonas anguilliseptica* strain BI exhibits an amino acid sequence identity 27–28% to intracellular CphB enzymes of cyanobacteria [47]. Today, extracellular CGPases has been found in a high variety of bacteria including Gram-positive, Gram-negative, aerobic and anaerobic strains. This indicates that the extracellular cleavage and utilization of CGP as carbon, nitrogen and energy source is a common principle in nature [47–53].

In 2007, in silico analysis showed that CphB homologs are widely distributed in eubacteria, proposing eight different groups including intracellular and extracellular CGPases. CGPases from cyanobacteria belong to group I, II and partially group III (CphB₁₋₃). Groups IV–VIII, including CphE, are present in a large variety of non-photosynthetic bacteria [25].

4.3. Aspartyl-arginine dipeptidase

The last step in catabolism of CGP is the cleavage of β -Asp-Arg dipeptides to monomeric amino acids, arginine and aspartate (**Figure 2**). In 1999, Richter et al. found β -Asp-Arg dipeptides hydrolyzing activity in extracts of *Synechocystis* sp. PCC 6803 [28]. In *Synechocystis* sp. PCC 6803, the ORF sll0422 as well as ORF all3922 from *Anabaena* sp. PCC 7120 is annotated as “plant-type asparaginase,” because of sequence similarities to the first cloned asparaginase from plants [54]. During characterization of plant-type asparaginase in general, including Sll0422 and All3922, Hejazi et al. were able to show that these enzymes are able to hydrolyze a wide range of isoaspartyl dipeptides [55]. Isoaspartyl peptides arise from two biological pathways: First, proteolytic degradation of modified proteins containing isoaspartyl residues and second, as primary degradation product of CGP cleavage from CGPases. Thus, the plant-type

asparaginases, SlI0422 and All3922, have not only a function in asparagine catabolism but also in the final step of CGP and protein degradation [55].

The mature isoaspartyl dipeptidases of *Synechocystis* sp. PCC 6803 and *Anabaena* sp. PCC 7120 consist of two protein subunits that are generated by autocleavage of the primary translation product between Gly-172 and Thr-173 (numbering according to *Synechocystis* sp. PCC 6803) within the conserved consensus sequence GT(I/V)G [55]. The native molecular weight of approximately 70kD of this enzyme suggests that it has a subunit structure of $\alpha_2\beta_2$ (α derived from the N-terminal part and β from the C-terminal part of the precursor) [55].

In *Anabaena* sp. PCC 7120, all genes involved in CGP metabolism as well as the isoaspartyl dipeptidases All3922 are expressed in vegetative cells and heterocysts but in different expression levels. Both, CGP synthetases and CGPases are much higher expressed in heterocysts than in vegetative cells [56]. However, asparaginase All3922 is present in significantly lower levels in heterocysts than in vegetative cells [57]. A deletion of All3922 in *Anabaena* sp. PCC 7120 causes an increased accumulation of CGP and β -Asp-Arg dipeptides. Furthermore, a deletion mutant shows an impaired diazotrophic growth similar to the phenotype known from CphB deletion mutants in *Anabaena* sp. PCC 7120 [18, 57]. This observation implies that the first step of CGP catabolism, the cleavage catalyzed by CphB, takes place in the heterocyst. The released β -Asp-Arg dipeptides are transported to the adjacent vegetative cells. Isoaspartyl dipeptidase All3922, present in the vegetative cells, cleaves the β -Asp-Arg dipeptides and releases monomeric aspartate and arginine [57]. When CGP synthesis is not possible, due to a deletion of CphA, arginine and aspartate might be transferred directly from heterocysts. This explains the minor effects on diazotrophic growth in a CphA deletion mutant [15]. These results identified β -Asp-Arg dipeptides as nitrogen vehicle in diazotrophic heterocyst forming cyanobacteria, next to glutamine and arginine alone or with aspartate [57–59]. A benefit of β -Asp-Arg dipeptides as nitrogen transport substance is avoiding the release of free arginine and aspartate in the heterocyst. This indicates that CGP metabolism has evolved in multicellular heterocyst-forming cyanobacteria to increase the efficiency of nitrogen fixation [57].

5. CGP regulation

5.1. Genetic organization of CphA and CphB

Usually, genes involved in CGP metabolism are clustered. The organization of these clusters can be different, depending on the respective organism [25]. In *Synechocystis* sp. PCC 6803, *cphA* and *cphB* are adjacent; however, they are expressed independently [60]. A hypothetical protein named slr2003 is located downstream of *cphA* and is transcribed in a polycistronic unit with *cphA* [60]. However, the function of Slr2003 is unknown. In the gene of CphB (slr2001), a small antisense RNA was detected (transcriptional unit 1486) [60].

In *Anabaena* sp. PCC 7120, two clusters containing CphA and CphB were identified [18]. In the *cph1* cluster, *cphB1* and *cphA1* were expressed under ammonia and nitrate supplemented growth, but the expression of both genes was higher in the absence of combined nitrogen in

heterocysts and vegetative cells. In the *cph1* operon, *cphB1* and *cphA1* were cotranscribed. In addition, *cphA1* can be expressed from independent promoters, of which one is constitutive and the other regulated by the global nitrogen control transcriptional factor NtcA [18].

In cluster *cph2*, the *cphB2* and *cphA2* genes were found in opposite orientation and both genes were expressed monocistronically. The genes were expressed under conditions of ammonia, nitrate or N₂ supplementation, but the expression was higher in the absence of ammonia. Generally, the expression of the *cph2* is lower compared to *cph1* [18].

In addition to these two gene clusters, a third set of ORFs containing putative *cphA* and *cphB* genes was found in *Nostoc punctiforme* PCC 73102 and *Anabaena variabilis* ATCC 29413 [25].

5.2. Dependence of CGP metabolism on arginine biosynthesis

Generally, CGP accumulation is triggered by cell growth arresting stress conditions, such as entry into stationary phase, light or temperature stress, limitation of macronutrients (with the exception of nitrogen starvation) or inhibition of translation by adding antibiotics like chloramphenicol [9, 10, 61]. All of these CGP triggering conditions result in a reduced or arrested growth. In exponential growth phase the amino acids arginine and aspartate are mostly used for protein biosynthesis with the consequence of a low intracellular level of free amino acids. Under growth-limiting conditions, protein biosynthesis is slowed down, which yields an excess of monomeric amino acids in the cytoplasm, triggering the CGP biosynthesis [10].

CGP accumulation also requires an excess of nitrogen. For the filamentous cyanobacterium *Calothrix* sp. strain PCC 7601, it was shown that CGP accumulation occurs preferably in the presence of ammonia [62]. The addition of amino acids to the media further increased CGP formation [63]. During process optimization studies for heterotrophic CGP production in the strain *Acinetobacter calcoaceticus* ADP1, it was shown that addition of arginine to the medium as sole carbon source increased CGP accumulation drastically. When, in *A. calcoaceticus* strain ADP1, CGP synthesis is induced by phosphate starvation, it accounts to 3.5% (w/w) of the cell dry matter (CDM) with ammonia as nitrogen source. Additional supply of the medium with arginine increases the CGP amount to 41.4% (w/w) (CDM). Notably, a combined supply of arginine and aspartate has a much lower stimulating effect to CGP accumulation than arginine alone [30].

A potential link between regulation of arginine biosynthesis and GCP metabolism was suggested in many previous studies. In a transposon mutagenesis study in the filamentous cyanobacterium *Nostoc ellipsosporum*, an arginine biosynthesis gene, *argL*, was interrupted by a transposon. This mutation partially impairs arginine biosynthesis but does not strictly result in L-arginine auxotrophy. Without arginine supplementation, heterocysts failed to fix nitrogen, akinetes were unable to germinate and CGP granules did not appear. However, when both nitrate and arginine are present in the media, the impaired arginine biosynthesis is bypassed. Under this condition, the mutant could form CGP and was able to differentiate functional akinetes, which contained CGP granules [64].

In metabolic engineering studies of the CGP production strain *Acinetobacter calcoaceticus* ADP1, several genes related to the arginine biosyntheses or its regulation were modified to yield higher amounts of arginine. As a consequence, significant higher CGP production was observed [65].

Bacteria produce arginine from glutamate in eight steps. The first five steps involving N-acetylated intermediates lead to ornithine. The conversion of ornithine to arginine requires three additional steps [66]. The second enzyme of ornithine biosynthesis is the N-acetylglutamate kinase (NAGK), which catalyzes the phosphorylation of N-acetyl glutamate to N-acetylglutamyl-phosphate. NAGK catalyzes the controlling step in arginine biosynthesis [67]. NAGK activity is subjected to allosteric feedback inhibition by arginine and is, moreover, positively controlled by the P_{II} signal transduction protein (see below) [67, 68]. Maheswaran et al. showed that arginine production and the following CGP accumulation depend on the catalytic activation of NAGK by the signal transduction protein P_{II} [69]. In a P_{II} -deficient mutant of *Synechocystis* sp. PCC 6803, NAGK remained in a low activity state, which caused impaired CGP accumulation [69].

The nitrogen-regulated response regulator NrrA also has influence on arginine and CGP biosynthesis. An NrrA-deficient mutant in *Synechocystis* sp. PCC 6803 shows reduced intracellular arginine levels and, consequently, reduced CGP amount [70].

All these results and observations point towards arginine as main bottleneck of CGP biosynthesis, while aspartate plays a minor role. CGP accumulation occurs as a result of arginine enrichment in the cytoplasm. Reasons for increased arginine content in the cell are lowered protein biosynthesis as a result of various growth limiting conditions. Furthermore, an excess of nitrogen and energy sensed by P_{II} leads to NAGK activation and thereby increased arginine biosynthesis.

5.3. P_{II} regulation of arginine metabolism

The P_{II} signal transduction proteins are widely distributed in prokaryotes and chloroplasts, where they play a coordinating role in the regulation of nitrogen assimilatory processes [71–73]. For this purpose, P_{II} senses the energy status of the cell by binding ATP or ADP in a competitive way [74]. Binding of ATP and synergistic binding of 2-oxoglutarate (2-OG) allows P_{II} to sense the current carbon/nitrogen status of the cell [75]. 2-OG is the carbon skeleton for the GS/GOGAT reactions and thereby links the carbon and nitrogen metabolism in all domains of life [76, 77]. The pool size of 2-OG reacts quickly to changes in nitrogen availability, wherefore 2-OG is an indicator of the carbon/nitrogen balance [78, 79]. Depending on the nitrogen supply, P_{II} may be phosphorylated at the apex of the T-loop at position Ser49 [80, 81]. Binding of the effector molecules ATP, ADP and 2-OG as well as phosphorylation leads to conformational rearrangements of the large surface-exposed T-loop, P_{II} 's major protein-interaction structure [82]. These conformational states direct the interaction of P_{II} with its various interaction partners and thereby regulate the cellular C/N balance [83].

In cyanobacteria, P_{II} regulates the global nitrogen control transcriptional factor NtcA, through binding to the NtcA co-activator PipX [84]. In common with other bacteria, cyanobacterial P_{II} proteins can interact with the biotin carboxyl carrier protein (BCCP) of acetyl-CoA carboxylase (ACC) and thereby control the acetyl-CoA levels [85]. Furthermore, P_{II} controls arginine biosynthesis via regulation of NAGK [68, 69, 86].

P_{II} proteins form a cylindrical-shaped homotrimer with 12–13 kDa per subunits. The T-loop, a large and surface-exposed loop, protrudes from each subunit. The effector binding sites are positioned in the three inter-subunit clefts [87, 88]. If sufficient energy and nitrogen are available,

indicated by a high ATP and low 2-OG level, non-phosphorylated P_{II} forms an activating complex with NAGK.

The crystal structure of the P_{II} -NAGK complex from *Synechococcus elongatus* strain PCC 7942 revealed two P_{II} trimers sandwiching a NAGK homohexamer (trimer of dimers) [88]. Each P_{II} subunit contacts one NAGK subunit [88]. Two parts of P_{II} are involved in interaction with NAGK. The first structure, called B-loop, is located on the P_{II} body and interacts with the C-domain of NAGK subunit, involving residue Glu85. The interaction of the B-loop is the first step in complex formation. Second, the T-loop must adopt a bent conformation and insert into the interdomain cleft of NAGK [89]. This enhances the catalytic efficiency of NAGK, with the V_{max} increasing fourfold and the K_m for N-acetylglutamate decreasing by a factor of 10 [86]. Furthermore, feedback inhibition of NAGK by arginine is strongly decreased in the presence of P_{II} [86].

During P_{II} mutagenesis, a P_{II} variant was identified that binds constitutively NAGK in vitro. This P_{II} variant exhibits a single amino acid replacement, Ile86 to Asn86, hereafter referred as $P_{II}(I86N)$ [89]. The crystal structure of $P_{II}(I86N)$ has been solved, showing an almost identical backbone than wild-type P_{II} . However, the T-loop adopts a compact conformation, which is a structural mimic of P_{II} in the NAGK complex [89, 90]. Addition of 2-OG in the presence of ATP normally leads to a dissociation of the P_{II} -NAGK complex, however $P_{II}(I86N)$ no longer responds to 2-OG [90].

The $P_{II}(I86N)$ variant enables a novel approach of metabolic pathway engineering by using custom-tailored P_{II} signaling proteins. By replacing the wild-type P_{II} with a P_{II} carrying the mutation for I86N in *Synechocystis* sp. PCC 6803, it was possible to engineer the first cyanobacterial CGP overproducer strain. Strain BW86, containing the $P_{II}(I86N)$ version, shows an increase of NAGK activity, which causes a more than 10-fold higher arginine content than the wild-type [10]. Under balanced growth conditions with nitrate as nitrogen source, strain BW86 accumulates up to $15.6 \pm 5.4\%$ CGP relative to the CDM, i.e., on average almost sixfold more than the wild type. Appropriate starvation conditions can further increase the CGP content of strain BW86 up to $47.4 \pm 2.3\%$ per CDM under phosphate starvation and $57.3 \pm 11.1\%$ per CDM under potassium starvation, without addition of arginine to the medium [10]. Furthermore, the CGP, which is produced by strain BW86, shows a high polydispersity ranging from 25 to 100 kDa, similar to the polydispersity of cyanobacterial wild-type CGP, which contrasts CGP from recombinant producer strains using heterologous expression systems with heterotrophic bacteria, yeasts or plants [10]. CGP isolated from those strains have a size ranging of 25–45 kDa [27, 31, 32].

6. Industrial applications

Industrial applications for CGP have previously mainly focused on chemical derivatives. CGP can be converted via hydrolytic β -cleavage to poly(α -L-aspartic acid) (PAA) and free arginine. PAA is biodegradable and has a high number of negatively charged carboxylic groups, making PAA a possible substituent for polyacrylates [48, 50, 91]. PAA can be employed as anti-scalant or dispersing ingredient in many fields of applications, including washing detergents or suntan lotions. Furthermore, PAA has potential application areas as an additive in paper, paint, building or oil industry [48, 50].

CGP can also serve as a source for dipeptides and amino acids in food, feed and pharmaceutical industry. The amino acids arginine (semi-essential), aspartate (non-essential) and lysine (essential) derived from CGP have a broad spectrum of nutritional or therapeutic applications. Large-scale production of these amino acids, as mixtures or dipeptides, is established in industry, with various commercial products already available on the market (reviewed by Sallam and Steinbuechel [92]).

Potential applications of non-modified CGP have been discussed but remain so far largely unexplored. This can partially be explained by the lack of research being conducted on the material properties of CGP. Recently in 2017, the first study regarding CGP material properties has been published. In this study, Khlystov et al. focused on the structural, thermal, mechanical and solution properties of CGP produced by recombinant *E. coli*, giving new insights in the nature of this polymer as bulk chemical [91]. They describe CGP as an amorphous, glassy polyzwitterion with high thermostability. The dry material is stiff and brittle. According to these properties, CGP could be used to synthesize zwitterionomeric copolymers or as reinforcing fillers [91].

7. Biotechnological production

Previous ventures to produce CGP in high amounts were mainly focused on heterotrophic bacteria, yeasts and plants as production host. These recombinant production hosts heterologously express CGP synthetase genes, mostly from cyanobacteria. In this way, heterotrophic bacteria, which are established in biotechnological industry including *E. coli*, *Corynebacterium glutamicum*, *Cupriavidus necator* (formally known as *Ralstonia eutropha*) and *Pseudomonas putida*, were used for heterologous production of CGP [93].

Strain *E. coli* DH1, containing *cphA* from *Synechocystis* sp. PCC6803, was used for large-scale production of CGP in a culture volume of up to 500 liter, allowing the isolation of CGP in a kilogram scale. During process optimization, the highest observed CGP content was 24% (w/w) per CDM. However, the synthesis of CGP was strongly dependent on the presence of complex components in the medium (terrific broth complex medium). In mineral salt medium, CGP accumulation only occurs in the presence of casamino acids [27]. An engineered version of *CphA* from *Nostoc ellipsosporum*, transformed in *E. coli*, shows a further increase in CGP production, up to 34.5% (w/w) of CDM. However, this production strain also requires expensive complex growth media to yield such a high amount of CGP [94].

Cupriavidus necator and *Pseudomonas putida* are known as model organisms for the industrial scale production of polyhydroxyalkanoates (PHA). Therefore, they have been considered as candidates for large scale CGP production [93, 95]. Metabolic engineering and process optimization studies of *Cupriavidus necator* and *Pseudomonas putida* harboring *cphA* from *Synechocystis* sp. PCC 6803 or *Anabaena* sp. PCC 7120 were performed. In these organisms, the accumulation of CGP is mainly depending on the origin of the *cphA* gene, the accumulation of other storage compounds like PHA as well as the addition of precursor components like arginine to the medium [96]. PHA-deficient mutants of *Cupriavidus necator* and *Pseudomonas putida* accumulate in general more CGP compared to the PHA containing strains [96]. During genetic modification of *cphA* expression in *Cupriavidus necator*, CGP accumulation turned out to be

strongly affected by the expression system. A stabilized multi-copy *cphA* expression system, using the KDPG-aldolase gene (*eda*)-dependent addition system, allows cultivation without antibiotic selection. The multi-copy *cphA* expression results in a CGP yield between 26.9% and 40.0% (w/w) of CDM. The maximum amount of 40.0% (w/w) of CDM was observed in a 30- and 500-l pilot plant. In the absence of the amino acids arginine and aspartic acid in the medium, the CGP amount was still between 26.9% and 27.7% (w/w) of CDM [97].

The industrially established host *Saccharomyces cerevisiae* has also been used for CGP production, by expression of *cphA* from *Synechocystis* sp. PCC 6803. *S. cerevisiae* harboring *cphA* accumulated up to 6.9% (w/w) of CDM. Two CGP species were observed in this strain: water-soluble and the typical water-insoluble CGP. Furthermore, the isolated polymer from this transgenic yeast contained 2 mol% lysine, which can be increased up to 10 mol% when cultivation occurs with lysine in the medium [31]. During metabolic engineering studies, several arginine biosynthesis mutants have been analyzed concerning their CGP accumulation abilities. Surprisingly, strains with defects in arginine degradation accumulated only 4% CGP (w/w) of CDM; however, arginine auxotrophic strains were able to accumulate up to 15.3%. Depending on the cultivation conditions, between 30 and 90% of the extracted CGP was soluble at neutral pH. In addition to arginine, aspartate and lysine, further amino acids, such as citrulline and ornithine, have been detected in isolated CGP from different arginine biosynthesis mutants [98]. Furthermore, it was also possible to produce CGP and CGP derivatives in *Pseudomonas putida* and the yeast *Pichia pastoris* [99, 100].

CGP and CGP derivatives are important sources for β -dipeptides for several applications. A large-scale method was developed to convert CGP into its constituting β -dipeptides by using CphE from *Pseudomonas alcaligenes*. This allows the large-scale production of customized β -dipeptides, depending on the composition of the CGP derivatives [92, 101].

Production of CGP has also been attempted in several transgenic plants. Here, ectopic expression of the primer-independent CphA from *Thermosynechococcus elongatus* BP-1 leads to an accumulation of CGP up to 6.8% (w/w) in tobacco leaves and to 7.5% (w/w) of CDM in potato tubers [102, 103]. CGP production and extraction in plants can be coupled with the production of other plant products like starch [103]. The peculiarities and challenges of plant-produced CGP have been reviewed by Nausch et al. [32].

Compared to bacteria that are used so far in biotechnological industry, cyanobacteria are unique as they use sunlight and CO₂ as energy and carbon source. Cyanobacteria have been identified as rich source of various biologically active compounds, biofertilizers, bioplastics, energy, food and feed [104]. Obviously, the importance of environmentally friendly production processes increases more and more. Hence, Cyanobacteria are expected to play a major role in future industry. *Synechocystis* sp. PCC 6803 strain BW86 is the first reported bulk chemical producing cyanobacterial strain in the literature. CGP production in *Synechocystis* BW86 does not require organic carbon or CGP precursor substances. Growth limiting conditions like phosphate and potassium starvation can further increase the CGP production up to $47.4 \pm 2.3\%$ and $57.3 \pm 11.1\%$ per CDM, respectively. The studies of Trautmann et al. showed that strain BW86 can be cultivated in flat plate photobioreactors (Midiplate reactor system [105]). During this optimization study, the optimal light intensity as well as the phosphate concentration was determined to maximize CGP synthesis. Under optimal production conditions, highest amount of CGP was around 40% of CDM with a total yield of 340 mg CGP per liter in 9 days [106].

The main bottleneck of CGP production in Cyanobacteria is the relatively slow growth rate, which is much lower than in biotechnologically established bacteria. Conventional cultivation methods of cyanobacteria reach a biomass of roughly 1 g dry mass per liter [107]. To overcome this limitation, a new cultivation method was developed, using a two-tier vessel with membrane-mediated CO₂ supply. By using this cultivation setup, it was possible to enable rapid growth of *Synechocystis* sp. PCC 6803 and *Synechococcus* sp. PCC 7002 up to 30 g CDM per liter [108]. *Synechocystis* sp. PCC 6803 strain BW86 was also used in this high-density cultivation setup. During this study, CGP amounts up to 1 g per liter were reached in 96 h. This is approximately four times higher compared to the maximum CGP yield observed during conventional cultivation after 12 days [106, 109].

In comparison, the recombinant *E. coli* strain DH1 harboring *cphA* from *Synechocystis* sp. PCC 6803 produces between 6.7 and 8.3 g CDM per liter culture in 16 h. CGP amounts during this fed-batch fermentations were between 21 and 24% of the CDM [27], resulting in a CGP production rate of 87.9 to 124.5 mg/l and hour. Although this exceeds the production rate in *Synechocystis* sp. PCC 6803 strain BW86 by a factor of 10, the recombinant *E. coli* requires terrific broth complex medium, while *Synechocystis* sp. PCC 6803 strain BW86 is cultivated in simple mineral medium and additionally sequesters hazardous greenhouse gas CO₂. Considering these super ordinate factors, production of biopolymers with cyanobacteria may in fact become an alternative to heterotrophic bacteria.

8. Conclusions

CGP is well researched and its occurrence in cyanobacteria is known for more than 100 years. However, many questions are still open. Most obviously, the cell biology of the CGP granules remains largely unknown. In the last decades, research on CGP mainly focused on biotechnological purposes, like strain or process optimization. Most work has been carried out with short-chain CGP from recombinant producer strains; however the biophysical properties of the long-chain native CGP remain largely unexplored. So far, heterotrophic bacteria were mainly used to produce industrial biocompounds including CGP. In this chapter, we discussed the possibility of a cyanobacterial CGP production strain. The main disadvantages of cyanobacteria, their slower growth and the low abundance of product can be compensated using genetic engineering together with appropriate production processes. Future industry has to cope with the manifold challenges to counteract environmental pollution and climate change. The use of cyanobacteria in CGP production and, more generally, in biotechnological applications for bioproduct synthesis provides an environmentally friendly alternative to conventional biotechnological approaches.

Acknowledgements

This work was supported by grants from the DFG (Fo195/9), the research training group GRK 1708 and the Baden-Württemberg foundation grant 7533-10-5-92B. We thank Iris Maldener for provision of the electron micrographs of *Anabaena* sp. PCC 7120 and *Synechocystis* sp. PCC 6803. We would also like to give thanks to Rebeca Pérez for provision of light micrographs of *Anabaena variabilis* ATCC 29413 and *Nostoc punctiforme* ATCC 29133.

Conflict of interest

The authors declare that they have no competing interests.

Author details

Björn Watzer and Karl Forchhammer*

*Address all correspondence to: karl.forchhammer@uni-tuebingen.de

Interfaculty Institute of Microbiology and Infection Medicine Tübingen, Eberhard Karls Universität Tübingen, Tübingen, Germany

References

- [1] Feng S, ZhiNan X. Microbial production of natural poly amino acid. *Science in China Series B*. 2007;**50**(3):291-303
- [2] Simon RD, Weathers P. Determination of the structure of the novel polypeptide containing aspartic acid and arginine which is found in cyanobacteria. *Biochimica et Biophysica Acta (BBA)—Protein Structure*. 1976;**420**(1):165-176
- [3] Borzi A. Le comunicazioni intracellulari delle Nostochinee. *Malpighia*. 1887;**1**:28-74
- [4] Wood P, Peat A, Whitton BA. Influence of phosphorus status on fine-structure of the cyanobacterium (blue-green-alga) *calothrix-parietina*. *Cytobios*. 1986;**47**(189):89-99
- [5] Lang NJ. The fine structure of blue-green algae. *Annual Review of Microbiology*. 1968;**22**:15-46
- [6] Lang NJ, Simon RD, Wolk CP. Correspondence of cyanophycin granules with structured granules in *Anabaena-Cylindrica*. *Archiv fur Mikrobiologie*. 1972;**83**(4):313
- [7] Allen MM, Weathers PJ. Structure and composition of cyanophycin granules in the cyanobacterium *Aphanocapsa 6308*. *Journal of Bacteriology*. 1980;**141**(2):959-962
- [8] Weathers PJ, Chee HL, Allen MM. Arginine catabolism in *Aphanocapsa 6308*. *Archives of Microbiology*. 1978;**118**(1):1-6
- [9] Allen MM, Hutchison F, Weathers PJ. Cyanophycin granule polypeptide formation and degradation in the Cyanobacterium *Aphanocapsa 6308*. *Journal of Bacteriology*. 1980;**141**(2):687-693
- [10] Watzer B, Engelbrecht A, Hauf W, Stahl M, Maldener I, Forchhammer K. Metabolic pathway engineering using the central signal processor PII. *Microbial Cell Factories*. 2015;**14**:192
- [11] Allen MM, Hutchison F. Nitrogen limitation and recovery in the Cyanobacterium *Aphanocapsa-6308*. *Archives of Microbiology*. 1980;**128**(1):1-7

- [12] Klotz A, Georg J, Budinska L, Watanabe S, Reimann V, Januszewski W, et al. Awakening of a dormant cyanobacterium from nitrogen chlorosis reveals a genetically determined program. *Current Biology*. 2016;**26**(21):2862-2872
- [13] Sherman LA, Meunier P, Colon-Lopez MS. Diurnal rhythms in metabolism: A day in the life of a unicellular, diazotrophic cyanobacterium. *Photosynthesis Research*. 1998;**58**(1): 25-42
- [14] Finzi-Hart JA, Pett-Ridge J, Weber PK, Popa R, Fallon SJ, Gunderson T, et al. Fixation and fate of C and N in the cyanobacterium *Trichodesmium* using nanometer-scale secondary ion mass spectrometry. *Proceedings of the National Academy of Sciences of the United States of America*. 2009;**106**(24):9931
- [15] Ziegler K, Stephan DP, Pistorius EK, Ruppel HG, Lockau W. A mutant of the cyanobacterium *Anabaena variabilis* ATCC 29413 lacking cyanophycin synthetase: Growth properties and ultrastructural aspects. *FEMS Microbiology Letters*. 2001;**196**(1):13-18
- [16] Burnat M, Herrero A, Flores E. Compartmentalized cyanophycin metabolism in the diazotrophic filaments of a heterocyst forming cyanobacterium. *Proceedings of the National Academy of Sciences of the United States of America*. 2014;**111**(10):3823-3828
- [17] Forchhammer K, Watzer B. Closing a gap in cyanophycin metabolism. *Microbiology*. 2016;**162**:727-729
- [18] Picossi S, Valladares A, Flores E, Herrero A. Nitrogen-regulated genes for the metabolism of cyanophycin, a bacterial nitrogen reserve polymer—Expression and mutational analysis of two cyanophycin synthetase and cyanophycinase gene clusters in the heterocyst-forming cyanobacterium *Anabaena* sp. PCC 7120. *The Journal of Biological Chemistry*. 2004;**279**(12):11582-11592
- [19] Sukenik A, Maldener I, Delhaye T, Viner-Mozzini Y, Sela D, Bormans M. Carbon assimilation and accumulation of cyanophycin during the development of dormant cells (akinetes) in the cyanobacterium *Aphanizomenon ovalisporum*. *Frontiers in Microbiology*. 2015;**6**:1067
- [20] Perez R, Forchhammer K, Salerno G, Maldener I. Clear differences in metabolic and morphological adaptations of akinetes of two Nostocales living in different habitats. *Microbiology*. 2016;**162**:214-223
- [21] Perez R, Wormer L, Sass P, Maldener I. A highly asynchronous developmental program triggered during germination of dormant akinetes of the filamentous diazotrophic cyanobacteria. *FEMS Microbiology Ecology*. 2018;**94**(1)
- [22] Sutherland JM, Reaston J, Stewart WDP, Herdman M. Akinetes of the Cyanobacterium *Nostoc* Pcc 7524—Macromolecular and biochemical-changes during Synchronous germination. *Journal of General Microbiology*. 1985;**131**(Nov):2855-2863
- [23] Krehenbrink M, Oppermann-Sanio FB, Steinbuechel A. Evaluation of non-cyanobacterial genome sequences for occurrence of genes encoding proteins homologous to cyanophycin

- synthetase and cloning of an active cyanophycin synthetase from *Acinetobacter* sp. strain DSM 587. *Archives of Microbiology*. 2002;**177**(5):371-380
- [24] Ziegler K, Deutzmann R, Lockau W. Cyanophycin synthetase-like enzymes of non-cyanobacterial eubacteria: Characterization of the polymer produced by a recombinant synthetase of *Desulfitobacterium hafniense*. *Zeitschrift für Naturforschung. Section C*. 2002;**57**(5-6):522-529
- [25] Fuser G, Steinbuchel A. Analysis of genome sequences for genes of cyanophycin metabolism: Identifying putative cyanophycin metabolizing prokaryotes. *Macromolecular Bioscience*. 2007;**7**(3):278-296
- [26] Simon RD. Cyanophycin granules from the blue-green alga *Anabaena cylindrica*: A reserve material consisting of copolymers of aspartic acid and arginine. *Proceedings of the National Academy of Sciences of the United States of America*. 1971;**68**(2):265-267
- [27] Frey KM, Oppermann-Sanio FB, Schmidt H, Steinbuchel A. Technical-scale production of cyanophycin with recombinant strains of *Escherichia coli*. *Applied and Environmental Microbiology*. 2002;**68**(7):3377-3384
- [28] Richter R, Hejazi M, Kraft R, Ziegler K, Lockau W. Cyanophycinase, a peptidase degrading the cyanobacterial reserve material multi-L-arginyl-poly-L-aspartic acid (cyanophycin)—Molecular cloning of the gene of *Synechocystis* sp. PCC 6803, expression in *Escherichia coli*, and biochemical characterization of the purified enzyme. *European Journal of Biochemistry*. 1999;**263**(1):163-169
- [29] Simon RD, Lawry NH, McLendon GL. Structural characterization of the cyanophycin granule polypeptide of *Anabaena cylindrica* by circular dichroism and Raman spectroscopy. *Biochimica et Biophysica Acta*. 1980;**626**(2):277-281
- [30] Elbahloul Y, Krehenbrink M, Reichelt R, Steinbuchel A. Physiological conditions conducive to high cyanophycin content in biomass of *Acinetobacter calcoaceticus* strain ADP1. *Applied and Environmental Microbiology*. 2005;**71**(2):858-866
- [31] Steinle A, Oppermann-Sanio FB, Reichelt R, Steinbuchel A. Synthesis and accumulation of cyanophycin in transgenic strains of *Saccharomyces cerevisiae*. *Applied and Environmental Microbiology*. 2008;**74**(11):3410-3418
- [32] Nausch H, Huckauf J, Broer I. Peculiarities and impacts of expression of bacterial cyanophycin synthetases in plants. *Applied Microbiology and Biotechnology*. 2016;**100**(4):1559-1565
- [33] Ziegler K, Diener A, Herpin C, Richter R, Deutzmann R, Lockau W. Molecular characterization of cyanophycin synthetase, the enzyme catalyzing the biosynthesis of the cyanobacterial reserve material multi-L-arginyl-poly-L-aspartate (cyanophycin). *European Journal of Biochemistry*. 1998;**254**(1):154-159
- [34] Wiefel L, Steinbuchel A. Solubility behavior of cyanophycin depending on lysine content. *Applied and Environmental Microbiology*. 2014;**80**(3):1091-1096

- [35] Simon RD. The biosynthesis of multi-L-arginyl-poly(L-aspartic acid) in the filamentous cyanobacterium *Anabaena cylindrica*. *Biochimica et Biophysica Acta*. 1976;**422**(2):407-418
- [36] Berg H, Ziegler K, Piotukh K, Baier K, Lockau W, Volkmer-Engert R. Biosynthesis of the cyanobacterial reserve polymer multi-L-arginyl-poly-L-aspartic acid (cyanophycin)—Mechanism of the cyanophycin synthetase reaction studied with synthetic primers. *European Journal of Biochemistry*. 2000;**267**(17):5561-5570
- [37] Hai T, Oppermann-Sanio FB, Steinbuechel A. Molecular characterization of a thermostable cyanophycin synthetase from the thermophilic cyanobacterium *Synechococcus* sp strain MA19 and in vitro synthesis of cyanophycin and related polyamides. *Applied and Environmental Microbiology*. 2002;**68**(1):93-101
- [38] Shively JM. *Inclusions in Prokaryotes*. Berlin ; New York: Springer; 2006. xii, 349 p
- [39] Arai T, Kino K. A cyanophycin synthetase from *Thermosynechococcus elongatus* BP-1 catalyzes primer-independent cyanophycin synthesis. *Applied Microbiology and Biotechnology*. 2008;**81**(1):69-78
- [40] Hai T, Oppermann-Sanio FB, Steinbuechel A. Purification and characterization of cyanophycin and cyanophycin synthetase from the thermophilic *Synechococcus* sp. MA19. *FEMS Microbiology Letters*. 1999;**181**(2):229-236
- [41] Aboulmagd E, Sanio FBO, Steinbuechel A. Purification of *Synechocystis* sp strain PCC-6308 cyanophycin synthetase and its characterization with respect to substrate and primer specificity. *Applied and Environmental Microbiology*. 2001;**67**(5):2176-2182
- [42] Krehenbrink M, Steinbuechel A. Partial purification and characterization of a non-cyanobacterial cyanophycin synthetase from *Acinetobacter calcoaceticus* strain ADP1 with regard to substrate specificity, substrate affinity and binding to cyanophycin. *Microbiology*. 2004;**150**(Pt 8):2599-2608
- [43] Berg H. *Untersuchungen zu Funktion und Struktur der Cyanophycin-Synthetase von Anabaena variabilis ATCC 29413*. Germany: Dissertation Humboldt-Universität zu Berlin; 2003
- [44] Klemke F, Nurnberg DJ, Ziegler K, Beyer G, Kahmann U, Lockau W, et al. CphA2 is a novel type of cyanophycin synthetase in N-2-fixing cyanobacteria. *Microbiology*. 2016;**162**:526-536
- [45] Simon RD. Inclusion bodies in the cyanobacteria: Cyanophycin, polyphosphate, polyhedral bodies. In: Fay P, Van Baalen C, editors. *The Cyanobacteria*: Elsevier Science Publishers B.V.; 1987. p. 199-225
- [46] Law AM, Lai SW, Tavares J, Kimber MS. The structural basis of beta-peptide-specific cleavage by the serine protease cyanophycinase. *Journal of Molecular Biology*. 2009;**392**(2):393-404
- [47] Obst M, Oppermann-Sanio FB, Luftmann H, Steinbuechel A. Isolation of cyanophycin-degrading bacteria, cloning and characterization of an extracellular cyanophycinase gene (cphE) from *Pseudomonas anguilliseptica* strain BI. The cphE gene from *P. anguilliseptica* BI encodes a cyanophycinhydrolyzing enzyme. *Journal of Biological Chemistry*. 2002;**277**(28):25096-25105

- [48] Rehm B. *Microbial Production of Biopolymers and Polymer Precursors: Applications and Perspectives*. Wymondham: Caister Academic; 2009. viii, 293 p, 1 p. of plates p.
- [49] Obst M, Sallam A, Luftmann H, Steinbuchel A. Isolation and characterization of gram-positive cyanophycin-degrading bacteria—Kinetic studies on cyanophycin depolymerase activity in aerobic bacteria. *Biomacromolecules*. 2004;**5**(1):153-161
- [50] Obst M, Steinbuchel A. Microbial degradation of poly(amino acid)s. *Biomacromolecules*. 2004;**5**(4):1166-1176
- [51] Obst M, Krug A, Luftmann H, Steinbuchel A. Degradation of cyanophycin by *Sedimentibacter hongkongensis* strain KI and *Citrobacter amalonaticus* strain G isolated from an anaerobic bacterial consortium. *Applied and Environmental Microbiology*. 2005; **71**(7):3642-3652
- [52] Sallam A, Steinbuchel A. Anaerobic and aerobic degradation of cyanophycin by the denitrifying bacterium *Pseudomonas alcaligenes* strain DIP1 and role of three other coisolates in a mixed bacterial consortium. *Applied and Environmental Microbiology*. 2008;**74**(11):3434-3443
- [53] Sallam A, Steinbuchel A. Cyanophycin-degrading bacteria in digestive tracts of mammals, birds and fish and consequences for possible applications of cyanophycin and its dipeptides in nutrition and therapy. *Journal of Applied Microbiology*. 2009;**107**(2):474-484
- [54] Lough TJ, Reddington BD, Grant MR, Hill DF, Reynolds PHS, Farnden KJF. The isolation and characterization of a cDNA clone encoding L-asparaginase from developing seeds of Lupin (*Lupinus arboreus*). *Plant Molecular Biology*. 1992;**19**(3):391-399
- [55] Hejazi M, Piotukh K, Mattow J, Deutzmann R, Volkmer-Engert R, Lockau W. Isoaspartyl dipeptidase activity of plant-type asparaginases. *The Biochemical Journal*. 2002;**364**: 129-136
- [56] Gupta M, Carr NG. Enzyme-activities related to cyanophycin metabolism in heterocysts and vegetative cells of *Anabaena* Spp. *Journal of General Microbiology*. 1981;**125**(Jul):17-23
- [57] Burnat M, Herrero A, Flores E. Compartmentalized cyanophycin metabolism in the diazotrophic filaments of a heterocyst-forming cyanobacterium. *Proceedings of the National Academy of Sciences of the United States of America*. 2014;**111**(10):3823-3828
- [58] Wolk CP, Austin SM, Bortins J, Galonsky A. Autoradiographic localization of N-13 after fixation of N-13-labeled nitrogen gas by a heterocyst-forming blue-green-alga. *The Journal of Cell Biology*. 1974;**61**(2):440-453
- [59] Thomas J, Meeks JC, Wolk CP, Shaffer PW, Austin SM, Chien WS. Formation of glutamine from [ammonia-N-13], [dinitrogen-N-13], and [glutamate-C-14] by heterocysts isolated from *Anabaena cylindrica*. *Journal of Bacteriology*. 1977;**129**(3):1545-1555
- [60] Mitschke J, Georg J, Scholz I, Sharma CM, Dienst D, Bantscheff J, et al. An experimentally anchored map of transcriptional start sites in the model cyanobacterium *Synechocystis* sp PCC6803. *Proceedings of the National Academy of Sciences of the United States of America*. 2011;**108**(5):2124-2129

- [61] Simon RD. The effect of chloramphenicol on the production of cyanophycin granule polypeptide in the blue green alga *Anabaena cylindrica*. *Archiv für Mikrobiologie*. 1973; **92**(2):115-122
- [62] Liotenberg S, Campbell D, Rippka R, Houmard J, deMarsac NT. Effect of the nitrogen source on phycobiliprotein synthesis and cell reserves in a chromatically adapting filamentous cyanobacterium. *Microbiology*. 1996; **142**:611-622
- [63] Sarma TA, Khattar JIS. Accumulation of cyanophycin and glycogen during sporulation in the blue-green-alga *Anabaena torulosa*. *Biochemie und Physiologie der Pflanzen*. 1986; **181**(3):155-164
- [64] Leganes F, Fernandez-Pinas F, Wolk CP. A transposition-induced mutant of *Nostoc ellipsosporum* implicates an arginine-biosynthetic gene in the formation of cyanophycin granules and of functional heterocysts and akinetes. *Microbiology*. 1998; **144**:1799-1805
- [65] Elbahloul Y, Steinbuechel A. Engineering the genotype of *Acinetobacter* sp strain ADP1 to enhance biosynthesis of cyanophycin. *Applied and Environmental Microbiology*. 2006; **72**(2):1410-1419
- [66] Cunin R, Glansdorff N, Pierard A, Stalon V. Biosynthesis and metabolism of arginine in bacteria. *Microbiological Reviews*. 1986; **50**(3):314-352
- [67] Caldovic L, Tuchman M. N-acetylglutamate and its changing role through evolution. *The Biochemical Journal*. 2003; **372**:279-290
- [68] Heinrich A, Maheswaran M, Ruppert U, Forchhammer K. The *Synechococcus elongatus* P signal transduction protein controls arginine synthesis by complex formation with N-acetyl-L-glutamate kinase. *Molecular Microbiology*. 2004; **52**(5):1303-1314
- [69] Maheswaran M, Ziegler K, Lockau W, Hagemann M, Forchhammer K. P-II-regulated arginine synthesis controls accumulation of cyanophycin in *Synechocystis* sp strain PCC 6803. *Journal of Bacteriology*. 2006; **188**(7):2730-2734
- [70] Liu D, Yang C. The nitrogen-regulated response regulator *NrrA* controls cyanophycin synthesis and glycogen catabolism in the *Cyanobacterium synechocystis* sp PCC 6803. *The Journal of Biological Chemistry*. 2014; **289**(4):2055-2071
- [71] Sant'Anna F, Trentini D, Weber SD, Cecagno R, da Silva SC, Schrank I. The PII superfamily revised: A novel group and evolutionary insights. *Journal of Molecular Evolution*. 2009; **68**(4):322-336
- [72] Chellamuthu VR, Alva V, Forchhammer K. From cyanobacteria to plants: Conservation of PII functions during plastid evolution. *Planta*. 2013; **237**(2):451-462
- [73] Forchhammer K. P(II) signal transducers: Novel functional and structural insights. *Trends in Microbiology*. 2008; **16**(2):65-72
- [74] Zeth K, Fokina O, Forchhammer K. Structural basis and target-specific modulation of ADP sensing by the *Synechococcus elongatus* PII signaling protein. *The Journal of Biological Chemistry*. 2014; **289**(13):8960-8972

- [75] Fokina O, Chellamuthu VR, Forchhammer K, Zeth K. Mechanism of 2-oxoglutarate signaling by the *Synechococcus elongatus* P-II signal transduction protein. Proceedings of the National Academy of Sciences of the United States of America. 2010;**107**(46):19760-19765
- [76] Huergo LF, Dixon R. The emergence of 2-oxoglutarate as a master regulator metabolite. Microbiology and Molecular Biology Reviews. 2015;**79**(4):419-435
- [77] Luddecke J, Francois L, Spat P, Watzler B, Chilczuk T, Poschet G, et al. PII protein-derived FRET sensors for quantification and live-cell imaging of 2-oxoglutarate. Scientific Reports. 2017;**7**(1):1437
- [78] Yuan J, Doucette CD, Fowler WU, Feng XJ, Piazza M, Rabitz HA, et al. Metabolomics-driven quantitative analysis of ammonia assimilation in *E. coli*. Molecular Systems Biology. 2009;**5**:302
- [79] Yan DL, Lenz P, Hwa T. Overcoming fluctuation and leakage problems in the quantification of intracellular 2-oxoglutarate levels in *Escherichia coli*. Applied and Environmental Microbiology. 2011;**77**(19):6763-6771
- [80] Forchhammer K, Tandeau de Marsac N. Phosphorylation of the PII protein (glnB gene product) in the cyanobacterium *Synechococcus* sp. strain PCC 7942: Analysis of in vitro kinase activity. Journal of Bacteriology. 1995;**177**(20):5812-5817
- [81] Forchhammer K, Hedler A. Phosphoprotein PII from cyanobacteria—Analysis of functional conservation with the PII signal-transduction protein from *Escherichia coli*. European Journal of Biochemistry. 1997;**244**(3):869-875
- [82] Radchenko M, Merrick M. The role of effector molecules in signal transduction by PII proteins. Biochemical Society Transactions. 2011;**39**(1):189-194
- [83] Forchhammer K, Luddecke J. Sensory properties of the PII signalling protein family. The FEBS Journal. 2016;**283**(3):425-437
- [84] Espinosa J, Forchhammer K, Contreras A. Role of the *Synechococcus* PCC 7942 nitrogen regulator protein PipX in NtcA-controlled processes. Microbiology. 2007;**153**:711-718
- [85] Hauf W, Schmid K, Gerhardt EC, Huergo LF, Forchhammer K. Interaction of the nitrogen regulatory protein GlnB (PII) with biotin carboxyl carrier protein (BCCP) controls acetyl-CoA levels in the Cyanobacterium *synechocystis* sp. PCC 6803. Frontiers in Microbiology. 2016;**7**:1700
- [86] Maheswaran M, Urbanke C, Forchhammer K. Complex formation and catalytic activation by the P-II signaling protein of N-acetyl-L-glutamate kinase from *Synechococcus elongatus* strain PCC 7942. The Journal of Biological Chemistry. 2004;**279**(53):55202-55210
- [87] Luddecke J, Forchhammer K. From PII signaling to metabolite sensing: A novel 2-oxoglutarate sensor that details PII-NAGK complex formation. PLoS One. 2013;**8**(12):e83181
- [88] Llacer JL, Contreras A, Forchhammer K, Marco-Marin C, Gil-Ortiz F, Maldonado R, et al. The crystal structure of the complex of PII and acetylglutamate kinase reveals how

- PII controls the storage of nitrogen as arginine. Proceedings of the National Academy of Sciences of the United States of America. 2007;**104**(45):17644-17649
- [89] Fokina O, Chellamuthu VR, Zeth K, Forchhammer K. A novel signal transduction protein P(II) variant from *Synechococcus elongatus* PCC 7942 indicates a two-step process for NAGK-P(II) complex formation. Journal of Molecular Biology. 2010;**399**(3):410-421
- [90] Zeth K, Fokina O, Forchhammer K. An engineered PII protein variant that senses a novel ligand: Atomic resolution structure of the complex with citrate. Acta Crystallographica Section D. 2012;**68**(8):901
- [91] Khlystov NA, Chan WY, Kunjapur AM, Shi WC, Prather KU, Olsen BD. Material properties of the cyanobacterial reserve polymer multi-L-arginyl-poly-L-aspartate (cyanophycin). Polymer. 2017;**109**:238-245
- [92] Sallam A, Steinbuechel A. Dipeptides in nutrition and therapy: Cyanophycin-derived dipeptides as natural alternatives and their biotechnological production. Applied Microbiology and Biotechnology. 2010;**87**(3):815-828
- [93] Aboulmagd E, Voss I, Oppermann-Sanio FB, Steinbuechel A. Heterologous expression of cyanophycin synthetase and cyanophycin synthesis in the industrial relevant bacteria *Corynebacterium glutamicum* and *Ralstonia eutropha* and in *Pseudomonas putida*. Biomacromolecules. 2001;**2**(4):1338-1342
- [94] Hai T, Frey KM, Steinbuechel A. Engineered cyanophycin synthetase (CphA) from *Nostoc ellipsosporum* confers enhanced CphA activity and cyanophycin accumulation to *Escherichia coli*. Applied and Environmental Microbiology. 2006;**72**(12):7652-7660
- [95] Diniz SC, Voss I, Steinbuechel A. Optimization of cyanophycin production in recombinant strains of *Pseudomonas putida* and *Ralstonia eutropha* employing elementary mode analysis and statistical experimental design. Biotechnology and Bioengineering. 2006;**93**(4):698-717
- [96] Voss I, Diniz SC, Aboulmagd E, Steinbuechel A. Identification of the *Anabaena* sp strain PCC7120 cyanophycin synthetase as suitable enzyme for production of cyanophycin in gram-negative bacteria like *Pseudomonas putida* and *Ralstonia eutropha*. Biomacromolecules. 2004;**5**(4):1588-1595
- [97] Voss I, Steinbuechel A. Application of a KDPG-aldolase gene-dependent addiction system for enhanced production of cyanophycin in *Ralstonia eutropha* strain H16. Metabolic Engineering. 2006;**8**(1):66-78
- [98] Steinle A, Bergander K, Steinbuechel A. Metabolic engineering of *Saccharomyces cerevisiae* for production of novel Cyanophycins with an extended range of constituent amino acids. Applied and Environmental Microbiology. 2009;**75**(11):3437-3446
- [99] Wiefel L, Broker A, Steinbuechel A. Synthesis of a citrulline-rich cyanophycin by use of *Pseudomonas putida* ATCC 4359. Applied Microbiology and Biotechnology. 2011;**90**(5):1755-1762

- [100] Steinle A, Witthoff S, Krause JP, Steinbuchel A. Establishment of cyanophycin biosynthesis in *Pichia pastoris* and optimization by use of engineered cyanophycin synthetases. *Applied and Environmental Microbiology*. 2010;**76**(4):1062-1070
- [101] Sallam A, Kast A, Przybilla S, Meiswinkel T, Steinbuchel A. Biotechnological process for production of beta-dipeptides from cyanophycin on a technical scale and its optimization. *Applied and Environmental Microbiology*. 2009;**75**(1):29-38
- [102] Huhns M, Neumann K, Hausmann T, Ziegler K, Klemke F, Kahmann U, et al. Plastid targeting strategies for cyanophycin synthetase to achieve high-level polymer accumulation in *Nicotiana tabacum*. *Plant Biotechnology Journal*. 2008;**6**(4):321-336
- [103] Huhns M, Neumann K, Hausmann T, Klemke F, Lockau W, Kahmann U, et al. Tuber-specific cphA expression to enhance cyanophycin production in potatoes. *Plant Biotechnology Journal*. 2009;**7**(9):883-898
- [104] Abed RMM, Dobretsov S, Sudesh K. Applications of cyanobacteria in biotechnology. *Journal of Applied Microbiology*. 2009;**106**(1):1-12
- [105] Dillschneider R, Steinweg C, Rosello-Sastre R, Posten C. Biofuels from microalgae: Photoconversion efficiency during lipid accumulation. *Bioresource Technology*. 2013; **142**:647-654
- [106] Trautmann A, Watzer B, Wilde A, Forchhammer K, Posten C. Effect of phosphate availability on cyanophycin accumulation in *Synechocystis* sp PCC 6803 and the production strain BW86. *Algal Research*. 2016;**20**:189-196
- [107] Beardall J, Raven JA. Limits to phototrophic growth in dense culture: CO₂ supply and light. In: Borowitzka MA, Moheimani NR, editors. *Algae for Biofuels and Energy*. Dordrecht: Springer Netherlands; 2013. pp. 91-97
- [108] Bahr L, Wüstenberg A, Ehwald R. Two-tier vessel for photoautotrophic high-density cultures. *Journal of Applied Phycology*. 2016;**28**(2):783-793
- [109] Lippi L, Bähr L, Wüstenberg A, Wilde A, Steuer R. Exploring the potential of high-density cultivation of cyanobacteria for the production of cyanophycin. *Algal Research*. 2018;**31**:363-366

6. Accepted publication

Watzer, B. & Forchhammer, K. (2018).

Cyanophycin synthesis optimizes nitrogen utilization in the unicellular cyanobacterium *Synechocystis* sp. PCC 6803.

Applied and environmental microbiology, 84: e01298-18



Cyanophycin Synthesis Optimizes Nitrogen Utilization in the Unicellular Cyanobacterium *Synechocystis* sp. Strain PCC 6803

Björn Watzer,^a Karl Forchhammer^a

^aInterfaculty Institute of Microbiology and Infection Medicine Tübingen, Department of Organismic Interactions, Eberhard Karls Universität Tübingen, Tübingen, Germany

ABSTRACT Cyanophycin is a carbon/nitrogen storage polymer widely distributed in most cyanobacterial strains and in a few heterotrophic bacteria. It is a nonribosomal polypeptide consisting of equimolar amounts of aspartate and arginine. Here, we focused on the physiological function and cell biology of cyanophycin in the unicellular nondiazotrophic cyanobacterium *Synechocystis* sp. strain PCC 6803. To study the cellular localization of the cyanophycin-synthesizing enzyme CphA during cyanophycin synthesis and degradation, we fused it to green fluorescent protein. When CphA was inactive, it localized diffusely in the cytoplasm. When cyanophycin synthesis was triggered, CphA first aggregated into foci and later localized on the surface of cyanophycin granules. In the corresponding cell extracts, localization of CphA on the cyanophycin granule surface required Mg²⁺. During cyanophycin degradation, CphA dissociated from the granule surface and returned to its inactive form in the cytoplasm. To investigate the physiological role of cyanophycin, we compared wild-type cells with a CphA-deficient mutant. Under standard laboratory conditions, the ability to synthesize cyanophycin did not confer a growth advantage. To mimic the situation in natural habitats, cells were cultured with a fluctuating and limiting nitrogen supplementation and/or day/night cycles. Under all of these conditions, cyanophycin provided a fitness advantage to the wild type over the mutant lacking cyanophycin. During resuscitation from nitrogen starvation, wild-type cells accumulated cyanophycin during the night and used it as an internal nitrogen source during the day. This demonstrates that cyanophycin can be used as a temporary nitrogen storage to uncouple nitrogen assimilation from photosynthesis.

IMPORTANCE We clarified the elusive biological function of cyanophycin in the nondiazotrophic cyanobacterium *Synechocystis* sp. PCC 6803. Cyanophycin is a dynamic carbon/nitrogen storage polymer (multi-arginyl-L-polyaspartate) that is conditionally present in most cyanobacteria and a few heterotrophic bacteria as cellular inclusion granules. Here, we show that the cyanophycin-synthesizing enzyme CphA in the nonactive state localizes diffusely in the cytoplasm. When cyanophycin synthesis is triggered, active CphA first aggregates into foci and then covers the surface of mature cyanophycin granules, which *in vitro* requires Mg²⁺ as a cofactor. Cyanophycin accumulation enables *Synechocystis* sp. to optimize nitrogen assimilation under nitrogen-poor conditions, in particular when the nitrogen supply fluctuates and during day/night cycles, by allowing continuous nitrogen assimilation and storage. Therefore, cyanophycin provides the wild-type cyanobacterium with a clear fitness advantage over non-cyanophycin-producing cells in natural environments with fluctuating nitrogen supply.

KEYWORDS CphA, cyanobacteria, cyanophycin, nitrogen storage, nitrogen utilization, *synechocystis*

Received 29 May 2018 Accepted 9 August 2018

Accepted manuscript posted online 17 August 2018

Citation Watzer B, Forchhammer K. 2018. Cyanophycin synthesis optimizes nitrogen utilization in the unicellular cyanobacterium *Synechocystis* sp. strain PCC 6803. *Appl Environ Microbiol* 84:e01298-18. <https://doi.org/10.1128/AEM.01298-18>.

Editor Claire Vieille, Michigan State University

Copyright © 2018 American Society for Microbiology. All Rights Reserved.

Address correspondence to Karl Forchhammer, karl.forchhammer@uni-tuebingen.de.

One of the most important steps in evolution on Earth was the appearance of oxygen in the atmosphere. This dramatic change in the redox state of our planet, called the “great oxidation event,” was triggered by the emergence of cyanobacteria capable of oxygenic photosynthesis (1).

Some of the cyanobacteria acquired the ability to fix atmospheric nitrogen, which allowed them to spread throughout the illuminated biosphere and fertilize it (2). Nitrogen is a necessary macronutrient for all life and therefore constitutes a growth-limiting factor in many terrestrial and aquatic ecosystems (3). Nondiazotrophic cyanobacteria can use a variety of combined nitrogen sources, such as nitrate or ammonia. In the absence of a usable nitrogen source, these cyanobacteria face nitrogen starvation, a situation that arrests anabolic metabolism, followed by a process known as chlorosis, which finally results in a state of dormancy (4). Chlorosis is characterized by the degradation of photosynthetic pigments, which leads to a color change from blue-green to yellow (5). Together with the degradation of light-harvesting phycobilisomes, the cells accumulate carbon-reserve polymers, e.g., glycogen or polyhydroxybutyrate, and arrest the cell cycle (6–8). When nitrogen deprivation is prolonged, cells further reduce their bulk of cellular proteins until they reach a final chlorotic stage, where they maintain a low residual level of photosynthetic activity. In this state, cells are able to survive long periods of starvation. After the addition of a nitrogen source, they are able to regreen and resume growth (9).

The process of resuscitation from nitrogen-starvation-induced chlorosis has been investigated in detail in the unicellular and nondiazotrophic cyanobacterium *Synechocystis* sp. strain PCC 6803 (here, *Synechocystis* sp.) (7, 10, 11). The addition of a usable nitrogen source triggers a tightly coordinated resuscitation program, which results in the restoration of the vegetative cell cycle within 48 h. This process can be divided into two major phases. First, the cells turn on glycogen catabolism, which provides energy and carbon skeletons for nitrogen assimilation (10); this is used to first reinstall the basic anabolic machinery, in particular, the translational apparatus (7, 12). After 12 to 16 h, transition to the second phase occurs, where the cells reassemble their photosynthetic apparatus. The cells regreen and engage oxygenic photosynthesis (7). After reaching full photosynthetic activity, the cells enter the vegetative cell cycle. During resuscitation from nitrogen starvation, the carbon/nitrogen storage polymer cyanophycin transiently accumulates (7, 13). Cyanophycin (also known as cyanophycin granule polypeptide) is present in most cyanobacterial species and in a few heterotrophic bacteria (14). It is a nonribosomal polypeptide consisting of equimolar amounts of arginine and aspartate. Every aspartyl moiety of the polyaspartate backbone is linked with an arginine residue via an isopeptide bond (15). In nondiazotrophic cyanobacteria, cyanophycin accumulates when excess nitrogen is supplied and during unbalanced growth that lowers the growth rate (e.g., during sulfate, phosphate, or potassium starvation) (16, 17).

With a C/N ratio of 2:1, cyanophycin is extremely rich in nitrogen and is therefore used as a nitrogen storage compound. This plays an important role in nitrogen-fixing cyanobacteria, in particular in those that differentiate heterocysts to fix nitrogen during the day. The heterocysts accumulate large cyanophycin structures at the contact sites to the vegetative cells, termed the polar nodes; these nodes play a role in nitrogen trafficking between the nitrogen-fixing heterocyst and the vegetative cells of the filament (18). Nonheterocystous strains, such as *Cyanothece* sp. strain ATCC 51142, synthesize cyanophycin at night during nitrogen fixation, where in the absence of photosynthetic activity, nitrogenase is protected from harmful oxygen. During the day, nitrogen fixation is arrested, and cyanophycin is degraded to mobilize the fixed nitrogen (19, 20).

Cyanophycin synthetase (CphA) builds cyanophycin from arginine and aspartate in an ATP-consuming elongation reaction that requires KCl, MgCl₂, and a sulfhydryl reagent (dithiothreitol [DTT] or β-mercaptoethanol) (21). The elongation reaction requires an unknown cyanophycin primer that must consist of at least three Asp-Arg building blocks (22) as a starting point. The primary structure of CphA consists of two

regions; both regions contain an active site and an ATP binding site (22, 23). The putative cyanophycin elongation cycle starts at the C terminus of the cyanophycin primer. First, the carboxylic acid group of the polyaspartate backbone is activated by phosphorylation with the γ -phosphoryl group of ATP. Subsequently, one aspartate is bound at the C terminus by its amino group, forming a peptide bond. The intermediate (β -Asp-Arg)_n-Asp is then transferred to the second active site of CphA and phosphorylated at the β -carboxyl group of aspartate. Finally, the α -amino group of arginine is linked via an isopeptide bond to the β -carboxyl group of aspartate (22). Cyanophycin accumulates in the form of opaque and light-scattering granules in the cell (6). CphB, an intracellular cyanophycinase, catalyzes the degradation of cyanophycin to β -Asp-Arg dipeptides (24). The last step in cyanophycin catabolism is the cleavage of the β -Asp-Arg dipeptides to monomeric arginine and aspartate, catalyzed by isoaspartyl dipeptidases (25).

Several previous studies have indicated that arginine availability is the main bottleneck of cyanophycin biosynthesis (17, 26–29). The committed step in arginine biosynthesis, the *N*-acetylglutamate kinase (NAGK) reaction, is regulated by the signal transduction protein P_{II} (30). P_{II} senses the energy status and the C/N ratio by binding 2-oxoglutarate and ATP (31, 32). Binding of P_{II} enhances the catalytic efficiency of NAGK and decreases its feedback inhibition by arginine (33), resulting in increased arginine production, followed by the accumulation of cyanophycin (17, 29).

In the last decades, research on cyanophycin has mainly focused on its potential use in different biotechnological and industrial applications, whereas the biology of cyanophycin, in particular in nondiazotrophic cyanobacteria, remains largely uninvestigated. Previous studies revealed an unexplained transient accumulation of cyanophycin during the outgrowth of dormant *Synechocystis* sp. cells from nitrogen starvation (7, 13). Here, we aimed at identifying the role of cyanophycin synthesis in the recovery of *Synechocystis* sp. cells from nitrogen starvation and, more generally, at clarifying its function during fluctuating ambient nitrogen supply.

RESULTS

CphA localization changes during resuscitation from nitrogen starvation. To investigate the intracellular localization of CphA, we fused *cphA* to the gene encoding enhanced green fluorescent protein (eGFP) (yielding eGFP fused to the C terminus of CphA) and inserted *cphA-eGFP* under the control of the native *cphA* promoter into the *Synechocystis* sp. shuttle vector pVZ322 (34). The resulting pVZ322-*cphA-eGFP* plasmid was introduced into *Synechocystis* sp. by triparental mating (34). The resulting strain, termed *Synechocystis* sp. strain CphA-eGFP, was used to investigate the cellular localization of CphA using comprehensive statistical analysis of microscopy images.

In the majority of nutrient-replete cells ($87\% \pm 3\%$; $n = 486$) in the mid-exponential phase of growth (optical density at 750 nm [OD₇₅₀], approximately 0.6), the GFP signal was uniformly distributed in the cytoplasm and did not colocalize with the fluorescence signal of the thylakoid membranes near the cell periphery (Fig. 1A to D). In the remaining cells ($13\% \pm 3\%$), distinct foci formed. Accordingly, the cyanophycin content during exponential growth was usually less than 1% of the cell dry mass, and visible cyanophycin granules were absent (6, 17, 35).

To reveal the localization of CphA during periods of cyanophycin accumulation or degradation, we monitored CphA-eGFP localization after the addition of nitrate to *Synechocystis* sp. cells that had been starved for nitrogen for 4 days. These conditions are known to induce transient cyanophycin accumulation (7, 13, 29). The *cphA* gene is constitutively expressed in different nitrogen regimes (7). In agreement, a recent quantitative proteomics analysis of resuscitating nitrogen-starved *Synechocystis* sp. cells revealed minor changes in the abundance of CphA. It increased by about 10% from cells starved of nitrogen for 21 days to fully recovered exponentially growing cells (11). In nitrogen-starved cells, the GFP signal was almost exclusively found as a diffuse signal in the cytoplasmic space ($98\% \pm 2\%$ of the cells) (see Fig. S1 in the supplemental material). Three hours after the addition of nitrate, the CphA-eGFP strain formed

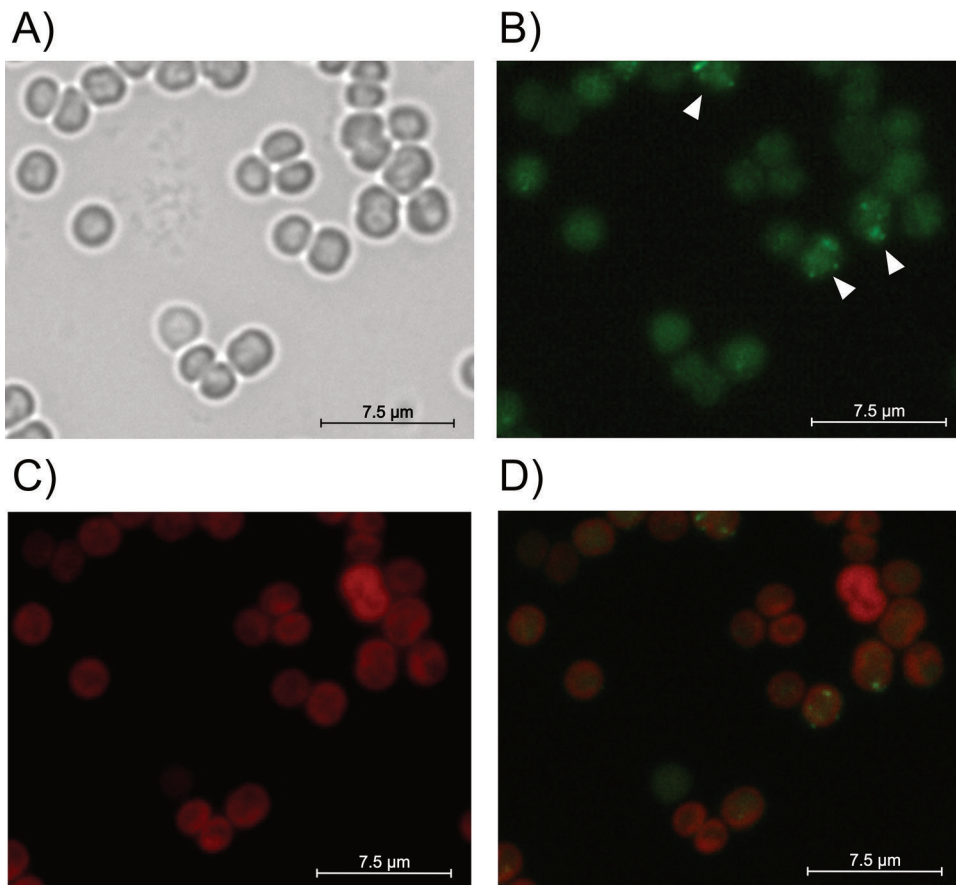


FIG 1 Localization of CphA-eGFP during exponential growth (OD_{750} of 0.6) of *Synechocystis* sp. (A) Bright-field image of cells. (B) GFP fluorescence; white arrows point to cells with CphA-eGFP foci. (C) Autofluorescence of thylakoid membranes. (D) Overlay of GFP and thylakoid membrane fluorescence images.

distinct foci in almost half of the cells (Fig. 2). After 6 h and up to 27 h after nitrate addition, the majority of cells contained CphA-eGFP foci ($83\% \pm 7\%$). As the foci appeared, their number per cell simultaneously increased, with a maximum between 6 and 12 h after nitrate addition (Fig. 2 and S2A); thereafter, the number of foci gradually decreased. The apparent diameter of the CphA-eGFP foci reached a maximum between 12 and 21 h after nitrate addition (Fig. S2B). To correlate the appearance of the CphA-eGFP foci with the occurrence of cyanophycin granules, we stained the granules

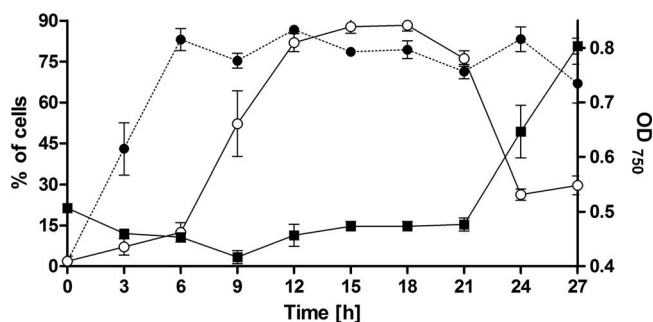


FIG 2 Number of CphA-eGFP foci and cyanophycin granules during 27 h of resuscitation of *Synechocystis* sp. cultures that were nitrogen starved for 4 days. Cells were resuscitated by adding 17.3 mM nitrate to starved cultures. Measurements are means of three biological replicates. Filled circles, percentage of cells with visible CphA-eGFP foci ($n \geq 200$ cells per time point); open circles, percentage of cells with cyanophycin granules visualized with the arginine-specific Sakaguchi stain ($n \geq 150$ cells per time point); filled squares, growth curve.

with the arginine-specific Sakaguchi stain. In bright-field images, the granules are opaque; the Sakaguchi stain enables a sensitive and clear identification of cyanophycin granules (17). Compared to the appearance of CphA-eGFP foci, the appearance of the cyanophycin granules was delayed. Six hours after nitrate addition, the number of cells containing cyanophycin granules increased dramatically, reaching a plateau of $87.8\% \pm 4.2\%$ of the cells at 15 h after nitrate addition. Eighteen hours after the addition of nitrate, both the number of cells with visible cyanophycin granules and the diameter of the foci decreased (Fig. 2 and S2B). As the cyanophycin granules degraded, the cells simultaneously started to grow again (Fig. 2).

During recovery from nitrogen starvation, cyanophycin is produced transiently, and the maximal level of accumulated cyanophycin was relatively low compared to other conditions that trigger cyanophycin accumulation (13, 17). Potassium starvation subjects cyanobacterial cells to an intense and immediate stress, which results in massive cyanophycin accumulation (17). This motivated us to analyze CphA localization under such conditions. Upon induction of potassium starvation, CphA relocalized from an initial diffuse cytoplasmic localization into distinct foci and later clearly localized on the surface of the cyanophycin granules, forming a halo-like structure (Fig. S3). Cyanophycin granules of larger diameter were amorphous and not spherical (Fig. S3). The proportion of cells with cyanophycin granules and CphA-eGFP foci increased during potassium starvation (Fig. S4A). Shifting the potassium-starved cells back to standard BG-11 medium restored the growth within approximately 24 h, concomitantly with the degradation of the cyanophycin granules. During cyanophycin degradation, it appeared in some cases that CphA-eGFP no longer colocalized with the granules (Fig. S3). The proportion of cells with cyanophycin granules and CphA-eGFP foci decreased accordingly. After 24 h, only about 20% of the cells contained cyanophycin granules. Simultaneously, 70% of the cells contained CphA-eGFP foci, while the remaining cells show the CphA-eGFP signal exclusively distributed in the cytoplasmic space (Fig. S4B). Furthermore, the average size of the granules decreased, while the number of granules per cell increased (Fig. S5), indicating that the granules disaggregate into smaller particles.

CphA localization on the cyanophycin granule surface requires Mg^{2+} . The above-mentioned results showed that CphA is homogeneously distributed in the cytoplasm as long as no cyanophycin synthesis occurs, and when cyanophycin accumulation is triggered, CphA relocalizes into foci and subsequently attaches to the surface of growing cyanophycin granules. *In vitro*, the elongation reaction of CphA requires cyanophycin primers, arginine, aspartate, $MgCl_2$, ATP, and a sulfhydryl reagent (β -mercaptoethanol or DTT) (21). To determine how these components affect the localization of CphA-eGFP in cell extracts, we analyzed cell lysates using anti-eGFP antibodies and immunoblots. Cell extracts were prepared from potassium-starved *Synechocystis* sp. cells that produced CphA-eGFP and separated into soluble and insoluble fractions, with the insoluble fractions containing the cyanophycin granules. We determined whether CphA remained associated with granules in the presence of different buffer components.

In potassium-starved *Synechocystis* sp. cells, CphA-eGFP appeared to be localized on the surface of the cyanophycin granule *in vivo* (Fig. S3). When these cells were lysed in a buffer containing 50 mM Tris-HCl (pH 7.4) and 4 mM EDTA, CphA was detected only in the soluble fraction (Fig. 3A). In contrast, when cells were lysed in a buffer containing 50 mM Tris-HCl (pH 8.2), 20 mM $MgCl_2$, and 20 mM KCl, CphA appeared in the insoluble fraction, which indicated that it remained granule associated, because cyanophycin granules remain in the insoluble fraction, owing to their insolubility at neutral pH (Fig. 3B). To test whether $MgCl_2$ is responsible for the persistent association of CphA with granules in cell extracts, cells were lysed in the same buffer containing different $MgCl_2$ concentrations (Fig. 3C). In the absence of Mg^{2+} , only residual amounts of CphA were detected in the insoluble fraction. Increasing amounts of Mg^{2+} led to increased

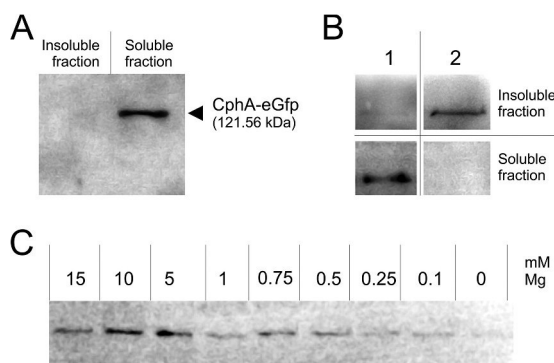


FIG 3 Immunoblot detection of CphA-eGFP using anti-GFP primary antibodies. Cell extracts of potassium-starved *Synechocystis* sp. cells were fractionated into soluble and insoluble fractions. (A) Cells lysed in a buffer containing 50 mM Tris-HCl (pH 7.4) and 4 mM EDTA. (B) Comparison of potassium-starved *Synechocystis* cells lysed in the presence of 4 mM EDTA (same buffer mentioned above) (lane 1) and a buffer without EDTA containing 50 mM Tris-HCl (pH 8.2), 20 mM MgCl₂, and 20 mM KCl (21) (lane 2). (C) Insoluble fraction of cells lysed in Tris-KCl buffer containing different MgCl₂ concentrations.

amounts of CphA in the insoluble fraction, with an apparent optimal concentration of 10 mM Mg²⁺ for *in vitro* association with cyanophycin granules (Fig. 3C).

Lack of CphA has no influence on the response to nitrogen starvation. To gain further insights into the physiological role of cyanophycin, we generated a *cphA* deletion mutant in which the *slr2002* (*cphA*) open reading frame was replaced with a kanamycin resistance cassette. Complete segregation of the mutant was confirmed by PCR (Fig. S6). The inability of the mutant to accumulate cyanophycin granule peptide (CGP) was confirmed by microscopy and cyanophycin extraction (data not shown). To investigate a possible influence of cyanophycin deficiency on the nitrogen starvation response, *Synechocystis* sp. wild-type and $\Delta cphA$ mutant cells were grown to an OD₇₅₀ of 0.4 to 0.6, washed, and resuspended in BG-11 lacking a combined nitrogen source. This treatment induces nitrogen chlorosis, which is visible as the degradation of the photosynthetic apparatus (9). We monitored the degradation of pigments during chlorosis by recording the UV-Vis spectra of the cells. In the course of chlorosis, the absorbance at 630 nm (phycobiliproteins; Fig. 4A) and at 680 nm (chlorophyll *a/b*; Fig. 4B) decreased in wild-type and $\Delta cphA$ mutant cultures similarly. After induction of nitrogen starvation, wild-type and $\Delta cphA$ mutant cells divided one more time, as indicated by the doubling of the OD₇₅₀ of the culture (Fig. 4C). After prolonged nitrogen starvation for 13 days, cells of both the wild type and the $\Delta cphA$ mutant completed chlorosis, and the cultures appeared yellowish (Fig. 4E). However, the pigment composition of long-term starved cultures of the $\Delta cphA$ mutant and wild type slightly differed; the peak heights at 440 nm and 680 nm in UV-Vis spectra in the $\Delta cphA$ mutant were higher, which indicated a higher residual amount of chlorophyll *a/b* (Fig. 4D).

Cyanophycin synthesis delays resuscitation from nitrogen starvation under standard laboratory conditions. As cyanophycin transiently accumulates during resuscitation from nitrogen starvation (7), we focused on this process to investigate the physiological role of cyanophycin. To determine whether cyanophycin synthesis influences the resuscitation process, *Synechocystis* sp. wild-type and $\Delta cphA$ mutant cells were first nitrogen starved for 2 weeks, and then resuscitation was initiated by the addition of 5 mM nitrate, adjusting the cultures to an OD₇₅₀ of 0.5. The cultures were incubated under continuous light with shaking. The time course of regreening was monitored by recording the UV-Vis spectra of the cultures.

Twelve hours after the addition of nitrate to the chlorotic cultures, the absorbance at 630 nm (phycobiliproteins; Fig. 5A) and at 680 nm (chlorophyll *a/b*; Fig. 5B) began to increase. The wild-type and $\Delta cphA$ mutant cultures regreened similarly (Fig. 5A to C). However, the $\Delta cphA$ mutant had a growth advantage over the wild type in liquid medium (as revealed by the optical density of the culture; see Fig. 5D). Thirty-six hours

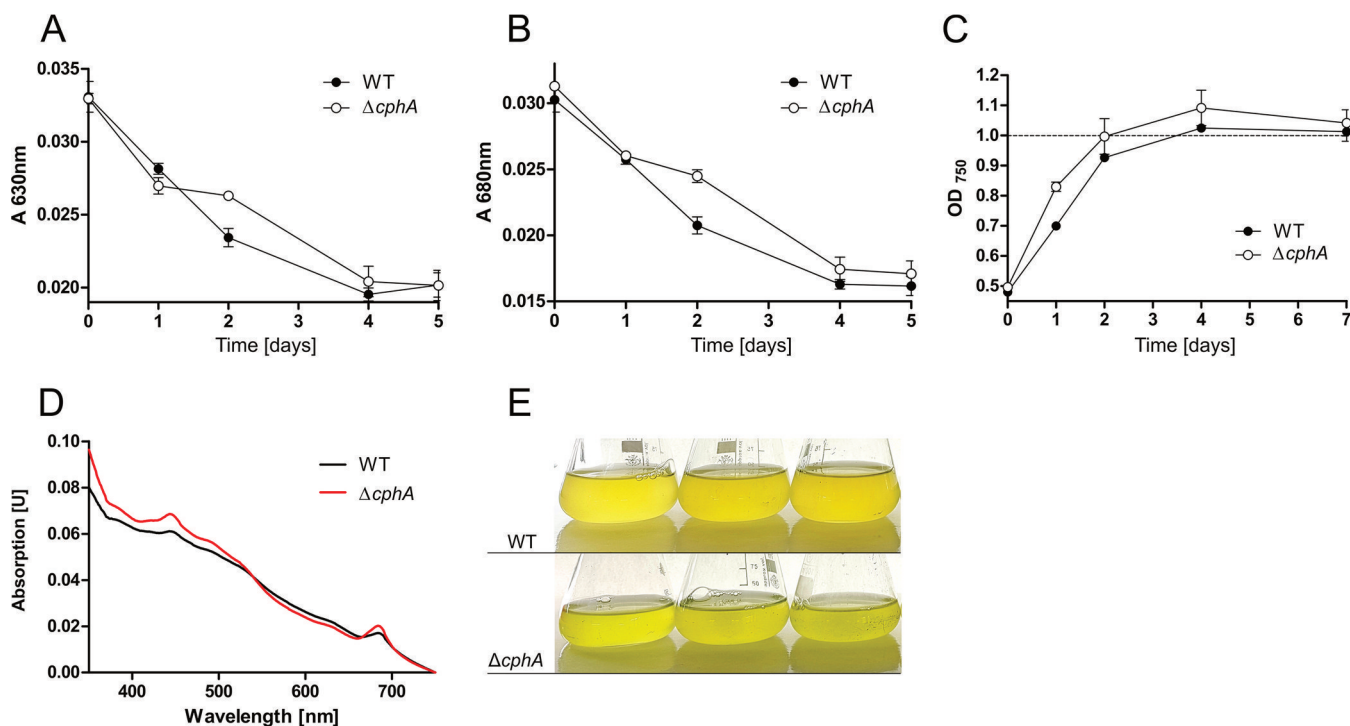


FIG 4 Changes in pigmentation and growth during nitrogen starvation of *Synechocystis* sp. wild type and a $\Delta cphA$ mutant under continuous light. Nitrogen starvation was induced by resuspending washed exponentially growing cells in BG-11 medium lacking a nitrogen source to an OD₇₅₀ of 0.5. The degradation of pigments during chlorosis was monitored by recording UV-Vis spectra, which were normalized to cultures of the same optical density at 750 nm. Shown are the means of three biological replicates. (A) Course of absorbance of phycobiliproteins at 630 nm. (B) Course of absorbance of chlorophyll *a/b* at 680 nm. (C) Growth curve (OD₇₅₀) of *Synechocystis* sp. during nitrogen starvation. (D) UV-Vis spectrum of *Synechocystis* sp. wild type and $\Delta cphA$ mutant cells that were nitrogen starved for 13 days. Spectra were normalized to cultures of the same optical density at 750 nm. (E) Three biological replicates of cultures of *Synechocystis* sp. wild type and $\Delta cphA$ mutant starved of nitrogen for 13 days.

after the addition of nitrogen, the difference in the optical density amounts to 0.07 OD₇₅₀ units. After 46 h, the $\Delta cphA$ mutant reached an OD₇₅₀ of 0.747 ± 0.045 compared to the wild type, with 0.64 ± 0.036 , which is a significant difference ($P = 0.0329$). This growth disadvantage of the wild type turned out even more clearly on solid medium (as revealed by the drop plate method; see Fig. 5E). In the drop plate method, the area of the $\Delta cphA$ mutant was green already after 2 days, which indicated a return to the vegetative cell cycle and growth; the wild type lagged behind in the greening process. This growth advantage of the $\Delta cphA$ mutant over the wild type continued until day 8 of recovery, at which time the two strains showed a similar degree of recovery.

Cyanophycin accumulation helps overcome a fluctuating or limiting nitrogen supply. The growth disadvantage of the cyanophycin-forming wild-type cells during resuscitation from nitrogen chlorosis was puzzling. We questioned whether this disadvantage was due to unnatural laboratory conditions (nitrogen-rich medium and continuous light). Therefore, we nitrogen starved *Synechocystis* wild-type and $\Delta cphA$ mutant cells for 9 days and compared their resuscitation with a fluctuating and/or limiting nitrogen supplementation by a modification of the drop plate method (Fig. 6), which allows nitrogen supplementation to be changed without imposing additional stress to the cells that occurs with harvesting, washing, and resuspending cells in another medium.

When chlorotic cells were exposed under continuous light to 6-h periods of nitrogen excess (17.3 mM nitrate) per day (6 h on BG-11 with nitrate and 18 h on nitrogen-free BG-11), the $\Delta cphA$ mutant grew slightly faster than the wild type during the first 3 days (Fig. 6A). After the fourth day, the wild type and $\Delta cphA$ mutant reached the same culture density. After 7 days, the wild type displayed a slight growth advantage. After 9 days, the wild type clearly had a growth advantage over the $\Delta cphA$ mutant.

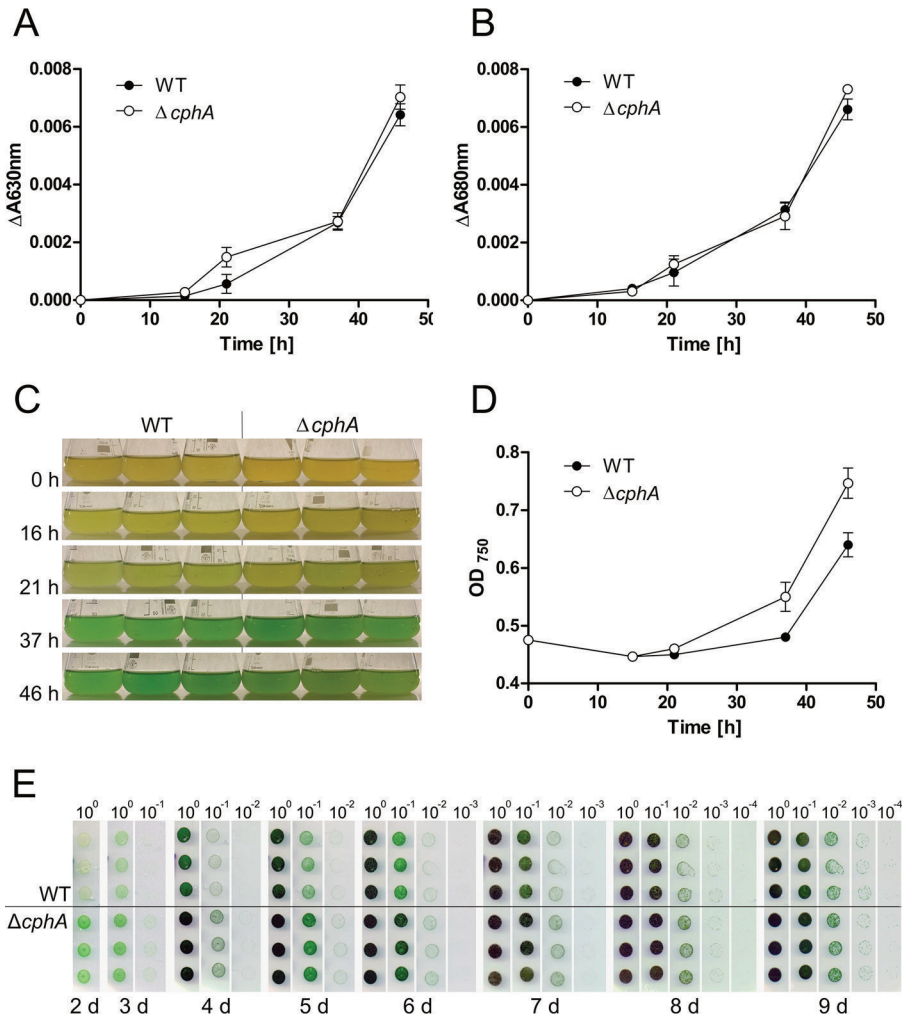


FIG 5 Resuscitation from 2-weeks-nitrogen-starved *Synechocystis* sp. wild-type and $\Delta cphA$ cultures in BG-11 liquid medium and on agar under continuous light. (A and B) Absorbance of phycobiliproteins at 630 nm (A) and absorbance of chlorophyll *a/b* at 680 nm (B) during regreening. Values shown are the means of three biological replicates. (C) Cultures of resuscitating wild type (WT) and the $\Delta cphA$ mutant; 0 h, induction of resuscitation. (D) Growth curve (OD_{750}) of wild-type and the $\Delta cphA$ mutant cultures during resuscitation. Values shown are the means of three biological replicates. (E) Drop plate method of resuscitating wild-type and $\Delta cphA$ mutant cells on BG-11 agar plates containing 17.3 mM nitrate (standard concentration in BG-11 medium). Cultures were adjusted to an OD_{750} of 1.0, diluted in a 10-fold dilution series, and cultivated under continuous light. Photos were taken starting after 2 days of cultivation. Assays were performed using three biological replicates per strain. d, days.

To test resuscitation with continuous but low nitrogen supplementation, chlorotic cells were exposed under continuous light to only 1.73 mM nitrate (10% of the standard concentration) and transferred to fresh plates containing 1.73 mM nitrate every day. Colonies of green cells of both strains appeared after 3 days (Fig. 6B), but the wild type showed a clear growth advantage over the $\Delta cphA$ mutant throughout the experiment (Fig. 6B).

In the next experiment, we combined nitrogen limitation and fluctuating nitrogen availability. A limiting amount of nitrogen (1.73 mM nitrate) was available for only 4 h per day under continuous light. Under these conditions, the wild type showed the clearest growth advantage over the $\Delta cphA$ mutant (Fig. 6C). Furthermore, a difference in the colors of the cultures of the two strains became apparent. Cultures of the $\Delta cphA$ mutant were more yellow than those of the wild type, which indicated that the $\Delta cphA$ cells could not fully recover their photosynthetic pigments and remained in a semi-chlorotic state.

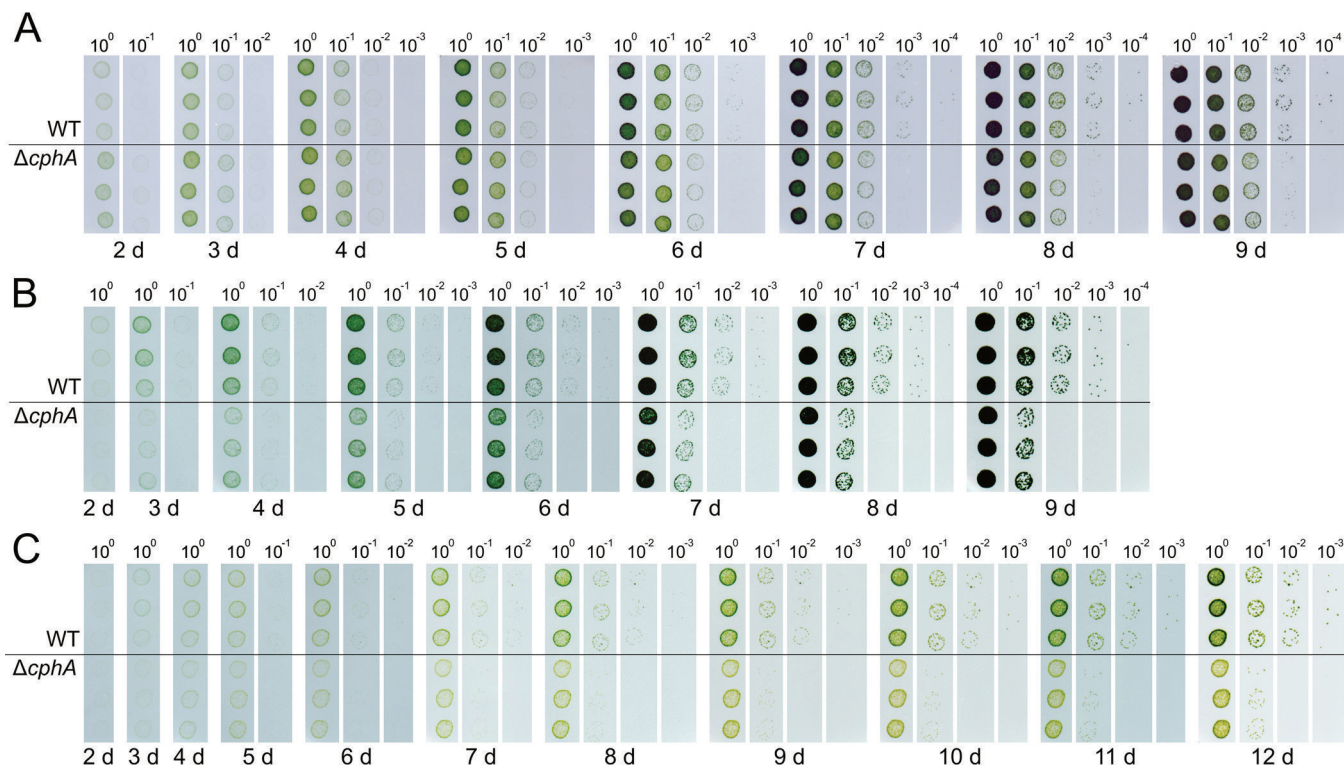


FIG 6 *Synechocystis* sp. wild-type and $\Delta cphA$ mutant cells starved of nitrogen for 9 days and resuscitated under continuous light on BG-11 agar plates supplying fluctuating or limiting nitrogen levels. Chlorotic cultures were adjusted to an OD_{750} of 1.0 and diluted in series. To enable fluctuating nitrogen supplementation, each cell suspension was dropped onto a transfer membrane, which was periodically moved to another plate containing a different nitrogen concentration. Photos were taken starting after 2 days of cultivation. Assays were performed using three biological replicates per strain. (A) Cells were exposed to 17.3 mM nitrate for 6 h per day and to no nitrogen for 18 h. (B) Cells were continuously exposed to a low concentration of nitrate (1.73 mM); to avoid nitrogen starvation, the transfer membrane was moved daily to a fresh plate containing 1.73 mM nitrate. (C) Both nitrogen limitation and fluctuating nitrogen availability were combined by exposing the cells to 1.73 mM nitrate for 4 h per day.

To determine whether the growth advantage under fluctuating nitrogen concentrations of wild-type cells over the $\Delta cphA$ mutant could also be observed in liquid culture, we provided nitrogen-starved liquid cultures of *Synechocystis* sp. wild-type and the $\Delta cphA$ mutant with 10 mM nitrate for 4 h, followed by 20 h with no nitrogen source; this cycle was repeated for 4 days (Fig. 7). After 2 days, both strains began to regreen, but the wild type regreened faster than the $\Delta cphA$ mutant (Fig. 7A and B). After 4 days, the growth advantage of the wild type was clearly visible, since the optical density of

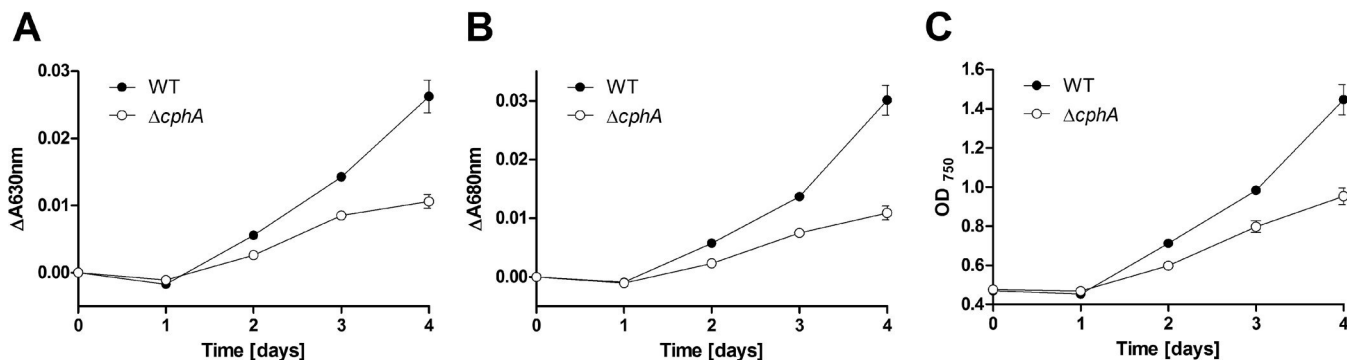


FIG 7 *Synechocystis* sp. wild-type and $\Delta cphA$ mutant cells starved of nitrogen for 9 days and resuscitated under continuous light in liquid medium supplying fluctuating nitrogen concentrations. Values are the means of three biological replicates. Chlorotic cultures were adjusted to an OD_{750} of 0.5. Resuscitation was induced by adding 10 mM nitrate. After 4 h of nitrogen availability, the cells were washed and resuspended in nitrogen-free BG-11 medium. This routine was repeated over 4 days. The progress of regreening was documented by measuring the absorbance of phycobiliproteins at 630 nm (A) and chlorophyll *a/b* at 680 nm (B). (C) Growth curve of the two strains.

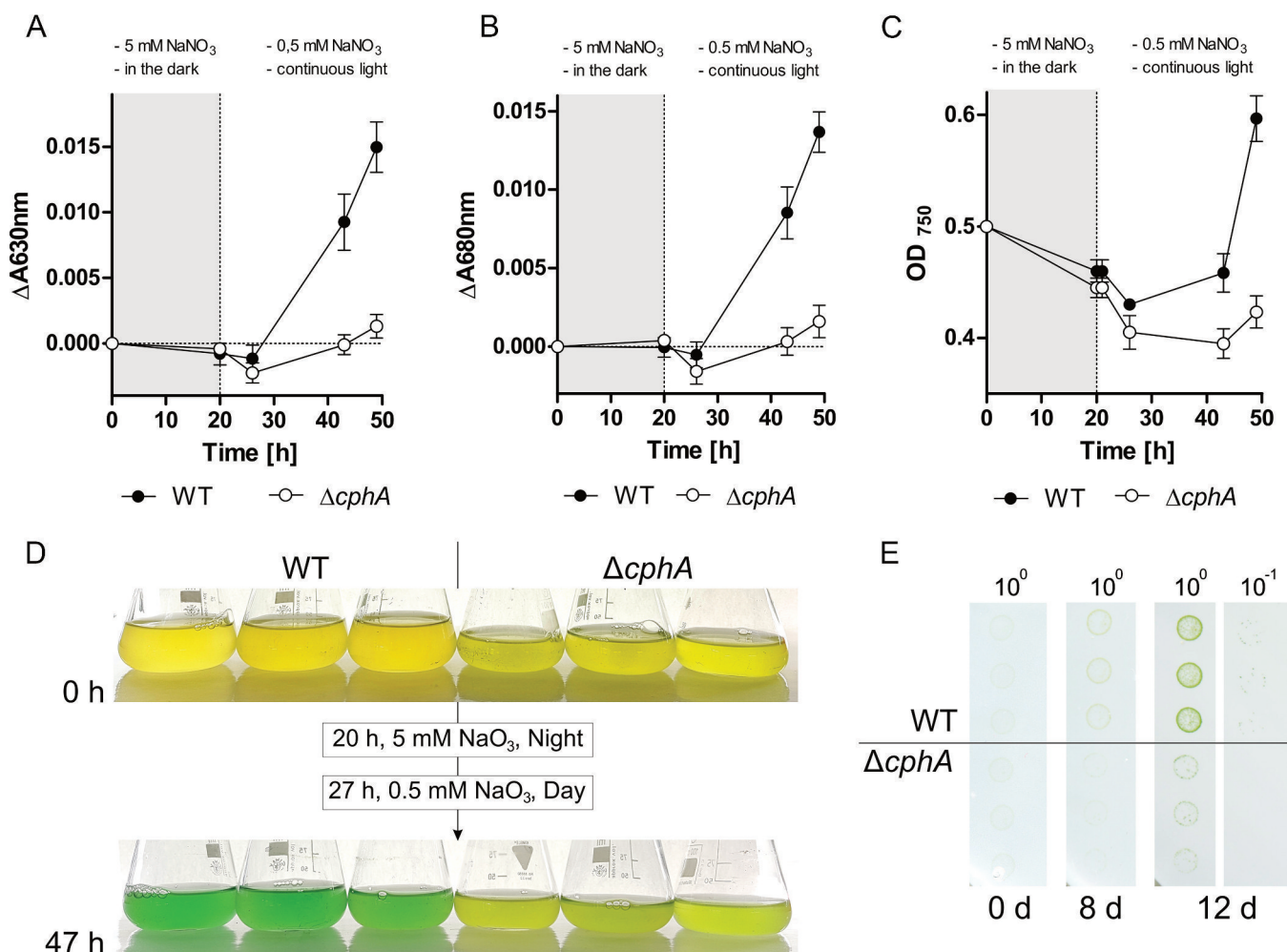


FIG 8 *Synechocystis* sp. wild-type and $\Delta cphA$ mutant strains starved of nitrogen for 1 week and resuscitated in liquid medium and on agar plates with fluctuating nitrogen supply and day/night cycles. Starved cultures of wild-type and the $\Delta cphA$ mutant were adjusted to an OD₇₅₀ of 0.5, and resuscitation was initiated by adding 5 mM nitrate in the absence of light. After 20 h of nitrogen availability in the dark, the cells were washed and resuspended in BG-11 medium containing residual amounts of nitrate (0.5 mM) and placed in the light. The progress of regreening was documented by measuring the absorbance of phycobiliproteins at 630 nm (A) and chlorophyll *a/b* at 680 nm (B). (C) Growth curve of the two strains. Gray areas in panels A to C indicate the night phase with nitrogen availability; white areas indicate the day phase with nitrogen limitation. Values are the means of three biological replicates. (D) Three liquid cultures of resuscitating *Synechocystis* sp. wild-type and the $\Delta cphA$ mutant. (E) Modified drop plate method of *Synechocystis* sp. strains starved of nitrogen for 1 week, with three biological replicates per strain. Starved cultures were adjusted to an OD₇₅₀ of 1.0 and diluted 10-fold in series, and the dilutions were dropped onto a transfer membrane. The cells on the membrane were exposed to a small amount of nitrogen (1.73 mM) once per day for 8 h in the absence of light.

the wild-type culture increased 3-fold, whereas that of the $\Delta cphA$ mutant increased only 2-fold (Fig. 7C).

Cyanophycin accumulated in the night can trigger resuscitation during the day. Photosynthetic organisms in nature have to deal with day-night changes and a fluctuating and limiting nutrient supplementation. We hypothesized that cyanophycin that accumulates in nondiazotrophic cyanobacteria in the night could be used as an intracellular nitrogen source during the day. To test this hypothesis, we combined nitrogen limitation and fluctuating nitrogen supplementation with day/night periods.

Nitrogen-starved liquid cultures of *Synechocystis* sp. wild-type and the $\Delta cphA$ mutant were exposed to 5 mM nitrate for 20 h without light. After this dark period, the cells were washed and resuspended into fresh medium containing a small amount of nitrate (0.5 mM) and exposed to light. After the 20-h dark period, the wild type accumulated cyanophycin to $3.7\% \pm 0.6\%$ of the cell dry mass, but the pigmentation of the wild type and $\Delta cphA$ mutant was still at its initial low level (Fig. 8A and B). Shortly after light exposure in low-nitrate medium, the wild type started to synthesize pigments, but the

$\Delta cphA$ mutant was not able to regreen (Fig. 8A, B, and D). Forty-seven hours after the first addition of nitrate, wild-type cultures appeared green and cultures began to grow (Fig. 8C and D), whereas the $\Delta cphA$ mutant was still chlorotic. We further analyzed the growth behavior with a modified version of the drop plate method, in which *Synechocystis* sp. wild-type and $\Delta cphA$ mutant cells starved of nitrogen for 1 week were grown on plates with fluctuating nitrogen supply and with day/night cycles (16-h day/8-h night). A small amount of nitrate (1.7 mM) was provided only during the night. Under these conditions, the overall growth of both strains was very low. Nevertheless, the wild type showed a clear growth advantage over the $\Delta cphA$ mutant; growth of the wild type and mutant was detected after 8 and 12 days of cultivation, respectively (Fig. 8E).

DISCUSSION

CphA localization switch indicates active and inactive forms. Our results revealed different localizations of the inactive and active forms of CphA in cells of *Synechocystis* species. Under conditions in which no cyanophycin synthesis occurs, such as during exponential growth or nitrogen starvation, CphA is inactive and mainly located in the cytoplasm. Immediately after the induction of cyanophycin synthesis, CphA aggregated in foci that were randomly distributed in the cell. Formation of the CphA foci may be a consequence the priming of the CphA enzyme. The primers could induce self-aggregation.

CphA in its primed state is ready to elongate the cyanophycin primer. During this elongation process, the CphA foci increase in size and become visible as cyanophycin granules. As cyanophycin accumulates, the numbers of foci and granules per cell continuously decrease, possibly as initial granules fuse to form larger aggregates. This behavior would also explain the amorphous structure of the large granules that we observed when the cellular cyanophycin content was high and which we also observed previously in electron micrographs of a cyanobacterial cyanophycin-overproducer strain (17). The observed ring-like appearance of the fluorescence signal around large cyanophycin granules in our study suggests that during cyanophycin accumulation, CphA-eGFP covers the surface of the granule.

Previous studies have shown that CphA activity *in vitro* requires cyanophycin primers, arginine, aspartate, $MgCl_2$, ATP, and a sulfhydryl reagent (21). Our results indicate that Mg^{2+} is strictly required for the association of CphA to the cyanophycin granules. The primary structure of CphA is composed of two regions (23), both of which show sequence similarities to ATP-dependent ligases of two superfamilies. Sequence alignments of the D-alanine-D-alanine ligase DdIB with cyanobacterial CphA show that key residues involved in binding of the ATP- Mg^{2+} complex are conserved in CphA (22). Accordingly, Mg^{2+} may stabilize the active conformation of CphA which is able to bind the C terminus of the cyanophycin substrate. In the absence of Mg^{2+} , CphA cannot maintain its enzymatic activity, which could lead to dissociation of the substrate and consequently to release from the granule surface.

Cyanophycin accumulation is triggered in the presence of combined nitrogen sources by several growth-limiting conditions that lead to growth arrest, and cyanophycin degradation can be triggered by restoring the growth of the arrested cells. During cyanophycin degradation, the localization of CphA-eGFP changed from the surface of the cyanophycin granule to the cytoplasm. This suggests that as cyanophycin degrades, CphA dissociates from the granule surface and distributes in an inactive form throughout the cytoplasm, where it remains silent until cyanophycin synthesis is triggered again by growth-arresting conditions. A model of the cyanophycin accumulation and degradation cycle during nitrogen-induced chlorosis and resuscitation is depicted in Fig. 9.

Our previous transcriptome study of nitrogen-depleted *Synechocystis* sp. cells has shown that the transcript levels of *cphA* in cells starved for nitrogen and of exponentially growing cells are very similar (1.2-fold upregulated during 14 days nitrogen starvation compared to nitrogen-supplemented cells). However, during resuscitation from nitrogen starvation, the *cphA* transcript level 24 h after the addition of nitrogen

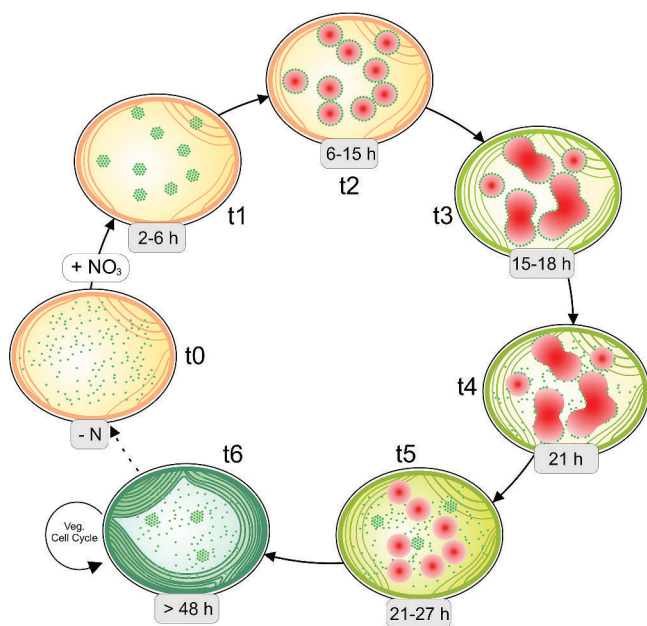


FIG 9 Hypothetical cycle of cyanophycin accumulation and degradation during resuscitation from nitrogen starvation. t0, when cyanophycin does not accumulate, such as during nitrogen starvation, CphA (green dots) is distributed in the cytoplasm; t1, 2 to 6 h after the addition of nitrogen, CphA aggregates in foci; t2, 6 to 15 h after the addition of nitrogen, the first cyanophycin granules (red) appear, with CphA localized on the surface of the growing granules; t3, 15 to 18 h after nitrogen addition, adjacent granules merge when they collide, building amorphous granules with CphA on their surface; t4, 21 h after nitrogen addition, when cyanophycin begins to degrade, CphA begins to dissociate from the granule surface; t5, 21 to 27 h after nitrogen addition, the granules become smaller, and CphA is distributed in the cytoplasm; t6, after the cell completes resuscitation after more than 48 h, it starts to divide, with CphA mainly distributed in the cytoplasm. Veg, vegetative.

is approximately 1.7-fold higher than in exponentially growing cells (7). In agreement, quantitative proteomics revealed that the level of CphA after 21 days of nitrogen starvation is slightly reduced compared to nitrate-supplemented cells and goes back to initial values during recovery (11).

The synthesis of cyanophycin is probably tuned by the cellular level of arginine, which increases under growth-limiting conditions because of lowered protein biosynthesis. High concentrations of arginine surpass the K_m of CphA for arginine and could therefore trigger the biosynthesis of cyanophycin (29). Whether CphA is subjected to additional activity control remains to be elucidated.

Cyanophycin-deficient mutant has a growth advantage under laboratory conditions. The ability to synthesize cyanophycin is widespread among cyanobacteria and other eubacteria. With a C/N ratio of 2:1, cyanophycin is perfectly suited as a nitrogen storage compound. However, the physiological significance of cyanophycin for nondiazotrophic cyanobacteria remained largely unknown. Here, we showed that in the nondiazotrophic unicellular cyanobacterium *Synechocystis* sp., the deletion of *cphA*, which causes the inability to produce cyanophycin, has no impact on the nitrogen starvation response. The wild type and the $\Delta cphA$ mutant responded to nitrogen starvation similarly, namely, with chlorosis. However, the $\Delta cphA$ mutant reproducibly retained slightly higher residual pigment content in the chlorotic state. Merritt et al. (36) reported in nitrogen-limited cells of *Synechocystis* sp. the presence of a cyanophycin-like polymer that contains glutamic acid instead of arginine (36). Such a compound could be synthesized by a side-reaction of CphA and could affect the degradation of pigments in a so-far-unknown manner.

Several earlier studies have reported the transient accumulation of cyanophycin in cyanobacteria during resuscitation from nitrogen starvation (7, 13). Allen et al. (1980) reported an immediate synthesis of cyanophycin with a peak of 5 to 6% of the cell dry

weight 8 to 12 h after the addition of NaNO_3 to nitrogen-starved *Synechocystis* sp. PCC 6308 cultures (13). Here, we show that under standard laboratory conditions with continuous light and nitrogen excess, the ΔcphA mutant showed a clear growth advantage over the wild type both in liquid medium and on agar plates. The synthesis of cyanophycin costs 1.3 ± 0.1 mol ATP per mol incorporated amino acid *in vitro* (37). Without using the benefit of cyanophycin as a storage compound, the synthesis of cyanophycin is only a burden to the cells, and consequently, the cyanophycin-deficient ΔcphA mutant has an advantage over the wild type. This is the case under artificial laboratory cultivation conditions, which provide an excess of nitrogen and light.

Cyanophycin is beneficial under natural conditions. In nature, microorganisms have to deal with a fluctuating and limiting nitrogen availability (3). We hypothesized that cyanophycin accumulation is a strategy to overcome temporal limitations in nitrogen availability. Growth and resuscitation experiments of *Synechocystis* sp. wild-type and the ΔcphA mutant confirmed this hypothesis. The ability to store nitrogen in the form of cyanophycin was beneficial during resuscitation under a fluctuating or limiting nitrogen supplementation, and the cells have a growth advantage over the cyanophycin-deficient mutant. When nitrogen fluctuation and limitation are combined, the cyanophycin-deficient mutant was not able to fully recover from chlorosis.

To further mimic natural conditions, we tested day/night cycles in addition to a fluctuating and/or limiting nitrogen supply. In the unicellular diazotrophic cyanobacterium *Cyanothece* sp. ATCC 51142 and the filamentous cyanobacterium *Trichodesmium* sp., cyanophycin acts as temporary nitrogen storage to enable the coexistence of nitrogen fixation and photosynthesis in the same cell (19, 20). These cyanobacteria fix nitrogen in the night and store the fixed nitrogen in the form of cyanophycin. During the day, when cells carry out photosynthesis, cyanophycin is degraded to mobilize the fixed nitrogen. Based on this behavior in diazotrophic cyanobacteria, we hypothesized that cyanophycin is involved in nitrogen storage also in nondiazotrophic cyanobacteria at night. Indeed, when we combined fluctuating nitrogen supplementation and day/night cycles, the resuscitation of *Synechocystis* sp. wild-type cells proceeded as fast as in continuous light, with growth restoration after 48 h. In contrast, the cyanophycin-deficient mutant was not able to resuscitate in this time period.

The first phase of resuscitation from nitrogen chlorosis occurs in a light-independent mode, where the cells catabolize glycogen using the parallel operating Entner-Doudoroff and oxidative pentose phosphate pathways (10). Only when the photosynthetic apparatus is reinstalled after approximately 12 to 16 h does metabolism switch back from the heterotrophic mode to a mixotrophic mode and finally to the fully autotrophic mode. Our data suggest that most of the nitrogen that is required for greening can be assimilated in the initial heterotrophic phase and stored as cyanophycin. The stored cyanophycin makes internal nitrogen available to the cells during the second phase of resuscitation, which can then proceed, even if the ambient nitrogen supply is again low.

Nitrate assimilation by cyanobacteria is tightly regulated at both the transcriptional and posttranslational levels (38, 39). Nitrate uptake is mediated by the bispecific nitrate/nitrite transporter encoded by the *nrtABCD* genes. This operon is only expressed in the absence of ammonium, and the nitrate/nitrite transporter is rapidly and reversibly inhibited by the addition of ammonia (38–40). The P_{II} signal transduction protein appears to be involved in this process, since a P_{II} -deficient mutant shows no ammonium-responsive inhibition of nitrate and nitrite uptake (41). In vegetative growing cells, in addition to the requirement for ammonium absence, the operation of the nitrate/nitrite transporter also requires CO_2 fixation, because the inhibition of photosynthetic CO_2 fixation results in the simultaneous inhibition of nitrate uptake (42). Newly assimilated nitrogen is incorporated in the central metabolism via the glutamine synthetase (GS) and glutamate synthase (GOGAT) cycle. GS activity is tightly regulated by light/dark transitions; induction of the inhibitory factor 7 (IF7) and IF17 in the dark causes GS to switch off (43–45). This leads to the inhibition of nitrogen assimilation in

the dark, both at the level of nitrate transport and by inhibition of the ammonium-assimilating GS. Our results showed that cyanophycin accumulates upon nitrate addition to chlorotic cells in the dark, which requires active nitrate assimilation. This contradicts the dark switch-off nitrate assimilation in vegetative cells. It is possible that the P_{II} signaling protein is directly involved in this behavior. Nonphosphorylated P_{II} mediates a light-dependent inhibition of nitrate utilization (41, 46). However, during nitrogen starvation, P_{II} is highly phosphorylated and remains in the highly phosphorylated state during the first period of resuscitation (11, 47). In this state, P_{II} is probably unable to inhibit nitrate uptake. In agreement, Reyes et al. (48) have shown that the inactivation of GS in the dark is attenuated under nitrogen depletion, which allows the cells to utilize nitrogen in the dark after a nitrogen starvation period (48). The GS inhibitory factors IF7 and IF17 are regulated by the global nitrogen control transcriptional factor NtcA, which is in turn controlled by 2-oxoglutarate levels and the PII-PipX network (49–51). Apparently, during nitrogen starvation, where NtcA is activated by elevated levels of 2-oxoglutarate and by binding PipX, the nocturnal derepression of the *gifA* and *gifB* genes appears to be abrogated (52, 53).

The occurrence of cyanophycin in cyanobacteria has been known for more than 100 years. However, fundamental questions on its biological function or the benefit of cyanophycin accumulation remained largely uninvestigated. Altogether, our study sheds new light on the process of cyanophycin accumulation and reveals new insights into the biological function of cyanophycin in nondiazotrophic cyanobacteria. Interestingly, artificial laboratory conditions do not provide any fitness advantage for cyanophycin-producing cells, and in a fluctuating environment, CphA becomes beneficial. As the *cphA* gene is constitutively expressed in *Synechocystis* sp., the cells are programmed to overcome fluctuating nitrogen supply and transient periods of starvation in a constantly changing environment.

MATERIALS AND METHODS

Cultivation conditions. Standard procedures for cloning in *Escherichia coli* NEB 10-beta (NEB) and *E. coli* XL1-Blue (Stratagene) were followed. Strains were grown in LB medium at 37°C with constant shaking at 300 rpm.

Synechocystis sp. strains were cultivated photoautotrophically in BG-11 medium supplemented with 5 mM NaHCO₃ (54) at 27°C with constant shaking at 120 rpm and illumination at 40 to 50 microeinsteins. Growth was monitored by measuring the optical density at 750 nm. BG-11 agar plates contained 1.5% (wt/vol) Bacto agar (Difco), 0.3% (wt/vol) sodium thiosulfate pentahydrate, and 10 mM *N*-tris(hydroxymethyl)methyl-2-aminoethanesulfonic acid (TES)-NaOH (pH 8) (Roth). Antibiotics were added to the medium when required.

For the induction of starvation conditions, cells of exponentially growing cultures (OD₇₅₀, 0.4 to 0.6) were harvested, washed, and resuspended in BG-11 medium lacking a specific nutrient. For nitrogen starvation, the cells were resuspended in BG-11 medium without a nitrogen source. For resuscitation from nitrogen starvation, chlorotic cultures were adjusted to an OD₇₅₀ of 0.5, harvested, and resuspended in BG-11 containing a nitrogen source. To introduce potassium starvation, cells were harvested, washed, and resuspended in BG-11 medium containing Na₂HPO₄ in an amount equimolar to that of the K₂HPO₄, it replaced. Regeneration from potassium starvation was induced by harvesting, washing, and resuspending cells in BG-11 medium containing a potassium source.

For the drop plate method, *Synechocystis* sp. cultures were adjusted to an OD₇₅₀ of 1. The cultures were diluted 10-fold in series in BG-11 medium lacking nitrogen. Drops (5 μl) of five dilutions (10⁰ to 10⁻⁴) were placed on BG-11 agar plates containing specific nitrate concentrations. When cells were to be shifted to different solid media, the drops were placed on mixed-cellulose ester transfer membranes (pore size, 0.45 μm; HATF; Merck Millipore). The transfer membranes were placed on different BG-11 agar plates at the intervals specified in the figure legends. To minimize carryover of the residual nitrate from the initial plate, the transfer membranes were placed on nitrogen-free BG-11 plates for 10 min. The plates were incubated at 27°C with illumination at 40 to 50 microeinsteins.

Construction of a $\Delta cphA$ mutant and a *cphA-egfp* fusion. PCR fragments were generated using high-fidelity Q5 polymerase (NEB) and oligonucleotides with overlapping regions. Genomic *Synechocystis* sp. DNA or plasmids served as the templates. The primers, plasmids, and strains used in this study are listed in Tables 1, 2, and 3, respectively.

To generate a $\Delta cphA$ mutant, 500-bp upstream and downstream genomic regions of *slr2002* (*cphA*) were amplified using the oligonucleotides up_for/up_rev and down_for/down_rev. The kanamycin resistance gene (816 bp) was amplified from pVZ322 (34) using primers kan_for and kan_rev. Upstream and downstream fragments and the kanamycin resistance cassette were fused and incorporated into the linear pJET1.2/blunt cloning vector (Thermo Scientific) by isothermal single-reaction DNA assembly, according to Gibson et al. (55). The resulting construct (pJET $\Delta cphA$) was introduced into competent *E. coli* NEB 10-beta by transformation. The correct length (1,816 bp) of the insert was confirmed via colony

TABLE 1 Oligonucleotides used in this study

Primer	Sequence (5'→3')
Up_for	GATGGCTCGAGTTTTTCAGCAAGATCGCTGGTGGATATGGCGGTG
Up_rev	TCCCGTTGAATATGGCTCATGATCTGTGTCAGTCAAGAAC
Down_for	TGCTCGATGAGTTTTTCTAAAGTTTTTCTCCCCCTTGCT
Down_rev	ATTGTAGGAGATCTTCTAGAAAGATGGGAAATTGTTCCGTTAACT
Kanr_for	GTTCTTGACTGACACAGATCATGAGCCATATCAACGGGA
Kanr_rev	AGCAAGGGGGAAGAAAACCTTTAGAAAACTCATCGAGCA
pJet_seq_for	CGACTCACTATAGGGAGAGCGGC
pJet_seq_rev	AAGAATCATGATTTTCCATGGCAG
seg_for	CCATTGAGTTAATTAAGCCC
cphA_for	GCTTTGCTTCCAGATGTATGCTCTTCTGCTCCTGCAGGTCGACGTGCCGAAATTGTGGTGATCAGC
cphA_rev	GAATTGGGACAACCTCCAGTGAAAAGTTCTTCTCTTTACTCATACCAATGGGTTTACGGGCTTTAATTAAC
gfp_for	GCTTTGCTTCCAGATGTATGCTCTTCTGCTCCTGCAGGTCGACGTGCCGAAATTGTGGTGATCAGC
gfp_rev	GAATGTTCCGTTGCGCTGCCGGATTACAGATCTCTAGAGTCGACTTAACAATATTTTAAAAATTGCCTACTG
pVZ322_seq_for	GAGCGCTGCCGCACAGCTCCATAGGC
pVZ322_seq_rev	GCGCTGCGCAGGGCTTTATTGATTC

PCR using the primers provided in the CloneJET PCR cloning kit (pJet_seq_for and pJet_seq_rev) (Thermo Scientific). *Synechocystis* sp. was transformed with pJET Δ cphA via natural competence (56). Transformants were selected on BG-11 agar plates supplemented with 50 μ g/ml kanamycin. Complete segregation was confirmed via PCR using primers seg_for, kan_for, and down_rev (Fig. S6).

For the *cphA-egfp* fusion, *cphA* including its promoter region was amplified using primers *cphA_for* and *cphA_rev*. Subsequently, the enhanced green fluorescent protein gene *egfp* derived from plasmid pCESL19 (57) was amplified using oligonucleotides *gfp_for* and *gfp_rev*. The *cphA* and *egfp* amplicons were fused and incorporated into XbaI-digested pVZ322 via DNA assembly according to Gibson et al. (55). The resulting plasmid, pVZ322 *cphA-egfp*, was introduced into competent *E. coli* XL1-Blue (Stratagene) cells by transformation. The sequence integrity of the plasmid was verified by sequencing using primers pVZ322_seq_for and pVZ322_seq_rev. *Synechocystis* sp. was transformed with pVZ322 *cphA-egfp* by triparental mating (34), and transformants were selected on BG-11 agar plates supplemented with 50 μ g/ml kanamycin and 5 μ g/ml gentamicin.

Microscopy and staining. Cells were observed by fluorescence microscopy using a Leica DM5500B microscope with a $\times 100/1.3$ oil objective. The GFP signal was detected with a BP470 40-nm excitation filter and a BP525 50-nm emission filter. Cyanobacterial autofluorescence was detected with a filter cube with excitation filter BP535/50 and suppression filter BP610/75. Images were acquired with a Leica DFC360FX black-and-white camera. Captured black-and-white pictures were colored using the Leica Application Suite Software (LAS AF) provided by Leica Microsystems. Bright-field images were exposed for 5 ms, and fluorescence images were exposed for 100 ms. Images, including those for counting fluorescent foci and measuring the diameter, were evaluated with the Leica Application Suite Software.

Cyanophycin granules were visualized using a staining method based on the arginine-selective Sakaguchi reaction, according to Watzer et al. (17). Photographs were taken with a Leica DM2500 microscope using a $\times 100/1.3$ oil objective. Images were acquired with a Leica DFC420C color camera and Leica Application Suite Software.

During all microscopy studies, microscope slides covered with a dried 2% (wt/vol) agarose solution were used to immobilize the cells.

Protein extract preparation. Potassium-starved *Synechocystis* sp. cells were harvested by centrifugation and resuspended in a buffer containing 50 mM Tris-HCl (pH 7.4), 4 mM EDTA, 1 mM DTT, and 0.5 mM benzamide, or optionally in a buffer containing 50 mM Tris-HCl (pH 8.2), 20 mM MgCl₂, 20 mM KCl, and 1 mM DTT (21). Cells were lysed using FastPrep-24 (MP Biomedicals) with 0.1-mm glass beads at a speed of 6.0 m/s for 20 s with five repeats and 5 min of resting after every repeat. Soluble and insoluble fractions were separated by centrifugation at 25,000 $\times g$ for 25 min at 4°C. The protein concentration was determined using the Bradford assay (58).

SDS-PAGE and immunoblotting. Proteins were separated by SDS-PAGE on a 12% polyacrylamide gel according to Sambrook and Russell (59). Total protein (10 μ g) was loaded on each lane. For immunoblot detection of CphA-eGFP, proteins were blotted onto a methanol-activated polyvinylidene difluoride (PVDF) membranes, as described previously (60). Membranes were blocked with 10% (wt/vol) milk powder in TBS buffer (50 mM Tris-HCl [pH 7.4], 75 mM NaCl) overnight. Afterwards, the membranes were transferred in 1% (wt/vol) milk powder in TBS buffer containing 1:2,500 diluted rabbit anti-GFP antibody (chromatin immunoprecipitation [ChIP] grade ab290; Abcam) and incubated for 2 h at ambient

TABLE 2 Plasmids used in this study

Plasmid	Description	Reference or source
pJET1.2	Cloning vector	Thermo Scientific
pVZ322	Broad-host-range vector	36
pJET Δ cphA	<i>cphA</i> (ORF <i>slr2002</i>) knockout plasmid	This study
pVZ322 <i>cphA-egfp</i>	eGFP fused to the C terminus of <i>cphA</i>	This study

TABLE 3 Strains used in this study

Strain	Description	Reference or source
<i>E. coli</i> RP4	Conjugation strain	36
<i>E. coli</i> NEB 10-beta	Cloning strain	NEB
<i>E. coli</i> XL1-Blue	Cloning strain	Stratagene
<i>Synechocystis</i> sp. strain PCC 6803	Wild type	Pasteur Culture Collection
CphA-eGFP	Wild type transformed with pVZ322 <i>cphA-egfp</i>	This study
Δ <i>cphA</i> mutant	Chromosomal deletion of <i>cphA</i> (ORF <i>slr2002</i>)	This study

temperature. Unbound primary antibodies were removed by washing the membranes three times with TBS buffer. Anti-rabbit IgG secondary antibody conjugated to horseradish peroxidase (anti-rabbit polyclonal goat antibody; Sigma-Aldrich) diluted 1:1,000 in 1% (wt/vol) milk powder in TBS buffer was applied to the membranes and incubated for 30 min at ambient temperature. Afterwards, the membranes were washed three times with TBS buffer to remove unbound secondary antibodies. Bands were visualized using the Lumi-Light detection system (Roche Diagnostics). Luminograms were taken with the Gel Logic 1500 imaging system (Kodak) with the associated software.

Cyanophycin extraction and quantification. Cyanophycin was extracted according to Watzler et al. (17) and quantified by determining the amount of arginine in the extracted sample using the modified Sakaguchi reaction, according to Messineo (61). The determined amount of cyanophycin was normalized to the cell dry mass. The cell dry mass was determined by centrifuging 10 ml of culture and washing and drying the pellet for 4 h at 60°C in a rotational vacuum concentrator. The dried pellets were weighed on an analytical balance.

SUPPLEMENTAL MATERIAL

Supplemental material for this article may be found at <https://doi.org/10.1128/AEM.01298-18>.

SUPPLEMENTAL FILE 1, PDF file, 1.2 MB.

ACKNOWLEDGMENTS

This work was supported by grants from the DFG (Fo195/9-2) and the research training group GRK 1708.

We thank Alicia Engelbrecht and Waldemar Hauf for help in constructing the CphA-eGFP strain, Daniel Hörömpöli for technical assistance in immunoblot analysis, and Karen A. Brune, Niels Neumann, Sofia Doello, and Moritz Koch for carefully reading the manuscript.

REFERENCES

- Blankenship RE. 2017. How cyanobacteria went green. *Science* 355:1372–1373. <https://doi.org/10.1126/science.aam9365>.
- Herrero A, Flores E. 2008. *The cyanobacteria: molecular biology, genomics, and evolution*. Caister Academic Press, Norfolk, United Kingdom.
- Vitousek PM, Howarth RW. 1991. Nitrogen limitation on land and in the sea: how can it occur? *Biogeochemistry* 13:87–115. <https://doi.org/10.1007/BF00002772>.
- Schwarz R, Forchhammer K. 2005. Acclimation of unicellular cyanobacteria to macronutrient deficiency: emergence of a complex network of cellular responses. *Microbiology* 151:2503–2514. <https://doi.org/10.1099/mic.0.27883-0>.
- Allen MM, Smith AJ. 1969. Nitrogen chlorosis in blue-green algae. *Arch Mikrobiol* 69:114–120. <https://doi.org/10.1007/BF00409755>.
- Allen MM. 1984. Cyanobacterial cell inclusions. *Annu Rev Microbiol* 38:1–25. <https://doi.org/10.1146/annurev.mi.38.100184.000245>.
- Klotz A, Georg J, Budinska L, Watanabe S, Reimann V, Januszewski W, Sobotka R, Jendrossek D, Hess WR, Forchhammer K. 2016. Awakening of a dormant cyanobacterium from nitrogen chlorosis reveals a genetically determined program. *Curr Biol* 26:2862–2872. <https://doi.org/10.1016/j.cub.2016.08.054>.
- Görl M, Sauer J, Baier T, Forchhammer K. 1998. Nitrogen-starvation-induced chlorosis in *Synechococcus* PCC 7942: adaptation to long-term survival. *Microbiology* 144:2449–2458. <https://doi.org/10.1099/00221287-144-9-2449>.
- Sauer J, Schreiber U, Schmid R, Volker U, Forchhammer K. 2001. Nitrogen starvation-induced chlorosis in *Synechococcus* PCC 7942. Low-level photosynthesis as a mechanism of long-term survival. *Plant Physiol* 126:233–243.
- Doello S, Klotz A, Makowka A, Gutekunst K, Forchhammer K. 2018. A specific glycogen mobilization strategy enables awakening of dormant cyanobacteria from chlorosis. *Plant Physiol* 177:594–603. <https://doi.org/10.1104/pp.18.00297>.
- Spät P, Klotz A, Rexroth S, Maček B, Forchhammer K. 2018. Chlorosis as a developmental program in cyanobacteria: the proteomic fundament for survival and awakening. *Mol Cell Proteomics* <https://doi.org/10.1074/mcp.RA118.000699>.
- Klotz A, Forchhammer K. 2017. Glycogen, a major player for bacterial survival and awakening from dormancy. *Future Microbiol* 12:101–104. <https://doi.org/10.2217/fmb-2016-0218>.
- Allen MM, Hutchison F. 1980. Nitrogen limitation and recovery in the cyanobacterium *Aphanocapsa* 6308. *Arch Microbiol* 128:1–7. <https://doi.org/10.1007/BF00422297>.
- Füser G, Steinbüchel A. 2007. Analysis of genome sequences for genes of cyanophycin metabolism: identifying putative cyanophycin metabolizing prokaryotes. *Macromol Biosci* 7:278–296. <https://doi.org/10.1002/mabi.200600207>.
- Simon RD, Weathers P. 1976. Determination of the structure of the novel polypeptide containing aspartic acid and arginine which is found in cyanobacteria. *Biochim Biophys Acta* 420:165–176. [https://doi.org/10.1016/0005-2795\(76\)90355-X](https://doi.org/10.1016/0005-2795(76)90355-X).
- Allen MM, Hutchison F, Weathers PJ. 1980. Cyanophycin granule polypeptide formation and degradation in the cyanobacterium *Aphanocapsa* 6308. *J Bacteriol* 141:687–693.
- Watzler B, Engelbrecht A, Hauf W, Stahl M, Maldener I, Forchhammer K. 2015. Metabolic pathway engineering using the central signal processor P_{ii}. *Microb Cell Fact* 14:192. <https://doi.org/10.1186/s12934-015-0384-4>.
- Burnat M, Herrero A, Flores E. 2014. Compartmentalized cyanophycin metabolism in the diazotrophic filaments of a heterocyst-forming cyano-

- nobacterium. *Proc Natl Acad Sci U S A* 111:3823–3828. <https://doi.org/10.1073/pnas.1318564111>.
19. Sherman LA, Meunier P, Colon-Lopez MS. 1998. Diurnal rhythms in metabolism: a day in the life of a unicellular, diazotrophic cyanobacterium. *Photosynth Res* 58:25–42. <https://doi.org/10.1023/A:1006137605802>.
 20. Finzi-Hart JA, Pett-Ridge J, Weber PK, Popa R, Fallon SJ, Gunderson T, Hutcheon ID, Nealson KH, Capone DG. 2009. Fixation and fate of C and N in the cyanobacterium *Trichodesmium* using nanometer-scale secondary ion mass spectrometry. *Proc Natl Acad Sci U S A* 106:6345–6350. <https://doi.org/10.1073/pnas.0810647106>.
 21. Simon RD. 1976. The biosynthesis of multi-L-arginyl-poly(L-aspartic acid) in the filamentous cyanobacterium *Anabaena cylindrica*. *Biochim Biophys Acta* 422:407–418. [https://doi.org/10.1016/0005-2744\(76\)90151-0](https://doi.org/10.1016/0005-2744(76)90151-0).
 22. Berg H, Ziegler K, Piotukh K, Baier K, Lockau W, Volkmer-Engert R. 2000. Biosynthesis of the cyanobacterial reserve polymer multi-L-arginyl-poly-L-aspartic acid (cyanophycin): mechanism of the cyanophycin synthetase reaction studied with synthetic primers. *Eur J Biochem* 267:5561–5570. <https://doi.org/10.1046/j.1432-1327.2000.01622.x>.
 23. Ziegler K, Diener A, Herpin C, Richter R, Deutzmann R, Lockau W. 1998. Molecular characterization of cyanophycin synthetase, the enzyme catalyzing the biosynthesis of the cyanobacterial reserve material multi-L-arginyl-poly-L-aspartate (cyanophycin). *Eur J Biochem* 254:154–159. <https://doi.org/10.1046/j.1432-1327.1998.2540154.x>.
 24. Richter R, Hejazi M, Kraft R, Ziegler K, Lockau W. 1999. Cyanophycinase, a peptidase degrading the cyanobacterial reserve material multi-L-arginyl-poly-L-aspartic acid (cyanophycin): molecular cloning of the gene of *Synechocystis* sp. PCC 6803, expression in *Escherichia coli*, and biochemical characterization of the purified enzyme. *Eur J Biochem* 263:163–169.
 25. Hejazi M, Piotukh K, Mattow J, Deutzmann R, Volkmer-Engert R, Lockau W. 2002. Isoaspartyl dipeptidase activity of plant-type asparaginases. *Biochem J* 364:129–136. <https://doi.org/10.1042/bj3640129>.
 26. Elbahloul Y, Krehenbrink M, Reichelt R, Steinbüchel A. 2005. Physiological conditions conducive to high cyanophycin content in biomass of *Acinetobacter calcoaceticus* strain ADP1. *Appl Environ Microbiol* 71:858–866. <https://doi.org/10.1128/AEM.71.2.858-866.2005>.
 27. Leganés F, Fernandez-Pinas F, Wolk CP. 1998. A transposition-induced mutant of *Nostoc ellipsosporum* implicates an arginine-biosynthetic gene in the formation of cyanophycin granules and of functional heterocysts and akinetes. *Microbiology* 144:1799–1805. <https://doi.org/10.1099/00221287-144-7-1799>.
 28. Elbahloul Y, Steinbüchel A. 2006. Engineering the genotype of *Acinetobacter* sp. strain ADP1 to enhance biosynthesis of cyanophycin. *Appl Environ Microbiol* 72:1410–1419. <https://doi.org/10.1128/AEM.72.2.1410-1419.2006>.
 29. Maheswaran M, Ziegler K, Lockau W, Hagemann M, Forchhammer K. 2006. P_{II}-regulated arginine synthesis controls accumulation of cyanophycin in *Synechocystis* sp. strain PCC 6803. *J Bacteriol* 188:2730–2734. <https://doi.org/10.1128/JB.188.7.2730-2734.2006>.
 30. Heinrich A, Maheswaran M, Ruppert U, Forchhammer K. 2004. The *Synechococcus elongatus* P_{II} signal transduction protein controls arginine synthesis by complex formation with N-acetyl-L-glutamate kinase. *Mol Microbiol* 52:1303–1314. <https://doi.org/10.1111/j.1365-2958.2004.04058.x>.
 31. Fokina O, Chellamuthu VR, Forchhammer K, Zeth K. 2010. Mechanism of 2-oxoglutarate signaling by the *Synechococcus elongatus* P_{II} signal transduction protein. *Proc Natl Acad Sci U S A* 107:19760–19765. <https://doi.org/10.1073/pnas.1007653107>.
 32. Forchhammer K. 2008. P_{II} signal transducers: novel functional and structural insights. *Trends Microbiol* 16:65–72. <https://doi.org/10.1016/j.tim.2007.11.004>.
 33. Maheswaran M, Urbanke C, Forchhammer K. 2004. Complex formation and catalytic activation by the P_{II} signaling protein of N-acetyl-L-glutamate kinase from *Synechococcus elongatus* strain PCC 7942. *J Biol Chem* 279:55202–55210. <https://doi.org/10.1074/jbc.M410971200>.
 34. Wolk CP, Vonshak A, Kehoe P, Elhai J. 1984. Construction of shuttle vectors capable of conjugative transfer from *Escherichia coli* to nitrogen-fixing filamentous cyanobacteria. *Proc Natl Acad Sci U S A* 81:1561–1565.
 35. Simon RD. 1973. Measurement of the cyanophycin granule polypeptide contained in the blue-green alga *Anabaena cylindrica*. *J Bacteriol* 114:1213–1216.
 36. Merritt MV, Sid SS, Mesh L, Allen MM. 1994. Variations in the amino acid composition of cyanophycin in the cyanobacterium *Synechocystis* sp. PCC 6308 as a function of growth conditions. *Arch Microbiol* 162:158–166.
 37. Aboulmagd E, Oppermann-Sanio FB, Steinbüchel A. 2000. Molecular characterization of the cyanophycin synthetase from *Synechocystis* sp. strain PCC6308. *Arch Microbiol* 174:297–306. <https://doi.org/10.1007/s002030000206>.
 38. Flores E, Herrero A. 1994. Assimilatory nitrogen metabolism and its regulation, p 487–517. In Bryant DA (ed), *The molecular biology of cyanobacteria*. Springer Netherlands, Dordrecht, The Netherlands.
 39. Flores E, Herrero A. 2005. Nitrogen assimilation and nitrogen control in cyanobacteria. *Biochem Soc Trans* 33:164–167. <https://doi.org/10.1042/BST0330164>.
 40. Kikuchi H, Aichi M, Suzuki I, Omata T. 1996. Positive regulation by nitrite of the nitrate assimilation operon in the cyanobacteria *Synechococcus* sp. strain PCC 7942 and *Plectonema boryanum*. *J Bacteriol* 178:5822–5825. <https://doi.org/10.1128/jb.178.19.5822-5825.1996>.
 41. Lee HM, Flores E, Herrero A, Houmard J, Tandeau de Marsac N. 1998. A role for the signal transduction protein P_{II} in the control of nitrate/nitrite uptake in a cyanobacterium. *FEBS Lett* 427:291–295. [https://doi.org/10.1016/S0014-5793\(98\)00451-7](https://doi.org/10.1016/S0014-5793(98)00451-7).
 42. Romero JM, Lara C, Guerrero MG. 1985. Dependence of nitrate utilization upon active CO₂ fixation in *Anacystis nidulans*: a regulatory aspect of the interaction between photosynthetic carbon and nitrogen-metabolism. *Arch Biochem Biophys* 237:396–401. [https://doi.org/10.1016/0003-9861\(85\)90291-7](https://doi.org/10.1016/0003-9861(85)90291-7).
 43. Marqués S, Merida A, Candau P, Florencio FJ. 1992. Light-mediated regulation of glutamine-synthetase activity in the unicellular cyanobacterium *Synechococcus* sp. PCC 6301. *Planta* 187:247–253. <https://doi.org/10.1007/BF00201947>.
 44. García-Domínguez M, Reyes JC, Florencio FJ. 1999. Glutamine synthetase inactivation by protein-protein interaction. *Proc Natl Acad Sci U S A* 96:7161–7166. <https://doi.org/10.1073/pnas.96.13.7161>.
 45. Galmozzi CV, Fernandez-Avila MJ, Reyes JC, Florencio FJ, Muro-Pastor MI. 2007. The ammonium-inactivated cyanobacterial glutamine synthetase I is reactivated *in vivo* by a mechanism involving proteolytic removal of its inactivating factors. *Mol Microbiol* 65:166–179. <https://doi.org/10.1111/j.1365-2958.2007.05773.x>.
 46. Kloft N, Forchhammer K. 2005. Signal transduction protein P_{II} phosphatase PphA is required for light-dependent control of nitrate utilization in *Synechocystis* sp. strain PCC 6803. *J Bacteriol* 187:6683–6690. <https://doi.org/10.1128/JB.187.19.6683-6690.2005>.
 47. Forchhammer K, Tandeau de Marsac N. 1995. Phosphorylation of the P_{II} protein (*glnB* gene product) in the cyanobacterium *Synechococcus* sp. strain PCC 7942: analysis of *in vitro* kinase activity. *J Bacteriol* 177:5812–5817. <https://doi.org/10.1128/jb.177.20.5812-5817.1995>.
 48. Reyes JC, Crespo JL, Garcíadomínguez M, Florencio FJ. 1995. Electron-transport controls glutamine-synthetase activity in the facultative heterotrophic cyanobacterium *Synechocystis* sp. PCC 6803. *Plant Physiol* 109:899–905.
 49. Espinosa J, Rodríguez-Mateos F, Salinas P, Lanza VF, Dixon R, de la Cruz F, Contreras A. 2014. PipX, the coactivator of NtcA, is a global regulator in cyanobacteria. *Proc Natl Acad Sci U S A* 111:E2423–E2430. <https://doi.org/10.1073/pnas.1404097111>.
 50. Vázquez-Bermúdez MF, Herrero A, Flores E. 2002. 2-Oxoglutarate increases the binding affinity of the NtcA (nitrogen control) transcription factor for the *Synechococcus glnA* promoter. *FEBS Lett* 512:71–74. [https://doi.org/10.1016/S0014-5793\(02\)02219-6](https://doi.org/10.1016/S0014-5793(02)02219-6).
 51. Paz-Yepes J, Flores E, Herrero A. 2003. Transcriptional effects of the signal transduction protein P_{II} (*glnB* gene product) on NtcA-dependent genes in *Synechococcus* sp. PCC 7942. *FEBS Lett* 543:42–46.
 52. Tanigawa R, Shirokane M, Maeda S, Omata T, Tanaka K, Takahashi H, Takahashi H. 2002. Transcriptional activation of NtcA-dependent promoters of *Synechococcus* sp. PCC 7942 by 2-oxoglutarate *in vitro*. *Proc Natl Acad Sci U S A* 99:4251–4255. <https://doi.org/10.1073/pnas.072587199>.
 53. García-Domínguez M, Reyes JC, Florencio FJ. 2000. NtcA represses transcription of *gifA* and *gifB*, genes that encode inhibitors of glutamine synthetase type I from *Synechocystis* sp. PCC 6803. *Mol Microbiol* 35:1192–1201.
 54. Rippka R, Deruelles J, Waterbury JB, Herdman M, Stanier RY. 1979. Generic assignments, strain histories and properties of pure cultures of cyanobacteria. *J Gen Microbiol* 111:1–61.
 55. Gibson DG, Young L, Chuang RY, Venter JC, Hutchison CA, Smith HO. 2009. Enzymatic assembly of DNA molecules up to several hundred kilobases. *Nat Methods* 6:343–345. <https://doi.org/10.1038/nmeth.1318>.
 56. Grigorieva G, Shestakov S. 1982. Transformation in the cyanobacterium

- Synechocystis* sp. 6803. FEMS Microbiol Lett 13:367–370. <https://doi.org/10.1111/j.1574-6968.1982.tb08289.x>.
57. Muro-Pastor AM, Olmedo-Verd E, Flores E. 2006. All4312, an NtcA-regulated two-component response regulator in *Anabaena* sp. strain PCC 7120. FEMS Microbiol Lett 256:171–177. <https://doi.org/10.1111/j.1574-6968.2006.00136.x>.
 58. Bradford MM. 1976. A rapid and sensitive method for the quantitation of microgram quantities of protein utilizing the principle of protein-dye binding. Anal Biochem 72:248–254. [https://doi.org/10.1016/0003-2697\(76\)90527-3](https://doi.org/10.1016/0003-2697(76)90527-3).
 59. Sambrook J, Russell D. 2001. Molecular cloning: a laboratory manual, 3rd ed, vol 1. Cold Spring Harbor Laboratory Press, Cold Spring Harbor, NY.
 60. Towbin H, Staehelin T, Gordon J. 1979. Electrophoretic transfer of proteins from polyacrylamide gels to nitrocellulose sheets: procedure and some applications. Proc Natl Acad Sci U S A 76:4350–4354.
 61. Messineo L. 1966. Modification of Sakaguchi reaction: spectrophotometric determination of arginine in proteins without previous hydrolysis. Arch Biochem Biophys 117:534–540. [https://doi.org/10.1016/0003-9861\(66\)90094-4](https://doi.org/10.1016/0003-9861(66)90094-4).

7. Manuscript in preparation

Watzel, B., Spät, P., Neumann, N., Koch, M., Hennrich, O. & Forchhammer, K.

The signal transduction protein P_{II} controls ammonium, nitrate and urea uptake in cyanobacteria

Preliminary Manuscript, version 07.12.2018

Submitted to *Frontiers in Microbiology* (ISSN 1664302x) on 09.04.2019

The signal transduction protein P_{II} controls ammonium, nitrate and urea uptake in cyanobacteria

1 Björn Watzler¹, Philipp Spät^{1,2}, Niels Neumann¹, Moritz Koch¹, Oliver Hennrich¹,
2 Karl Forchhammer^{1*}

3 ¹Interfaculty Institute of Microbiology and Infection Medicine Tuebingen, Department of
4 Organismic Interactions, Eberhard Karls Universität Tübingen

5 ²Proteome Center Tuebingen, Eberhard Karls Universität Tübingen,

6 * Correspondence:

7 Karl Forchhammer

8 karl.forchhammer@uni-tuebingen.de

9 **Keywords: P_{II} signaling protein, GlnB, Cyanobacteria, Nitrogen regulation, Nitrate**
10 **uptake, Ammonia uptake, Urea uptake, ABC transporters**

11

12 Abstract

13 P_{II} signal transduction proteins are widely spread among all domains of life where they
14 regulate a multitude of carbon and nitrogen metabolism related processes. Non-diazotrophic
15 cyanobacteria can utilize a high variety of organic and inorganic nitrogen sources. In recent
16 years, several studies demonstrated an involvement of the cyanobacterial P_{II} protein in
17 regulation of ammonium, nitrate/nitrite and cyanate uptake. However, information regarding
18 the involvement of the P_{II} protein in nitrogen uptake are largely scattered in literature. In this
19 study, we concretize the dependence of P_{II} for nitrogen uptake regulation in the unicellular
20 and non-diazotrophic cyanobacterium *Synechocystis* sp. PCC 6803. By using biochemical and
21 physiological approaches we could demonstrate that P_{II} regulates ammonium uptake by
22 interacting with the Amt1 ammonium permease; similar to the regulation of the P_{II}
23 homologue GlnK and the ammonium permease AmtB described for *E. coli*. We could further
24 clarify that P_{II} mediates the light and ammonium depending inhibition of nitrate uptake by
25 interacting with the NrtC and NrtD subunit of the nitrate/nitrite transporter NrtABCD. Both
26 interactions, with the Amt1 permease and the NrtC/D subunits, require the large surface
27 exposed T-loop structure of P_{II}. In course of this study we further identified the ABC-type
28 urea transporter UrtABCDE as novel P_{II} target. We could demonstrate the involvement of P_{II}
29 in regulation of the urea uptake by interacting with the UrtE subunit in a T-loop independent
30 manner. The deregulation of urea uptake in a P_{II} deletion mutant causes an ammonium
31 excretion when urea is provided as nitrogen source. Furthermore, we found evidences for a
32 regulation of the urea hydrolyzing urease by P_{II}. Overall, this study underlines the great
33 importance of the P_{II} signal transduction protein in the regulation of nitrogen utilization in
34 cyanobacteria.

35 1 Introduction

36 Around 2.3 billion years ago, the biologically induced accumulation of oxygen in earth's
37 atmosphere represents one of the most important turning points in the development of life and
38 enabled the evolution of our present flora and fauna. This change in the redox-state of earth's
39 atmosphere were triggered by the emergence of the oxygenic photosynthesis by ancestors of
40 present cyanobacteria (Soo et al., 2017). Down to the present day, cyanobacteria occupy a
41 high variety of illuminated habitats, where they represent one of the quantitatively most
42 abundant organisms (Whitton, 2012). As primary producer, cyanobacteria are essential
43 contributors to the global carbon cycle. A part of the cyanobacterial strains acquired the
44 ability to fix atmospheric nitrogen. These diazotrophic cyanobacteria are the dominant N₂-
45 fixers in the oceans, making them key players in the global nitrogen turnover (Herrero and
46 Flores, 2008). Nitrogen represents a necessary macronutrient for all living organisms and
47 therefore constitutes an important growth limiting factor in most ecosystems (Vitousek and
48 Howarth, 1991). The regulation of the nitrogen metabolism in cyanobacteria mainly depends
49 on the fine-tuned network of the signal transduction protein P_{II}, the global nitrogen
50 transcription factor NtcA and the NtcA co-activator PipX (Vegapalas et al., 1992; Espinosa et
51 al., 2006; Espinosa et al., 2007; Forchhammer, 2008; Espinosa et al., 2014).

52 P_{II} signal-transduction proteins are widely spread in all three domains of life, where they
53 represent one of the largest and most ancient families of signaling proteins in nature
54 (Chellamuthu et al., 2013; Forchhammer and Luddecke, 2016). P_{II} proteins are involved in the
55 regulation of various nitrogen and carbon metabolism associated processes (Forchhammer,
56 2004; 2008). Canonical P_{II} proteins are homo-trimeric with three characteristic loop regions,
57 designated as B-, C- and T-loops. The B- and T-loops of one subunit form a binding pocket
58 for adenylnucleotides in the inter-subunit cleft together with the C-loop of the neighboring
59 subunit (Cheah et al., 1994; Xu et al., 2003; Forchhammer, 2004; Llacer et al., 2007;
60 Forchhammer, 2008; Fokina et al., 2010a; Zhao et al., 2010; Zeth et al., 2014). Canonical P_{II}
61 proteins can sense the energy status of the cell by the competitive binding of ADP or ATP
62 (Zeth et al., 2014). Binding of ATP and synergistic binding of 2-oxoglutarate (2-OG) allows
63 P_{II} to sense the current carbon/ nitrogen status of the cell (Fokina et al., 2010a). 2-OG is an
64 intermediate of the TCA-cycle that provides the carbon skeleton for inorganic nitrogen
65 incorporation by the GS/GOGAT cycle. Due to this, 2-OG represents the link between the
66 carbon and nitrogen metabolism and therefore acts as an indicator for the intracellular
67 carbon/nitrogen balance (Muro-Pastor et al., 2001; Fokina et al., 2010a). Besides effector
68 molecule binding, post translational modifications of P_{II} represent a second level of
69 regulation. Depending on the nitrogen availability, the cyanobacterial P_{II} can be
70 phosphorylated at the apex of the T-loop at position Ser49 (Forchhammer and Tandeau de
71 Marsac, 1995; Forchhammer and Hedler, 1997). In cells grown in presence of ammonium, P_{II}
72 is completely non-phosphorylated. In nitrate growing cells, an intermediate level of
73 phosphorylation can be observed, while the highest phosphorylation level occurs under
74 nitrogen starvation (Forchhammer and Demarsac, 1995). In other prokaryotes, like *E.coli*, P_{II}
75 is modified by uridylylation in dependence of nitrogen availability instead of phosphorylation
76 (Jiang et al., 1998). Binding of ATP, ADP and 2-OG as well as post translational
77 modifications lead to conformational rearrangements of the surface-exposed T-loop.
78 Depending on the conformational state, P_{II} can interact with a variety of interaction partners
79 and thereby regulate the cellular C/N balance (Radchenko and Merrick, 2011; Forchhammer
80 and Luddecke, 2016). In cyanobacteria, P_{II} regulates the global nitrogen control
81 transcriptional factor NtcA through binding of the NtcA co-activator PipX (Espinosa et al.,

2007). In common with other bacteria, the cyanobacterial P_{II} protein can control the acetyl-CoA levels by interacting with the biotin carboxyl carrier protein (BCCP) of acetyl-CoA carboxylase (ACC) (Hauf et al., 2016). Furthermore, P_{II} regulates the arginine biosynthesis by interacting with the enzyme N-acetylglutamate kinase (NAGK), which catalyzes the key rate-limiting step in the arginine biosynthesis (Caldovic and Tuchman, 2003; Heinrich et al., 2004; Llacer et al., 2007; Watzer et al., 2015). If sufficient energy and nitrogen is available, indicated by a high intracellular ATP and low 2-OG level, non-phosphorylated P_{II} can interact with NAGK (Heinrich et al., 2004). This complex formation enhances the catalytic efficiency of NAGK and relieves the feedback inhibitory effect of arginine to its reaction (Heinrich et al., 2004; Maheswaran et al., 2004; Llacer et al., 2007). The accumulation of the carbon/nitrogen storage polymer cyanophycin (multi-l-arginyl-poly-l-aspartate) is mainly depending on the availability of arginine. Therefore, P_{II} regulates directly the arginine biosynthesis and indirectly the cyanophycin synthesis via NAGK regulation (Maheswaran et al., 2006; Watzer et al., 2015). In P_{II} mutagenesis experiments, a P_{II} variant was identified with a single amino acid substitution, Ile86 to Asn86, hereafter referred as P_{II}(I86N), that binds NAGK constitutively *in vitro* (Fokina et al., 2010b). By replacing the wild-type P_{II} with a I86N variant in *Synechocystis* sp. PCC 6803 (hereafter *Synechocystis* sp.), it was previously possible to generate a strain which strongly overproduces arginine and cyanophycin (Watzer et al., 2015). Since cyanophycin is of high commercial interest, process optimization was performed to further increase the total cyanophycin yield of the P_{II}(I86N) strain. In experiments to define the best nitrogen source, it surprisingly turned out that strain P_{II}(I86N) is impaired in ammonium utilization (Watzer et al., 2015).

Non-diazotrophic cyanobacteria can utilize a high variety of organic and inorganic nitrogen sources, including ammonium, nitrate, nitrite, urea and several amino acids (Labarre et al., 1987; Flores and Herrero, 1994; Whitton, 2012; Esteves-Ferreira et al., 2018). These nitrogen sources are utilized in a hierarchical order, in which ammonia is the preferred nitrogen sources. As a consequence, when ammonia is provided together with other suitable nitrogen sources, ammonia will be utilized primarily (Muro-Pastor et al., 2005). At high pH, a major fraction of ammonium is present in form of ammonia, which is able to diffuse passively through biological membranes at high concentrations (Kleiner, 1981). However, in most natural habitats, the ammonia availability is low, what leads to the necessity of high affinity ammonia permeases (Rees et al., 2006). In the unicellular and non-diazotrophic cyanobacterium *Synechocystis* sp., the Amt1 permeases are mainly responsible for ammonia uptake (Montesinos et al., 1998). The ammonium transporter family (Amt) is widely spread among all domains of life (Wirén and Merrick, 2004). In *E. coli*, the P_{II} homologue GlnK regulates the ammonium permease AmtB by direct protein-protein interaction. In case of an ammonia excess, the intracellular 2-OG level decreases rapidly and the GlnK T-loop becomes de-uridylyated. In its ADP bound and non-deuridylyated state, GlnK blocks the ammonia influx by inserting the apex of the T-loop into the cytoplasmic exits of the AmtB pores to prevent uncontrolled influx of ammonia (Conroy et al., 2007).

Nitrate and nitrite are the most abundant nitrogen sources for cyanobacteria in their natural habitat (Guerrero et al., 1981; Rees et al., 2006). For the assimilation of nitrate, an active nitrate transporter, a nitrate reductase (NR) and a nitrite reductase (NiR) are required (Ohashi et al., 2011). Two types of nitrate transporter were found among cyanobacteria, a high-affinity nitrate/nitrite permease NrtP and the ABC type transporter NrtABCD (Omata et al., 1993a; Luque et al., 1994; Sakamoto et al., 1999; Ohashi et al., 2011). NrtABCD is a bispecific nitrate and nitrite transporter showing high affinity for both substrates (Maeda and Omata,

129 1997). Intracellular nitrate is first reduced to nitrite by NR and subsequently reduced to
130 ammonium by NiR. The reduction of nitrate requires two electrons whereas six electrons are
131 required for the reduction of nitrite. Afterwards, ammonium is directly assimilated in the
132 GS/GOGAT cycle (Flores and Herrero, 1994). Both, NR and NiR, use photosystem I reduced
133 ferredoxin as an electron donor, indicating a coupling of photosynthesis and nitrate
134 assimilation (Manzano et al., 1976; Flores and Herrero, 1994). Since ammonium is the
135 preferred nitrogen source, the addition of ammonia to nitrate adapted cells result in an
136 immediate inhibition of nitrate uptake and a repression of proteins involved in nitrate
137 assimilation (NR and NiR). The ammonium induced inhibition of NrtABCD is regulated by
138 the P_{II} protein and the C-terminal domain of NrtC (Kobayashi et al., 1997; Lee et al., 1998).
139 The ammonium depended regulation of NrtABCD by P_{II} occurs independently of its
140 phosphorylation since phosphorylation mimicking mutants of P_{II} showed ammonium promoted
141 inhibition of nitrate uptake like the wild-type (Lee et al., 2000). Furthermore, ammonium
142 induced inhibition of nitrate utilization was not effected in a P_{II} phosphatase deletion mutant
143 (PphA), which exhibits a continuous high phosphorylated P_{II}. In contrast, a P_{II} deletion mutant
144 shows an impaired regulation in nitrate uptake (Kloft and Forchhammer, 2005). Both P_{II}
145 signaling deficient mutants, the P_{II} deletion mutant and the PphA deletion mutant, excrete
146 nitrite in the medium under conditions of limited photosystem I reduced ferredoxin (low light).
147 The excretion of nitrite is due to an excess of reduction of nitrate along with an impaired
148 reduction of nitrite (Forchhammer and Demarsac, 1995; Kloft and Forchhammer, 2005). This
149 effect can be restored by increasing the level of photosystem I reduced ferredoxin (high light).
150 This behavior indicates that non-phosphorylated P_{II} regulates the utilization of nitrate in
151 response to light intensity and the coupled redox-state of the cell (Kloft and Forchhammer,
152 2005).

153 The ability to utilize urea as nitrogen source is widely distributed among bacteria, fungi and
154 algae (Baker et al., 2009; Solomon et al., 2010; Esteves-Ferreira et al., 2018). Urea is usually
155 present at ambient concentrations below 1 μ M in aquatic ecosystems (Mitamura and Saijo,
156 1980; Antia et al., 1991). Generally, the urea concentrations in aquatic ecosystems are lower
157 than those of nitrate or ammonium; however, urea concentrations may occasionally exceed
158 the concentrations of these inorganic nitrogen forms (Solomon et al., 2010). In common with
159 other bacteria, the cyanobacteria *Synechocystis* sp. and *Anabaena* sp. PCC 7120 process a
160 high affinity urea ABC-type transporter, which is capable of urea import at concentrations
161 lower than 1 μ M (Valladares et al., 2002). The gene cluster *urtABCDE*, encoding all subunits
162 of this ABC-type urea transporter, are transcriptional controlled by the global transcription
163 factor NtcA (Valladares et al., 2002).

164 The impaired ammonium utilization of *Synechocystis* sp. which harbors the P_{II}(I86N) variant,
165 implied a relation between P_{II} signaling and ammonium uptake in cyanobacteria. This
166 observation goes in line with several other studies which document a connection between P_{II}
167 signaling and utilization of different suitable nitrogen sources. To analyze a possible
168 regulation of the cyanobacterial Amt1 permease by P_{II}, we found further evidence for an
169 involvement of P_{II} in the regulation of the nitrate/ nitrite transporter NrtABCD and the urea
170 transporter UrtABCDE in *Synechocystis* sp.

171 **2 Materials and Methods**

172 **2.1 Cultivation conditions**

173 Standard procedures for cloning were performed in *Escherichia coli* NEB 10-beta (NEB).
174 Strains were grown in LB-medium at 37°C with constant shaking at 300 rpm.

175 *Synechocystis* sp. strains were grown photoautotrophically in BG-11 medium supplemented
176 with 5 mM NaHCO₃ and nitrate, ammonia or urea as nitrogen source (Rippka et al., 1979).
177 BG-11 agar plates were produced by adding 1.5 % (w/v) Bacto-agar (Difco), 0.3 % (w/v)
178 sodium thiosulfate pentahydrate and 10 mM TES-NaOH pH 8 (Roth) to liquid BG-11
179 Medium. Antibiotics were added when required. Cultivation of liquid cultures occurs in 50,
180 100 or 500 ml Erlenmeyer flasks, at 28°C and with constant shaking of 120 rpm. Cultures
181 were continuously illuminated with a photon flux rate of 40–50 μE. Growth rates were
182 determined by measuring the optical density at 750 nm.

183 For induction of nitrogen starvation conditions, exponentially growing cells (OD₇₅₀ 0.4–0.8)
184 were harvested by centrifugation (3000 x g for 10 min at room temperature), washed and
185 resuspended in BG-11 medium lacking a suitable nitrogen source.

186 For drop-agar assays, *Synechocystis* sp. cultures were adjusted to an OD₇₅₀ of 1. A dilution
187 series to the power of 10 was made using BG-11 medium lacking nitrogen. 5 μl of every
188 dilution step (10⁰–10⁻⁴) were dropped on BG-11 agar plates. Plates were cultivated at 28°C
189 with constant illumination of 40–50 μE.

190

191 **2.2 Bacterial two-hybrid assay**

192 Plasmids were constructed by PCR amplification using high-fidelity Q5 polymerase (NEB)
193 and oligonucleotides with overlapping regions. Genomic *Synechocystis* sp. DNA or plasmids
194 served as the templates. PCR fragments were inserted in linearized bacterial two hybrid
195 vectors pUT18 and pKT25 containing the either the T18 or T25 subunit of the adenylate
196 cyclase CyaA (Karimova et al., 2001) by isothermal, single-reaction DNA assembly
197 according to Gibson *et al* (Gibson et al., 2009). Since the multiple cloning site of pKT25 is
198 located downstream of the T25 subunit, allowing only N-terminal localization of the tag, we
199 constructed plasmid pKT25n to achieve a C-terminal fusion of the tag to the gene of interest.
200 Therefore plasmid pKT25 was linearized using PCR and the gene of interest was fused
201 upstream of the T25 subunit. Primers, plasmids, and strains used in this study are listed in
202 Tables 4, 5, and 6, respectively.

203 *E.coli* BTH101 cells were co-transformed with plasmid pUT18 and plasmid pKT25 or
204 pKT25n (table 5). Plasmid pKT25 or pKT25n encodes a possible P_{II} interaction partner fused
205 N- or C-terminal to the T25 subunit. Plasmid pUT18 encodes a fusion of the P_{II}-encoding
206 *glnB* gene or a genetically modified *glnB* gene containing the I86N mutation [Ile (5'ATC) at
207 codon position 86 to Asn (5'AAC)] with the T18 subunit. The *glnB* gene and the modified
208 *glnB* gene containing the I86N mutation were always fused N-terminal with the T18 subunit,
209 since the C-terminus of P_{II} is necessary for interactions. Co-transformants were plated on LB-
210 plates (supplemented with 100 μg ml⁻¹ ampicillin and 50 μg ml⁻¹ kanamycin) and cultivated
211 for 2 days at 30°C.

The signal transduction protein P_{II} controls ammonium, nitrate and urea uptake in cyanobacteria

212 To achieve a reasonable level of heterogeneity 5 clones from each plate were picked to
 213 inoculate 5 ml LB- medium (containing 100 µg ml⁻¹ ampicillin and 50 µg ml⁻¹ kanamycin).
 214 Cultures were cultivated overnight at 37°C. Overnight culture were diluted 1:100 in 3 ml
 215 fresh LB-medium (containing 100 µg ml⁻¹ ampicillin and 50 µg ml⁻¹ kanamycin) and grown to
 216 an OD₆₀₀ of 0.7. 3µl of each culture were plated on X-Gal (containing 100 µg mL⁻¹
 217 ampicillin, 50 µg mL⁻¹ kanamycin, 1mM IPTG, 40µg mL⁻¹ X-Gal) and MacConkey
 218 (containing 100 µg mL⁻¹ ampicillin, 50 µg mL⁻¹ kanamycin, 1mM IPTG, 1% maltose)
 219 reporter plates. Reporter plates were incubated for 3 days at 25°C.

220 Table 1 Oligonucleotides used in this study

Primer	Sequence
glnB_fw	TGTGTGGAATTGTGAGCGGATAACAATTTACACAGGAAACAGCTATGAAAAAAGTAGAAGCGATTATTC
glnB_rev	CTCGCTGGCGGCTGAATTCGAGCTCGGTACCCGGGGATCAATAGCTTCGGTATCCTTTTC
pipX_fw	TTCACACAGGAAACAGCTATGAGTAACGAAATTTACCTTAAC
pipX_rev	GATGCGATTGCTGCATGGTAAAAAGTGTTTTATGTAACTTTG
pipX_pKT25n_fw	AAGTTACATAAAAAACTTTTACCATGCAGCAATCGCATCAG
pipX_pKT25n_rev	TAAGGTAAATTTTCGTTACTCATAGCTGTTTCCTGTGTGAAATTG
amt1_pKT25_fw	CTGGCGCGCACGGCGGGCTGCAGGGTCGACTCTAGAGATGTCTAATTCGATATTGTCTAAAC
amt1_pKT25_rev	AAAACGACGGCCGAATTCCTTAGTTACTTAGGTACCCGGGGATCTTATTCAGGGACAGTGG
amt1_fw	AACAATTTACACAGGAAACAGCTATGTCTAATTCGATATTGTCTAAAC
amt1_rev	TGATGCGATTGCTGCATGGTTTCAGGGACAGTGGCACCG
amt1_pKT25n_fw	TCTCCGGTGCCACTGTCCCTGAAACCATGCAGCAATCGCATC
amt1_pKT25n_rev	ACAATATCGAATTAGACATAGCTGTTTCCTGTGTGAAATTGTTATCCGC
nrtC_pKT25_fw	CGCGCACGGCGGGCTGCAGGGTCGACTCTAGAGGATCCCCCTTCATTGAAATTGATCATGTTG
nrtC_pKT25_rev	AGTCACGACGTTGTAACGACGGCCGAATTCCTAGTTATTGATTAAGTTGATCAATTTGGTCGATGAG
nrtC_fw	AATTTACACAGGAAACAGCTATGCCCTTCATTGAAATTGATCATG
nrtC_rev	CTGATGCGATTGCTGCATGGTTTGATTAAGTTGATCAATTTGG
nrtC_pKT25n_fw	AAATTGATCAAGTTAATCAAACCATGCAGCAATCGCATCAG
nrtC_pKT25n_rev	TCAATTTCAATGAAGGGCATAGCTGTTTCCTGTGTGAAATTG
nrtD_pKT25_fw	CGCACGGCGGGCTGCAGGGTCGACTCTAGAGGATCCCCAAACAATGAATGTCAATGACCCTATCC
nrtD_pKT25_rev	CCCAGTCACGACGTTGTAACGACGGCCGAATTCCTAGTTAAGACCCTTCCATGGATTCCACTGAGGGGGTAG
nrtD_fw	AATTTACACAGGAAACAGCTATGCAACAATGAATGTCAATGACCCTATC
nrtD_rev	CTGATGCGATTGCTGCATGGTAGACCCTTCCATGGATTCCACTGAG

The signal transduction protein P_{II} controls ammonium, nitrate and urea uptake in cyanobacteria

nrtD_pKT25n_fw	TGGAATCCATGGAAGGGTCTACCATGCAGCAATCGCATCAG
nrtD_pKT25n_rev	ATTGACATTCATTGTTTGCATAGCTGTTTCCTGTGTGAAATTG
urtD_pKT25_fw	CGCACGCGGGGGCTGCAGGGTCTAGAGGATCCCACCAGCAAAATCTTAGAAATTCAAG
urtD_pKT25_rev	CCCAGTCACGACGTTGTA AACGACGGCCGAATCTTAGCTAATCTCCATCCTCATCAAC
urtD_fw	ACACAGGAAACAGCTATGACCAGCAAAATCTTAGAAATTCAAGAC
urtD_rev	GATGCGATTGCTGCATGGTATCTCCATCCTCATCAACACTG
urtD_pKT25n_fw	AGTGTTGATGAGGATGGAGATACCATGCAGCAATCGCATCAG
urtD_pKT25n_rev	TTCTAAGATTTTGCTGGTCATAGCTGTTTCCTGTGTGAAATTG
urtE_fw	GCGCGCACGCGGGGGCTGCAGGGTCTAGAGGATGCTATGTTATCCTTTCCCCATTCTTG
urtE_rev	CCCAGTCACGACGTTGTA AACGACGGCCGAATCTTAGTTATACTGCCAAAAATTTTGGATAAC
urtE_fw	ACAATTCACACAGGAAACAGCTATGGCTATGTTATCCTTTCCC
urtE_rev	TGATGCGATTGCTGCATGGTACTGCCAAAAATTTTGGATAACC
urtE_pKT25n_fw	TATCCAAAAATTTTGGCAGTAACCATGCAGCAATCGCATCAG
urtE_pKT25n_rev	GGGAAAGGATAACATAGCCATAGCTGTTTCCTGTGTGAAATTG

221

222 Table 2 Plasmids used in this study

Plasmid	Tag localization	Description	Reference
pPD-CFLAG		Encoding the 3×FLAG tag	(Chidgey et al., 2014)
pKT25		Encoding T25 fragment of adenylate cyclase CyaA (amino acids 1–224)	(Karimova et al., 2001)
pKT25n		Derived from pKT25. Upstream of the T25 fragment	This study
pUT18		Encoding T18 fragment of adenylate cyclase CyaA (amino acids 225–399)	(Karimova et al., 2001)
pUT18 <i>glnB</i>	N-terminal	Derived from pUT18. Encoding <i>glnB</i>	This study
pUT18 <i>glnB</i> (I86N)	N-terminal	Derived from pUT18. Encoding <i>glnB</i> containing the I86N mutation	This study
pKT25n <i>pipX</i>	C-terminal	Derived from pKT25. Sequence encoding <i>pipX</i> . Positive control	This study

pKT25 <i>pipX</i>	N-terminal	Derived from pKT25. Sequence encoding <i>pipX</i> . Positive control	This study
pKT25n <i>amt1</i>	C-terminal	Derived from pKT25. Sequence encoding <i>amt1</i>	This study
pKT25 <i>amt1</i>	N-terminal	Derived from pKT25. Sequence encoding <i>amt1</i>	This study
pKT25n <i>nrtC</i>	C-terminal	Derived from pKT25. Sequence encoding <i>nrtC</i>	This study
pKT25 <i>nrtC</i>	N-terminal	Derived from pKT25. Sequence encoding <i>nrtC</i>	This study
pKT25n <i>nrtD</i>	C-terminal	Derived from pKT25. Sequence encoding <i>nrtD</i>	This study
pKT25 <i>nrtD</i>	N-terminal	Derived from pKT25. Sequence encoding <i>nrtD</i>	This study
pKT25n <i>urtD</i>	C-terminal	Derived from pKT25. Sequence encoding <i>urtD</i>	This study
pKT25 <i>urtD</i>	N-terminal	Derived from pKT25. Sequence encoding <i>urtD</i>	This study
pKT25n <i>urtE</i>	C-terminal	Derived from pKT25. Sequence encoding <i>urtE</i>	This study
pKT25 <i>urtE</i>	N-terminal	Derived from pKT25. Sequence encoding <i>urtE</i>	This study

223

224 Table 3 Strains used in this study

Strains	Description	Reference
<i>E.coli</i> NEB 10-beta	Cloning strain	NEB
<i>E.coli</i> BTH101	Bacterial two-hybrid host strain	Euromedex
<i>Synechocystis</i> sp. PCC 6803	Wild type	Pasteur Culture Collection
<i>Synechocystis</i> sp. P _{II} (I86N)	Genomic P _{II} (I86N) mutant	(Watzer et al., 2015)
<i>Synechocystis</i> sp. ΔP _{II}	Chromosomal deletion of <i>glnB</i>	(Hisbergues et al., 1999)
<i>Synechocystis</i> sp. ΔP _{II} + P _{II} -Venus	<i>Synechocystis</i> sp. ΔP _{II} transformed with pVZ322 encoding a P _{II} -Venus fusion	(Hauf et al., 2016)

225

226 2.3 Construction and cultivation of the *Synechocystis* sp. P_{II}-3xFLAG tag strain

227 The previously described pPD-CFLAG plasmid was used to construct a P_{II} fusion protein
 228 with a C-terminal 3xFLAG tag and insert it together with a kanamycin resistance cassette in
 229 the *Synechocystis* sp. PCC 6803 wild-type genome by homologous recombination, replacing
 230 the *psbAII* gene (Chidgey et al., 2014). Transformants were selected and segregated by
 231 kanamycin resistance. For pull down experiments, 2 L batch cultures were inoculated to an
 232 optical density at 750 nm (OD₇₅₀) of 0.2 in BG11 medium (Rippka et al., 1979) and
 233 propagated photoautotrophically under constant illumination with 60 μmol photons m⁻² s⁻¹
 234 and magnetic stirring at 120 rpm at 26 °C. Cultures were bubbled with ambient air,
 235 supplemented with 2% CO₂ v/v. For growth on urea (5 mM) as exclusive nitrogen source,
 236 NaNO₃ (17.7 mM) was substituted in BG11 medium. Cell harvesting was performed at an
 237 OD₇₅₀ of 0.6 by mixing the cultures with ice in a 2:1 ratio for rapid metabolic inactivation and
 238 centrifugation at 7,477 × g for 10 min. Cell pellets were subsequently washed with nitrogen-
 239 free BG11 at 4 °C and snap frozen in liquid nitrogen. For experimental controls, the wild-type

240 strain was similarly cultivated and subjected to pull down assays followed by MS analyses as
241 described below. Two independent replicates were prepared per condition.

242

243 **2.4 Preparation of cell extracts and Anti-FLAG Pull down**

244 Frozen cell pellets were resuspended in 5 mL IP buffer, containing 25 mM MES/NaOH; pH
245 6.5, 5 mM CaCl₂, 10 mM MgCl₂, and 20 % glycerol for washing and subsequently in 3 mL IP
246 buffer, including protease inhibitors (cOmplete EDTA-free; Roche) for cell lysis. Therefore,
247 an equal volume of glass beads was added and cells were broken using a FastPrep24
248 Ribolyser (MP Biomdicals) with five 20 s cycles at 6.5 m s⁻¹ and 4 °C. After centrifugation
249 for 5 min at 3,314 × g and 4 °C, the supernatant was transferred and adjusted with IP buffer to
250 a final volume of 6 mL. For membrane protein solubilization, 1.5% w/v
251 dodecyl-β-D-maltoside (DDM; Carl Roth) was added and incubated under agitation for 1 h at
252 4 °C, before insoluble cell debris was removed by centrifugation for 20 min at 20,000 × g and
253 4 °C. Obtained supernatants from 2 L culture were subjected to the P_{II}-FLAG pull down
254 procedure: for this, 400 μL of resuspended anti-FLAG-M2-agarose (Sigma) was added into
255 empty SPE-columns and washed twice with each 1 mL IP buffer, supplemented with 0.04%
256 w/v DDM, before the supernatants were incubated for 5 min and removed by gravity flow.
257 Repeated washing steps with each 5 mL DDM supplemented IP buffer were performed
258 similarly, until the flow through appeared colorless. Elution of coupled proteins from the anti-
259 FLAG resin was performed by incubation in 600 μL DDM supplemented IP buffer containing
260 3 mg/mL FLAG peptide (Sigma) for 5 min.

261

262 **2.5 Proteomics workflow, nanoLC-MS/MS analysis and data processing**

263 Eluates from pull downs were subjected to acetone/methanol precipitation and resulting
264 protein pellets were resuspended in denaturation buffer for subsequent tryptic digestion as
265 described elsewhere (Spat et al., 2015). Resulting peptide mixtures were subjected to stage tip
266 purification (Rappsilber et al., 2007). Qualitative MS for protein identification was performed
267 as described previously (Spat et al., 2015): in brief, purified peptides were loaded on an
268 EASY-LC system (Proxeon Biosystems) onto a 15 cm reversed-phase C₁₈ nanoHPLC column
269 and separated in a 90 min segmented linear gradient. Eluted peptides were ionized in the on-
270 line coupled ESI source and injected in a LTQ Orbitrap XL mass spectrometer (Thermo
271 Scientific). MS spectra were acquired in the positive-ion mode with, per scan cycle, one initial
272 full (MS) scan followed by fragmentation of the 15 most intense multiply charged ions
273 through collision induced dissociation (CID) for MS/MS scans. The scan range was m/z 300–
274 2000 for precursor ions at resolution 60,000 and sequenced precursors were dynamically
275 excluded for fragmentation for 90 s. The lock mass option was enabled for real time mass
276 recalibration (Olsen et al., 2005). All raw spectra were processed with the MaxQuant software
277 (version 1.5.2.8) (Cox and Mann, 2008) at default settings. Peak lists were searched with the
278 following database search criteria against a target-decoy database of *Synechocystis* sp. PCC
279 6803 with 3,671 protein sequences, retrieved from Cyanobase (Nakao et al., 2010) (July
280 2014), and against 245 common contaminants: trypsin was defined as a cleaving enzyme and
281 up to two missed cleavages were allowed; carbamido-methylation of cysteines was defined as
282 a fixed modification and methionine oxidation and protein N-terminal acetylation as variable
283 modifications. The experimental design template is described in supplementary Information

284 XY. False discovery rates retrieved from MaxQuant of peptides and proteins were limited to
285 1%, each. Raw data acquired by mass spectrometry was deposited at the ProteomeXchange
286 Consortium via the Pride partner repository (Vizcaino et al., 2013) under the identifier XYZ.

287

288 **2.6 Determination of nitrate, nitrite, ammonium and urea in cell-free culture medium**

289 To determine the nitrate, ammonium or urea uptake, exponentially growing cells (OD₇₅₀ 0.4–
290 0.8) were harvest by centrifugation (3000 xg for 10 min at room temperature) and washed
291 twice with BG-11 medium lacking nitrogen. Subsequently, the cultures were adjusted to an
292 OD₇₅₀ of 1 with nitrogen nitrogen-free BG11 medium. The assays were started by adding
293 either 200 μM NaNO₃, 200 μM NH₄ or 150 μM Urea, respectively. Cells were cultivated
294 under constant shaking of 120 rpm and illumination of 40–50 μE. 1 ml aliquots of the cell
295 suspensions were taken and subsequently centrifuged (13,000 xg for 5 min at room
296 temperature) to remove the cells.

297 For nitrate quantification the absorbance at 210 nm was measured in the cell-free medium.
298 Since both nitrate and nitrite absorb at 210 nm, the apparent nitrate values were corrected for
299 the presence of nitrite (Kloft and Forchhammer, 2005). Nitrite concentration of the cell-free
300 medium was determined using the modified Griess reaction according to (Fiddler, 1977).

301 The ammonium concentration of cell-free medium was measured by using the Nessler
302 reaction (Vogel et al., 1989). Urea was quantified by using the urea nitrogen (BUN)
303 colorimetric detection kit (Invitrogen).

304

305 **2.7 Microscopy procedures and Image evaluation**

306 Fluorescence microscopy was performed using a Leica DM5500B microscope with a
307 100 ×/1.3 oil objective. For the detection of Venus fluorescence, an ET500/20x excitation
308 filter and an ET535/30m emission filter were used referred as YFP-channel. To detect
309 cyanobacterial autofluorescence, an excitation filter BP 535/50 and a suppression filter BP
310 610/75 were used. Image acquisition was done with a Leica DFC360FX black-and-white
311 camera. Captured images were colored with the Leica Application Suite Software (LAS AF)
312 provided by Leica Microsystems. Bright-field images were exposed for 6 ms, Venus
313 fluorescence images for 150 ms and autofluorescence images for 100 ms. Microscope slides
314 covered with dried 2 % (w/v) agarose solution were used to immobilize the cells during all
315 microscopical examinations.

316 Image evaluation including fluorescence intensity measurements were performed using the
317 open-source software ImageJ (Fiji) (Schindelin et al., 2012). To compare the fluorescence
318 intensities in different cell compartments, a linear profile of the gray values across the plasma
319 membrane and cytoplasm were determined. The maximum gray levels of the plasma
320 membrane were normalized to the average gray levels of the cytoplasm. An example of this
321 profile data quantification is given in supplementary figure 1.

322

323

324 **3 Results**

325 **3.1 P_{II} signaling mutants show ammonia toxicity**

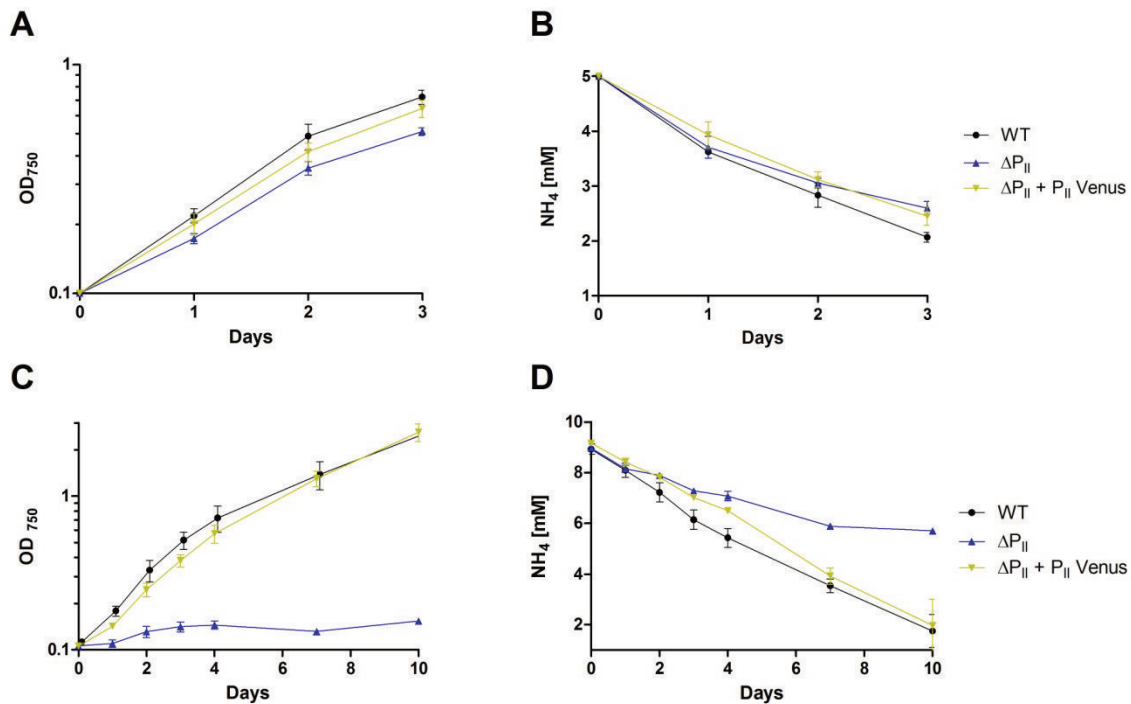
326

327 In *E. coli*, it is known that the P_{II} homologue GlnK regulates the ammonium influx by direct
328 protein-protein interaction with the ammonium permease AmtB. The observation of impaired
329 ammonium utilization of *Synechocystis* sp. harboring the P_{II}(I86N) mutation indicated a
330 similar regulation in cyanobacteria. The P_{II}(I86N) variant exhibits a modified T-loop
331 structure, while the P_{II} backbone appears almost identical with the P_{II} wild-type structure
332 (Fokina et al., 2010b). Therefore, the impaired ammonium utilization of a P_{II}(I86N) mutant
333 could be attributable to the altered T-loop structure. In order to proof this suggestion, we
334 tested the ammonium utilization of different P_{II} signaling mutants, including a P_{II} deletion
335 mutant (Δ P_{II}) (Hisbergues et al., 1999) and a complementation strain (Δ P_{II} + P_{II}-Venus)
336 (Hauf et al., 2016). The complementation strain was previously generated by introducing a
337 *Synechocystis* sp. shuttle vector (pVZ322) encoding a P_{II}-Venus fusion, in the P_{II} deletion
338 mutant (Δ P_{II}) (Hauf et al., 2016). To avoid sterical inhibition of the T-loop, the Venus
339 fluorescent protein was fused to the C-terminus of P_{II}. However, fusion to the C-terminus
340 could lead to a sterical inhibition of the B- and C-Loop. The recombinant P_{II}-Venus is
341 transcriptionally controlled by the native *glnB* promoter of *Synechocystis* sp.

342 When grown in presence of 5 mM ammonium in liquid medium, the *Synechocystis* sp. wild-
343 type, the Δ P_{II} and the Δ P_{II} + P_{II}-Venus complementation strains show similar growth rates and
344 ammonium consumption (figure 1 A, B). However, with an elevated ammonium
345 concentration of 10 mM, only the wild-type and the Δ P_{II} + P_{II}-Venus complementation could
346 maintain normal growth, while the Δ P_{II} mutant is unable to grow (figure 1 C). The ammonium
347 utilization of the wild-type and the Δ P_{II} + P_{II}-Venus complementation is similar under this
348 condition (figure 1 D). In contrast, the Δ P_{II} mutant shows a similar ammonium utilization rate
349 as the wild-type and the Δ P_{II} + P_{II}-Venus complementation within the first 24 h. After 48 h,
350 the ammonium consumption of the Δ P_{II} mutant decreases over time (figure D). Similar
351 observations haven been documented for *Synechocystis* sp. harboring the P_{II}(I86N) variant.
352 When grown at 10 mM ammonium, the P_{II}(I86N) mutant utilizes ammonium in a similar rate
353 as the wild-type in the first 48 h. Afterwards, the utilization rate of the P_{II}(I86N) mutant
354 reduces and its growth is impaired (Watzer et al., 2015).

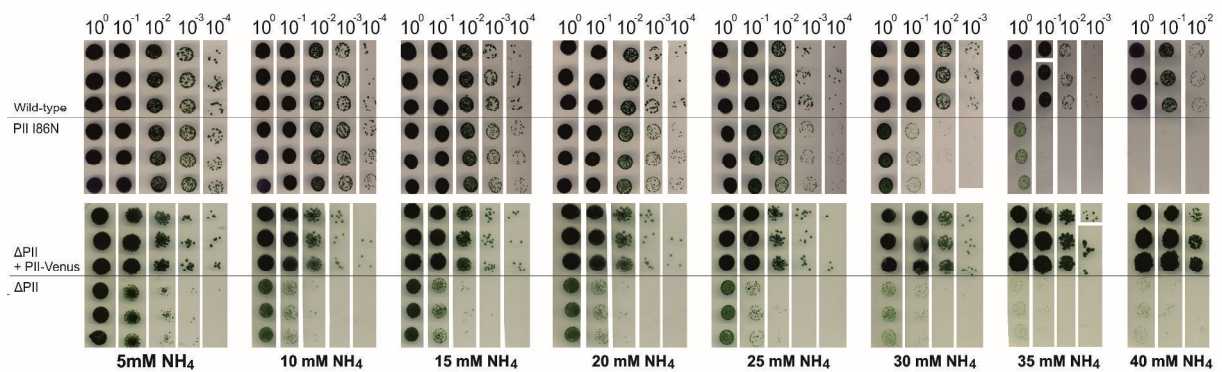
355 Although ammonium represents the preferred nitrogen source, it becomes toxic for many
356 photosynthetic organisms at higher concentrations (Drath et al., 2008). Our observation
357 implied an intoxication of the Δ P_{II} and P_{II}(I86N) mutant by ammonium, while the wild-type
358 and the Δ P_{II} + P_{II}-Venus complementation maintain a higher tolerance. To confirm that the
359 reduced growth and impaired ammonium utilization occurs in response to ammonium
360 intoxication, we performed a drop plate method with increasing amounts of ammonium
361 (figure 2). Over a range from 5 mM to 40 mM ammonium, the wild-type and Δ P_{II} + P_{II}-Venus
362 complementation show similar growth and ammonium tolerance. However, the P_{II}(I86N)
363 mutant shows impaired growth at 25 mM and the Δ P_{II} mutant already at 5 mM ammonium
364 (figure 2). Both mutants show reduced ammonium tolerance while the Δ P_{II} mutant is more
365 sensitive than the P_{II}(I86N) mutant.

The signal transduction protein P_{II} controls ammonium, nitrate and urea uptake in cyanobacteria



366

367 Figure 1 Ammonium supplemented growth and ammonium utilization of *Synechocystis* sp.
 368 wild-type, ΔP_{II} and $\Delta P_{II} + P_{II}$ -Venus. Values are the means of three biological replicates. (A)
 369 Growth curve in presence of 5 mM Ammonium. (B) Ammonium concentration in culture
 370 supernatants of *Synechocystis* sp. strain grown in BG-11 medium with 5 mM ammonium. (C)
 371 Growth curve in presence of 10 mM Ammonium. (D) Ammonium concentration in culture
 372 supernatants of *Synechocystis* sp. strain grown in BG-11 medium with 10 mM ammonium.



373

374 Figure 2 Drop plate method of *Synechocystis* sp. strains with three biological replicates per
 375 strain. Starved cultures were adjusted to an OD₇₅₀ of 1.0 and diluted tenfold in series. The
 376 dilutions were dropped onto BG-11 agar plates containing increasing concentrations of
 377 ammonia (5 mM to 40 mM).

378 **3.2 Pull down method identifies novel P_{II} interaction partner**

379 The uncontrolled influx of ammonia and following intoxication of the ΔP_{II} and P_{II}(I86N)
380 mutants grown in presence of high concentrations of ammonia suggested an involvement of
381 P_{II} in the ammonium uptake. The ammonium uptake in *Synechocystis* sp. is mainly depending
382 on the Amt1 permease (Montesinos et al., 1998). In order to verify a possible interaction
383 between P_{II} and Amt1, we performed pull down assays using a C-terminal 3xflag-tagged P_{II}
384 protein as bait. The P_{II} 3xFlag fusion protein was under control of a strong *psbA* promoter,
385 which was transformed in the *Synechocystis* sp. wild-type background. The resulting
386 *Synechocystis* sp. P_{II} 3xFlag was grown in presence of nitrate as nitrogen source. The fusion
387 protein and its interacting targets were purified by immunoprecipitation and subsequently
388 identified by mass spectrometry (MS). As a negative control, we used the *Synechocystis* sp.
389 wild-type and processed it in the same way as the *Synechocystis* sp. P_{II} 3xFlag strain to
390 identify unspecific binding proteins.

391 As proof of principle, we were able to identify P_{II} and the known P_{II} interacting protein PipX.
392 Both proteins show a higher sequence coverage (SC) and intensity in the flag-tag pull down
393 compared to the wild-type control in both replicas (Table 1). A similar enrichment in both
394 replicas can also be documented for the ammonium permease Amt1, supporting our
395 suggestion that Amt1 represents a P_{II} binding target in cyanobacteria. Surprisingly, besides
396 Amt1, we could also identify subunits of the NrtABCD nitrate/nitrite transporter and the
397 UrtABCDE urea transporter in our pull down experiment. All subunits of both transporters
398 are enriched in the flag-tag pull down compared to the wild-type control, instead of the
399 periplasmatic substrate binding protein NrtA and UrtA (Table 1). To further validate the
400 enrichment of UrtABCDE subunits, we performed a similar experiment with cells grown on
401 urea as unique nitrogen source. In agreement with the previous pull down experiment, we
402 were able to document an enrichment of the P_{II} target PipX, the ammonium permease Amt1,
403 the nitrate/ nitrite transporter NrtABCD and the urea transporter UrtABCDE (Table 2).

404

The signal transduction protein P_{II} controls ammonium, nitrate and urea uptake in cyanobacteria

405 Tabel 4. Pull down assay of nitrate supplemented *Synechocystis* sp. wild-type (control) and *Synechocystis* sp. P_{II} 3xFlag (Flag-tag Pull down). SC,
406 Sequence coverage [%]; R1 and R2, replicas 1 and 2, respectively.

Protein IDs		Mol. weight [kDa]	Control		Flag-tag Pulldown		Control		Flag-tag Pulldown	
			SC R1 [%]	SC R2 [%]	SC R1 [%]	SC R2 [%]	Intensity R1	Intensity R2	Intensity R1	Intensity R2
ssl0707	P _{II} /P _{II} - FLAG	15,425	59,1	82,5	98,5	98,5	1,2E+08	2,6E+08	6,2E+10	4,3E+10
ssl0105	PipX	10,448	0	0	22,7	22,7	0	0	1,2E+08	2,5E+08
sll0108	Amt1	53,58	0,0	8,1	9,7	9,7	0	7,6E+06	4,4E+09	2,4E+09
sll0374	UrtE	27,424	0	0	25,7	22,1	0	0	1,2E+08	2,5E+07
sll0764	UrtD	41,194	0	0	30,3	29,0	0	0	2,6E+08	2,6E+07
slr1201	UrtC	45,084	0	0	18,3	13,2	0	0	6,8E+07	1,1E+07
slr1200	UrtB	41,681	0	0	2,8	2,8	0	0	1,9E+07	5,3E+06
slr0447	UrtA	48,359	22,2	13,9	8,3	4,0	1,2E+08	7,4E+06	5,7E+06	6,8E+05
sll1451	NrtB	29,72	0	0	12,0	4,0	0	0	6,2E+07	2,6E+07
sll1453;slr0044	NrtD	36,564	11,1	3,9	57,2	54,2	1,9E+07	1,5E+05	1,9E+09	1,7E+08
sll1452	NrtC	75,1	0	0	46,1	45,5	0	0	1,2E+09	3,5E+08
sll1450;slr0040	NrtA	48,966	14,8	14,8	18,2	8,7	1,0E+08	7,7E+06	1,6E+07	2,4E+06

407

408

The signal transduction protein P_{II} controls ammonium, nitrate and urea uptake in cyanobacteria

409 Tabel 5. Pull down assay of urea supplemented *Synechocystis* sp. wild-type (control) and *Synechocystis* sp. P_{II} 3xFlag (Flag-tag Pull down). SC,
410 Sequence coverage [%]; R1 and R2, replicas 1 and 2, respectively.

411

Protein IDs		Mol. weight [kDa]	Control		Flag-tag Pulldown		Control		Flag-tag Pulldown	
			SC R1 [%]	SC R2 [%]	SC R1 [%]	SC R2 [%]	Intensity R1	Intensity R2	Intensity R1	Intensity R2
ssl0707	P _{II} /P _{II} - FLAG	15,425	60,6	31,4	91,2	60,6	2,5E+08	1,3E+07	3,2E+10	2,4E+08
ssl0105	PipX	10,448	0	0	22,7	0	0	0	1,8E+08	0
sll0108	Amt1	53,58	1,6	2,0	10,1	2,0	1,7E+06	1,2E+07	4,9E+09	2,4E+07
sll0374	UrtE	27,424	0	11,6	70,7	21,7	0	2,6E+06	3,3E+09	4,8E+07
sll0764	UrtD	41,194	0	2,9	59,5	23,6	0	3,8E+05	8,0E+09	4,5E+07
slr1201	UrtC	45,084	0	3,4	21,7	12,0	0	1,1E+05	1,0E+09	1,0E+07
slr1200	UrtB	41,681	0	0	8,5	5,4	0	0	6,1E+08	1,2E+06
slr0447	UrtA	48,359	10,8	4,0	6,7	6,3	6,4E+06	6,1E+04	1,3E+07	5,0E+05
sll1451	NrtB	29,72	0	3,6	11,6	3,6	0	1,1E+05	1,8E+07	1,2E+06
sll1453;slr0044	NrtD	36,564	3,9	0	61,1	15,1	6,3E+06	0	5,6E+08	7,3E+05
sll1452	NrtC	75,1	0	0	58,8	0	0	0	1,6E+09	0
sll1450;slr0040	NrtA	48,966	0	0	2,5	0	0	0	1,2E+06	0

412

413 **3.3 Bacterial two-hybrid assay**

414 To further confirm the interaction of P_{II} with the identified nitrogen transports we performed
 415 bacterial two-hybrid assays. Next to wild-type P_{II} we also included the P_{II}(I86N) variant to
 416 test how the altered T-loop conformation influences the interactions. Due to their localization
 417 on the cytoplasmic site of the plasma membrane we tested the ATP-binding proteins of the
 418 ABC-type transporters (Omata et al., 1993b; Valladares et al., 2002). Interactions for Amt1,
 419 NrtC, NrtD, UrtD, UrtE have been tested for possible interactions, while the P_{II} - PipX and
 420 leucin zipper interaction were used as a positive controls. In case of a positive interaction
 421 cAMP is formed within a cAMP deficient *E.coli* host cells. This can be detected on X-Gal and
 422 MacConkey reporter plates. Table 3 shows the observed interactions in the bacterial two-
 423 hybrid assays.

424 Both, wild-type P_{II} and P_{II}(I86N) show interaction with the known P_{II} interaction partner
 425 PipX. While the wild-type P_{II} shows interaction with the Amt1 permease, the P_{II}(I86N)
 426 variant loses this ability, in agreement with our previous observations regarding the impaired
 427 ammonium utilization of *Synechocystis* sp. P_{II}(I86N). We could further confirm an interaction
 428 of wild-type P_{II} with the ATP-binding proteins NrtC and NrtD for the nitrate/nitrite
 429 transporter as well as UrtE for the urea transporter. However, interaction of wild-type P_{II} and
 430 the NrtC subunit appear very weak. Therefore the interaction of P_{II} and NrtC cannot be fully
 431 confirmed but also not negate. The P_{II}(I86N) variant doesn't show interaction with NrtC and
 432 NrtD, but maintain the ability to interact UrtE. Accordingly, the nitrate utilization could be
 433 impaired while the urea utilization could be unaffected in *Synechocystis* sp. P_{II}(I86N).

434 Table 6 Bacterial two-hybrid interactions observed for wild-type P_{II} and P_{II}(I86N). +,
 435 interaction; - no interaction; (+), weak interaction.

436	Interaction partners	Wild-typeP _{II}	P _{II} (I86N)
437	PipX (pos. control)	+	+
438	NrtC	(+)	-
439	NrtD	+	-
440	UrtD	-	-
441	UrtE	+	+
442	Amt1	+	-

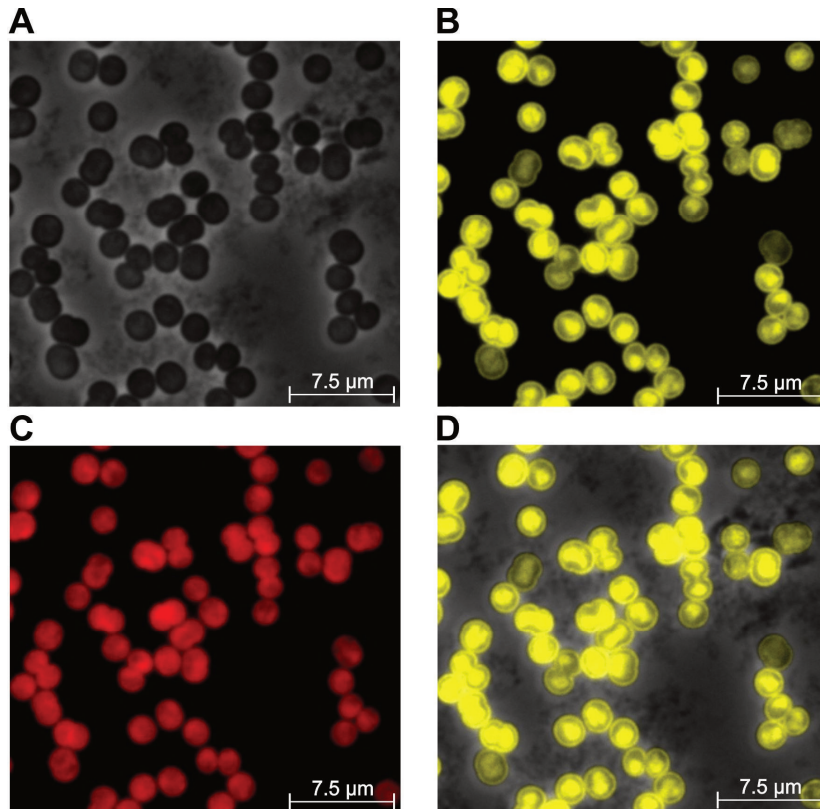
443 3.4 P_{II} localization changes upon addition of nitrate, ammonium and urea

444 Our previous pull down experiments and bacterial two-hybrid assays clearly show interaction
445 of P_{II} with Amt1, NrtABCD and UrtABCDE in *Synechocystis* sp. Since all these transporters
446 are plasma membrane associated, we tried to monitor P_{II} localization on the plasma
447 membrane. The *Synechocystis* sp. Δ P_{II} + P_{II}-Venus complementation was used to investigate
448 the cellular localization of P_{II} under different nitrogen supplementations.

449 Nitrate-replete *Synechocystis* sp. cells in the mid-exponential growth phase (OD₇₅₀ approx.
450 0.5) show P_{II}-Venus fluorescence heterogeneously distributed in the cell. The majority of cells
451 harbor a strong fluorescence signal in the center and periphery (figure 3 A). The intense signal
452 in the center corresponds to the cytoplasm where several metabolic reactions are located. P_{II}
453 localization in the cytoplasm indicates an interaction with different soluble proteins, like
454 NAGK. The P_{II}-Venus fluorescence in the periphery corresponds to the plasma membrane,
455 where Amt1, NrtABCD and UrtABCDE are located. The areas with low Venus fluorescence
456 are occupied by thylakoid membranes (figure 3 C).

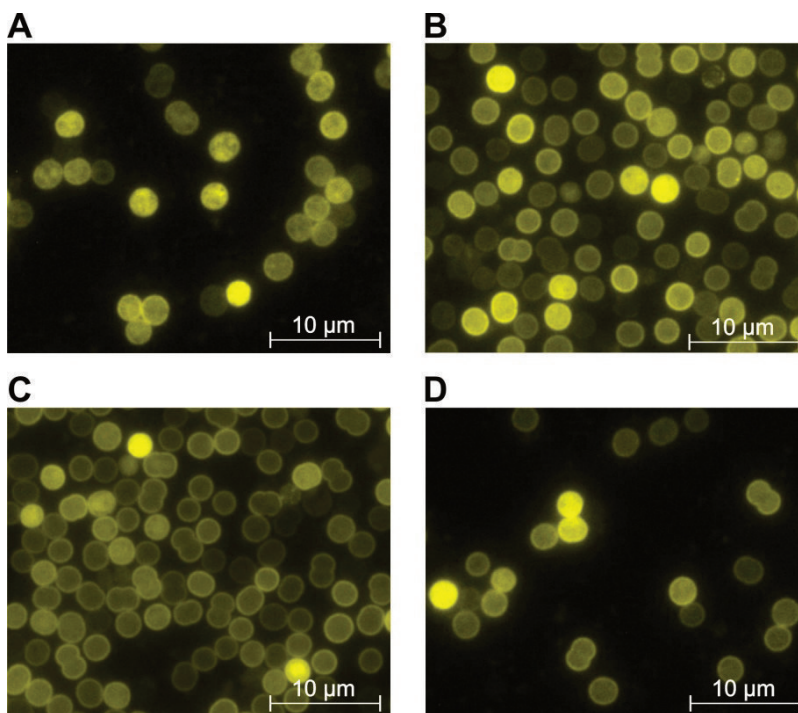
457 To monitor the P_{II} localization under nitrogen depletion, cells were grown to an OD₇₅₀ of 0.4
458 – 0.6, washed, and resuspended in BG-11 lacking a combined nitrogen source. After one
459 week of nitrogen starvation, the P_{II}-Venus signal is more evenly distributed throughout the
460 whole cell and its localization on the plasma membrane is not as distinct as during nitrogen
461 supplemented exponential growth (figure 4 A). To test the localization during resuscitation
462 from nitrogen starvation, one week nitrogen starved *Synechocystis* sp. cultures were
463 resuscitated by adding 5 mM NO₃, 5 mM NH₄ or 5 mM Urea, respectively. Immediately after
464 the addition of a combined nitrogen source a change in the P_{II} localization becomes visible.
465 The majority of cells show distinct plasma membrane localization, while the remaining
466 cytosol shows homogenous fluorescence intensity. The migration of P_{II} to the plasma
467 membrane turns out more clearly by the addition of ammonia compared to nitrate and urea
468 (figure 4 A,B,C).

469 In order to quantify the movement of P_{II} towards the plasma membrane, a linear profile of the
470 fluorescence intensities across the plasma membrane and cytoplasm was determined. The
471 maximum intensity of the plasma membrane was normalized to the average intensity value of
472 the cytoplasm. Under nitrogen depletion, the majority of the cells show a slightly higher
473 cytoplasmic P_{II}-Venus localization than plasma membrane localization (figure 5). The
474 addition of a nitrogen source directly induces a translocation of P_{II} towards the plasma
475 membrane. Thereby the addition of nitrate and urea show similar translocation of P_{II} in the
476 first two hours (figure 5 A, C, D). Two hours after the addition of nitrate, P_{II} starts to
477 dissociate from the plasma membrane and goes back in its cytoplasmic localization (figure 5
478 A). In contrast, urea addition induces a slow and constant migration of P_{II} towards the plasma
479 membrane during the whole four hours (figure 5 C). Ammonium addition induces migration
480 of P_{II} to plasma membrane in the first hour much stronger than nitrate or urea (figure 5 B).
481 After the immediate translocation towards the plasma membrane, P_{II} starts to dissociate and
482 migrates back into the cytoplasm after two hours.



483

484 Figure 3 Localization of P_{II}-Venus during exponential growth (OD₇₅₀ of 0.5) of *Synechocystis*
485 sp. (A) Phase contrast image of cells. (B) Venus fluorescence. (C) Autofluorescence of
486 thylakoid membranes. (D) Overlay of Venus fluorescence and phase contrast images.

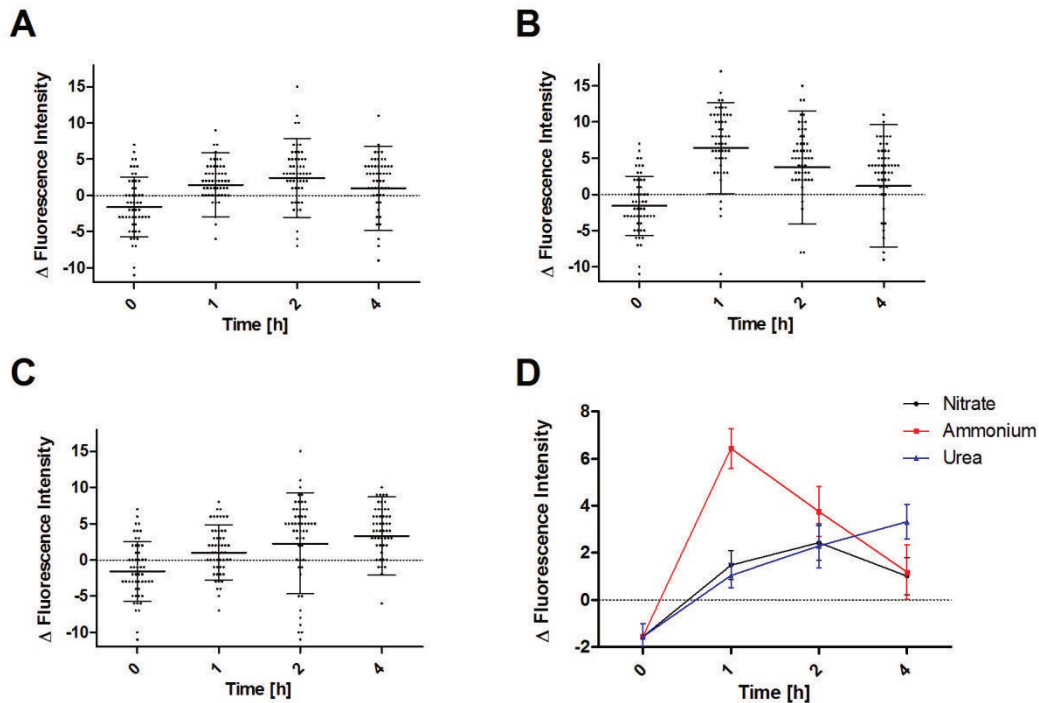


487

488 Figure 4 P_{II}-Venus localization under different nitrogen supplemented conditions. (A) P_{II}-
489 Venus fluorescence of one week nitrogen starved *Synechocystis* sp. cultures. (B-D) P_{II}-Venus
490 fluorescence of *Synechocystis* sp. during resuscitation from nitrogen starvation. One week
491 nitrogen starved *Synechocystis* sp. cultures were resuscitated by adding 5 mM NO₃ (B), 5 mM

492 NH₄ (C), or 5 mM Urea (D). Fluorescence images were taken 1 hour after addition of the
 493 nitrogen source.

494



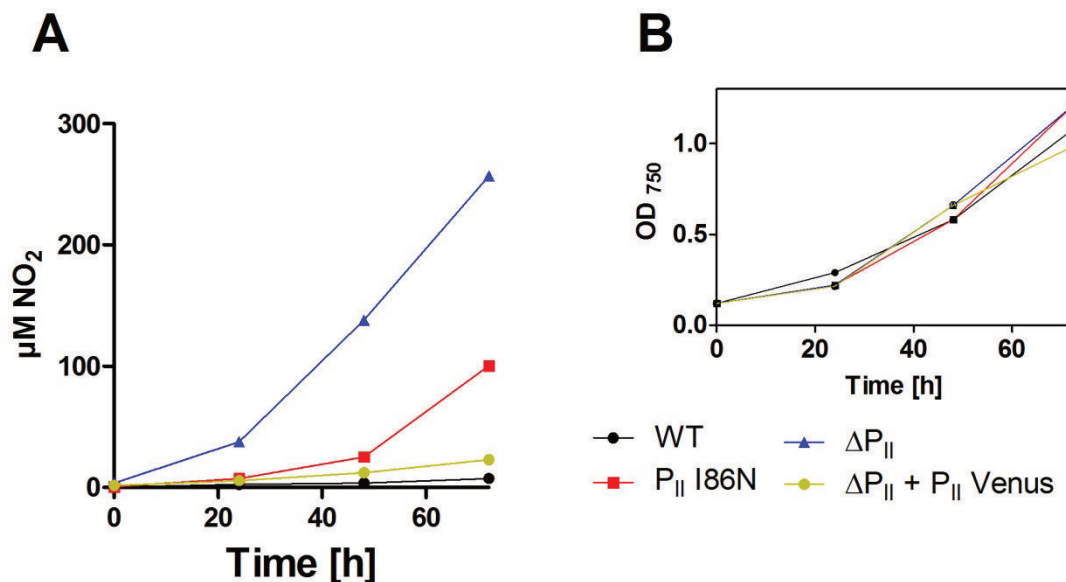
495

496 Figure 5 Quantification of the P_{II}-Venus migration towards the plasma membrane in response
 497 to the addition of different nitrogen sources to nitrogen starved *Synechocystis* sp. cultures. A
 498 linear profile of the fluorescence intensities across the plasma membrane and cytoplasm were
 499 determined. The maximum intensity of the plasma membrane was normalized to the average
 500 intensity value of the cytoplasm. Fluorescence intensity values < 0 indicate a stronger
 501 cytoplasmic localized signal, while values > 0 show a stronger plasma membrane association.
 502 Resuscitation of one week nitrogen starved *Synechocystis* sp. cultures were induced by adding
 503 either 5 mM NO₃ (A), 5 mM NH₄ (B), or 5 mM Urea (C). 50-60 cells were measured per time
 504 point. Dots indicate single cell measurements; whiskers showing the standard-deviations;
 505 thick black lines show the arithmetic mean. (D) Direct comparison of the mean Δ
 506 fluorescence intensities from NO₃, NH₄ and Urea induced resuscitation.

507 3.5 P_{II} deletion mutant and P_{II}(I86N) mutant secrete nitrite

508 Our previous results showed an involvement of P_{II} in regulation of nitrate utilization by direct
509 protein-protein interaction with the NrtD and NrtC subunit of the NrtABCD nitrate/nitrite
510 transporter. This regulation has also been suggested by several previous studies which
511 documented altered nitrate utilization properties of P_{II} deletion and signaling mutants
512 (Kobayashi et al., 1997; Lee et al., 1998; Lee et al., 2000; Kloft and Forchhammer, 2005).
513 One characteristic phenotype which has been described for a P_{II} deletion mutant grown in the
514 presence of nitrate is the excretion of nitrite in the medium (Forchhammer and Demarsac,
515 1995; Kloft and Forchhammer, 2005). The reduction of nitrate requires two electrons whereas
516 six electrons are needed for the reduction of nitrite to ammonium. Due to the lower costs of
517 nitrate reduction, the nitrite reduction becomes limiting in case of an uncontrolled nitrate
518 influx. As a consequence, nitrite accumulates and is excreted. In agreement, this nitrite
519 excretion phenotype can be restored by increasing the light intensity due to the elevated level
520 of photosystem I reduced ferredoxin (Kloft and Forchhammer, 2005). We wondered if the
521 *Synechocystis* sp. P_{II}(I86N) strain shows a similar phenotype when grown on nitrate and if the
522 P_{II}-Venus complementation is able to restore the nitrite excretion phenotype of a P_{II} deletion
523 mutant.

524 When grown with nitrate as only nitrogen source and constant illumination of 40–50 μ E,
525 *Synechocystis* sp. wild-type, P_{II}(I86N), Δ P_{II} and the Δ P_{II} + P_{II}-Venus complementation obtain
526 the same growth rate (figure 6). Under this condition, both, the P_{II}(I86N) and Δ P_{II} mutant,
527 secrete nitrite into the medium. However, the P_{II}(I86N) mutant excretes much lower amounts
528 than the P_{II} deletion mutant. The *Synechocystis* sp. wild-type and P_{II}-Venus complementation
529 doesn't secrete nitrite, indicating that the insertion of P_{II}-Venus in the Δ P_{II} mutant restores the
530 wild-type phenotype.



531
532 Figure 6 (A) Nitrite excretion of *Synechocystis* sp. wild-type, P_{II}(I86N), Δ P_{II} and the Δ P_{II} +
533 P_{II}-Venus complementation grown in BG11 medium supplemented with Nitrate and
534 illuminated with illumination of 40–50 μ E. (B) Corresponding growth curve.

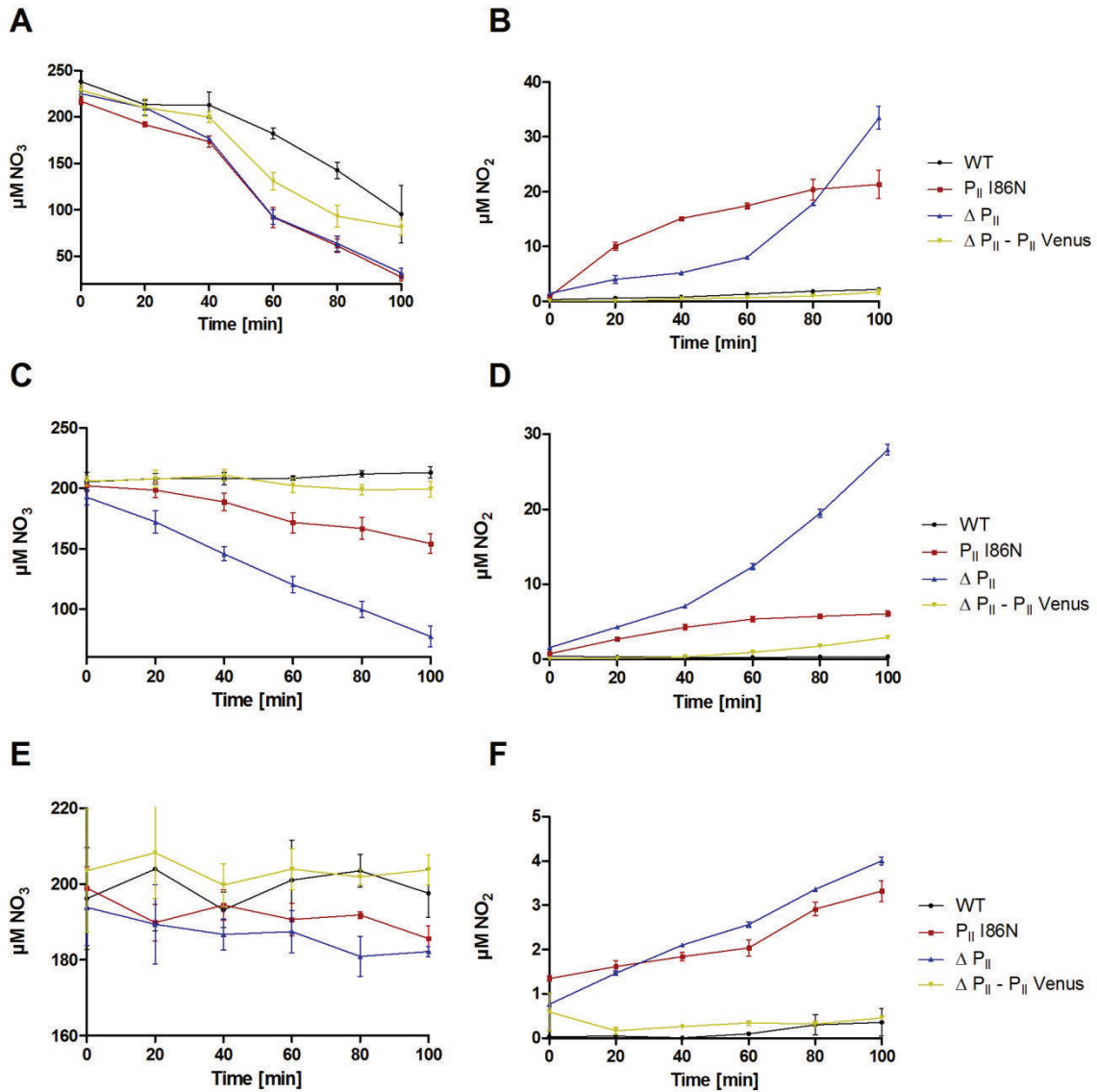
535

536 3.6 P_{II} is responsible for nitrate utilization inhibition

537 Excretion of nitrite by the P_{II}(I86N) strain indicates an uncontrolled nitrate influx similar to
538 the P_{II} deletion mutant. To gain further insights in the P_{II} depending regulation of nitrate
539 uptake, we measured nitrate consumption rates of the P_{II}-signaling mutants under different
540 conditions. For this purpose, exponential growing cells were washed and subsequently
541 incubated in BG-11 Medium, containing 200 μM NO₃ as nitrogen source. Nitrate utilization
542 was quantified by determining the nitrate concentration in cell free culture supernatant over
543 time. Under constant illumination of 40–50 μE, *Synechocystis* sp. wild-type and the ΔP_{II} + P_{II}-
544 Venus strain show low nitrate consumption while the P_{II}(I86N) and ΔP_{II} mutant show similar
545 higher nitrate utilization (figure 7 A). In agreement with our previous results, we observed
546 excretion of nitrate by the P_{II}(I86N) and ΔP_{II} mutant (figure 7 B). Interestingly, while the
547 nitrate utilization rate of the P_{II}(I86N) and ΔP_{II} mutant appear almost identical, both mutants
548 differ in their nitrite excretion rate. While the course of nitrite excretion of the ΔP_{II} mutant
549 appears progressive, the course of nitrite excretion of the P_{II}(I86N) appears digressive.

550 Since ammonium is the preferred nitrogen source, the addition of ammonia to cells grown on
551 nitrate leads to an immediate inhibition of the nitrate uptake (Lee et al., 1998). This
552 ammonium dependent inhibition of nitrate uptake is regulated by the P_{II} protein (Lee et al.,
553 1998). Since the P_{II}(I86N) mutant behaves similar as the ΔP_{II} mutant in case of nitrate uptake
554 and nitrite excretion, we tested if the P_{II}(I86N) mutant maintains the ammonium depending
555 nitrate uptake inhibition. For this purpose, we determined the nitrate consumption by
556 measuring the remaining nitrate concentration in the culture supernatant in presence of 2 mM
557 ammonium. Both, *Synechocystis* sp. wild-type and the ΔP_{II} + P_{II}-Venus mutant, show a
558 complete inhibition of nitrate utilization by the addition of ammonium (figure 7 C). In
559 contrast, the P_{II}(I86N) and ΔP_{II} mutant maintain the nitrate utilization. Here the P_{II}(I86N)
560 mutant utilizes lower amounts of nitrate compared to the ΔP_{II} mutant (figure 7 C). The
561 uncontrolled nitrate uptake of the P_{II}(I86N) and ΔP_{II} mutant leads to an elevated excretion
562 nitrite. Due to the lower consumption of nitrate by the P_{II}(I86N) mutant, the nitrite excretion
563 is also lower compared to the ΔP_{II} mutant (figure 7 D).

564 Next to the requirement of ammonium absence, active nitrate transport also requires
565 photosynthetic CO₂ fixation (Romero et al., 1985). Nitrogen assimilation is tightly regulated
566 by light / dark transitions. A transition from light to dark causes an immediate inhibition of
567 nitrate uptake and an inhibition of the ammonium assimilating GS (Romero et al., 1985;
568 Marques et al., 1992). To test if the P_{II}(I86N) mutant maintains the light dependent inhibition
569 of nitrate utilization, we measured the nitrate consumption without light. In the dark, the
570 overall nitrate consumption is low in all tested mutants (figure 7 E). However, the P_{II}(I86N)
571 and ΔP_{II} mutant show slightly higher nitrate utilization rates compared to the wild-type and
572 the ΔP_{II} + P_{II}-Venus mutant, which maintain a constant nitrate concentration in the medium.
573 Furthermore, P_{II}(I86N) and ΔP_{II} mutant excrete similar small amounts of nitrite, supporting
574 the suggestion that the P_{II}(I86N) and ΔP_{II} mutant are unable to fulfill light depending nitrate
575 uptake inhibition.



576

577 Figure 7 Nitrate utilization and nitrite excretion of *Synechocystis* sp. wild-type, P_{II}(I86N), ΔP_{II}
 578 and the ΔP_{II} + P_{II}-Venus complementation. Exponentially growing and nitrate supplemented
 579 *Synechocystis* sp. cells were washed and resuspended in a medium containing 200 µM nitrate.
 580 Shown are the means of three biological replicates. (A) Nitrate utilization and (B) nitrite
 581 excretion under constant illumination of 40–50 µE. (C) Nitrate utilization and (D) nitrite
 582 excretion in presence of 2 mM ammonium and under constant illumination of 40–50 µE. (E)
 583 Nitrate utilization and (F) nitrite excretion in the dark.

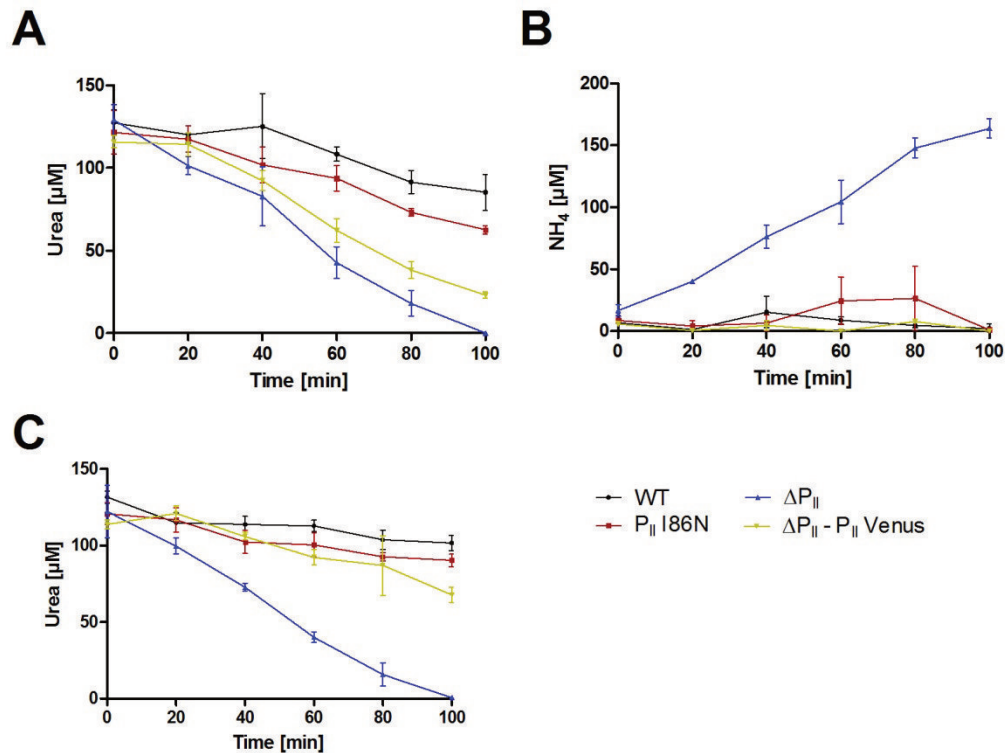
584 3.7 P_{II} signaling mutants show impaired urea utilization

585 Our previous results showed an involvement of P_{II} in regulation of nitrate and ammonium
586 utilization. Both interactions of P_{II} with the Amt1 permease and the nitrate transporter are T-
587 loop depending, since the P_{II}(I86N) mutant, which exhibits an altered T-loop conformation,
588 shows a similar behavior than a P_{II} deletion mutant. We could also confirm that the impaired
589 ammonium and nitrate utilization can be restored by inserting the P_{II}-Venus variant, which
590 exhibits not effected T-loop conformation. Next to Amt1 and NrtABCD we could also show
591 an interaction of P_{II} with the UrtE subunit of the urea transporter UrtABCDE. In order to
592 analyze the biological significance of this interaction we monitored the urea utilization
593 abilities of our P_{II} signaling mutants under different conditions. For this purpose exponential
594 growing cells were washed and incubated in BG-11 Medium containing 150 μ M Urea as
595 nitrogen source.

596 Under constant illumination of 40–50 μ E the *Synechocystis* sp. wild-type and P_{II}(I86N)
597 mutant utilize similar amounts of urea (figure 8 A). In contrast, the Δ P_{II} and Δ P_{II} + P_{II}-Venus
598 mutants consume similarly higher amounts of urea compared to the wild-type and P_{II}(I86N)
599 mutant. Unlike the utilization of ammonium and nitrate, the Δ P_{II} + P_{II}-Venus cannot
600 complement the P_{II} deletion while the P_{II}(I86N) variant behaves like the wild-type (figure 8
601 A). This could indicate that the interaction with UrtE is T-loop independent. The P_{II}-Venus
602 variant which exhibits a native T-loop conformation is unable to block the UrtABCDE
603 transporter. The C-terminal Venus fusion could interfere with the B- and C-loop by sterical
604 inhibition, leading to the suggestion that P_{II} - UrtE interaction is B- and/or C-loop dependent.

605 In cyanobacteria, urea is hydrolyzed to CO₂ and two molecules of ammonium by the enzyme
606 urease (Mobley and Hausinger, 1989; Esteves-Ferreira et al., 2018). Since uncontrolled nitrate
607 influx leads to an excretion of nitrite, we wonder if an uncontrolled influx of urea could lead
608 to an excretion of ammonium. To test this, we measured ammonium concentrations in culture
609 supernatant of cells which are incubated with urea as the only nitrogen source. Indeed, we
610 were able to detect ammonium excretion of the Δ P_{II} mutant proportional to its urea utilization
611 (figure 8 B). In contrast, only minor amounts of ammonium could be detected in the culture
612 supernatant of the *Synechocystis* sp. wild-type, P_{II}(I86N) mutant and Δ P_{II} + P_{II}-Venus mutant
613 (figure 8 B).

614 *Synechocystis* sp. utilizes available nitrogen sources in a hierarchical order. In presence of
615 ammonium the uptake of outer nitrogen sources is blocked (Muro-Pastor et al., 2005). To test
616 the inhibition of urea utilization, we determined urea consumption in presence of 2 mM
617 ammonium. The *Synechocystis* sp. wild-type, P_{II}(I86N) and Δ P_{II} + P_{II}-Venus strain show a
618 clear inhibition in urea utilization by the addition of ammonium. While *Synechocystis* sp.
619 wild-type and the P_{II}(I86N) mutant behave very similar, the Δ P_{II} + P_{II}-Venus strain showed
620 slightly higher urea consumption. In contrast, the Δ P_{II} mutant shows the complete
621 consumption of 150 μ M urea in 100 min with and without the addition of ammonium (figure
622 8 A, C), indicating the complete inability to block the urea utilization.



623

624 Figure 8 Urea utilization and ammonium excretion of the *Synechocystis* sp. wild-type,
 625 P_{II}(I86N), ΔP_{II} and the ΔP_{II} + P_{II}-Venus strain. Exponentially growing and nitrate
 626 supplemented *Synechocystis* sp. cells were washed and resuspended in a medium containing
 627 150 μM urea. Shown are the means of three biological replicates. (A) Urea utilization and (B)
 628 ammonium excretion under constant illumination of 40–50 μE. (C) Urea utilization in
 629 presence of 2 mM ammonium and under constant illumination of 40–50 μE.

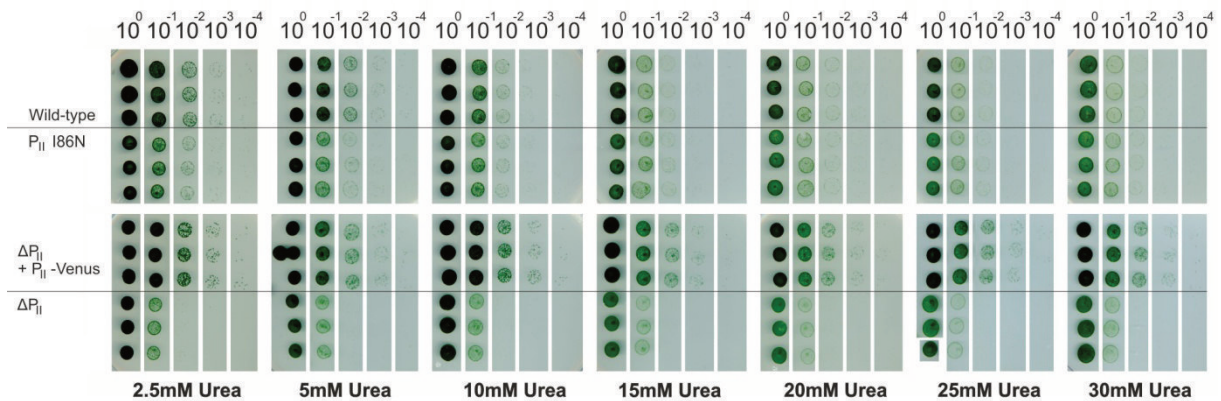
630

631 3.8 P_{II} influences urea supplemented growth

632 Our previous experiment indicates a regulation of the urea transporter UrtABCDE by the
 633 interaction of P_{II} with the UrtE subunit. This interaction is properly T-loop independent, since
 634 the P_{II}(I86N) variant show the same behavior in UrtE binding than the wild-type P_{II} and
 635 mediate the same urea utilization properties than *Synechocystis* sp. wild-type. The P_{II}-Venus
 636 variant is partially unable to complement the impaired urea utilization phenotype of the P_{II}
 637 deletion mutant, since ammonium still inhibits urea uptake. We wanted to test how this
 638 impaired regulation of the urea utilization effects the growth of *Synechocystis* sp. in presence
 639 of urea. In order to analyze the growth behavior, we performed a drop agar method with
 640 increasing urea concentrations.

641 Under low urea concentrations of 2.5 to 5 mM, *Synechocystis* sp. wild-type and ΔP_{II} + P_{II}-
 642 Venus mutant show similar growth, while the P_{II}(I86N) and ΔP_{II} mutant show impaired
 643 growth. Here the P_{II}(I86N) mutant grew slightly faster than the ΔP_{II} mutant at concentrations
 644 of 2.5 to 10 mM Urea. Surprisingly, under higher concentrations of urea (> 15 mM) the wild-
 645 type shows similar growth rates as the P_{II}(I86N) and ΔP_{II} mutant. In contrast, the ΔP_{II} + P_{II}-
 646 Venus complementation strain maintains a high growth though all concentrations. In our
 647 previous experiments the ΔP_{II} and ΔP_{II} + P_{II}-Venus complementation strain showed impaired

648 regulation in urea uptake, therefore the high urea tolerance and growth rate of the $\Delta P_{II} + P_{II}$ -
 649 Venus complementation strain was unexpected. However, these opposing results indicate that
 650 urea tolerance and utilization do not only depend on urea uptake.



651

652 Figure 9 Drop plate method of *Synechocystis* sp. strains with three biological replicates per
 653 strain. One week nitrogen starved cultures were adjusted to an OD₇₅₀ of 1.0 and diluted
 654 tenfold in series. The dilutions were dropped onto BG-11 agar plates containing increasing
 655 concentrations of urea (2.5 mM to 30 mM).

656

657 4 Discussion

658 4.1 P_{II} regulates ammonium uptake by interacting with the Amt1 ammonium 659 permease in *Synechocystis* sp.

660 In *E. coli*, the P_{II} homolog GlnK regulates AmtB by direct protein-protein interaction to
 661 control the influx of ammonia. Our results revealed a similar function of GlnB by regulating
 662 the Amt1 permease in the unicellular and non-diazotrophic cyanobacterium *Synechocystis*
 663 sp.

664 Pull-down and bacterial two-hybrid assays identified Amt1 as an interaction partner of P_{II} in
 665 *Synechocystis* sp. Examination of the binding properties of P_{II}-signaling mutants by bacterial
 666 two-hybrid assays give strong evidence that the P_{II} interaction with the Amt1 permease is T-
 667 loop depending, similar to GlnK - AmtB interaction in *E. coli*. In *E. coli* GlnK can block the
 668 ammonia influx by inserting the tip of its T-loops into the cytoplasmic exits of the AmtB-
 669 pores (Conroy et al., 2007). The structure of the P_{II}(I86N) variant exhibits a tightly bended
 670 conformation of the T-loop, which mimics the T-loop conformation of the P_{II} - NAGK
 671 complex (Fokina et al., 2010b). This bended conformation leads to an impaired interaction
 672 with Amt1. In agreement, *Synechocystis* sp. harboring the P_{II}(I86N) variant show similar
 673 impaired regulation of the ammonium uptake as a P_{II} deletion mutant, which leads to
 674 intoxication at high ambient ammonium concentrations. However, *Synechocystis* sp. P_{II}(I86N)
 675 exhibits a higher ammonium tolerance as the ΔP_{II} mutant. In a P_{II} deletion mutant, NAGK
 676 remain in a low activity state (Maheswaran et al., 2006). In contrast, *Synechocystis* sp.
 677 P_{II}(I86N) shows a highly enhanced NAGK activity followed by a high intra cellular arginine
 678 and cyanophycin content (Watzel et al., 2015). The high NAGK activity of the *Synechocystis*
 679 sp. P_{II}(I86N) strain could promote faster ammonium assimilation and therefore protect the cell
 680 from a toxic intracellular ammonium accumulation.

681 The *E. coli* AmtB-GlnK complex responds to the ATP/ADP ration. While ADP exhibits a
682 complex stabilization, ATP and synergistic bound 2-OG promotes its dissociation (Durand
683 and Merrick, 2006; Gruswitz et al., 2007; Rodrigues et al., 2011). According to our data we
684 suggest a different regulation in nitrogen starved *Synechocystis* sp. Under nitrogen starvation,
685 phosphorylated P_{II} shows a homogenous localization in the cytoplasm. Nitrogen starvation
686 induced dormancy is marked by a low ATP (Doello et al., 2018) and high 2-OG level. Only
687 one hour after the addition of ammonium P_{II} shows a strong migration to the plasma
688 membrane. Simultaneously in this first hour of resuscitation the ATP level increases two fold
689 (Doello et al., 2018). Providing ammonium to nitrogen starved cells also triggers a rapid
690 decrease of the 2-OG levels. Therefore, the immediate rise of ATP and drop of the 2-OG level
691 could trigger the translocation of phosphorylated P_{II}. Once the Amt1-cannels are closed, no
692 further ammonium will enter the cell. As a consequence, the 2-OG level increases, which lead
693 in combination with the elevated ATP level to a dissociation of the P_{II}-Amt1 complex. This
694 would explain the dissociation of P_{II} from the plasma membrane after one hour of nitrogen
695 availability. Since P_{II} remains a highly phosphorylated state during the first 24 h of
696 resuscitation from nitrogen starvation, this model is only valid in case of highly
697 phosphorylated P_{II}.

698

699 **4.2 P_{II} regulate nitrate uptake by interacting NrtD and NrtC**

700 Several previous studies documented an involvement of P_{II} in regulation of nitrate/nitrite
701 uptake. Our data provide new insights regarding the regulation of the NrtABCD transporter
702 by P_{II}. NrtABCD is directly regulated by the interaction of P_{II} with the NrtC and NrtD
703 subunit. This interaction is T-loop depending, since the P_{II}(I86N) variant (exhibiting an
704 altered T-loop conformation) shows impaired regulation of NrtABCD. A P_{II} deletion or
705 changed T-loop conformation leads to the inability to control the nitrate influx. In
706 consequence, those mutants excrete nitrite in the medium due to excess reduction of nitrate
707 along with impaired reduction of nitrite.

708 P_{II} interaction with the NrtC and NrtD subunit permit the ammonium and light induced
709 inhibition of nitrate uptake. Under nitrogen starvation P_{II} obtain a highly phosphorylated state.
710 After the addition of nitrate, phosphorylated P_{II} migrates to the plasma membrane.
711 Simultaneously in this first hour of resuscitation the ATP level increases (Doello et al., 2018)
712 leading to the suggestion that phosphorylated P_{II} interacts with NrtC and NrtD in an ATP-
713 bound state. Two hours after addition of nitrate, P_{II} begins to slightly dissociate from the
714 plasma membrane. This dissociation could occur in response to a temporary increased 2-OG
715 level, which appears due to the initially closed NrtABCD transporters. Kloft and coworkers
716 observed an uncontrolled influx of nitrate in a P_{II} phosphatase (PphA) deletion mutant under
717 low light conditions (Kloft and Forchhammer, 2005). This mutant exhibits a high
718 phosphorylated P_{II}. High light conditions, which generate a high ATP level, could restore the
719 uncontrolled nitrate uptake and nitrite excretion (Kloft and Forchhammer, 2005).
720 Furthermore, nitrogen starved cells are able to utilize nitrate in absence of light (low ATP)
721 (Watzer and Forchhammer, 2018), while exponentially growing cells inhibited nitrate
722 utilization in the dark (Romero et al., 1985). According to this data we conclude that
723 phosphorylated P_{II} interacts with NrtC and NrtD in an ATP bound state, while ADP or
724 ATP/2-OG leads to a dissociation of the complex. Additionally, non-phosphorylated P_{II} can
725 block nitrate utilization even in an ADP bound state, since exponentially growing cells close
726 the NrtABCD transporter in absence of light.

727 The ammonium induced inhibition of nitrate utilization occurs independently from the
728 phosphorylation status (Lee et al., 2000; Kloft and Forchhammer, 2005). We suggest that the
729 rapid drop in 2-OG level induces the ammonium dependent nitrate uptake inhibition. In
730 agreement, the presence of L-methionine-d,l-sulfoximine (MSX) or azaserine (both inhibitors
731 of the GS/GOGAT pathway) lead to an accumulation of 2-OG followed by an impaired
732 ammonium induced nitrate uptake inhibition (Flores et al., 1980).

733

734 **4.3 P_{II} regulate urea uptake by interacting the UrtE subunit**

735 Cyanobacterial P_{II} is verifiable involved in regulation of different ABC-type transporters like
736 the bispecific nitrate/nitrite NrtABCD transporter and the bispecific cyanate/nitrite CynABC
737 transporter (Chang et al., 2013). Next to this two known P_{II} targets, our data identified the
738 ABC-type UrtABCDE transporter as a novel P_{II} target. Regulation of the UrtABCDE Urea
739 transporter is depending on the interaction between P_{II} and the UrtE subunit. The interaction
740 of P_{II} and the UrtE is likely T-loop independent, since our bacterial two-hybrid assay showed
741 interaction between the P_{II}(I86N) variant and UrtE. In agreement, *Synechocystis* sp. harboring
742 the P_{II}(I86N) variant behaves like the wild-type regarding the urea utilization properties. The
743 P_{II}(I86N) variant enables a tightly bend T-loop conformation; however, the P_{II}(I86N)
744 backbone is almost identical with that of the wild-type P_{II} (Fokina et al., 2010b). In contrast,
745 *Synechocystis* sp. harboring the P_{II}-Venus fusion is impaired in regulation of the urea
746 utilization. The Δ P_{II} + P_{II}-Venus strain shows elevated urea uptake and a slightly impaired
747 ammonium induced urea uptake inhibition. The Venus fusion on the C-terminus could lead to
748 a sterical inhibition of the B- and C-loop while the T-loop remains unaffected. According to
749 this data, we strongly suggest an involvement of the B- and C-loop in the interaction of P_{II}
750 with the UrtE subunit.

751 Surprisingly, the P_{II} deletion mutant excretes ammonium in response to the uncontrolled urea
752 uptake. This ammonium excretion could be causal to limited ammonium assimilation by the
753 GS/GOGAT cycle. The ammonium excretion only occurs in the P_{II} deletion mutant.
754 Interestingly, the Δ P_{II} + P_{II}-Venus complementation strain, which also obtain an impaired
755 urea uptake regulation, shows no ammonium excretion. This inconsistency can be explained
756 by the Amt1 ammonium permesase, which probably operates in both directions. The P_{II}-
757 Venus variant maintains the ability to interact with Amt1, while the P_{II} deletion mutant is
758 unable to block the Amt1 permease. Due to this behavior, the P_{II}-Venus version could block
759 the Amt1 permease and therefore avoid the ammonium excretion, which occurs in response to
760 uncontrolled urea influx. The absence of ammonium excretion of the P_{II}-Venus
761 complementation strain could also indicate a lower urease activity. Our pull down
762 experiments identified the urease as possible interaction partner of P_{II}. A high urease activity
763 in the Δ P_{II} mutant could lead to an accumulation of ammonium and therefore causes an
764 excretion. The P_{II}-Venus variant could maintain the ability to regulate the urease.
765 Accordingly, a reduced urease activity in the Δ P_{II} + P_{II}-Venus strain could prevent an
766 ammonium accumulation and no excretion occurs.

767 Quantification of urea consumption showed impaired regulation of urea uptake in the Δ P_{II} and
768 the Δ P_{II} + P_{II}-Venus strain. According to this we expected impaired growth of the Δ P_{II} and the
769 Δ P_{II} + P_{II}-Venus strain when urea is provided as only nitrogen source, while *Synechocystis* sp.
770 wild-type and the P_{II} (I86N) strain should grow normally. Surprisingly, *Synechocystis* sp.
771 wild-type enables a growth advantage against the P_{II} (I86N) strain at low urea concentrations
772 (<10 mM Urea), while both strains behave similar at higher urea concentrations. The P_{II}
773 deletion causes a growth disadvantage against the wild-type and the P_{II} (I86N) strain also only

774 at low urea concentration. This observation supports the importance of P_{II} regulation of the
775 UrtABCDE transporter, especially at low concentrations, while urea tolerance is only minorly
776 influenced by P_{II}. Furthermore, our drop plate method showed an unexpected high growth rate
777 and urea tolerance of the $\Delta P_{II} + P_{II}$ -Venus strain. The high urea tolerance of the $\Delta P_{II} + P_{II}$ -
778 Venus strain could be due to the increased copy number of the plasmid encoded P_{II}-Venus,
779 which causes a slight over-expression. The slight over-expression of P_{II}-Venus could somehow
780 compensate the impaired urea uptake regulation and therefore result in an increased growth.
781 All together this unexpected result indicates that urea tolerance and utilization do not only
782 depend on urea uptake regulation. Regulation of the urease activity and ammonium
783 assimilation rate of the GS/GOGAT cycle also strongly influence the urea tolerance and urea
784 supplemented growth.

785

786 **5 Conflict of Interest**

787 The authors declare that the research was conducted in the absence of any commercial or
788 financial relationships that could be construed as a potential conflict of interest.

789

790 **6 Author Contributions**

791 BW designed, performed and evaluated cyanobacterial growth experiments, drop plate
792 methods, quantifications of nitrate, nitrite, ammonium and urea utilization and
793 microscopically localization studies. PS and OH performed Anti-Flag Pull down experiments.
794 PS performed and evaluated protein identification by nanoLC-MS/MS. MK designed and
795 constructed bacterial two-hybrid vectors. NN performed and evaluated bacterial two-hybrid
796 assays. KF supervised the study and wrote the manuscript with BW. All authors gave input
797 and approved the manuscript.

798

799 **7 Funding**

800 This work was supported by grants from the DFG (Fo195/9-2) and the research training group
801 GRK 1708.

802

803 **8 References**

- 804 Antia, N.J., Harrison, P.J., and Oliveira, L. (1991). The role of dissolved organic nitrogen in
805 phytoplankton nutrition, cell biology and ecology. *Phycologia* 30(1), 1-89. doi: DOI
806 10.2216/i0031-8884-30-1-1.1.
- 807 Baker, K.M., Gobler, C.J., and Collier, J.L. (2009). Urease gene sequences from algae and
808 heterotrophic bacteria in axenic and nonaxenic phytoplankton cultures. *Journal of*
809 *Phycology* 45(3), 625-634. doi: 10.1111/j.1529-8817.2009.00680.x.
- 810 Caldovic, L., and Tuchman, M. (2003). N-acetylglutamate and its changing role through
811 evolution. *Biochem J* 372(Pt 2), 279-290. doi: 10.1042/BJ20030002.
- 812 Chang, Y.J., Takatani, N., Aichi, M., Maeda, S., and Omata, T. (2013). Evaluation of the
813 Effects of P-II Deficiency and the Toxicity of PipX on Growth Characteristics of the

- 814 P-II-Less Mutant of the Cyanobacterium *Synechococcus elongatus*. *Plant and Cell*
815 *Physiology* 54(9), 1504-1514. doi: 10.1093/pcp/pct092.
- 816 Cheah, E., Carr, P.D., Suffolk, P.M., Vasudevan, S.G., Dixon, N.E., and Ollis, D.L. (1994).
817 Structure of the *Escherichia coli* signal transducing protein P_{II}. *Structure* 2(10), 981-
818 990.
- 819 Chellamuthu, V.R., Alva, V., and Forchhammer, K. (2013). From cyanobacteria to plants:
820 conservation of P_{II} functions during plastid evolution. *Planta* 237(2), 451-462. doi:
821 10.1007/s00425-012-1801-0.
- 822 Chidgey, J.W., Linhartova, M., Komenda, J., Jackson, P.J., Dickman, M.J., Canniffe, D.P., et
823 al. (2014). A cyanobacterial chlorophyll synthase-HliD complex associates with the
824 Ycf39 protein and the YidC/Alb3 insertase. *Plant Cell* 26(3), 1267-1279. doi:
825 10.1105/tpc.114.124495.
- 826 Conroy, M.J., Durand, A., Lupo, D., Li, X.D., Bullough, P.A., Winkler, F.K., et al. (2007).
827 The crystal structure of the *Escherichia coli* AmtB-GlnK complex reveals how GlnK
828 regulates the ammonia channel. *Proc Natl Acad Sci U S A* 104(4), 1213-1218. doi:
829 10.1073/pnas.0610348104.
- 830 Cox, J., and Mann, M. (2008). MaxQuant enables high peptide identification rates,
831 individualized p.p.b.-range mass accuracies and proteome-wide protein quantification.
832 *Nature Biotechnology* 26(12), 1367-1372. doi: 10.1038/nbt.1511.
- 833 Doello, S., Klotz, A., Makowka, A., Gutekunst, K., and Forchhammer, K. (2018). A specific
834 glycogen mobilization strategy enables awakening of dormant cyanobacteria from
835 chlorosis. *Plant Physiol.* doi: 10.1104/pp.18.00297.
- 836 Drath, M., Kloft, N., Batschauer, A., Marin, K., Novak, J., and Forchhammer, K. (2008).
837 Ammonia triggers photodamage of photosystem II in the cyanobacterium
838 *Synechocystis* sp strain PCC 6803. *Plant Physiology* 147(1), 206-215. doi:
839 10.1104/pp.108.117218.
- 840 Durand, A., and Merrick, M. (2006). In vitro analysis of the *Escherichia coli* AmtB-GlnK
841 complex reveals a stoichiometric interaction and sensitivity to ATP and 2-
842 oxoglutarate. *Journal of Biological Chemistry* 281(40), 29558-29567. doi:
843 10.1074/jbc.M602477200.
- 844 Espinosa, J., Forchhammer, K., Burillo, S., and Contreras, A. (2006). Interaction network in
845 cyanobacterial nitrogen regulation: PipX, a protein that interacts in a 2-oxoglutarate
846 dependent manner with P_{II} and NtcA. *Mol Microbiol* 61(2), 457-469. doi:
847 10.1111/j.1365-2958.2006.05231.x.
- 848 Espinosa, J., Forchhammer, K., and Contreras, A. (2007). Role of the *Synechococcus* PCC
849 7942 nitrogen regulator protein PipX in NtcA-controlled processes. *Microbiology-Sgm*
850 153, 711-718. doi: 10.1099/mic.0.2006/003574-0.
- 851 Espinosa, J., Rodriguez-Mateos, F., Salinas, P., Lanza, V.F., Dixon, R., de la Cruz, F., et al.
852 (2014). PipX, the coactivator of NtcA, is a global regulator in cyanobacteria. *Proc*
853 *Natl Acad Sci U S A* 111(23), E2423-2430. doi: 10.1073/pnas.1404097111.
- 854 Esteves-Ferreira, A.A., Inaba, M., Fort, A., Araujo, W.L., and Sulpice, R. (2018). Nitrogen
855 metabolism in cyanobacteria: metabolic and molecular control, growth consequences
856 and biotechnological applications. *Crit Rev Microbiol*, 1-20. doi:
857 10.1080/1040841X.2018.1446902.
- 858 Fiddler, R.N. (1977). Collaborative study of modified AOAC method of analysis for nitrite in
859 meat and meat products. *J Assoc Off Anal Chem* 60(3), 594-599.
- 860 Flores, E., Guerrero, M.G., and Losada, M. (1980). Short-Term Ammonium Inhibition of
861 Nitrate Utilization by *Anacystis-Nidulans* and Other Cyanobacteria. *Archives of*
862 *Microbiology* 128(2), 137-144. doi: Doi 10.1007/Bf00406150.

- 863 Flores, E., and Herrero, A. (1994). "Assimilatory nitrogen metabolism and its regulation," in
864 *The Molecular Biology of Cyanobacteria*, ed. D.A. Bryant. (Dordrecht: Springer
865 Netherlands), 487-517.
- 866 Fokina, O., Chellamuthu, V.R., Forchhammer, K., and Zeth, K. (2010a). Mechanism of 2-
867 oxoglutarate signaling by the *Synechococcus elongatus* P_{II} signal transduction protein.
868 *Proc Natl Acad Sci U S A* 107(46), 19760-19765. doi: 10.1073/pnas.1007653107.
- 869 Fokina, O., Chellamuthu, V.R., Zeth, K., and Forchhammer, K. (2010b). A novel signal
870 transduction protein P(II) variant from *Synechococcus elongatus* PCC 7942 indicates a
871 two-step process for NAGK-P(II) complex formation. *J Mol Biol* 399(3), 410-421.
872 doi: 10.1016/j.jmb.2010.04.018.
- 873 Forchhammer, K. (2004). Global carbon/nitrogen control by P-II signal transduction in
874 cyanobacteria: from signals to targets. *Fems Microbiology Reviews* 28(3), 319-333.
875 doi: 10.1016/j.femsre.2003.11.001.
- 876 Forchhammer, K. (2008). P_{II} signal transducers: novel functional and structural insights.
877 *Trends Microbiol* 16(2), 65-72. doi: 10.1016/j.tim.2007.11.004.
- 878 Forchhammer, K., and Demarsac, N.T. (1995). Functional-Analysis of the Phosphoprotein P-
879 Ii (GlnB Gene-Product) in the Cyanobacterium *Synechococcus* Sp Strain Pcc-7942.
880 *Journal of Bacteriology* 177(8), 2033-2040. doi: DOI 10.1128/jb.177.8.2033-
881 2040.1995.
- 882 Forchhammer, K., and Hedler, A. (1997). Phosphoprotein P_{II} from cyanobacteria--analysis of
883 functional conservation with the P_{II} signal-transduction protein from *Escherichia coli*.
884 *Eur J Biochem* 244(3), 869-875.
- 885 Forchhammer, K., and Luddecke, J. (2016). Sensory properties of the P_{II} signalling protein
886 family. *FEBS J* 283(3), 425-437. doi: 10.1111/febs.13584.
- 887 Forchhammer, K., and Tandeau de Marsac, N. (1995). Phosphorylation of the P_{II} protein
888 (glnB gene product) in the cyanobacterium *Synechococcus* sp. strain PCC 7942:
889 analysis of in vitro kinase activity. *J Bacteriol* 177(20), 5812-5817.
- 890 Gibson, D.G., Young, L., Chuang, R.Y., Venter, J.C., Hutchison, C.A., and Smith, H.O.
891 (2009). Enzymatic assembly of DNA molecules up to several hundred kilobases.
892 *Nature Methods* 6(5), 343-U341. doi: 10.1038/Nmeth.1318.
- 893 Gruswitz, F., O'Connell, J., and Stroud, R.M. (2007). Inhibitory complex of the
894 transmembrane ammonia channel, AmtB, and the cytosolic regulatory protein, GlnK,
895 at 1.96 Å. *Proceedings of the National Academy of Sciences of the United States of*
896 *America* 104(1), 42-47. doi: 10.1073/pnas.0609796104.
- 897 Guerrero, M.G., Vega, J.M., and Losada, M. (1981). The assimilatory nitrate-reducing system
898 and its regulation. *Annual Review of Plant Physiology and Plant Molecular Biology*
899 32, 169-204. doi: DOI 10.1146/annurev.pp.32.060181.001125.
- 900 Hauf, W., Schmid, K., Gerhardt, E.C., Huergo, L.F., and Forchhammer, K. (2016). Interaction
901 of the nitrogen regulatory protein GlnB P_{II} with biotin carboxyl carrier protein (BCCP)
902 controls acetyl-CoA levels in the cyanobacterium *Synechocystis* sp. PCC 6803. *Front*
903 *Microbiol* 7, 1700. doi: 10.3389/fmicb.2016.01700.
- 904 Heinrich, A., Maheswaran, M., Ruppert, U., and Forchhammer, K. (2004). The
905 *Synechococcus elongatus* P_{II} signal transduction protein controls arginine synthesis by
906 complex formation with N-acetyl-L-glutamate kinase. *Mol Microbiol* 52(5), 1303-
907 1314. doi: 10.1111/j.1365-2958.2004.04058.x.
- 908 Herrero, A., and Flores, E. (2008). *The cyanobacteria : molecular biology, genomics, and*
909 *evolution*. Norfolk, UK: Caister Academic Press.
- 910 Hisbergues, M., Jeanjean, R., Joset, F., de Marsac, N.T., and Bedu, S. (1999). Protein P_{II}
911 regulates both inorganic carbon and nitrate uptake and is modified by a redox signal in
912 *Synechocystis* sp PCC 6803. *Febs Letters* 463(3), 216-220. doi: Doi 10.1016/S0014-
913 5793(99)01624-5.

- 914 Jiang, P., Peliska, J.A., and Ninfa, A.J. (1998). Enzymological characterization of the signal-
915 transducing uridylyltransferase/uridylyl-removing enzyme (EC 2.7.7.59) of
916 *Escherichia coli* and its interaction with the P_{II} protein. *Biochemistry* 37(37), 12782-
917 12794. doi: DOI 10.1021/bi980667m.
- 918 Karimova, G., Ullmann, A., and Ladant, D. (2001). Protein-protein interaction between
919 *Bacillus stearothermophilus* tyrosyl-tRNA synthetase subdomains revealed by a
920 bacterial two-hybrid system. *Journal of Molecular Microbiology and Biotechnology*
921 3(1), 73-82.
- 922 Kleiner, D. (1981). The transport of NH₃ and NH₄⁺ across biological membranes. *Biochim*
923 *Biophys Acta* 639(1), 41-52.
- 924 Kloft, N., and Forchhammer, K. (2005). Signal transduction protein P_{II} phosphatase PphA is
925 required for light-dependent control of nitrate utilization in *Synechocystis* sp. strain
926 PCC 6803. *J Bacteriol* 187(19), 6683-6690. doi: 10.1128/JB.187.19.6683-6690.2005.
- 927 Kobayashi, M., Rodriguez, R., Lara, C., and Omata, T. (1997). Involvement of the C-terminal
928 domain of an ATP-binding subunit in the regulation of the ABC-type nitrate/nitrite
929 transporter of the cyanobacterium *Synechococcus* sp. strain PCC 7942. *Journal of*
930 *Biological Chemistry* 272(43), 27197-27201. doi: DOI 10.1074/jbc.272.43.27197.
- 931 Labarre, J., Thuriaux, P., and Chauvat, F. (1987). Genetic-Analysis of Amino-Acid-Transport
932 in the Facultatively Heterotrophic Cyanobacterium *Synechocystis* Sp Strain 6803.
933 *Journal of Bacteriology* 169(10), 4668-4673. doi: DOI 10.1128/jb.169.10.4668-
934 4673.1987.
- 935 Lee, H.M., Flores, E., Forchhammer, K., Herrero, A., and de Marsac, N.T. (2000).
936 Phosphorylation of the signal transducer P-II protein and an additional effector are
937 required for the P-II-mediated regulation of nitrate and nitrite uptake in the
938 cyanobacterium *Synechococcus* sp PCC 7942. *European Journal of Biochemistry*
939 267(2), 591-600. doi: DOI 10.1046/j.1432-1327.2000.01043.x.
- 940 Lee, H.M., Flores, E., Herrero, A., Houmard, J., and de Marsac, N.T. (1998). A role for the
941 signal transduction protein P-II in the control of nitrate/nitrite uptake in a
942 cyanobacterium. *Febs Letters* 427(2), 291-295. doi: Doi 10.1016/S0014-
943 5793(98)00451-7.
- 944 Llacer, J.L., Contreras, A., Forchhammer, K., Marco-Marin, C., Gil-Ortiz, F., Maldonado, R.,
945 et al. (2007). The crystal structure of the complex of P_{II} and acetylglutamate kinase
946 reveals how P_{II} controls the storage of nitrogen as arginine. *Proc Natl Acad Sci U S A*
947 104(45), 17644-17649. doi: 10.1073/pnas.0705987104.
- 948 Luque, I., Flores, E., and Herrero, A. (1994). Nitrate and Nitrite Transport in the
949 Cyanobacterium *Synechococcus* Sp Pcc-7942 Are Mediated by the Same Permease.
950 *Biochimica Et Biophysica Acta-Bioenergetics* 1184(2-3), 296-298. doi: Doi
951 10.1016/0005-2728(94)90236-4.
- 952 Maeda, S.I., and Omata, T. (1997). Substrate-binding lipoprotein of the cyanobacterium
953 *Synechococcus* sp strain PCC 7942 involved in the transport of nitrate and nitrite.
954 *Journal of Biological Chemistry* 272(5), 3036-3041. doi: DOI 10.1074/jbc.272.5.3036.
- 955 Maheswaran, M., Urbanke, C., and Forchhammer, K. (2004). Complex formation and
956 catalytic activation by the P-II signaling protein of N-acetyl-L-glutamate kinase from
957 *Synechococcus elongatus* strain PCC 7942. *Journal of Biological Chemistry* 279(53),
958 55202-55210. doi: 10.1074/jbc.M410971200.
- 959 Maheswaran, M., Ziegler, K., Lockau, W., Hagemann, M., and Forchhammer, K. (2006). P_{II}-
960 regulated arginine synthesis controls accumulation of cyanophycin in *Synechocystis* sp
961 strain PCC 6803. *J Bacteriol* 188(7), 2730-2734. doi: 10.1128/Jb.188.7.2730-
962 2734.2006.

- 963 Manzano, C., Candau, P., Gomez-Moreno, C., Relimpio, A.M., and Losada, M. (1976).
964 Ferredoxin-dependent photosynthetic reduction of nitrate and nitrite by particles of
965 *Anacystis nidulans*. *Mol Cell Biochem* 10(3), 161-169.
- 966 Marques, S., Merida, A., Candau, P., and Florencio, F.J. (1992). Light-mediated regulation of
967 glutamine-synthetase activity in the unicellular cyanobacterium *Synechococcus* sp
968 PCC6301. *Planta* 187(2), 247-253.
- 969 Mitamura, O., and Saijo, Y. (1980). Insitu measurement of the urea decomposition rate and its
970 turnover rate in the pacific-ocean. *Marine Biology* 58(2), 147-152. doi: Doi
971 10.1007/Bf00396126.
- 972 Mobley, H.L., and Hausinger, R.P. (1989). Microbial ureases: significance, regulation, and
973 molecular characterization. *Microbiol Rev* 53(1), 85-108.
- 974 Montesinos, M.L., Muro-Pastor, A.M., Herrero, A., and Flores, E. (1998).
975 Ammonium/methylammonium permeases of a cyanobacterium. Identification and
976 analysis of three nitrogen-regulated amt genes in *Synechocystis* sp. PCC 6803. *J Biol*
977 *Chem* 273(47), 31463-31470.
- 978 Muro-Pastor, M.I., Reyes, J.C., and Florencio, F.J. (2001). Cyanobacteria perceive nitrogen
979 status by sensing intracellular 2-oxoglutarate levels. *Journal of Biological Chemistry*
980 276(41), 38320-38328.
- 981 Muro-Pastor, M.I., Reyes, J.C., and Florencio, F.J. (2005). Ammonium assimilation in
982 cyanobacteria. *Photosynth Res* 83. doi: 10.1007/s11120-004-2082-7.
- 983 Nakao, M., Okamoto, S., Kohara, M., Fujishiro, T., Fujisawa, T., Sato, S., et al. (2010).
984 CyanoBase: the cyanobacteria genome database update 2010. *Nucleic Acids Research*
985 38, D379-D381. doi: 10.1093/nar/gkp915.
- 986 Ohashi, Y., Shi, W., Takatani, N., Aichi, M., Maeda, S., Watanabe, S., et al. (2011).
987 Regulation of nitrate assimilation in cyanobacteria. *Journal of Experimental Botany*
988 62(4), 1411-1424. doi: 10.1093/jxb/erq427.
- 989 Olsen, J.V., de Godoy, L.M.F., Li, G.Q., Macek, B., Mortensen, P., Pesch, R., et al. (2005).
990 Parts per million mass accuracy on an orbitrap mass spectrometer via lock mass
991 injection into a C-trap. *Molecular & Cellular Proteomics* 4(12), 2010-2021. doi:
992 10.1074/mcp.T500030-MCP200.
- 993 Omata, T., Andriessse, X., and Hirano, A. (1993a). Identification and Characterization of a
994 Gene-Cluster Involved in Nitrate Transport in the Cyanobacterium *Synechococcus* Sp-
995 Pcc7942. *Molecular & General Genetics* 236(2-3), 193-202. doi: Doi
996 10.1007/Bf00277112.
- 997 Omata, T., Andriessse, X., and Hirano, A. (1993b). Identification and characterization of a
998 gene-cluster involved in nitrate transport in the cyanobacterium *Synechococcus* sp
999 PCC 7942. *Molecular & General Genetics* 236(2-3), 193-202. doi: Doi
1000 10.1007/Bf00277112.
- 1001 Radchenko, M., and Merrick, M. (2011). The role of effector molecules in signal transduction
1002 by P_{II} proteins. *Biochem Soc Trans* 39(1), 189-194. doi: 10.1042/BST0390189.
- 1003 Rappsilber, J., Mann, M., and Ishihama, Y. (2007). Protocol for micro-purification,
1004 enrichment, pre-fractionation and storage of peptides for proteomics using StageTips.
1005 *Nature Protocols* 2(8), 1896-1906. doi: 10.1038/nprot.2007.261.
- 1006 Rees, A.P., Woodward, E.M.S., and Joint, I. (2006). Concentrations and uptake of nitrate and
1007 ammonium in the Atlantic ocean between 60 degrees N and 50 degrees S. *Deep-Sea*
1008 *Research Part Ii-Topical Studies in Oceanography* 53(14-16), 1649-1665. doi:
1009 10.1016/j.dsr2.2006.05.008.
- 1010 Rippka, R., Deruelles, J., Waterbury, J.B., Herdman, M., and Stanier, R.Y. (1979). Generic
1011 assignments, strain histories and properties of pure cultures of cyanobacteria. *J Gen*
1012 *Microbiol* 111(Mar), 1-61. doi: 10.1099/00221287-111-1-1.

- 1013 Rodrigues, T.E., Souza, V.E.P., Monteiro, R.A., Gerhardt, E.C.M., Araujo, L.M., Chubatsu,
1014 L.S., et al. (2011). In vitro interaction between the ammonium transport protein AmtB
1015 and partially uridylylated forms of the P-II protein GlnZ. *Biochimica Et Biophysica*
1016 *Acta-Proteins and Proteomics* 1814(9), 1203-1209. doi:
1017 10.1016/j.bbapap.2011.05.012.
- 1018 Romero, J.M., Lara, C., and Guerrero, M.G. (1985). Dependence of nitrate utilization upon
1019 active CO₂ fixation in *Anacystis Nidulans* - a regulatory aspect of the interaction
1020 between photosynthetic carbon and nitrogen-metabolism. *Arch Biochem Biophys*
1021 237(2), 396-401. doi: Doi 10.1016/0003-9861(85)90291-7.
- 1022 Sakamoto, T., Inoue-Sakamoto, K., and Bryant, D.A. (1999). A novel nitrate/nitrite permease
1023 in the marine cyanobacterium *Synechococcus* sp. strain PCC 7002. *J Bacteriol*
1024 181(23), 7363-7372.
- 1025 Schindelin, J., Arganda-Carreras, I., Frise, E., Kaynig, V., Longair, M., Pietzsch, T., et al.
1026 (2012). Fiji: an open-source platform for biological-image analysis. *Nature Methods*
1027 9(7), 676-682. doi: 10.1038/Nmeth.2019.
- 1028 Solomon, C.M., Collier, J.L., Berg, G.M., and Glibert, P.M. (2010). Role of urea in microbial
1029 metabolism in aquatic systems: a biochemical and molecular review. *Aquatic*
1030 *Microbial Ecology* 59(1), 67-88. doi: 10.3354/ame01390.
- 1031 Soo, R.M., Hemp, J., Parks, D.H., Fischer, W.W., and Hugenholtz, P. (2017). On the origins
1032 of oxygenic photosynthesis and aerobic respiration in cyanobacteria. *Science*
1033 355(6332), 1436-1439. doi: 10.1126/science.aal3794.
- 1034 Spat, P., Macek, B., and Forchhammer, K. (2015). Phosphoproteome of the cyanobacterium
1035 *Synechocystis* sp PCC 6803 and its dynamics during nitrogen starvation. *Frontiers in*
1036 *Microbiology* 6. doi: ARTN 248
1037 10.3389/fmicb.2015.00248.
- 1038 Valladares, A., Montesinos, M.L., Herrero, A., and Flores, E. (2002). An ABC-type, high-
1039 affinity urea permease identified in cyanobacteria. *Molecular Microbiology* 43(3),
1040 703-715. doi: DOI 10.1046/j.1365-2958.2002.02778.x.
- 1041 Vegapalas, M.A., Flores, E., and Herrero, A. (1992). Ntca, a global nitrogen regulator from
1042 the cyanobacterium *Synechococcus* that belongs to the Crp family of bacterial
1043 regulators. *Molecular Microbiology* 6(13), 1853-1859. doi: DOI 10.1111/j.1365-
1044 2958.1992.tb01357.x.
- 1045 Vitousek, P.M., and Howarth, R.W. (1991). Nitrogen limitation on land and in the sea - how
1046 can it occur. *Biogeochemistry* 13(2), 87-115.
- 1047 Vizcaino, J.A., Cote, R.G., Csordas, A., Dianes, J.A., Fabregat, A., Foster, J.M., et al. (2013).
1048 The proteomics identifications (PRIDE) database and associated tools: status in 2013.
1049 *Nucleic Acids Research* 41(D1), D1063-D1069. doi: 10.1093/nar/gks1262.
- 1050 Vogel, A.I., Furniss, B.S., and Vogel, A.I. (1989). *Vogel's Textbook of practical organic*
1051 *chemistry*. London, New York: Longman Scientific & Technical ; Wiley.
- 1052 Watzer, B., Engelbrecht, A., Hauf, W., Stahl, M., Maldener, I., and Forchhammer, K. (2015).
1053 Metabolic pathway engineering using the central signal processor P_{II}. *Microb Cell*
1054 *Fact* 14, 192. doi: 10.1186/s12934-015-0384-4.
- 1055 Watzer, B., and Forchhammer, K. (2018). Cyanophycin synthesis optimizes nitrogen
1056 utilization in the unicellular cyanobacterium *Synechocystis* sp. PCC 6803. *Appl*
1057 *Environ Microbiol*. doi: 10.1128/AEM.01298-18.
- 1058 Whitton, B.A. (2012). *Ecology of cyanobacteria II : their diversity in space and time*. New
1059 York: Springer.
- 1060 Wirén, N.v., and Merrick, M. (2004). "Regulation and function of ammonium carriers in
1061 bacteria, fungi, and plants," in *Molecular Mechanisms Controlling Transmembrane*
1062 *Transport*. (Berlin, Heidelberg: Springer Berlin Heidelberg), 95-120.

- 1063 Xu, Y.B., Carr, P.D., Clancy, P., Garcia-Dominguez, M., Forchhammer, K., Florencio, F., et
1064 al. (2003). The structures of the P_{II} proteins from the cyanobacteria *Synechococcus* sp
1065 PCC 7942 and *Synechocystis* sp PCC 6803. *Acta Crystallographica Section D-*
1066 *Biological Crystallography* 59, 2183-2190. doi: 10.1107/S09074444903019589.
- 1067 Zeth, K., Fokina, O., and Forchhammer, K. (2014). Structural basis and target-specific
1068 modulation of ADP sensing by the *Synechococcus elongatus* P_{II} signaling protein.
1069 *Journal of Biological Chemistry* 289(13), 8960-8972. doi: 10.1074/jbc.M113.536557.
- 1070 Zhao, M.X., Jiang, Y.L., Xu, B.Y., Chen, Y., Zhang, C.C., and Zhou, C.Z. (2010). Crystal
1071 structure of the cyanobacterial signal transduction protein P_{II} in complex with PipX. *J*
1072 *Mol Biol* 402(3), 552-559. doi: 10.1016/j.jmb.2010.08.006.

1073

X. Acknowledgements

Allen voran möchte ich mich bei Herr Prof. Dr. Forchhammer bedanken, der meine Promotion überhaupt erst ermöglichte. Im Wintersemester 2011 besuchte ich erstmalig eine Ihrer Vorlesungen. Anders wie die meisten Dozenten, referierten Sie auf eine sehr enthusiastische und engagierte Art, wodurch Sie bei Ihren Zuhörern Interesse für das Thema wecken konnten und mich veranlassten meine Masterarbeit an Ihrem Institut zu schreiben. Auch bei der späteren Betreuung meiner Promotion, schafften Sie es immer wieder, mich zu motivieren. Häufig kommt es im Laufe einer Promotion vor, dass Experimente nicht die erwarteten Ergebnisse bringen, was sich demotivierend auswirkt. War dies aber der Fall, nahmen Sie sich immer Zeit, berieten mich und gaben mir wieder Optimismus und Zuversicht. Dafür vielen Dank!

Des Weiteren möchte ich mich bei Frau Prof. Brötz-Oesterhelt für das Erstellen des Zweitgutachtens bedanken.

Am Institut für organismische Interaktionen ist man Teil eines Teams, bei dem man sich gegenseitig hilft und unterstützt. Mein Dank geht daher an alle Kolleginnen und Kollegen, auf deren Unterstützung ich mich immer verlassen konnte. Es hätte keine bessere Arbeitsatmosphäre geben können. Besonderer Dank geht in diesem Zusammenhang auch an die ehemaligen Doktoranden aus der "letzten Generation": Waldemar Hauf, Alexander Klotz, Jan Lüddecke und Philipp Spät.

Ebenfalls bedanke ich mich bei der aktuellen Besetzung von 9P13: Sofia Doello, Moritz Koch, Niels Neumann und seit Kurzem auch Markus Burkhardt. Es war mir eine Freude, mit euch zu arbeiten.

Besonderer Dank geht an meine Freundin Sarah Schwarzenborfer: Dein Eifer und Engagement waren für mich immer eine Inspiration. Ich bin mir sicher, dass du eine hervorragende Lehrerin wirst.

Zu guter Letzt bedanke ich mich bei meinen Freunden und meiner Familie. Hervorheben möchte ich meinen Vater Reinhard Watzer und Oma Margarete Watzer. Ohne Eure Unterstützung wäre diese Arbeit nicht möglich gewesen.
